UNIVERSIDADE FEDERAL DA PARAÍBA
CENTRO DE CIÊNCIAS DA SAÚDE
PROGRAMA DE PÓS-GRADUAÇÃO EM PRODUTOS NATURAIS E SINTÉTICOS BIOATIVOS

ALEX FRANCE MESSIAS MONTEIRO

TRIAGEM VIRTUAL HÍBRIDA, PREDIÇÕES ADMET E MODELAGEM MOLECULAR DE COMPOSTOS 2-AMINOTIOFENOS FRENTE AO HIV-1

João Pessoa

2021

UNIVERSIDADE FEDERAL DA PARAÍBA
CENTRO DE CIÊNCIAS DA SAÚDE
PROGRAMA DE PÓS-GRADUAÇÃO EM PRODUTOS NATURAIS E SINTÉTICOS BIOATIVOS

TRIAGEM VIRTUAL HÍBRIDA, PREDIÇÕES ADMET E MODELAGEM MOLECULAR DE COMPOSTOS 2-AMINOTIOFENOS FRENTE AO HIV-1

Tese apresentada ao Programa de Pós-Graduação em Produtos Naturais e Sintéticos Bioativos do Centro de Ciências da Saúde da Universidade Federal da Paraíba, em cumprimento às exigências para obtenção do título de Doutor em Produtos Naturais e Sintéticos Bioativos.

Área de concentração: Farmacoquímica

Orientadora: Profa. Dra. Luciana Scotti

Coorientador: Prof. Dr. Francisco Jaime Bezerra Mendonça Júnior

João Pessoa

2021

FICHA CATALOGRAFICA

Catalogação de Publicação na Fonte. UFPB - Biblioteca Central

M775t Monteiro, Alex France Messias.
Triagem virtual híbrida, predições ADMET e modelagem molecular de compostos 2-aminotiofenos frente ao HIV-1 / Alex France Messias Monteiro. - João Pessoa, 2021.
147 f. : il.

Orientação: Luciana Scotti.
Coorientação: Francisco Jaime B. Mendonça Júnior.
Tese (Doutorado) - UFPB/CCS.

1. HIV. 2. Docking molecular. 3. 2-aminotiofeno. 4. Trancriptase reversa. 5. AIDS. I. Scotti, Luciana. II. Mendonça Júnior, Francisco Jaime B. III. Título.

UFPB/BC CDU 616.98:578.828(043)

ALEX FRANCE MESSIAS MONTEIRO

TRIAGEM VIRTUAL HÍBRIDA, PREDIÇÕES ADMET E MODELAGEM MOLECULAR DE COMPOSTOS 2-AMINOTIOFENOS FRENTE AO HIV-1

Aprovada em 20/08/2021

COMISSÃO EXAMINADORA

Luciana Scotti

_____

Profa. Dra. Luciana Scotti - Orientadora

Francisco Jaime B. Mendonça Jr.

_____

Prof. Dr. Francisco Jaime Bezerra Mendonça Júnior- Coorientador

Kristensen R. de Luna Freire

_____

Prof. Dr. Kristensen Reinaldo de Luna Freire

_____

Profa. Dra. Maria de Fátima Vanderlei de Souza

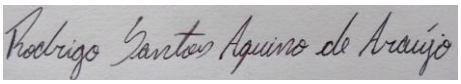

Prof. Dr. Rodrigo Santos Aquino de Araújo

Prof. Dr. Gustavo Henrique Goulart Trossini

“*A imaginação é mais importante que o conhecimento, porque o conhecimento é limitado, ao passo que a imaginação abrange o mundo inteiro*.” **(Albert Einstein)**

AGRADECIMENTOS

A **Deus** por me dar o sopro de vida e a oportunidade de trilhar meus próprios caminhos nas buscas dos meus objetivos me guiando até aqui.

Aos meus pais **Almir Monteiro e Cirleide Pereira** por serem exemplos de caráter, os quais sempre buscarei honrar e respeitar, por entenderem minha ausência em sair da minha cidade para estudar aqui na Paraíba, amo muito vocês!!!

Ao Prof. Dr. **Damião Pergentino** por ter estado comigo na seleção para o doutorado aqui no programa, mesmo que não tenha continuado em seu grupo de trabalho, saiba que minha admiração quanto pesquisadora não mudou, muito obrigado!

Aos **professores da minha banca de qualificação e da tese**, guardarei suas considerações acerca do meu estudo, e levarei para minha vida profissional, sou muito grato a cada um.

Aos **professores do curso** pelos ensinamentos valiosos, e que me ajudaram a tornar-me doutor, em especial o coordenador do laboratório de Quimioinformática o Prof. Dr. Marcus Tullius Scotti pela grande oportunidade em participar do grupo de trabalho e pelas inúmeras dúvidas tiradas.

A meu coorientador o Prof. Dr. **Francisco Jaime Bezerra Mendonça Júnior** por ajudar-me com as moléculas testadas, serei sempre muito grato pela parceria, também lhe admiro muito!

A minha orientadora a Profa. Dra. **Luciana Scotti**, eu nunca vou poder retribuir a grande mãe que a senhora foi em todo meu doutorado, me acolheu, me ensinou, me orientou. Sem dúvidas a senhora foi a figura mais importante em toda minha vida acadêmica, uma pesquisadora humana, uma amiga para os momentos mais difíceis. Serei eternamente grato por todas as portas que a senhora me abriu ao longo de mais de 3 anos de trabalho, muito obrigado!

RESUMO

O HIV é um vírus que afeta mais de 37 milhões de pessoas em todo o mundo, onde apenas 23,3 milhões recebiam tratamento retroviral em 2018, de acordo com a OMS, apenas 62% recebiam tratamento anti-HIV. Muitos grupos de pesquisa estão em busca de novos medicamentos para tratar e combater infecções crônicas causadas pelo vírus no corpo. Entre esses alvos estão três enzimas envolvidas no ciclo de vida do HIV: a transcriptase reversa, que é uma enzima responsável pela biossíntese do DNA viral do corpo. O RNA do vírus, a enzima protease responsável pela clivagem do DNA viral em unidades menores e funcionais, e a integrase, que é uma enzima responsável pela integração dessas unidades menores e funcionais no DNA dos linfócitos T CD4 +, dando a possibilidade de multiplicação retroviral e morte prematura. dessas células de defesa, cuja diminuição da concentração no organismo, deixa o infectado suscetível à doença oportunista devido à síndrome da imunodeficiência adquirida. Por conta disso, muitas pesquisas objetivam inibir uma dessas enzimas para tentar combater a progressão da AIDS, esta pesquisa teve como objetivo verificar através de técnicas *in silico* a possível atividade inibitória de um conjunto de derivados 2-aminotiofênicos contra essas três enzimas. , conceitos de planejamento racional de medicamentos, como triagem virtual e modelagem molecular, foram empregados, usando diferentes ferramentas computacionais como modelos de predição, taxa de absorção baseada na área topológica total, violação da regra de Lipinski, docking molecular e análise. de metabólitos hepáticos. Após todas as análises foi possível concluir que 07 compostos dos 180 inicialmente testados poderiam ter atividade potencial contra o HIV-1 com baixo efeito toxicológico.

Palavras-chave: HIV, transcriptase reversa, modelagem molecular e 2-aminotiofenos.

ABSTRACT

HIV is a virus that affects more than 37 million people worldwide, where only 23.3 million were receiving retroviral treatment in 2018, according to the WHO, only 62% received anti-HIV treatment. Many research groups are looking for new drugs to treat and fight chronic infections caused by the virus in the body. Among these targets are three enzymes involved in the HIV life cycle: reverse transcriptase, which is an enzyme responsible for the biosynthesis of the body's viral DNA. Virus RNA, the protease enzyme responsible for cleavage of viral DNA into smaller, functional units, and integrase, which is an enzyme responsible for integrating these smaller, functional units into the DNA of CD4+ T lymphocytes, giving the possibility of retroviral multiplication and premature death. of these defense cells, whose reduced concentration in the organism, makes the infected person susceptible to opportunistic disease due to the acquired immunodeficiency syndrome. Because of this, many researches aim to inhibit one of these enzymes to try to fight the progression of AIDS, this research aimed to verify through *in silico* techniques the possible inhibitory activity of a set of 2-aminothiophenic derivatives against these three enzymes. , concepts of rational drug planning, such as virtual screening and molecular modeling, were employed, using different computational tools such as prediction models, absorption rate based on the total topological area, violation of Lipinski's rule, molecular docking and analysis. of hepatic metabolites. After all the analyzes it was possible to conclude that 07 compounds of the 180 initially tested could have potential activity against HIV-1 with low toxicological effect.

Keywords: HIV, reverse transcriptase, molecular modeling and 2-aminothiophenes.

LISTA DE FIGURAS

LISTA DE TABELAS

LISTA DE ABREVIATURAS

ABREVIATURA	DESCRIÇÃO
%ABS	Taxa de absorção
ADMET	Absorção, distribuição, metabolismo, excreção e toxidade.
AIDS	*Acquired Immunodeficiency Syndrome*
CAR	Carcinogenicidade
ChEMBL	Banco de dados de estruturas químicas online
CPCA	*Consensus Principal Component Analysis* - Análise de componentes principais por consenso
DNA	Ácido desoxirribonucleico
ESR	Efeito tóxico no sistema reprodutor
HIV	*Human Immunodeficiency Virus*
IC_{50}	Concentração mínima inibitória de 50%
IN	Integrase
INIB	Proteína de inibição
IRR	Irritabilidade
LBVS	*Ligand based virtual scree*n – triagem virtual baseada no ligante
LIP	Violação a regra de Lipinski
MUT	Mutagênicidade
MVD	Molegro Virtual Docker
NVP	Inibidor da transcriptase reversa (PDB ID 3LP0)
PCA	*Principal Component Analysis* – Análise de componentes principais
PDB	Protein Data Bank – banco de dados de proteínas cristalografada
PLS	*Partial Least Squares* - Regressão parcial de mínimos quadrados
PN	Produto natural
PPE	Profilaxia Pós-exposição
PR	Protease
PrEP	Profilaxia Pré-Exposição
QSAR	*Quantitative structure-activity relationship* – relação estrutura atividade)
RF	*Random Forest* (Modelo de florestas randômicas de decisão)
RMSD	*Root-Mean-Square Deviation* - Desvio médio quadrático
RMSF	*Rocky Mountain Spotted Fever*
RNA	Ácido ribonucleico
ROC	*Receiver Operating Characteristic* - Característica de Operação do Receptor
SBVS	*Structure based virtual screen* – triagem virtual baseada na estrutura
SDF	Arquivo contendo estruturas químicas
SMILES	*Simplified Molecular Input Line Entry Specification* - representação de estruturas químicas usando caracteres ASCII

SUS	Sistema único de saúde
TOX	Citotoxidade total
TPSA	Área de Superfície Topológica Total
TPV2	Inibidor de protease (PDBB ID 6DIF)
TR	Transcriptase reversa
UNAIDS	Programa das Nações Unidas criado em 1996 e que tem a função de criar soluções e ajudar nações no combate à AIDS
WHO	*World Health Organization*
WPRED	Weka Predictor 3.7
WYSIWYG 2D	Sistema de plotagem bidimensional

SUMÁRIO

1. INTRODUÇÃO

A AIDS é considerada um problema de saúde pública, que acomete pessoas do mundo todo, independentemente de classe social, gênero, raça e outros. Está associada a prática sexual de comportamentos de risco, o compartilhamento de seringas para usuários de drogas injetáveis, contato direto com sangue contaminado e transmissão vertical de mãe para filho. (MACHADO-ZALDÍVAR *et al.*, 2021;BROEK, VAN DEN, 2021)

A grande maioria dos casos de infecção dão-se pela relação sexual sem o uso do preservativo, sendo o mais eficaz método profilático da doença recomendado pelos órgãos de saúde. A conscientização de hábitos sexualmente seguros e que propiciam menor exposição ao vírus do HIV é realizada através de campanhas educativas destinadas a todas as idades. (STONE *et al.*, 2021;PRESANIS *et al.*, 2021)

Segundo a WHO a faixa de vulnerabilidade está entre 15 a 49 anos, e milhões de pessoas morrem anualmente vítimas de complicações decorrentes a infecção pelo HIV, é verídica a informação de que a AIDS propriamente dita não capaz de provocar diretamente a morte do infectado, porém, contudo a diminuição das células imunológicas devido a infecção pelo retrovírus também diminui gradativamente a capacidade de defesa contra os microrganismos invasores, devido a fragilidade causada pela AIDS o indivíduo pode vir a óbito decorrentes de ações infecciosas secundárias como a pneumonia, tuberculose, meningite e outros. (MELO *et al.*, 2021)

Atualmente existem quatro linhas de pesquisas na produção de fármacos retrovirais para o HIV e suas mutações, cada linha corresponde a um alvo farmacológico diferente, o primeiro alvo está no camada de glicoproteínas com os inibidores de fusão (o impedimento da aproximação entre o vírus e célula normalmente não permite que o processo infeccioso inicie), o segundo alvo seria a protease uma enzima responsável por clivar em unidades menores e funcionais a cadeia proteica viral, o terceiro alvo seria a enzima integrase responsável por inserir a unidade viral no material genético da célula hospedeira, como último alvo tem-se a transcriptase reversa que é uma DNA polimerase

responsável pela síntese do material genético viral. (ZHU *et al.*, 2021; STEENKAMP, [s.d.])

As mutações sofridas pelo HIV que o torna resistente às drogas impulsiona pesquisas na busca de novas alternativas terapêuticas com bioativos isolados ou combinados. Motivadas pelo número de casos anuais de novas infecções, apesar de muitos esforços a infecção por HIV é crescente no mundo todo, assim como as variações do agente infecioso, assim, pesquisa como esta é necessário para o desenvolvimento científico da área. (YEO *et al.*, 2021; LI, Y. *et al.*, 2021)

No desenvolvimento de novos fármacos é possível contar com o auxílio da quimioinformática com o planejamento racional de novos bioativos, através das ferramentas *in silico* cientistas são capazes de predizer uma determinada atividade biológica analisando vários parâmetros estruturais, das moléculas cuja atividade ainda é desconhecida com base nas estruturas de moléculas cujas atividades já foram testadas. (MONICA *et al.*, 2021; BRIAN, 2021)

Estudos de QSAR e outros métodos computacionais reduzem custos vinculados as pesquisas, e preveem possíveis resultados satisfatórios, contudo, os métodos *in silico* possuem suas margens de erros inerentes dos processos, mas estes podem ser reduzidos através de cuidadosas validações que vão se aprimorando ao longo da aplicabilidade das ferramentas de química computacional. (DING *et al.*, 2021; BHOLE *et al.*, 2021)

A química computacional também trata de informações estruturais visando uma aplicabilidade biológica, segundo teorias da gestão da informação, o aumento da probabilidade de sucesso em um estudo voltado a análise de dados depende diretamente da qualidade da observação e do tratamento desse conjunto de informações. (ANDRIANOV *et al.*, 2021)

Para esta pesquisa foi escolhido derivados de 2-aminotiofeno por se tratar de uma linha de pesquisa bem consolidado, em síntese de produtos químicos orgânicos, desenvolvidos na Universidade Estadual da Paraíba, como os efeitos antivirais são conhecidos para essa classe de compostos, esperou-se apontar efeito anti-HIV.

Para isso, foram realizadas análises ligand-based e structure-based realizando uma triagem virtual hibrida para proposição de bioativos frente a transcriptase reversa do HIV-1.

2. FUNDAMENTAÇÃO TEÓRICA

2.1 HIV – Vírus de Imunodeficiência Adquirida

O HIV é um vírus cujo material genético é o RNA, por isso, é considerado um retrovírus e sua família é a *Retroviridae*, apresenta um longo período de incubação que pode chegar até 20 anos, com isso, seu gênero taxonômico é *Lentivirus.* O HIV é provoca uma doença imunopatológica causadora de uma infecção crônica responsável pela diminuição das células do sistema imunológico, o indivíduo infectado fica susceptível a várias outras doenças, impossibilitando o organismo de combater possíveis ataques de microrganismos invasores, esta infecção dar-se o nome de AIDS (*Acquired Immunodeficiency Syndrome*). (STOLBOV *et al.*, 2020; FERRANTE; RE, 2020; IMAMICHI, H. *et al.*, 2020)

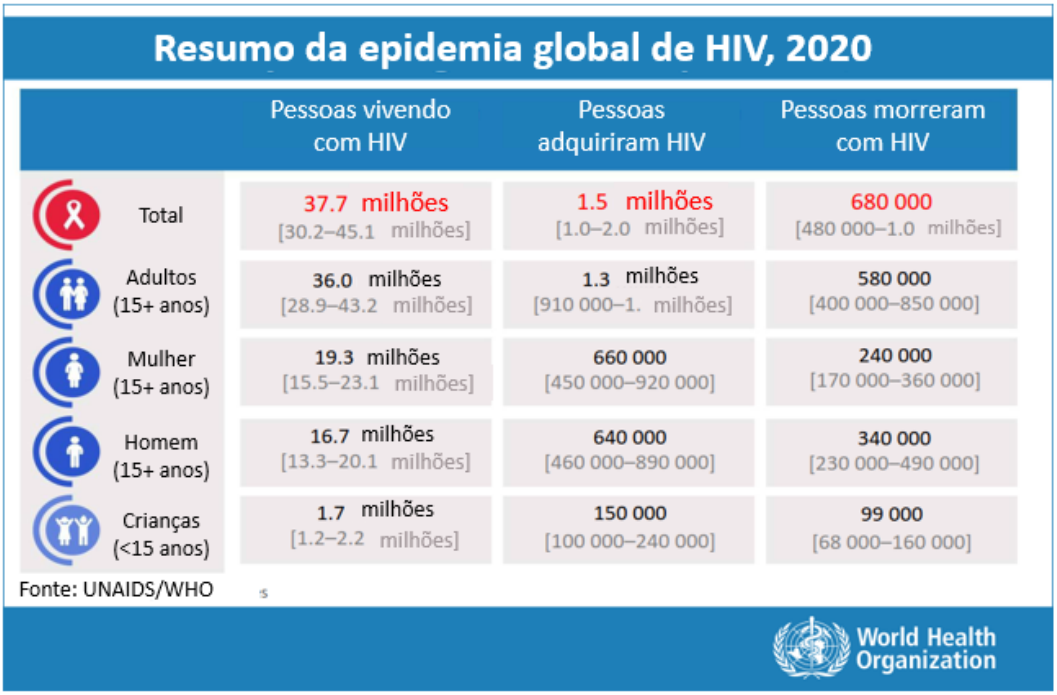

Figura 1. Dados estatísticos do HIV no mundo segundo a WHO.

De acordo com a WHO muitas pessoas vivem com o HIV, segundo dados a população infectada em 2020 foi cerca de 37,7 milhões, dos quais 19,3 milhões foram mulheres, segundo o boletim epidemiológico, houveram 1,5 milhões de

novos casos de infecção no mundo. Em crianças abaixo de 15 anos de idade corresponde a cerca de 1,7 milhões do total com 150mil novos casos no ano passado, conforme mostrado na Figura 1. (GIROIR, 2020;JIANG; ZHOU, Y.; TANG, 2020)

2.2 Morfologia do HIV-1, multiplicação viral e terapias

O HIV é um vírus de 100 a 150 nm de diâmetro que possui RNA como seu material genético cuidadosamente protegido por uma camada de proteínas idênticas chamada de capsídeo, que lembra uma membrana celular normal, motivo pelo qual há dificuldade das células de defesa em reconhecer o HIV como invasor. O invólucro é recoberto por poros eletropositivos que auxiliam na fixação através dos poliânions celulares, cuja composição é estimada em 1.300 proteínas totalizando cerca de 4 milhões de átomos. (ZHAO *et al.*, 2021; DEVANATHAN; KASHUBA, 2021)

Devido ao papel importante e o fato de a pouco tempo a estrutura do capsídeo ter sido desvendada, este passou de um simples envelope para um alvo farmacológico promissor, uma vez que, caso vírus seja impossibilitado de fixar-se à célula hospedeira, a infecção não poderá ser iniciada e, com isso, o capsídeo passou a ser compreendido como alvo farmacológico no combate ao HIV, a partir dos conhecidos inibidores de fusão. (XIAO; CAI; CHEN, B., 2021; VVZHU *et al.*, 2021)

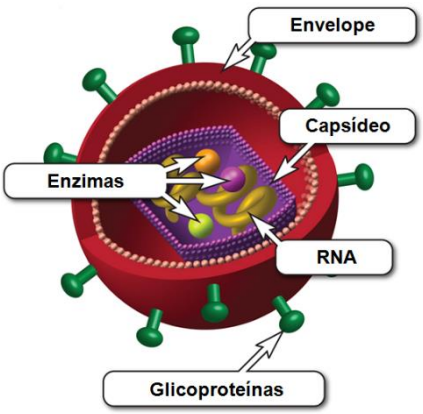

Figura 2. Esquema morfológico simplificado do HIV (Adaptado do AIDSinfo GLOSSARY)

Além do material genético, no meio intraviral também são encontradas enzimas importantes para a multiplicação como a protease (PR), integrase (IN) e a transcriptase reversa (TR), sendo esta última exclusiva em retrovírus como o HIV, essas três proteínas são indispensáveis para a evolução para o quadro infeccioso provocado pelo HIV.

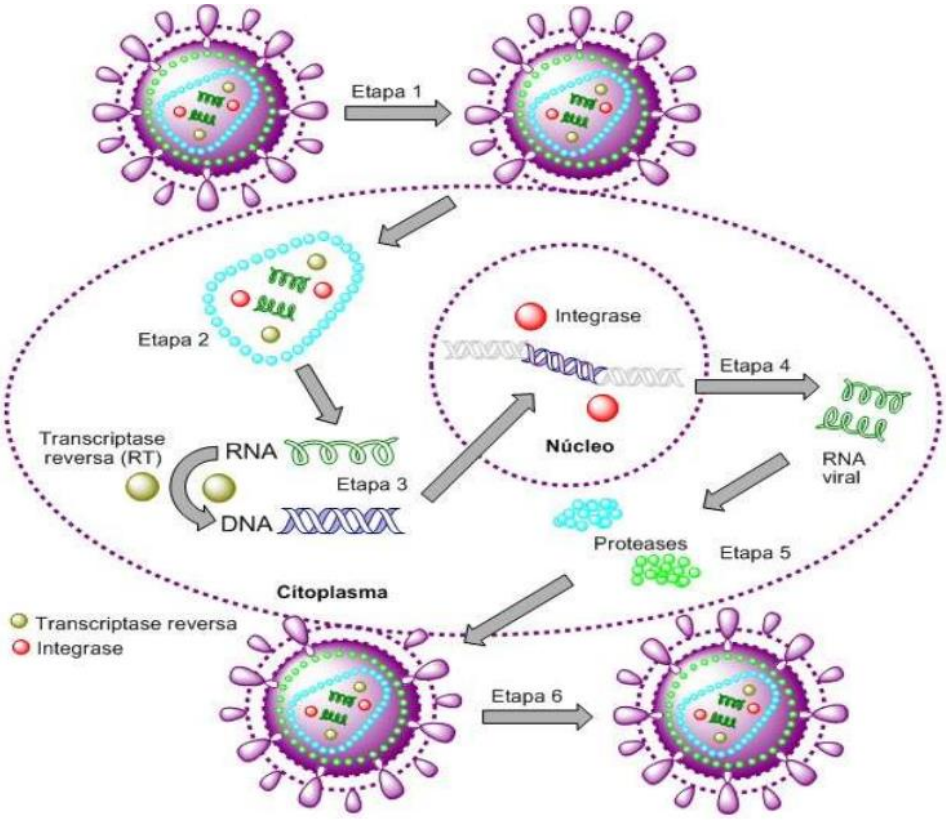

Figura 3. Esquema do ciclo de vida completo do HIV.

A contaminação pelo HIV consiste na fusão da unidade viral com as células normais do sistema imunológico (Figura 3), após isso, o envelope se abre permitindo que o capsídeo passe para o meio intracelular desintegrando-se no citoplasma, assim o material genético viral entra no interior da célula hospedeira. (IYER *et al.*, 2021; SABNIS, 2021)

A transcriptase reversa traduz o RNA viral e com isso biossintetiza o DNA viral, a integrase transporta e funde o DNA viral recém-criado ao DNA celular da célula hospedeira no núcleo celular. Assim, com a ajuda da protease, começa a produção de partículas virais que serão dispersos no citoplasma, formando novos vírus que, ao sair do meio celular, causam a morte da célula hospedeira,

reduzindo a quantidade das células de defesa do organismo, vulnerabilizando o indivíduo infectado, assim, devido a importância no processo de multiplicação viral, essas enzimas são alvos de pesquisavas que buscam o enfrentamento ao HIV. (CILENTO; KIRBY; SARAFIANOS, 2021; FENG, D. *et al.*, 2021)

Hoje o tratamento anti-HIV pode ser dividido em duas classes a PrEP e a PPE, a profilaxia pré-exposição (PrEP) consiste nos procedimentos médicos, farmacológicos ou sanitários que impedem a evolução infecciosa do patógeno que o indivíduo foi exposto, já a profilaxia pós-exposição (PrEP) consiste no tratamento após o início do processo infecioso. (ASSAF *et al.*, 2021)

Com relação ao HIV, a PrEP é gratuitamente oferecida, dando-se prioridade a indivíduos expostos por vulnerabilidade mental, física ou social (abuso sexual, rompimento de preservativo, entre outros). Existem centros médicos espalhados pelo mundo, inclusive em território nacional, em todos os estados que são habilitados e autorizados em administrar a PrEP no combate a disseminação do HIV em até 72h após a exposição. (JUNIOR; CAMOZZATO, 2021)

O tratamento medicamentoso é gratuito oferecido pelo SUS (Sistema Único de Saúde) juntamente com um acompanhamento psicológico que também é oferecido gratuitamente. Cabe salientar que a demanda de pacientes expostos por suas vulnerabilidades vem crescendo ao longo dos anos, facilitado pelo acesso à informação da existência da PrEP, contudo o uso do preservativo é indispensável para a profilaxia assegurada. (JUNIOR; CAMOZZATO, 2021)

Muitos medicamentos usados na terapia retroviral foram lançados, alguns como a estavudina (Figura 4a) e o indinavir (Figura 4b) deixaram de ser distribuídos pela rede pública de saúde devido a seus efeitos toxicológicos acentuados. Em 1990 foi aprovada a droga zidovudina (Figura 4c). (REES, 2021)

(a) (b) (c)

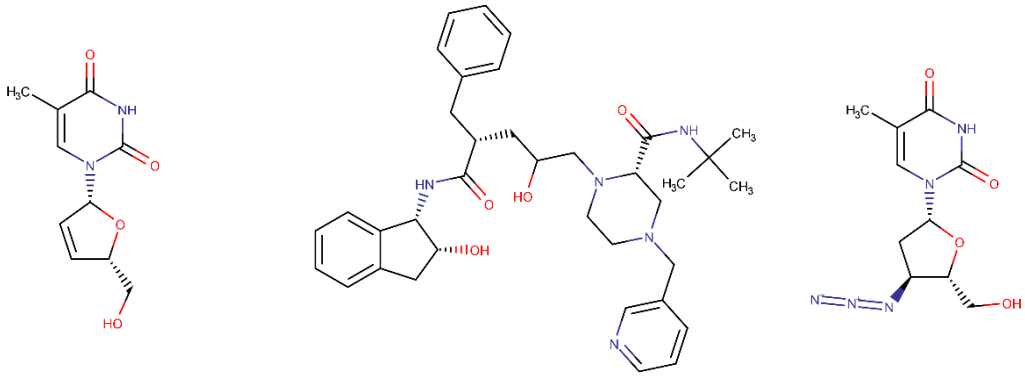

Figura 4. Algumas drogas usadas no tratamento anti-HIV.

Desde 2014 foi aprovada pelo ministério da saúde a dose tripla combinada (Figura 5) pelos medicamentos tenofovir (300mg) + lamivudina (300mg) + efavirez (600mg) de acordo com o protocolo clínico e diretrizes terapêuticas de tratamento de adultos com HIV e AIDS lançado no final de 2013 vigorando a partir de 2014 (SAÚDE, 2013), pois combinados demonstraram eficiência farmacológica frente ao HIV diminuindo a possibilidade de ineficiência do tratamento por mutação e resistência às drogas usadas. (WATERS *et al.*, 2021; TEIRA *et al.*, 2021)

(tenofovir) (lamivudina) (efavirez)

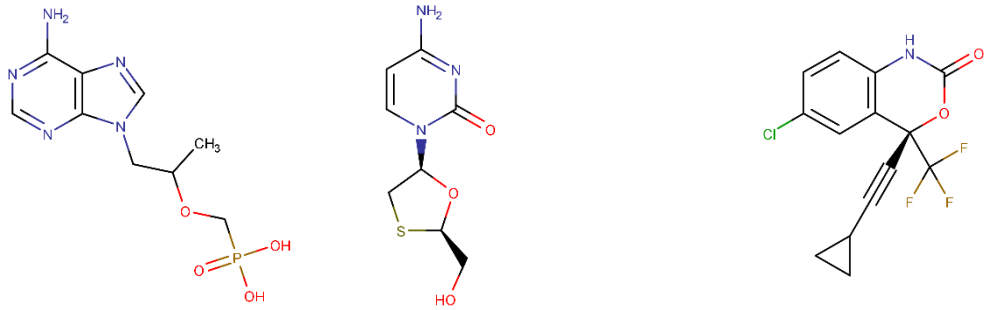

Figura 5. Substâncias da dose tripla combinada anti-HIV.

Existe uma gama de produtos sintéticos sendo produzidos e testados frente as cepas de HIV, contudo, no geral essas substâncias apresentam toxidade considerável no organismo dos pacientes infectados, seja devido à ao próprio bioativo ou de metabólitos secundários no momento do bioprocessamento da substância. Além dos produtos sintéticos, muitos grupos de pesquisas apostam na inserção de produtos naturais (PN), ou seus análogos,

para a proposição de candidatos a fármacos anti-HIV, como exemplo se tem o viridicatol (Figura 6), o qual está presente em vários estudos anti-HIV. (FRANCA RODRIGUES, DA *et al.*, 2018)

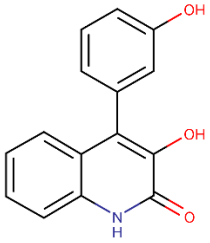

Figura 6. Estrutura 2D do viridicatol.

Em uma recente publicação, de agosto de 2017, Mohammad et al. (SADRAEIAN *et al.*, 2017) supervisionado pelo professor Drº. Francisco Guimarães do Instituto de Física da USP, em parceria com a Universidade de Louisiana, realizaram a extração da substância pulchelina A (Figura 7a) das sementes da planta *Abrus pulchellus tenuiflorus* (Figura 7b) encontrada na caatinga do Nordeste brasileiro, a qual causava a apoptose de cerca de 90% das células virais do HIV, incluindo as em estado latente, sem atingir as células sadias.

(a) (b)

Figura 7. a) A Estrutura 2D da pulchelina A e b) uma foto da semente de *Abrus pulchellus tenuiflorus*

2.3 Derivados 2-amino-tiofenos

Os derivados 2-amino-tiofenos são heterocíclicos do enxofre que possuem o grupamento amina (Figura 8a), podendo seu esqueleto ser

modificado ao longo de sua obtenção de acordo com o design dos reagentes utilizados (SUÁREZ *et al.*, 2021; NARENDER, 2021):

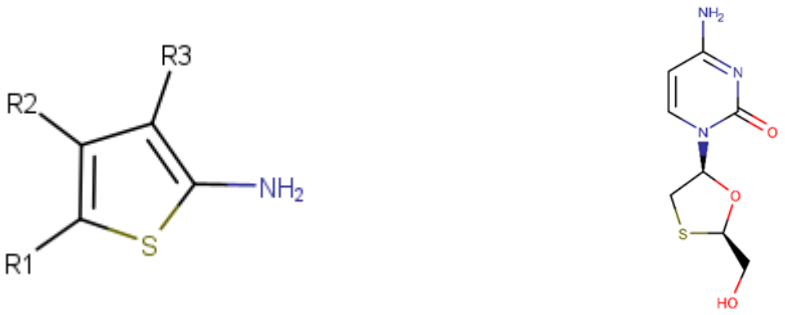

Figura 8. Estruturas 2D a) esqueleto base do 2-amino-tiofeno e b) o fármaco comercial lamivudina para HIV.

Para o tratamento do HIV comumente são encontrados heterocíclicos de cinco membros, como também é possível observar a presença do anel pentacíclico funcionalizado com enxofre em medicamentos de combate a infecção do HIV, como é o caso da lamivudina (Figura 8b). (FRANCA RODRIGUES, DA *et al.*, 2018; NEVES, W. W. *et al.*, 2020)

A versatilidade da reação de Gewald deu origem a várias metodologias de síntese desses compostos, cada variação emprega reagentes diferenciados, é possível destacar quatro variações a serem empregadas nesse projeto. A primeira variação consiste na utilização de α-sulfanilaldeídos ou α-sulfanilcetonas tratadas com acetonitrilas na presença de base orgânica, como mostra a Figura 9 abaixo (LUNA, 2017; ROCHA, [s.d.]):

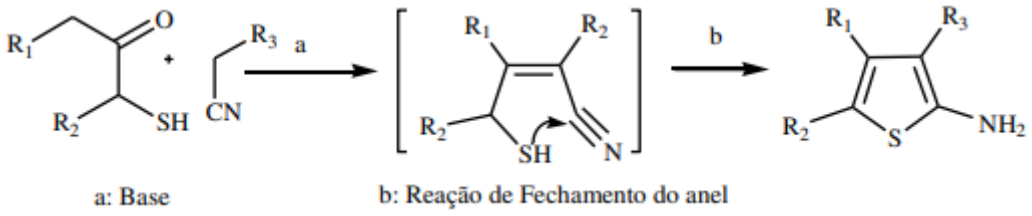

Figura 9. Esquema reacional envolvendo compostos α-sulfanilcarbonados para obtenção dos derivados 2-amino-tiofenos.

A segunda variação da reação de Gewald consiste na reação de um compostos α-metileno carbonilado, acetonitrilas ativada e enxofre, levando até a 95% de rendimentos em alguns casos relatados na literatura, conforme a Figura 10 (LI, J. J., 2021):

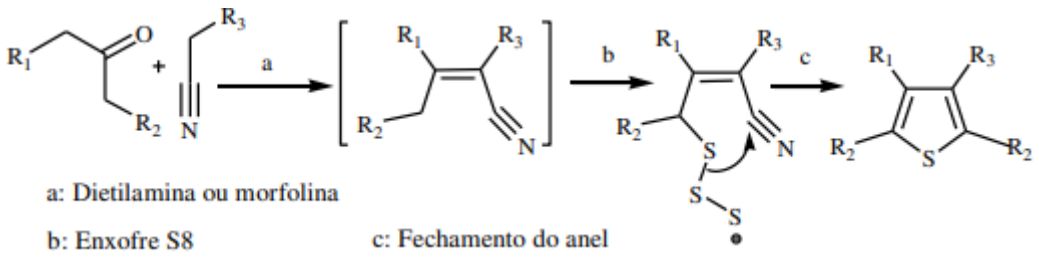

Figura 10. Esquema reacional envolvendo compostos α-metilenos carbonados para obtenção dos derivados tiofenos.

A terceira variação consiste na obtenção de derivados 2-amino-tiofenicos através da condensação de Knoevenagel-Cope, que consiste na reação entre utilizando nitrilas α-β-insaturadas e enxofre conforme mostrada na Figura 11 abaixo (BARI; GHANI; SYED, 2021):

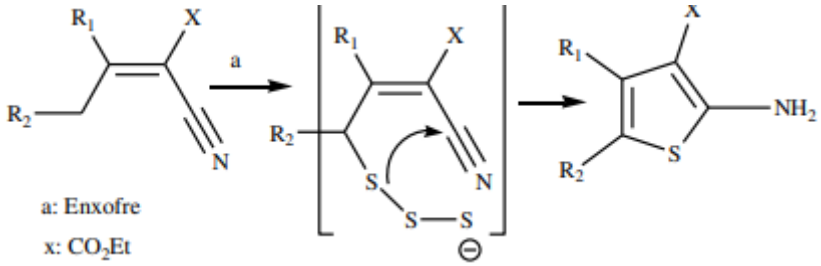

Figura 11. Esquema reacional através da condensação de Knoevenagel-Cope para obtenção dos derivados 2-amino-tiofenos.

Por fim, a quarta variação para obter esses heterocíclicos utiliza-se acetonitrilas com ditiane dióis na presença de base orgânica obtendo derivados 2-amino-tiofenicos, como segue o esquema da Figura 12:

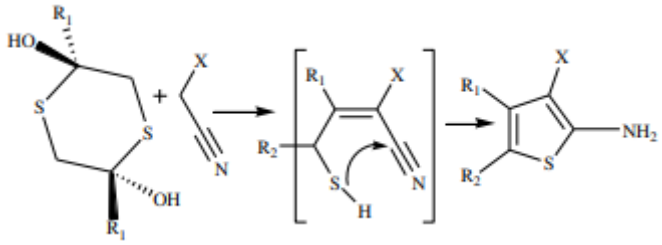

Figura 12. Esquema reacional através da reação de acetonitrilas com ditiane dióis para obtenção dos derivados 2-amino-tiofenos.

2.4 Importância da quimioinformática no desenvolvimento, inovação e tecnologia de medicamentos

A quimioinformática vem crescendo ao longo dos anos, tendo uma contribuição importante nas áreas das ciências farmacêuticas, com ela é possível inclusive planejar de forma racional bioativos para o tratamento de doenças, seja pela criação ou modificação estrutural dos que já existem no mercado. (MALAS *et al.*, 2021)

Atualmente uma das propostas de validação bastante empregadas são as análises em consenso, assim, um estudo utiliza duas ferramentas diferentes para uma mesma análise, diminui o erro inerente de cada método. Programas diferentes possuem algoritmos diferentes e, consequentemente, formas de cálculos diferentes, possuindo variabilidade se comparado com outros softwares. (GUERRERO-ALONSO; ANTUNEZ-MOJICA; MEDINA-FRANCO, 2021)

Os métodos *in silico* ajudaram a químicos sintéticos, químicos de produtos naturais e farmacologistas a diminuírem seus custos com insumos e tempo de trabalho, uma vez que a triagem por uma atividade biológica específica pode ser feita através de ferramentas computacionais, com menos recursos que uma experimentação laboratorial clássica. (SCANDELAI, 2021)

Com as ferramentas modernas é possível, triar, com base em características moleculares convenientes a cada atividade biológica analisar as energias e as interações ligante-receptor em um determinado sítio ativo, verificar a estabilidade e o comportamento dinâmico de um ligante em um determinado receptor realizar análises quimiométricas como PLS, PCA e CPCA e estudos de farmacóforo teórico até propor estruturas com perfil biológico mais promissores. (CHEN, Y. *et al.*, 2021)

A entrada de dados pode ser de um banco de estruturas químicas ou pela leitura de artigos científicos, o mais importante é que todas as estruturas possuam o mesmo tipo de atividade biológica (IC_{50}, EC_{50}, Ki e outros) frente ao mesmo organismo e tipo de teste (organismo, cepa, forma ou proteína isolada).

O cálculo dos descritores moleculares é imprescindível, pois eles serão a identidade estrutural de cada molécula, e juntamente com os dados

classificatórios do *docking* molecular é possível perceber as moléculas que apresentam maiores probabilidades de apresentarem características estruturais promissoras.

Através do aprendizado de máquina é possível interligar cada método ou dados de ferramentas *in silico* na intenção de um determinado estudo, essa proposta diminui ainda mais o tempo de obtenção dos dados e o automático tratamento de dados, como já foi falado é parte fundamental na manipulação de dados. (MONTE; OLIVEIRA ALVIM, DE, 2021)

Comumente essa automação é realizada através do uso de mapas auto-organizáveis, com os quais são possíveis tratar os dados, cruzar resultados, classificar, predizer e obter dados físico-químicos e quimio-farmacológicos de um conjunto de estruturas químicas em um curto espaço de tempo. (SRIVASTAVA; SELVARAJ; SINGH, 2021)

Com os avanços tecnológicos, a criação de novas ferramentas cada vez mais eficientes, a robustez, velocidade de processamento dos computadores mais modernos e a possibilidade de uso de supercomputadores (*clusters*) transformam a quimioinformática em uma boa aliada em estudos químicos e farmacológicos. (KUMAR, R. *et al.*, 2021)

A triagem virtual consiste na classificação de substâncias com base nas características que melhor explicam a atividade biológica a ser observada, estas características servem para nortear análogos com atividade promissora a partir das melhorias realizadas nessas características. Esta abordagem é conhecida como planejamento racional de fármacos, muito usada em pesquisas na área de química de fármacos, contribuindo ainda, para a diminuição do tempo de bancada na síntese de novos bioativos. (SAHIN, 2021)

Incluídos na triagem virtual, ainda é possível considerar a predição dos riscos de toxidade para cada molécula, dos quais, no geral analisa características de fragmentos de cada estrutura bem como o possível metabolismo de cada bioativo analisado, dando a possibilidade de um estudo completo para a proposição de candidatos a fármacos. Sendo, bastante útil para estudos nas áreas das ciências da saúde e química medicinal. (ADZHUBEI *et al.*, 2021; LANGARIZADEH *et al.*, 2021)

O planejamento racional de fármacos surgiu a partir do desenvolvimento da quimioinformática, no qual leva em considerações os resultados *in silico* para buscar novas ideias na área de inovação, aperfeiçoamento e desenvolvimento de novos medicamentos, dando a possibilidade de análise de características químicas, físicas, farmacológicas, farmacodinâmicas, farmacocinéticas e adequadas tecnologias de formulações farmacêuticas. (IMANI *et al.*, 2021)

3. OBJETIVOS

3.1 Objetivo Geral

Realizar a triagem virtual hibrida (baseado no ligante e na estrutura do receptor) de um grupo de 180 moléculas derivadas do 2-aminotiofeno frente a transcriptase reversa do HIV-1, levando em consideração além da predição da atividade biológica, algumas propriedades ADMET.

3.2 Objetivos Específicos

- Elaborar um modelo de predição de atividade anti-HIV no KNIME;
- Elaborar um modelo de predição para a absorção intestinal e permeabilidade intestinal;
- Predizer a taxa de absorção por via oral e os riscos de toxidade baseada na similaridade química de compostos que apresentem toxidade conhecida;
- Predizer os possíveis metabólitos secundários das moléculas com melhor perfil;
- Estimar a toxidade dos metabólitos de maior abundância;
- Selecionar as moléculas mais promissoras;
- Realizar o *docking molecular* e discutir as interações existentes entre as 3 moléculas propostas mais promissoras frente a atividade inibitória para a transcriptase reversa do HIV-1;
- Discutir características estruturais preditas desses compostos para tentar identificar padrões que melhor contribuam para a expressão da atividade anti-HIV.

4. METODOLOGIA

Neste trabalho foi realizado inicialmente uma triagem virtual híbrida que consiste em uma abordagem baseada no ligante juntamente com uma abordagem proteica de forma combinada. Assim foi possível obter as moléculas com melhores perfis farmacológicos *in silico*, analisando assim a biodisponibilidade, a absorção, os riscos de toxidade, a interação ligante-receptor a estabilidade no sítio ativo e a predição de atividade biológica.

A Figura 13 mostra um esquema completo da combinação de várias técnicas *in silico* para a proposição de novas moléculas com base em um estudo de farmacóforo teórico de um banco de dados criado por moléculas disponibilizadas em um banco de dados de estruturas químicas ou em artigos científicos. Este esquema foi norteador para o desenvolvimento desta pesquisa.

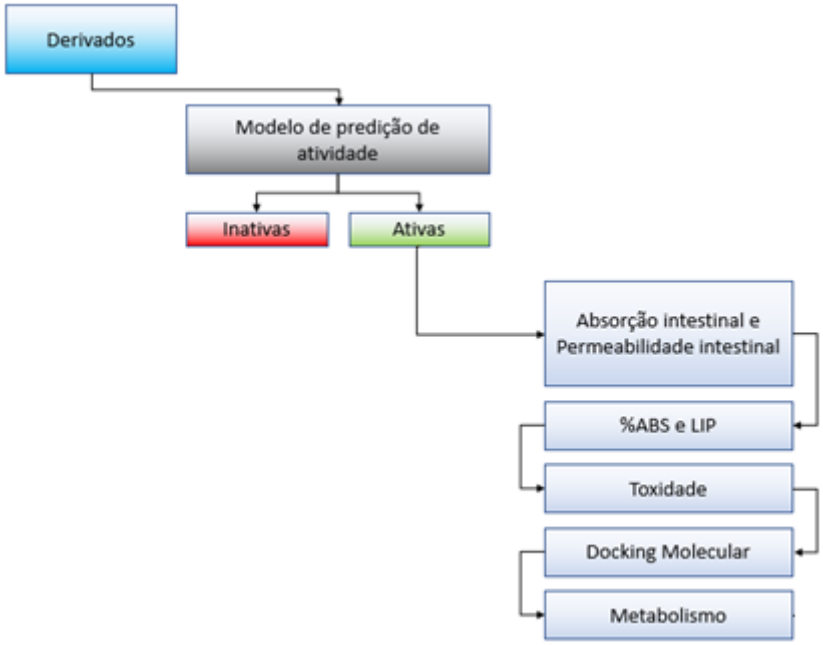

Figura 13. Esquema geral norteador para proposição de análogos promissores neste estudo.

4.1 Fármacos usados como controle

08 moléculas (Tabela 1) foram usadas como controles, estas moléculas correspondem a estruturas químicas de fármacos que são comumente usadas no tratamento anti-HIV.

Tabela 1. Controles usados na pesquisa.

ID	Inibição	Nome	Sigla	%ABS	MUT	CAR	ESR	IRR	TOX
C01	TR	Tenofovir	TDF	58.56	Não	Não	Não	Não	Não
C02	TR	Etravirina	ETR	67.38	Não	Não	Não	Não	Não
C03	TR	Lamivudina	3TC	69.86	Não	Não	Sim	Não	Sim
C04	TR	Zidovudina	AZT	72.83	Sim	Sim	Sim	Não	Sim
C05	TR	Abacavir	ABC	73.85	Não	Não	Não	Não	Não
C06	TR	Didanosina	DDL	78.38	Não	Não	Não	Não	Não
C07	TR	Nevirapina	NVP	88.95	Não	Não	Não	Não	Não
C08	TR	Efavirenz	EFZ	95.78	Não	Sim	Não	Não	Sim

4.2 Conjunto de dados utilizado

A princípio foi construído um conjunto de dados para esta pesquisa a partir das moléculas disponibilizadas gratuitamente no banco de dados de estruturas químicas ChEMBL (https://www.ebi.ac.uk/chembl) sendo usado como palavra-chave "*Human Immunodeficiency Virus 1"* como alvo e "*single protein*" como tipo de alvo. Foram considerados moléculas que apresentaram IC_{50} (nM) como resposta a ação inibitória para protease (ID: CHEMBL243), integrase (ID: CHEMBL3471) e transcriptase reversa (ID: CHEMBL247). Estes conjuntos de dados foram agrupados em uma única planilha utilizando o Microsoft Office Excel 365 apresentando 4.573 bioativos anti-HIV registrados na literatura (disponíveis do ChEMBL).

As 4.573 estruturas 3D dos bioativos selecionadas do banco de dados ChEMBL (https://www.ebi.ac.uk/chembl) foram obtidas a partir de seus receptivos códigos de SMILES através do software Standardizer 18.21.0 da ChemAxon©, agrupadas em um arquivo SDF contendo os dados e coordenadas espaciais de cada estrutura.

Para poder usá-las, as planilhas de um banco de dados de estruturas precisam de um conjunto de tratamentos de dados, este conjunto de procedimentos garantem que em cada linha da planilha esteja preenchida com informações de uma molécula exclusiva com relação às moléculas totais da planilha, este procedimento inicial é conhecido como remoção das duplicadas, e pode ser feito através de vários softwares como *Microsoft Office Excel*, HIT QSAR e outros. Junto com ele outro procedimento também é necessário, a padronização das unidades químicas envolvidas, principalmente de um conjunto de dados referente a mesma propriedade química, assim, o uso de conversões de unidades muitas vezes é empregado em planilhas baixadas *online*.

Em uma planilha com dados para serem usados em quimioinformática a remoção das duplicadas e a padronização das unidades são imprescindíveis para o sucesso das análises *in silico*, ou seja, a qualidade dos dados de saída para cada análise computacional depende da qualidade dos dados de entrada.

As estruturas químicas são a base para qualquer procedimento quimioinformático, a partir dessas estruturas é possível o cálculo de descritores moleculares com base no objetivo de cada estudo, além da padronização das unidades químicas, a padronização das estruturas químicas podem fazer com que um cientista de dados ganhe bastante tempo de análises que possivelmente dariam erradas ou gerariam dados sem qualidades, essa padronização consiste na adição de hidrogênios que faltam na estrutura, a remoção de misturas ou sais, conversão para estrutura em 3D, aromaticidade e muitos outros procedimentos. Nesta pesquisa, os ajustes nas estruturas quando necessários foram feitos com o auxílio do software Standardizer.

4.3 Descritores Moleculares

Os Descritores moleculares correspondem às características estruturais de cada molécula, e podem ser divididos em 5 tipos: descritores híbridos, descritores constitucionais, descritores topológicos, descritores eletrônicos e descritores geométricos. Cada tipo com seus descritores moleculares, e cada um com seu significado particular.

Os descritores são calculados a partir da importação do arquivo de entrada, que geralmente é um arquivo SDF contendo todas as estruturas

químicas a serem analisadas, então o cálculo dos descritores é iniciado. Existem muitos programas para geração de descritores moleculares, dos mais simples aos mais complexos, como exemplo o aplicativo gratuito em Java CDK Descriptor Calculator 4.8 (http://www.rguha.net/code/java/cdkdesc.html) e o software não livre Volsurf+.

Como os descritores são imprescindíveis para a construção de um modelo de predição e que cada software pode calcular alguns descritores diferentes uns dos outros, foram realizados dois modelos preditivos, um com base nos descritores calculados pelo CDK e outro com os descritores calculados pelo Volsurf, assim é possível obter uma predição por consenso, ao cruzar mais de uma predição a confiabilidade aumenta e dá maior robustez a metodologia.

4.4 Modelo de predição de atividade biológica

A predição da atividade biológica foi feita através de um modelo usando o software estatístico KNIME Analytics Platforms 3.6 com ele é possível elaborar um mapa auto organizável integrando diversos nós de dados, que juntos formam o modelo de predição, o fluxo de trabalho usados nesta pesquisa pode ser encontrado disponível online (https://doi.org/10.6084/m9.figshare.7588595).

Este modelo consiste na aplicabilidade de inteligência artificial, aprendizado de máquina, no qual o modelo ensina a máquina a classificar cada estrutura cuja atividade deseja-se predizer, com base em suas características estruturais. Esta comparação na busca de similaridades é feita com base nas moléculas classificadas como ativas no momento da construção do modelo. Uma vez a máquina sabendo as características das moléculas ativas e inativas, por comparação, ela pode classificar moléculas cuja predição de uma determinada atividade biológica não tenha sido relatada na literatura.

Nesta pesquisa foi usado como algoritmo de classificação integrado com o aprendizado de máquina o *Random Forest* (FASHOTO, S. G. *et al.*, 2018, TANEJA, 2018), que consiste em um conjunto de árvores de decisões que analisam moléculas randomicamente, com ele é possível classificar cada molécula através de uma análise de consenso entre as diversas árvores de decisão. Para isso, o banco contendo os bioativos usados para construir o modelo foi particionado em treino (80%) e teste (20%) (FORTI, 2018, VAZ, 2017),

no qual a classificação final é dada pela maioria de ocorrência de uma classificação em cada molécula.

Após particionar o banco de dados (neste caso retirados do ChEMBL), a máquina começa a aprender a classificar cada estrutura através da similaridade com as estruturas inicialmente admitidas como ativas quanto mais similar com moléculas ativas e dentro do domínio de aplicabilidade, maior a probabilidade da estrutura que está tendo a atividade ou propriedade predita ser também ativa.

A similaridade é analisada com base nos descritores moleculares onde os descritores das moléculas do modelo são comparados com os das moléculas cuja atividade é desconhecida. Dividindo-se a tabela das moléculas usadas na construção do modelo, com base no seguinte critério: divide-se o conjunto das moléculas usadas para a construção do modelo ao meio, as moléculas com pIC_{50} ($-\log(IC_{50})$) mais altos são atribuídas a atividade “A” (ativas) e as demais como “I” (inativas), assim a máquina é capaz de classificar qualquer outra estrutura que esteja dentro do domínio de aplicabilidade do modelo.

Estatisticamente para a predição ser aceitável a molécula cuja predição está sendo feita deve estar inserida no domínio de aplicabilidade. Esse domínio garante que as características das moléculas testadas são conhecidas pelo modelo criado. Como o modelo toma como base na comparação por similaridade, o domínio de aplicabilidade garante que a molécula cuja predição está sendo feita apresenta características estruturais representadas no espaço químico das moléculas usadas na construção do modelo, quando as moléculas testadas e as moléculas do modelo estão no mesmo espaço químico, aumenta-se a confiabilidade da predição, quanto maior a porcentagem da aplicabilidade mais confiável é a predição para a molécula analisada.

Para a predição da atividade foi utilizado o *Weka Predictor 3.7* para realizar a classificação das moléculas cuja atividade anti-HIV não é conhecida. Agregando-se o aprendizado de máquina do RF e a classificação da WPRED, o mapa auto organizável criado na *workflows* do KNIME vem ganhando as atenções de muitos pesquisadores na área de quimioinformática pela sua eficiência na predição e facilidade de configuração.

A tabela de confusão informa os valores de verdadeiro positivo, verdadeiro negativo, falso positivo e falso negativo conforme a Figura 14. Para avaliar a confiabilidade do modelo serão considerados, com base na tabela de confusão gerada pelo modelo, a acurácia acima de 75% e o coeficiente de correlação de Matthews acima de 60%, estes são parâmetros estatísticos que garantem a qualidade das predições realizadas. Outros parâmetros também serão analisados na discussão dos dados e da eficiência preditiva do modelo, que são: as curvas ROC do teste e da validação interna e o domínio de aplicabilidade.

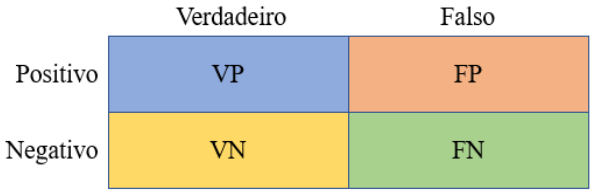

Figura 14. Esquema da tabela confusão de um modelo de predição.

Além da atividade biológica tomando como base o IC_{50} de moléculas com atividade anti-HIV conhecidas, ainda foram criados modelos para a predição da solubilidade e absorção intestinal com planilhas fornecidas pelo admetSAR @ LMMD (http://lmmd.ecust.edu.cn/admetsar1/download) gentilmente fornecidas pelo pesquisador Dr. Feixiong Cheng, nas três predições realizadas nesta pesquisa foi usado o mesmo fluxo de trabalho, variando apenas as tabelas para a construção dos modelos.

4.5 Violações a regra de Lipinski e %ABS

Para estimar as violações a regra de Lipinski foi usado o programa gratuito DruLiTo (http://www.niper.gov.in/pi_dev_tools/DruLiToWeb/DruLiTo_index.html), no qual as moléculas são importadas e dados como massa, Log*P*, aceptores e doadores de ligações de hidrogênio, TPSA, número total de átomos e outras características estruturais podem também ser calculadas simultaneamente.

A grande maioria dos fármacos retrovirais usados no tratamento anti-HIV apresentam-se na forma de comprimidos ou cápsulas, sendo administrados facilmente por via oral a pacientes contaminados, sendo assim, é possível calcular a taxa de absorção de bioativos baseados em sua área de superfície topológica total através da equação:

%ABS=109-(TPSAx0.345) (AHSAN *et al.*, 2016; GONZALEZ *et al.*, 2018; TUNCBILEK *et al.*, 2018)

Ao utilizar a taxa de absorção como parâmetro de exclusão na triagem virtual, apenas são consideradas as moléculas que apresentam %ABS igual ou superior à menor taxa dentre os fármacos usados como controle.

4.6 Predição dos riscos de toxidade

As moléculas foram importadas para o software gratuito OSIRIS DataWarrior 5.0 (http://www.openmolecules.org/datawarrior), neste programa os riscos de toxidade foram preditos pela comparação entre um banco de dados interno, no qual o programa busca fragmentos conhecidos nas moléculas analisadas, esses fragmentos quando encontrados geram um alerta de toxidade em quatro parâmetros: mutagenicidade, carcinogenicidade, efeito no sistema reprodutor e irritabilidade na pele. À toxidade total é atribuída o valor “Não” quando uma molécula não apresenta alertas para nenhum dos quatro parâmetros analisado pelo OSIRIS.

Analisando os riscos de toxidade como parâmetro de seleção de moléculas, o critério adotado foi não apresentar nenhum risco de toxidade em nenhum dos parâmetros já mencionados, assim, diminui-se a probabilidade de a molécula apresentar efeito tóxico.

4.7 Ancoragem ligante-receptor – *Docking Molecular*

Para a ancoragem das moléculas foi usado, nesta pesquisa, o software não livre Molegro Virtual Docker 6.0 no qual as moléculas são importadas juntamente com a proteína baixada no site *Protein Data Bank* (www.rcsb.org) (BERMAN *et al.*, 2000), os *templates* foram criados baseados nos inibidores complexados juntos às proteínas estudadas.

Na interpretação dos resultados do docking além das energias é possível analisar os tipos de interações, que no Molegro são três: hidrogênio (linhas tracejadas azuis), eletrostáticas (linhas tracejadas verdes) e estéricas (linhas tracejadas vermelhas). Ainda mais, é possível ver os resíduos de aminoácidos envolvidos em cada interação entre os ligantes e os respectivos receptores, com

isso, tenta-se identificar possíveis resíduos comuns entre os análogos e os controles e/ou inibidores complexados juntos a cada proteína na busca de relacionar a importância dessas interações para a atividade biológica.

4.8 Estudos *in silico* de metabolismo

Para realizar um estudo metabólico através de métodos computacionais, nesta pesquisa, foi utilizado o software não livre METASITE 6.0 da Molecular Discovery, este prediz as possíveis transformações sofridas por um conjunto de moléculas em um ou mais citocromos em alguns regiões específicas do corpo como pele, cérebro, fígado e outros. Cada citocromo, que é de constituição proteica, é responsável em transformar, através de reações químicas, as substâncias ingeridas, para promover sua eliminação através da polarização da estrutura.

Uma vez estimados pelo software as estruturas químicas 3D dos metabólitos secundários provenientes do metabolismo no fígado, cérebro e/ou pele, nesta pesquisa foram consideradas apenas as transformações no fígado, e os metabólitos secundários gerados foram submetidos a um modelo de predição de atividade biológica e seus riscos de toxidade, comparados com as suas respectivas abundâncias metabólicas.

Cada metabólito secundário teve seus riscos de toxidade preditos, através do OSIRIS, pois os bioativos que apresentavam parâmetros citotóxicos como alta mutagenicidade e/ou alta carcinogenicidade em seus metabólitos com abundância acima de 75% era desconsiderado para a seleção dos análogos de melhor perfil. Compreende-se para esta pesquisa que um candidato a fármaco deve apresentar baixa ou nula toxidade como também seus metabólitos mais abundantes.

5. RESULTADOS E DISCUSSÃO

5.1 Modelos de predição anti-HIV, HIA e CACO-2

Inicialmente 180 tiofenos foram submetidos a 4 modelo de predição de atividade anti-HIV, um modelo utilizando os descritores moleculares do Dragon 5, do CDK, do RDKIT e do Volsurf frente a enzima transcriptase reversa, pois trata-se de uma enzima específica dos retrovírus, assim serão apresentados os dados separadamente e depois o consenso entre os quatro modelos.

Com relação ao modelo utilizando-se os descritores Dragon, quatro moléculas apresentaram possível atividade com probabilidades ALX026 com 50,46%, ALX038 com 51,12%, ALX118 com 52.81% e ALX175 com 51,92% com domínio de similaridade confiável:

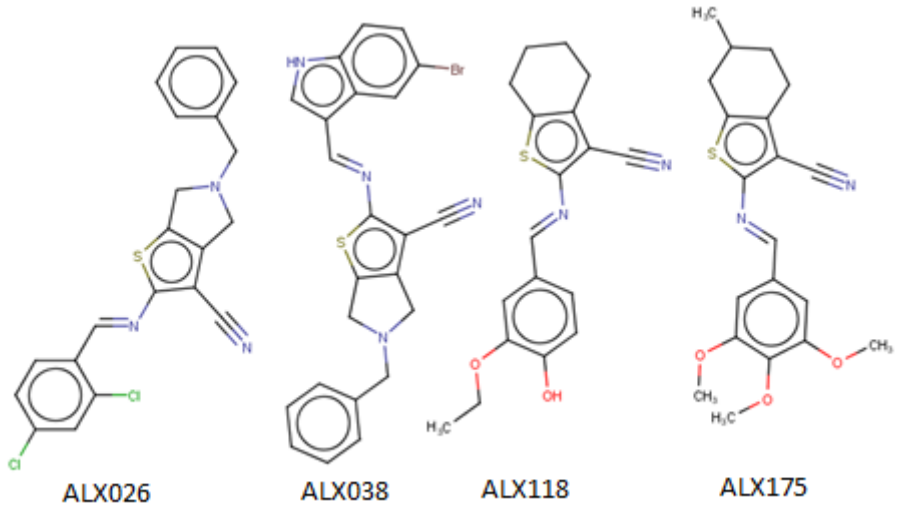

Figura 15. Estruturas químicas 2D dos compostos aprovados pelo modelo anti-HIV usando descritores Dragon.

De acordo com o resultado da predição do modelo utilizando descritores do Dragon, é possível perceber que as cinco moléculas aprovadas possuíram o anel tiofeno conjugado a um anel de cinco membros, com substituição do hidrogênio da amina cíclica por grupos benzoicos (ALX026 e ALX038), outra característica molecular observada nessas estruturas é a presença de grupos aromáticos policíclicos (indólicos), como podem ser observados na estrutura ALX038.

Tabela 2. Dados estatísticos do modelo de predição anti-HIV usando Dragon.

	Teste	Validação interna
Precisão	0.82	0.76
Sensibilidade	0.80	0.80
Especificidade	0.82	0.77
MCC	0.63	0.58
Acurácia	0.81	0.78
Curva ROC	87.61%	84.87%

Analisando a confiabilidade do modelo com base na sua estatística, apresentada na Tabela 2, é possível perceber que o modelo apresentou 80% de sensibilidade, que corresponde a capacidade de classificar como ativo a molécula que realmente pode ser ativa (verdadeiro positivo). Além da sensibilidade podemos apontar a acurácia do modelo que vai de 78% a 81% significando um bom acerto total nas predições, assim como também o coeficiente de correlação de Matthews (MCC) que diz respeito a avaliação global do modelo variando de 0.58 a 0.63.

Uma vez demostrada através da estatística do modelo a confiabilidade e a boa capacidade preditiva do modelo de predição de atividade biológica frente a enzima transcriptase reversa do HIV-1 utilizando os descritores Dragon, será apresentado os dados de predição para a mesma proteína, porém utilizando descritores CDK é possível perceber que apenas a molécula ALX175 foi aprovada com 50.66% de provável atividade anti-HIV.

Tabela 3. Dados estatísticos do modelo de predição anti-HIV usando CDK.

ALX175

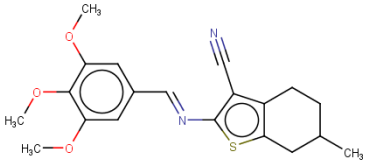

	Teste	Validação interna
Precisão	0.81	0.76
Sensibilidade	0.81	0.81
Especificidade	0.81	0.77
MCC	0.62	0.58
Acurácia	0.81	0.79
Curva ROC	87.91%	85.41%

Corroborando com a discussão do modelo anterior, o modelo utilizando descritores CDK também apresenta boa sensibilidade (81%) e especificidade (0.77% a 81%), assim como bons resultados de MCC como é visto para o grupo de teste 0.62 e para a validação interna cruzada 0.58.

A molécula ALX175 possui um substituinte 3,4,5-trimetroxibenzílico formando dupla ligação com a amina alifática do anel tiofeno, que por sua vez está conjugado a um anel hexaciclico não aromático, esses grupos trimetoxilados já são conhecidos na literatura pela sua atividade biológica, principalmente antitumoral, antimicrobiana e antiviral.

Para a transcriptase reversa foi feito um modelo de predição da atividade retroviral para o HIV-1 utilizando descritores do pacote RDKIT no KNIME conforme descrito na metodologia, de acordo com a predição 32 moléculas apresentaram probabilidade de atividade, a figura abaixo mostra as estruturas química 2D desses compostos, bem como as respectivas probabilidades de possível atividade:

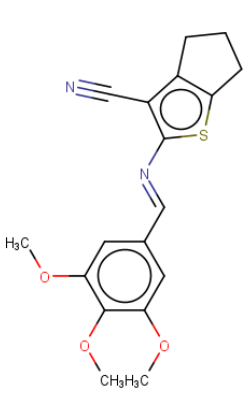

ALX008 - 55.85%

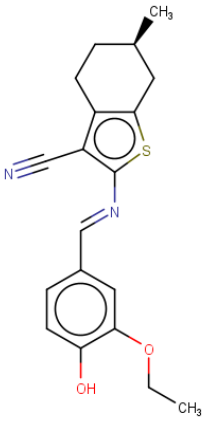

ALX011- 56.77%

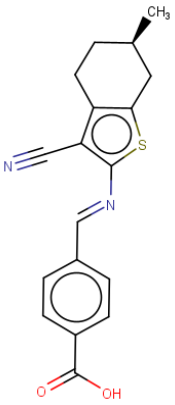

ALX012 - 54.22%

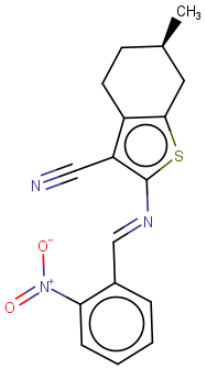

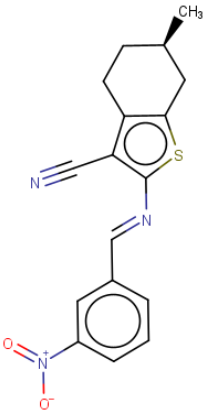

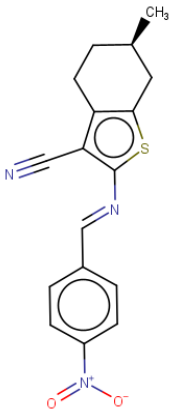

ALX014 -55.57%	ALX015 -58.26%	ALX016 -57.76%
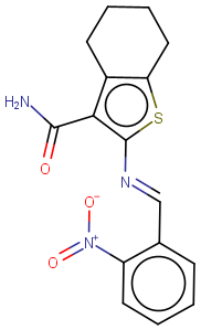	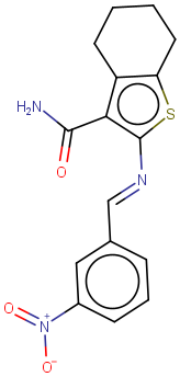	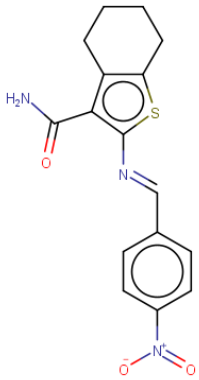
ALX064 -57.43%	**ALX066 -56.63%**	**ALX067 -56.43%**
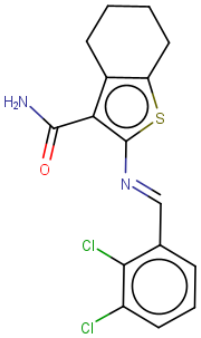	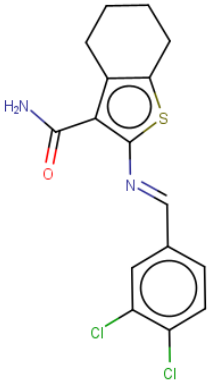	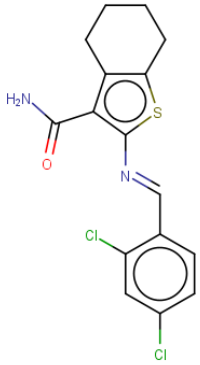
ALX071 -52.61%	**ALX072 -52.39%**	**ALX073 -52.09%**
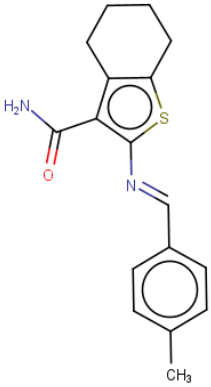	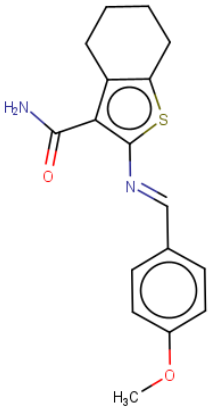	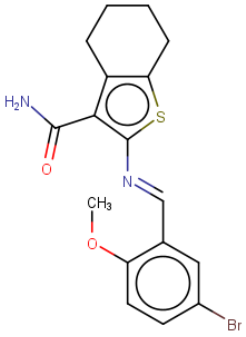
ALX074 -56.53%	**ALX075 -60.59%**	**ALX078 -56.27%**

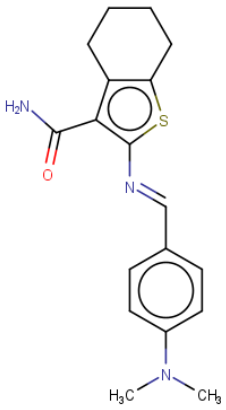

ALX081 -52.53%

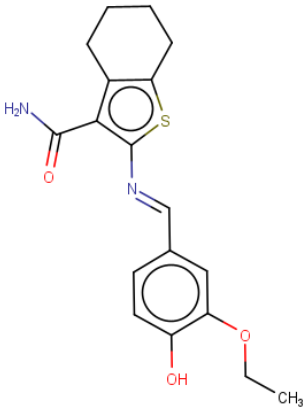

ALX082 -55.25%

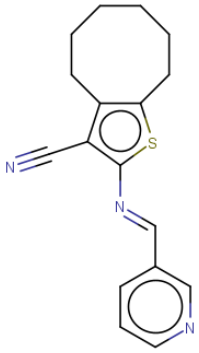

ALX084 -54.53%

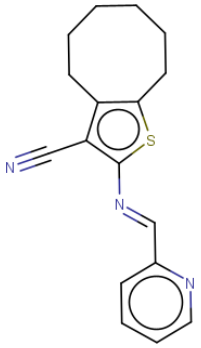

ALX085 -54.78%

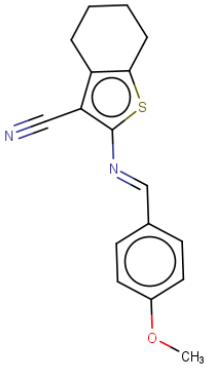

ALX113 -50.12%

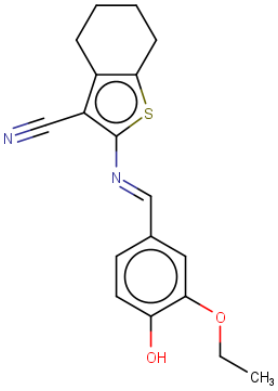

ALX118 -58.80%

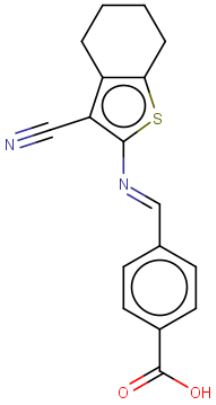

ALX122 -58.46%

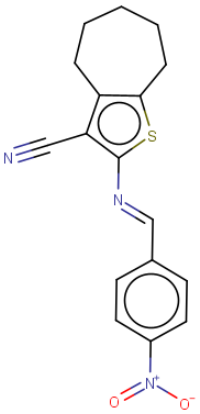

ALX132 -55.94%

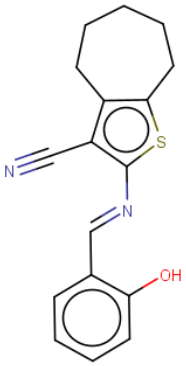

ALX135 -52.30%

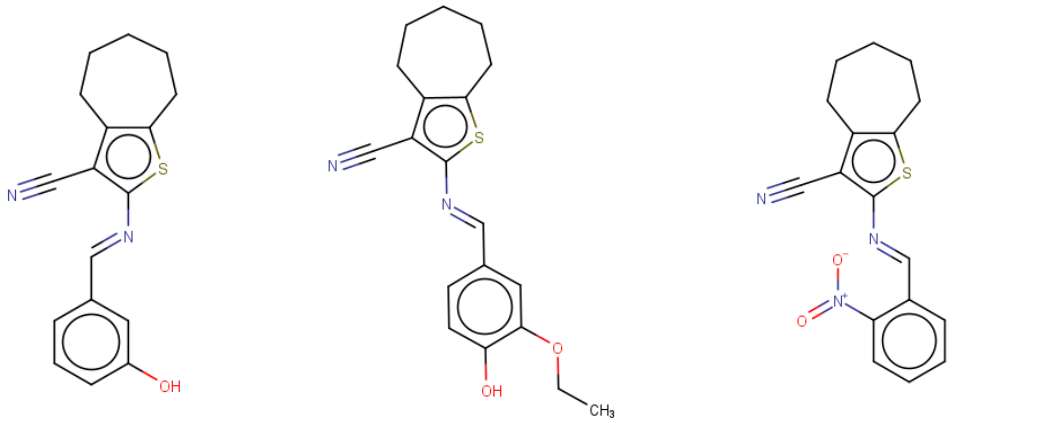

ALX136 -51.93%	ALX138 -59.72%	ALX139 -58.23%

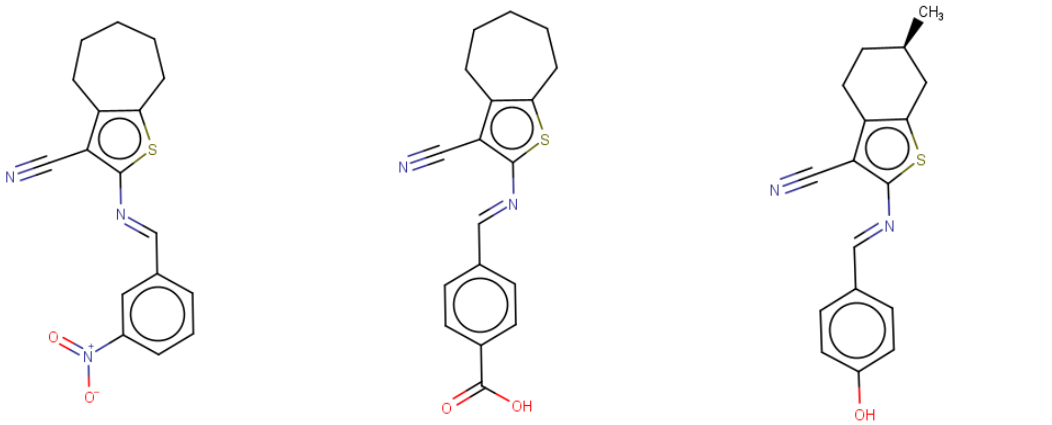

ALX140 -55.94%	ALX142 -52.54%	ALX176 -51.43%

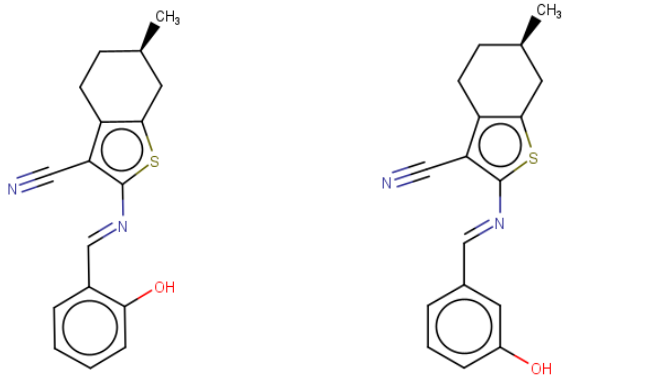

ALX178 -51.01%	ALX179 -51.43%

Figura 16. Estruturas químicas 2D dos compostos aprovados pelo modelo anti-HIV usando descritores CDK.

De acordo com a figura anterior, a molécula com a menor probabilidade de possível atividade foi a ALX113 com 50,12%, esta estrutura apresenta o anel tiofeno condensado a ciclohexano, com uma nitrila, sua amina alifática forma

dupla ligação com o p-metoxi-benzíla, um substituinte que sofre efeito indutivo com contribuição de ressonância que vai do substituinte dessa amina até o núcleo tiofeno. Em contra partida, a molécula com maior probabilidade foi ALX075 com estrutura bem semelhante à de menor probabilidade, contudo esta molécula não apresenta a nitrila, mas sim a C-C formamida, conferindo melhor deslocamento eletrônico e consequentemente melhor estabilização do efeito indutivo criado pelo substituinte da amina.

Após as discussões acerca dos resultados do modelo utilizando descritores RDKIT, é conveniente discutir os dados estatísticos que comprovaram a confiabilidade das predições apresentadas, conforme mostrado na tabela abaixo:

Tabela 4. Dados estatísticos do modelo de predição anti-HIV usando RDKIT.

	Teste	Validação interna
Precisão	0.78	0.72
Sensibilidade	0.79	0.79
Especificidade	0.78	0.72
MCC	0.57	0.51
Acurácia	0.78	0.75

É possível considerar o modelo criado na predição anterior devido os dados apresentados na tabela acima, o modelo apresenta boa capacidade preditiva com relação aos verdadeiros ativos (sensibilidade, 79%) e para os verdadeiros negativos (especificidade, 72-78%), assim como o acerto total (acurácia, 75-78%) e MCC 0.57 para o grupo de teste e 0.51 para a validação interna cruzada, outro dado importante corresponde a curva ROC do modelo, conforme mostrado na Figura abaixo:

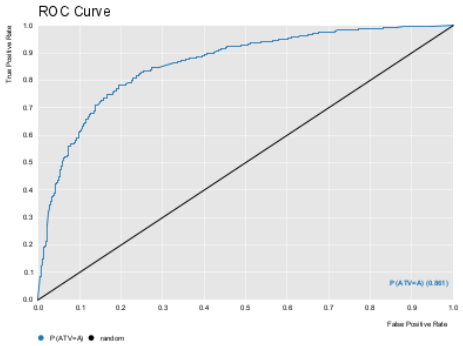

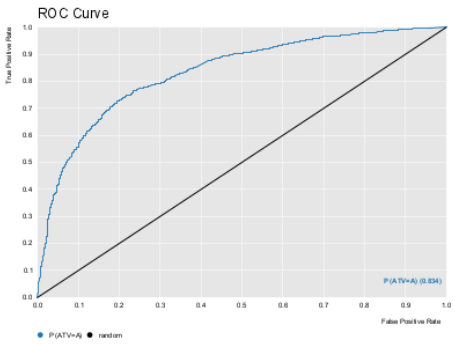

Teste: 86,1%	Validação cruzada: 83,1%

Figura 17. Curva ROC do modelo anti-HIV RDKIT.

Na Figura 17, mostra que a predição está acima da região dos dados aleatórios, segundo o gráfico ROC apresentado, o modelo apresentou boa performance preditiva com, sendo os resultados apresentados neste estudo confiáveis.

Por fim, o quarto modelo gerado foi utilizando os descritores Volsurf que apresentou 87 compostos com probabilidade de atividade que variou de 50,02-79,03%, dois quais 32 já foram apresentados na figura anterior: ALX008, ALX011, ALX012, ALX014, ALX015, ALX016, ALX064, ALX066, ALX067, ALX071, ALX072, ALX073, ALX074, ALX075, ALX078, ALX081, ALX082, ALX084, ALX085, ALX113, ALX118, ALX122, ALX132, ALX135, ALX136, ALX138, ALX139, ALX140, ALX142, ALX176, ALX178, ALX179. Assim seguem descriminados os derivados 2-aminotiofenos que apresentaram probabilidade de possível atividade retroviral para HIV-1 os 55 compostos restantes:

Tabela 5. Estruturas químicas 2D dos compostos aprovados pelo modelo anti-HIV usando descritores Volsurf.

ID	Molécula	%ATIVIDADE
ALX001	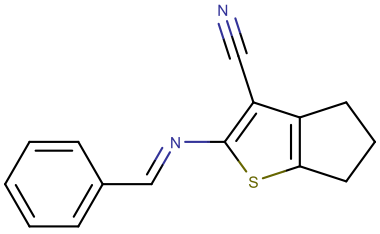	50.68

ALX004	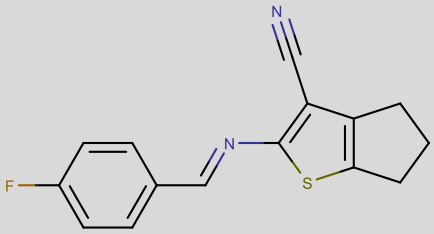	62.91
ALX009	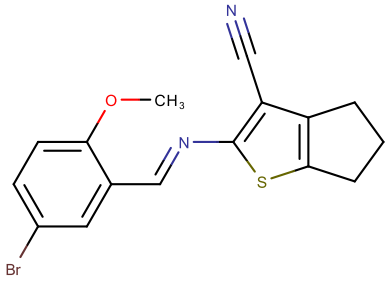	59.88
ALX010	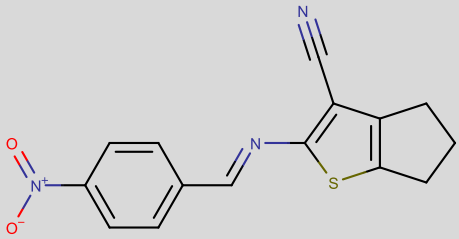	56.30
ALX013	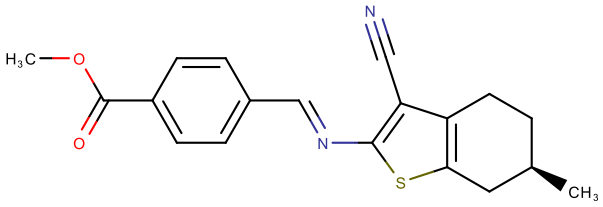	57.05
ALX019	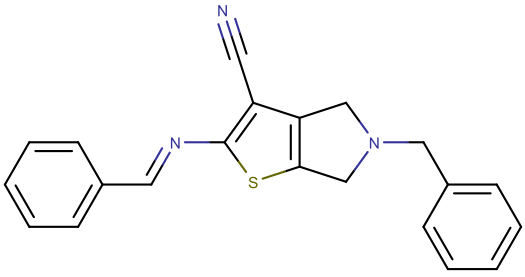	64.93
ALX020	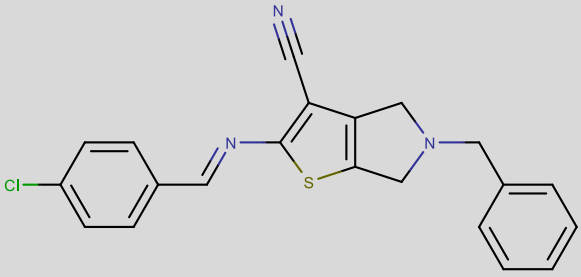	60.49

ALX021	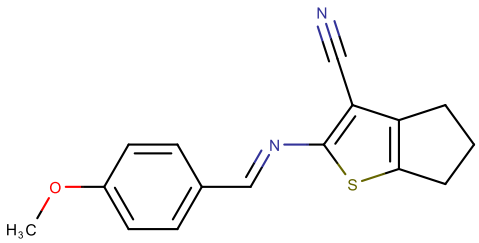	63.27
ALX022	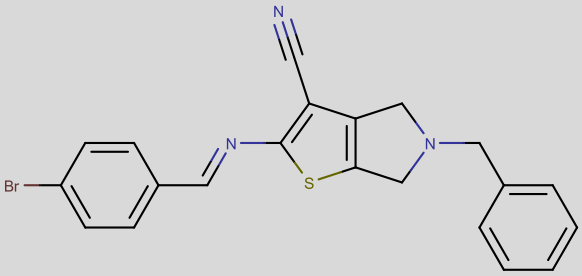	61.23
ALX023	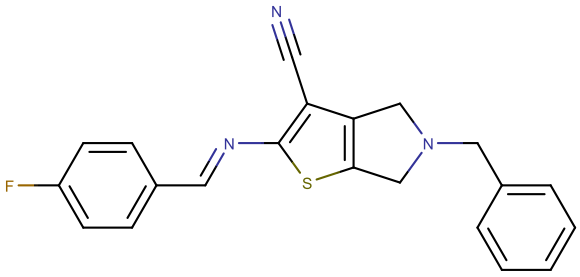	60.15
ALX024	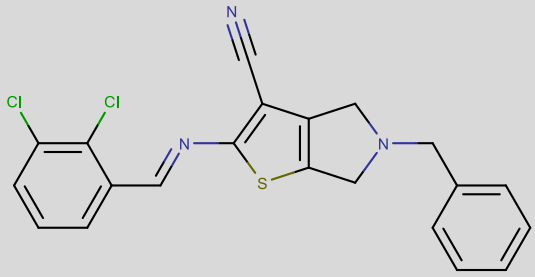	70.25
ALX025	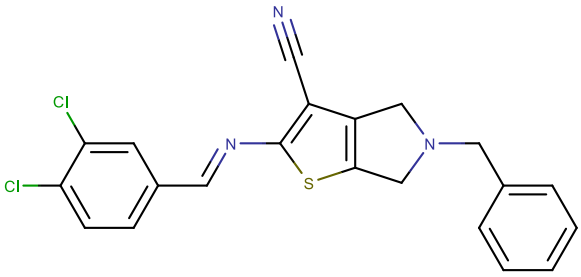	72.21
ALX026	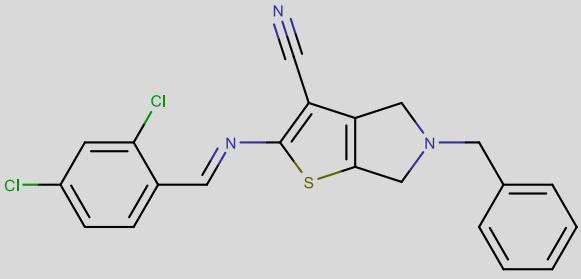	74.63

ALX027	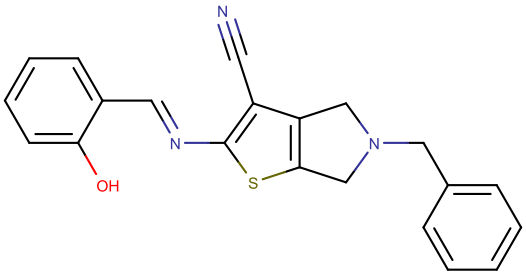	59.27
ALX028	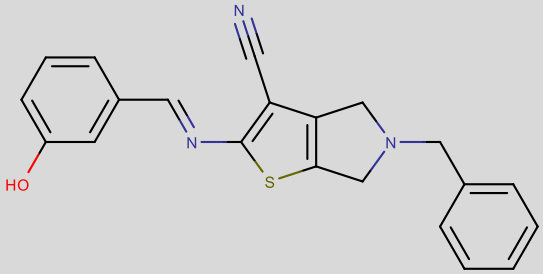	50.54
ALX029	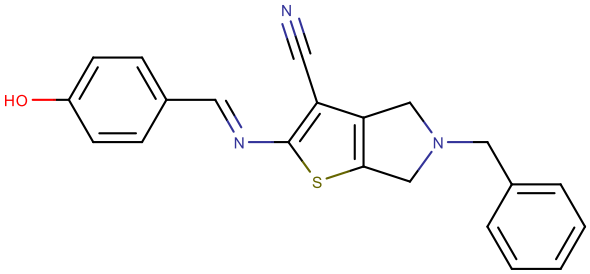	55.77
ALX030	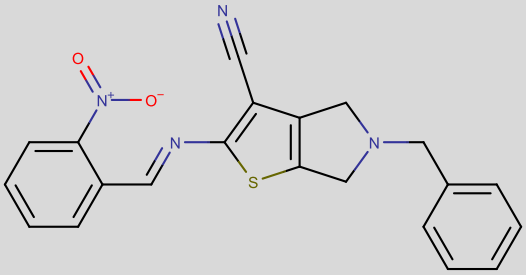	56.83
ALX031	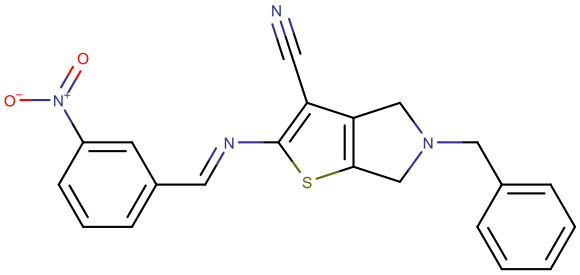	56.35
ALX033	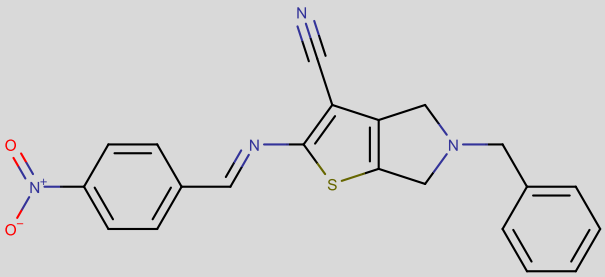	53.71

ALX035	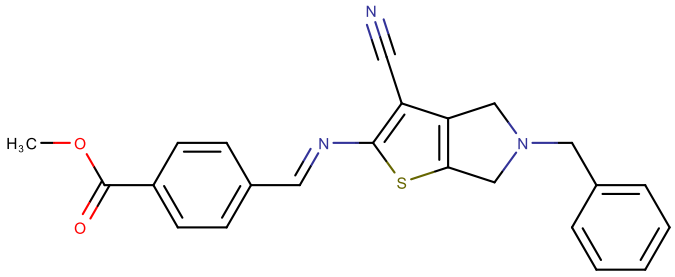	59.87
ALX036	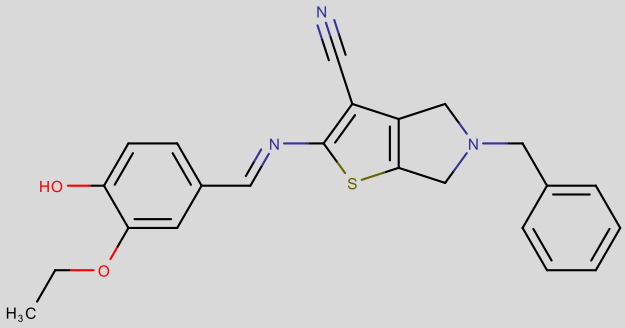	59.76
ALX037	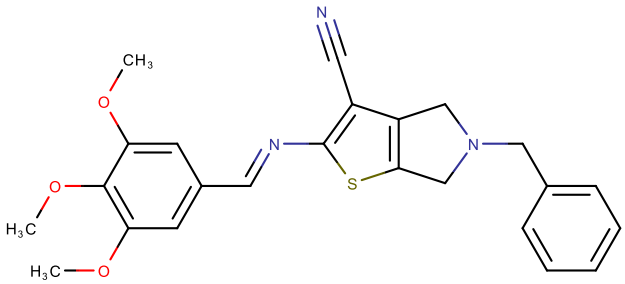	55.54
ALX038	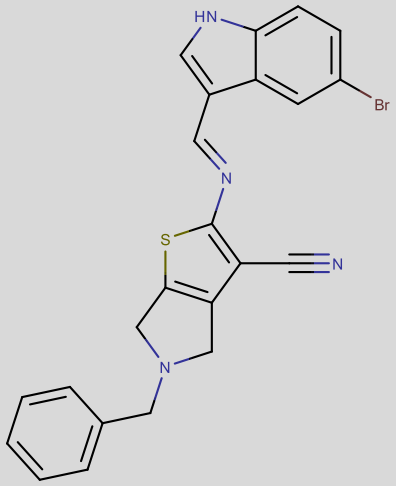	79.03
ALX039	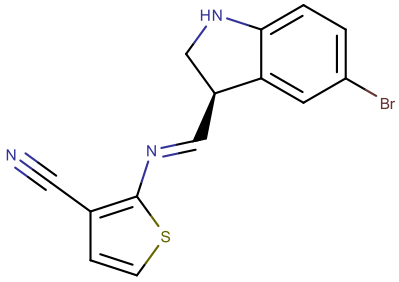	60.46

ALX051	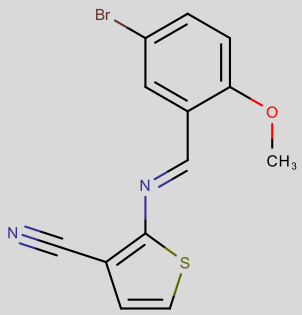	55.72
ALX052	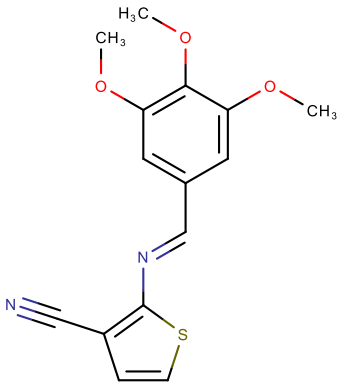	58.69
ALX053	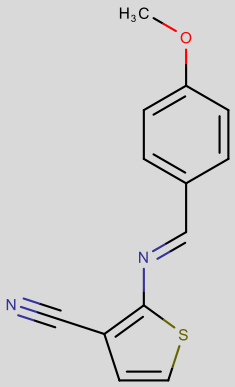	53.77
ALX056	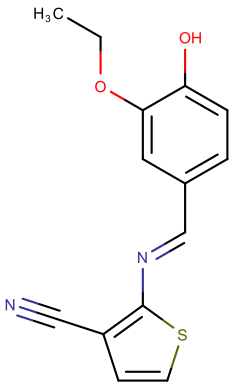	50.99

ALX059	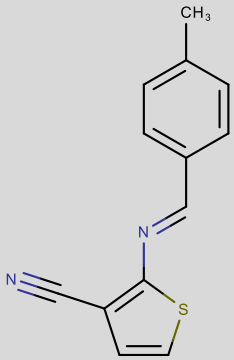	50.98
ALX070	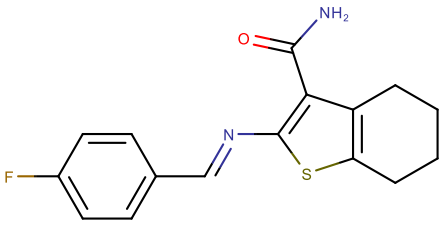	50.02
ALX076	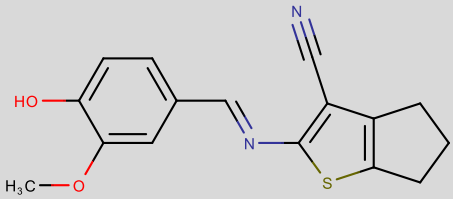	54.18
ALX083	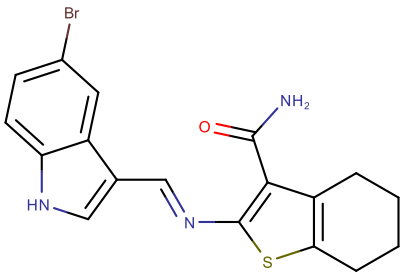	54.97
ALX087	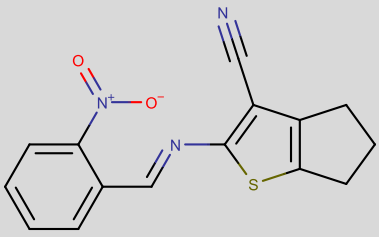	53.46
ALX089	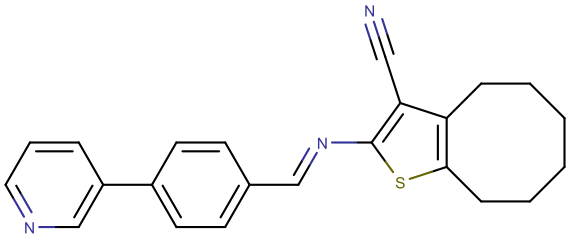	56.10

ALX092	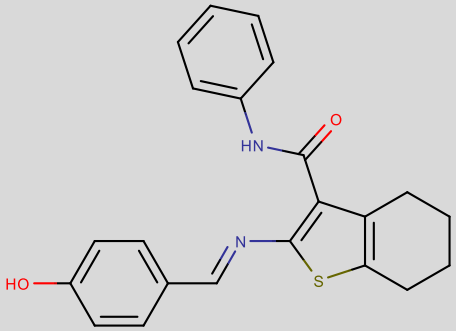	51.33
ALX097	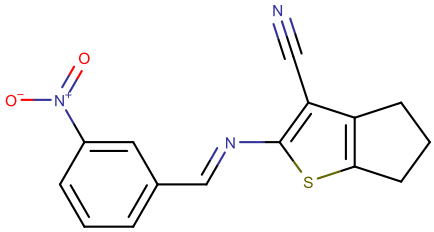	54.08
ALX101	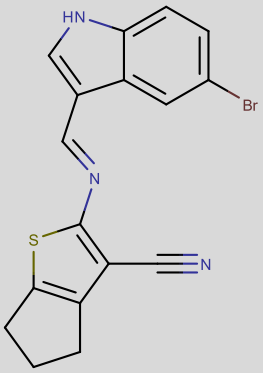	51.51
ALX106	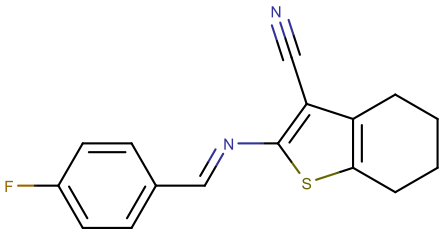	57.55
ALX110	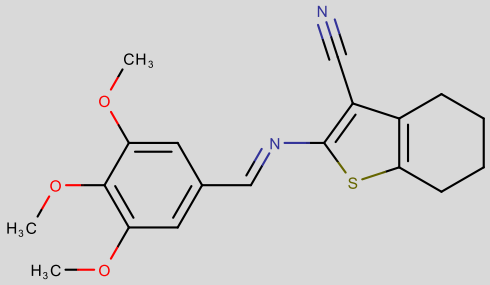	57.40
ALX112	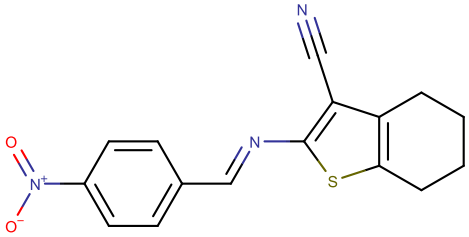	54.79

ALX119	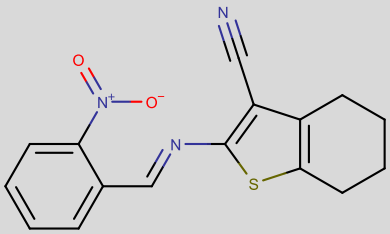	50.92
ALX120	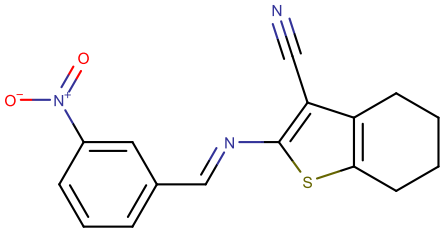	54.63
ALX121	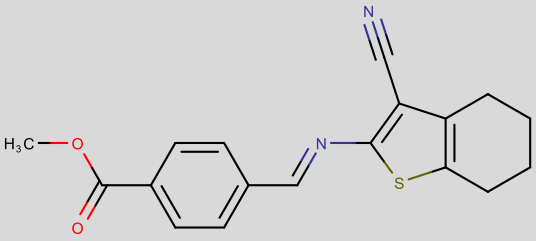	58.25
ALX126	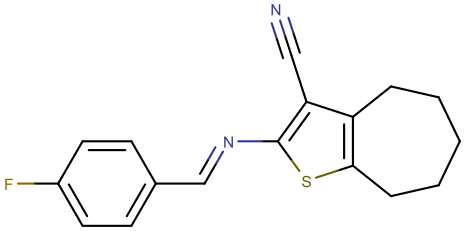	60.49
ALX130	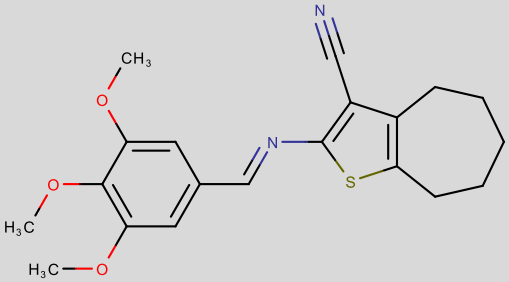	58.79
ALX133	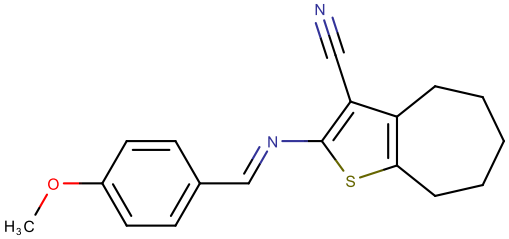	62.26
ALX137	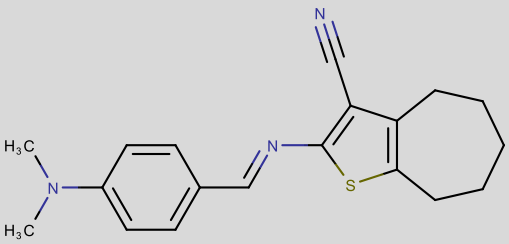	52.08

ALX141	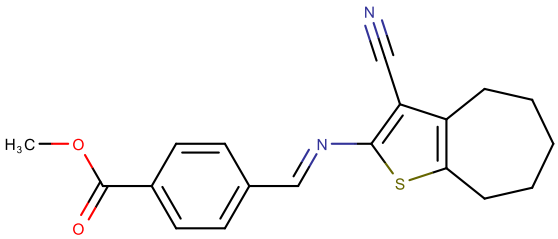	55.47
ALX152	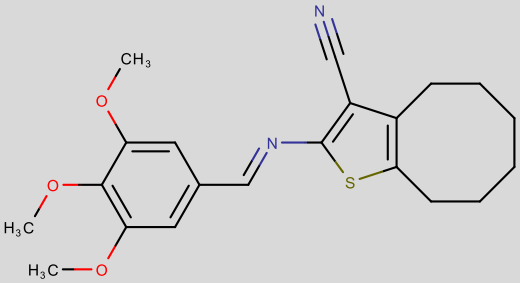	54.45
ALX156	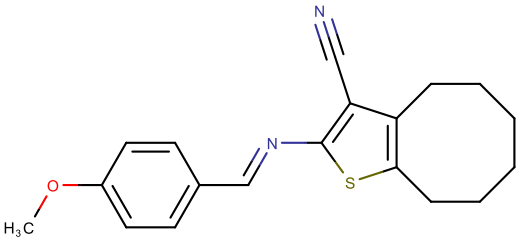	50.34
ALX158	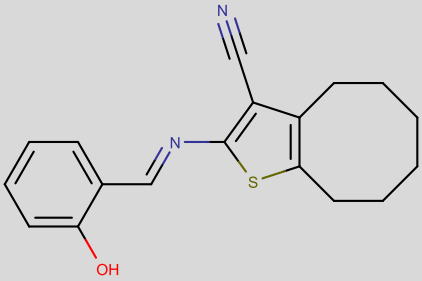	51.61
ALX159	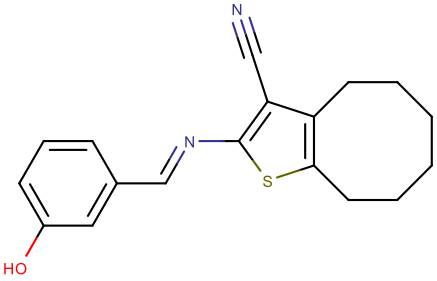	50.78
ALX161	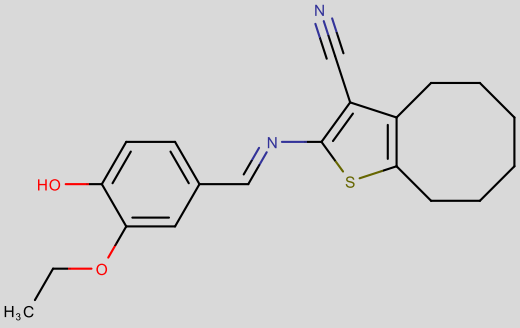	58.32

ALX171	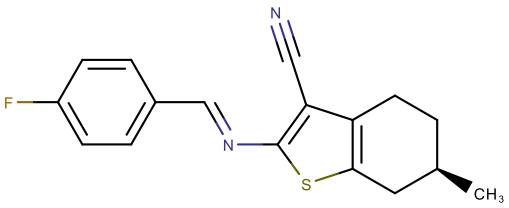	50.79
ALX175	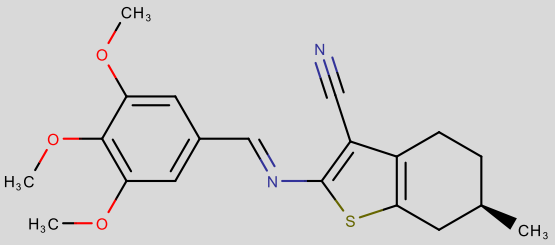	56.70

O composto ALX070 apresentou a menor probabilidade 50,02%, esta estrutura apresentou o átomo de flúor, bastante eletronegativo, ligado ao grupo benzíla que substitui a amina alifática do anel tiofeno, por ser um grupo bastante eletroretirador, a ressonância existente ao longo da estrutura que vai dessa substituição até a amida da posição 3 do tiofeno condensado com ciclohexano é prejudicada, tendo em vista que a densidade eletrônica da nuvem que deveria ser distribuída ao longo da estrutura, passa a ser atraída e deslocada para o átomo eletronegativo, o flúor é um elemento químico pequeno, cujo núcleo exerce uma atração forte pelos elétrons, desestabilizando a estrutura.

Analisando a estrutura do composto ALX038, que apresentou maior probabilidade de possível atividade (79,03%), é possível perceber que a estabilidade da ressonância é importante, a estrutura apresenta um grupo indeno ligado a amina alifática do tiofeno, é possível notar que nesse grupo apresenta um átomo de bromo, que apesar de também ser eletronegativo é um átomo pesado com pouco efeito desestabilizante.

Outra característica importante no composto ALX038 é que o anel tiofeno está conjugado com uma pentamina terciária fazendo ligação com o grupo benzíla, ou seja, além do contribuinte de ressonância da amina alifática, este composto também apresenta efeito ressonante nessa parte cíclica da molécula, assim, estabilizando ainda mais a densidade eletrônica.

Tabela 6. Dados estatísticos do modelo de predição anti-HIV usando Volsurf.

	Teste	Validação interna

Precisão	0.81	0.74
Sensibilidade	0.80	0.78
Especificidade	0.82	0.75
MCC	0.62	0.53
Acurácia	0.81	0.76

Com relação aos dados estatísticos do modelo utilizando os descritores Volsurf, é possível verificar com base no que foi discutido anteriormente nesta pesquisa, que o modelo apresentou boa capacidade preditiva, tendo em vista os dados da Tabela 6 que mostra que esse modelo apresentou sensibilidade 78-80%, especificidade 75-82%, acerto total de 76-81% e acerto global de até 63% em toda a predição.

Quanto a performance desse modelo, pode ser avaliado através da sua curva ROC, que no caso do modelo usando os descritores moleculares obtidos no Volsurf, conforme mostra a figura abaixo, para o grupo de teste foi de 86,91% e para a validação interna cruzada foi 83,19%, assim as predições ficaram longe da região de valores aleatórios, conferindo ao modelo uma boa performance preditiva.

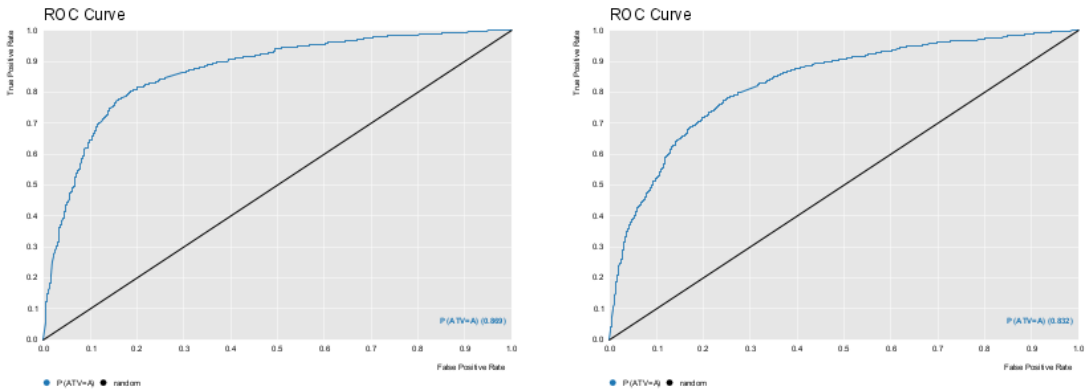

Teste – 86,91% Validação cruzada – 83,19%

Figura 18. Curva ROC do modelo anti-HIV Volsurf.

Após analisar os modelos para cada descritor molecular, foi realizada uma análise em consenso entre os modelos, que leva em consideração a probabilidade de cada molécula nos 4 modelos realizados. Apresentando 7

moléculas com probabilidades que variam de 50,32-55,81%, são as moléculas ALX011, ALX024, ALX025, ALX026, ALX038, ALX118, ALX138. As moléculas aprovadas pelo modelo de consenso estão descriminadas abaixo:

Tabela 7. Estruturas químicas 2D dos compostos aprovados pelo consenso entre os modelos anti-HIV.

ID	Molécula	%Atividade
ALX011	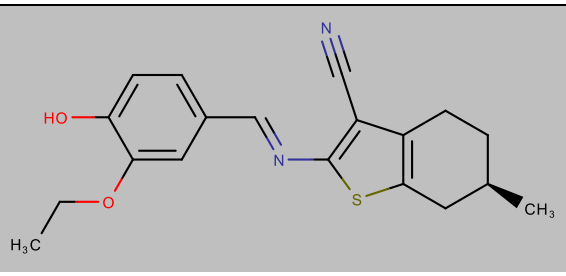	50.32
ALX024	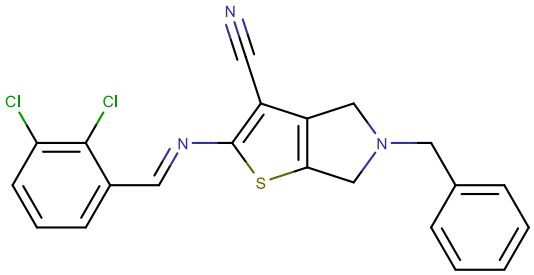	51.00
ALX025	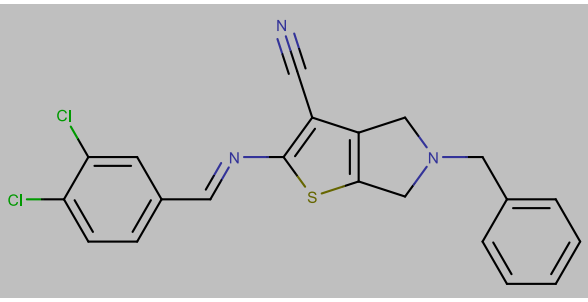	51.24
ALX026	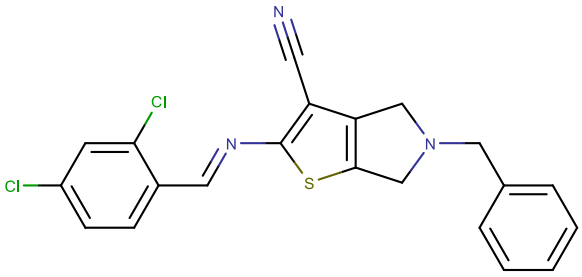	53.40

ALX038	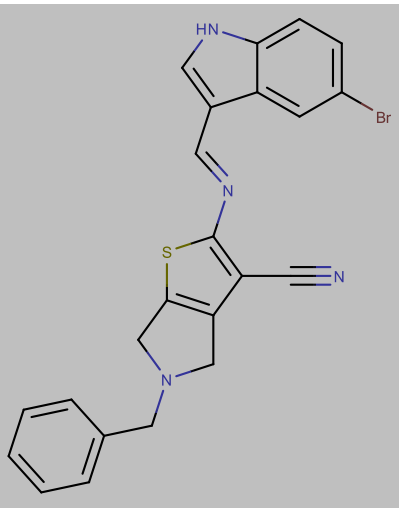	55.81
ALX118	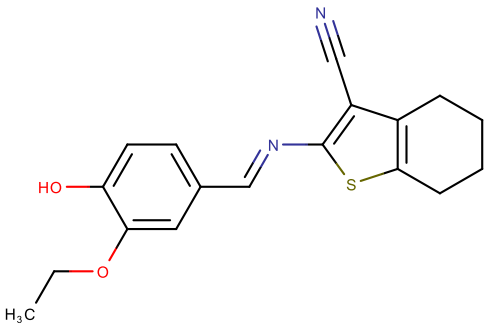	51.64
ALX138	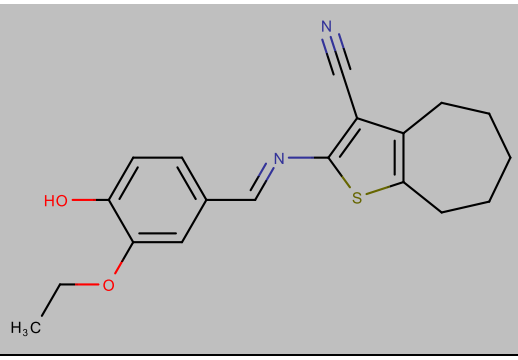	50.39

A molécula ALX011 apresenta o 3-etoxi-4-hidroxibenzil fazendo ligação dupla com a amina alifática do anel tiofeno, cujo tiofeno está conjugado a um ciclohexano. Analisando essa estrutura percebe-se que o efeito ressonante esperado conforme discussões anteriores foi prejudicado pela nitrila ligada ao anel tiofeno. Contudo, mais uma vez o composto ALX038 apresentou probabilidade de provável atividade inibitória da enzima transcriptase reversa do HIV-1.

Assim as 8 moléculas aprovadas pela análise de consenso foram submetidas ao modelo de permeabilidade intestinal (CACO-2) e absorção intestinal (HIA), conforme é possível ver através da tabela a seguir:

Tabela 8. Resultados da predição de HIA e CACO-2.

		HIA			CACO-2	
ID	Domínio	Atividade	%Atividade	Domínio	Atividade	%Atividade
ALX011		HIA+	57,00		CACO+	56,50
ALX024		HIA+	61,50		CACO+	57,00
ALX025		HIA+	58,00		CACO+	55,00
ALX026	Confiável	HIA+	63,50	Confiável	CACO+	60,00
ALX038		HIA+	63,50		CACO+	62,00
ALX118		HIA+	57,50		CACO+	50,00
ALX138		HIA-	49,50		CACO+	55,50

De acordo com os modelos realizados apresentados na tabela acima, apenas a molécula ALX138 não apresentou absorção intestinal, contudo todas as moléculas permeiam o intestino, tornando-as promissores bioativos se levarmos em consideração toda a discussão apresentada nesta pesquisa até então.

Como se tratam de modelos de predição realizados no KNIME, cabe avaliar os parâmetros estatísticos desses modelos, de acordo com os dados apresentados na tabela seguinte, assim como os demais modelos, estes apresentaram boa capacidade preditiva das propriedades de interesse.

Tabela 9. Dados estatísticos do modelo de predição de HIA e CACO-2.

	HIA		CACO-2	
	Teste	Validação interna	Teste	Validação interna
Precisão	0.75	0.66	0.75	0.66
Sensibilidade	0.79	0.78	0.79	0.78
Especificidade	0.71	0.62	0.72	0.61
MCC	0.50	0.51	0.51	0.59
Acurácia	0.75	0.70	0.75	0.69
Curva ROC	83.19	77.57	83.56	77.56

Em ambos os modelos, assim como as predições anti-HIV, os dados estatísticos foram muitos bons, comprovando a performance superior a 83% da capacidade preditiva, com acerto dos positivos de 79% e negativo 72%, assim como 50-59% do acerto total.

5.2 Absorção oral, regra de Lipinski e riscos de toxidade

Um fármaco que é administrado por via oral precisa permear e ser absorvido pelo intestino para que chegue ao fígado, assim, uma fração desse fármaco não biotransformado chega na corrente sanguínea, desprezando a princípio o conceito de latenciação de fármacos. Após chegar à corrente sanguínea, esse fármaco poderá então desenvolver o efeito terapêutico. Assim, para uma triagem virtual é muito importante o cálculo da taxa de absorção por via oral, porém, nesta pesquisa será calculado também essa taxa para os fármacos comerciais inibidores de transcriptase reversa para servir como parâmetro de comparação, conforme mostrado a seguir:

Tabela 10. TPSA, %ABS e LIP dos inibidores de transcriptase reversa usados como controles.

Controle	TPSA	%ABS	LIP
Abacavir	101.88	73.85	0
Didanosina	88.74	78.38	0
Efavirenz	38.33	95.78	0
Etravirina	120.64	67.38	0
Lamivudina	113.45	69.86	0
Nevirapina	58.12	88.95	0
Tenofovir	146.19	58.56	0
Zidovudina	104.83	72.83	0

Dentre os fármacos usados como controle, o tenofovir apresentou a menor taxa de absorção por via oral (58,56%), assim, esta taxa foi usada como parâmetro de exclusão nesta pesquisa, assim, os derivados 2-amino-tiofenos que apresentaram taxas inferiores não serão considerados para a próxima etapa. Assim o %ABS foi calculado para os 8 derivados aprovados pelo modelo de predição anti-HIV por consenso, assim como as violações a regra de Lipinski, conforme mostrado na tabela a seguir:

Tabela 11. Resultados de LIP, TPSA e %ABS para os derivados 2-aminotiofenos aprovados pelo consenso.

ID	LIP	TPSA	%ABS
ALX011	0	65.61	86.36
ALX024	0	39.39	95.41
ALX025	0	39.39	95.41
ALX026	0	39.39	95.41

ALX038	0	55.18	89.96
ALX118	0	65.61	86.36
ALX138	0	65.61	86.36

Observando os resultados dispostos na Tabela 11 é possível perceber que todos os 8 derivados 2-amino-tiofeno não violaram nenhuma das regras de Lipinski e nem taxa de absorção abaixo do controle definido nesta pesquisa, assim, todos os compostos serão considerados para a análise dos riscos de toxidade.

Tabela 12. Resultados da predição dos riscos de toxidade.

ID	MUT	CAR	ESR	IRR	Toxidade
ALX011	Nenhum	Nenhum	Nenhum	Nenhum	Não
ALX024	Nenhum	Nenhum	Nenhum	Nenhum	Não
ALX025	Nenhum	Nenhum	Nenhum	Nenhum	Não
ALX026	Nenhum	Nenhum	Nenhum	Nenhum	Não
ALX038	Nenhum	Nenhum	Nenhum	Nenhum	Não
ALX118	Nenhum	Nenhum	Nenhum	Nenhum	Não
ALX138	Nenhum	Nenhum	Nenhum	Nenhum	Não

MUT: Mutagenicidade
CAR: Carcinogenicidade
ESR: Efeito tóxico no sistema reprodutor
IRR: Irritante

Conforme a metodologia desta pesquisa, foi analisado 4 parâmetros diferentes e a toxidade foi definida de acordo com os riscos que foram evidenciados, para os 8 compostos derivados estudados, não ouve nenhum risco de toxidade em nenhum dos parâmetros analisados, reforçando a expectativa da candidatura destas estruturas a bioativos promissores. Assim todas as moléculas seguiram para a etapa.

5.3 Docking molecular

Foram utilizados 5 diferentes arquivos de transcriptase reversa com os dados cristalográficos das respectivas estruturas químicas, para a ancoragem molecular com os 8 derivados do 2-aminotiofeno que foram aprovados até esta etapa desta pesquisa, os dados da energia de acoplamento ligante-receptor podem ser observados na Tabela abaixo:

Tabela 13. Resultados de energia de acoplamento obtidas no docking molecular.

ID	1DTQ (RMSD 0.23Å) [kcal/mol]	1EP4 (RMSD 0.27Å) [kcal/mol]
Abacavir	-93.41	-118.53
Didanosina	-102.41	-93.71
Efavirenz	-130.65	-86.67
Etravirina	-13.27	-126.06
Lamivudina	-81.77	-69.10
Nevirapina	-93.55	-89.64
Tenofovir	-91.21	-100.52
Zidovudina	-112.44	-94.59
Inibidor	-157.10	-198.84
ALX011	-75.99	-133.47
ALX024	-113.60	-126.86
ALX025	-117.12	-125.80
ALX026	-97.14	-132.05
ALX038	-84.66	-114.41
ALX118	-91.42	-109.80
ALX138	-119.21	-137.61

5.3.1 Transcriptase reversa PDB ID 1DTQ

A primeira ancoragem molecular foi realizada utilizando a proteína cristalográfica da transcriptase reversa (TR) do HIV-1 complexada com feniletiltiazoliltioureia (PETT-1), este composto corresponde a uma série de inibidores de TR de alta eficiência, de acordo com a Tabela anterior e com a próxima figura que mostra a representação gráfica das energias para essa proteína PDB ID 1DTQ:

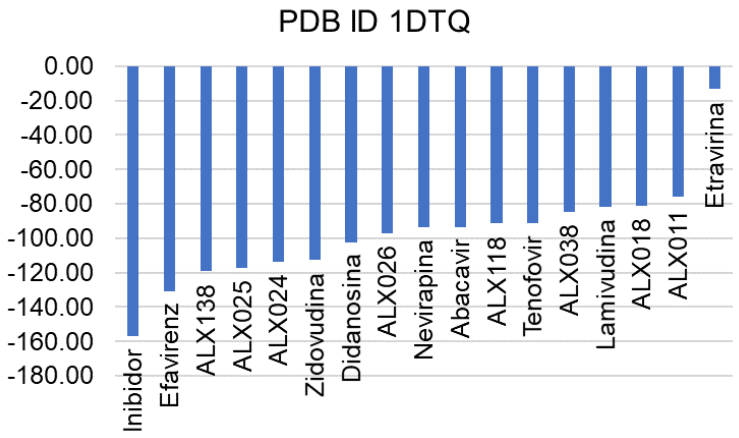

Figura 19. Gráfico representando graficamente os valores de energia no docking molecular para o PDB ID 1DTQ.

De acordo com o gráfico representado na Figura 19, os compostos ALX024 (-113.60 Kcal/mol), ALX025 (-117.12 Kcal/mol) e ALX138 (-119.21 Kcal/mol) apresentaram melhores energias de interação que os fármacos zidovudina (-112.44 Kcal/mol), didanosina (-102.41 Kcal/mol), nevirapina (-93.55 Kcal/mol), abacavir (-93.41 Kcal/mol), tenofovir (-91.21 Kcal/mol), lamivudina (-81.77 Kcal/mol) e etravirina (-13.27 Kcal/mol). Contudo o inibidor complexado junto a proteína no arquivo PDB apresentou energia de acoplamento de -157.10 Kcal/mol, seguido do fármaco efavirez -130.65 kcal/mol, mais baixos que qualquer um dos derivados 2-aminotiofenos estudados nesta etapa.

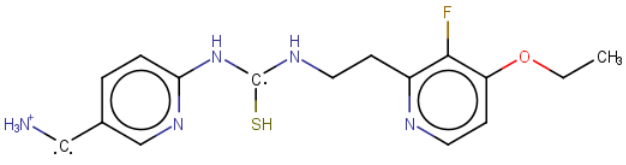

Inibidor – eniletiltiazoliltioureia (PETT-1)

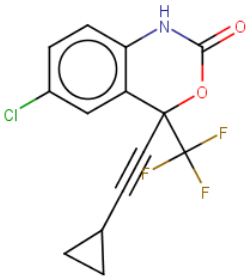

Efavirez

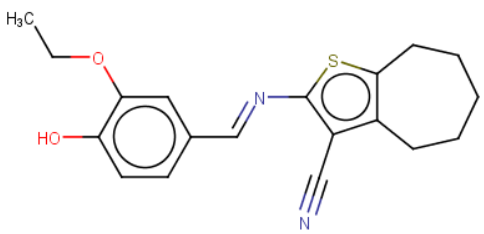

ALX138

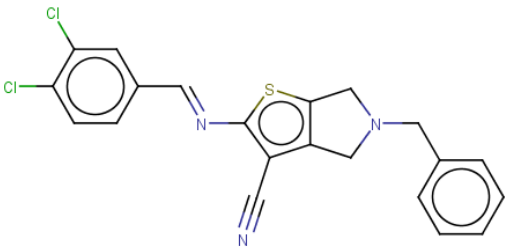

ALX025

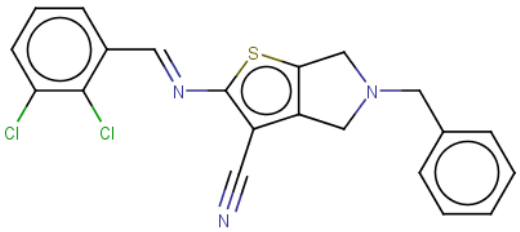

ALX024

Figura 20. Estruturas 2D do PETT-1, Efavirez, ALX024, ALX025 e ALX138.

Analisando a estrutura químicas dos 3 melhores derivados, na Figura 20, no inibidor complexado e do efavirez, é possível perceber que todos as estruturas apresentam anéis aromáticos funcionalizados, o PETT-1 é uma estrutura radicalar com 2 anéis piridínicos com várias aminas substituídas, inclusive grupo amoníaco e mercaptol estão presentes em sua estrutura, explicando a reatividade deste composto. Todas as estruturas apresentam nitrogênio com um dos seus heteroátomos, e a grande maioria apresentam contribuintes de ressonância, corroborando a discussão apresentada no início dos resultados desta pesquisa. Para compreender vamos analisar detalhadamente cada interação realizada por esses compostos, começando pelo inibidor, as interações mais fortes são as de hidrogênio, o inibidor que vem junto a proteína cristalográfica apresentou três destas interações, duas com o resíduo de aminoácido Lys101(A) e uma com Pro236(A) conforme mostrado na Figura 21.

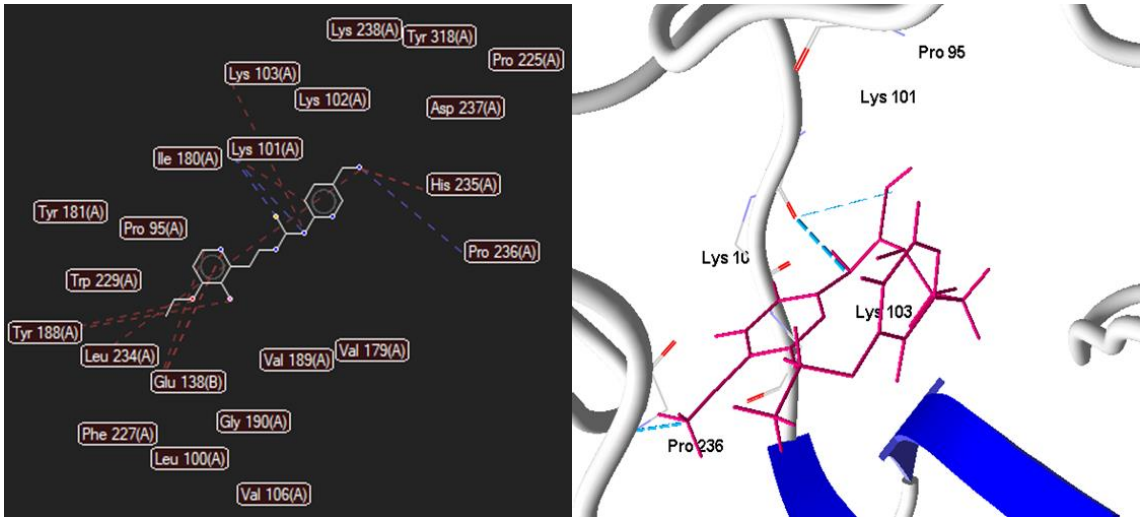

Figura 21. Docking molecular do inibidor da proteína PDB ID 1DTQ.

Contudo também apresentou interações estéricas com os resíduos 1Lys103, 1Lys101, 1His235, 2Tyr188, 1Leu234 e 2Glu138, a maior parte dessas interações deram-se nos anéis piridínicos, contudo as ligações de hidrogênio identificadas apresentaram-se nas aminas alifáticas da estrutura. Com relação ao efavirez, na figura mostra as interações encontradas:

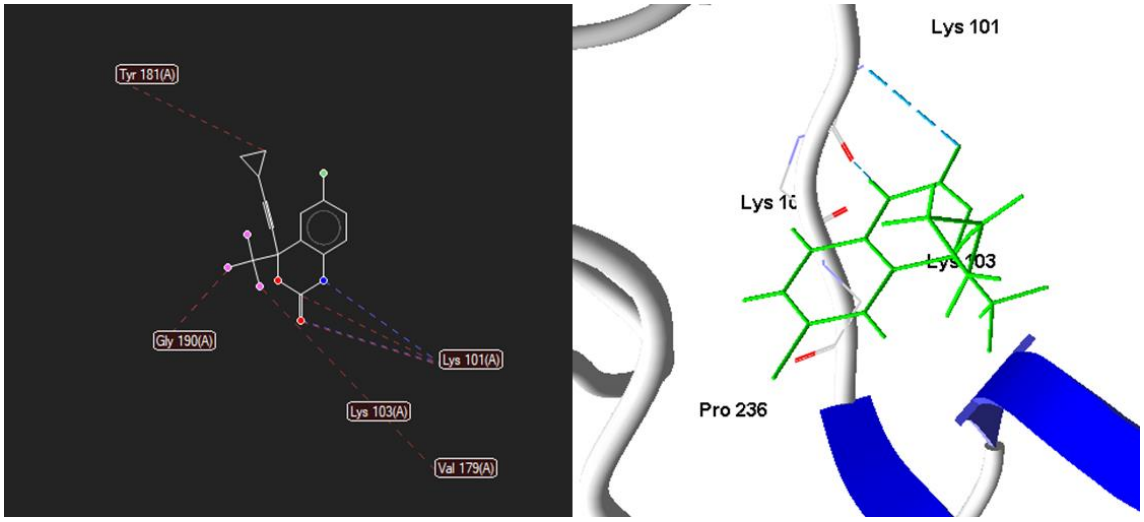

Figura 22. Docking molecular do efavirez (PDB ID 1DTQ).

Semelhante ao inibidor, o efavirez apresentou duas interações de hidrogênio com o Lys101, e interações estéricas com os resíduos 1Tyr181 com o anel de três membros, 1Gly190 com um átomo de flúor, 1Val179 também com um átomo de flúor e 2Lys101 nos dois oxigênios presentes no ciclohexano funcionalizado conjugado ao anel aromático. Semelhante ao mostrado na Figura 23 o ALX138, que dentre os derivados estudados foi o que apresentou melhor resultado de acoplamento com a proteína PDB ID 1DTQ.

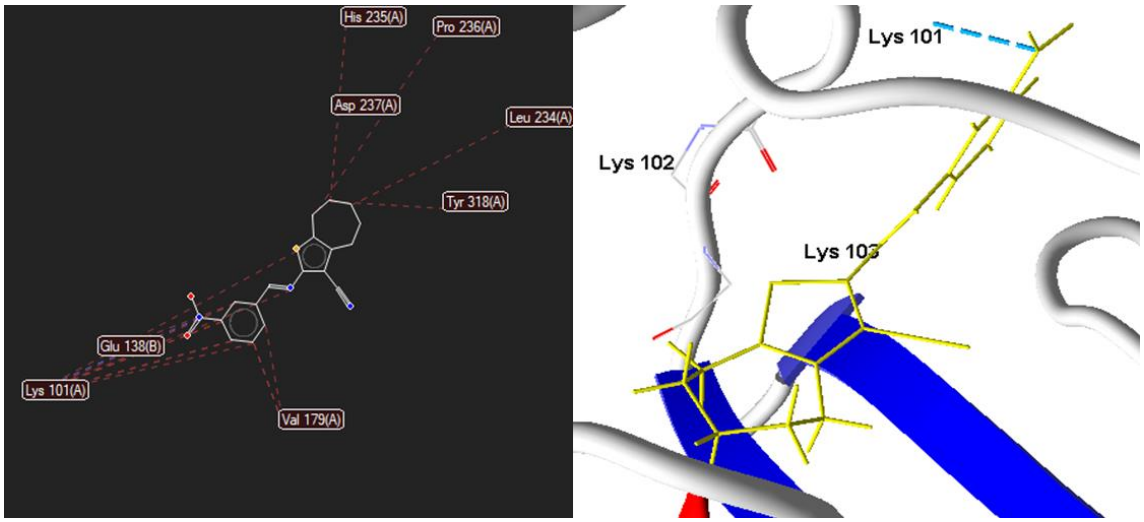

Figura 23. Docking molecular do ALX138 (PDB ID 1DTQ).

Na figura anterior, mostra que a estrutura apresentou interação de hidrogênio com o resíduo Lys101 através do nitrogênio do grupo nitro da posição meta do anel aromático do substituinte do anel tiofeno. Com relação a outras interações, a estrutura apresentou estéricas com os resíduos 1Val179, 6Lys101, 1Gly138, 1His235, 1Pro236, 1Lys234 e 1Tyr318. Nesta estrutura o átomo de enxofre estabeleceu interação estérica com o Lys101, assim como também com a amina alifática.

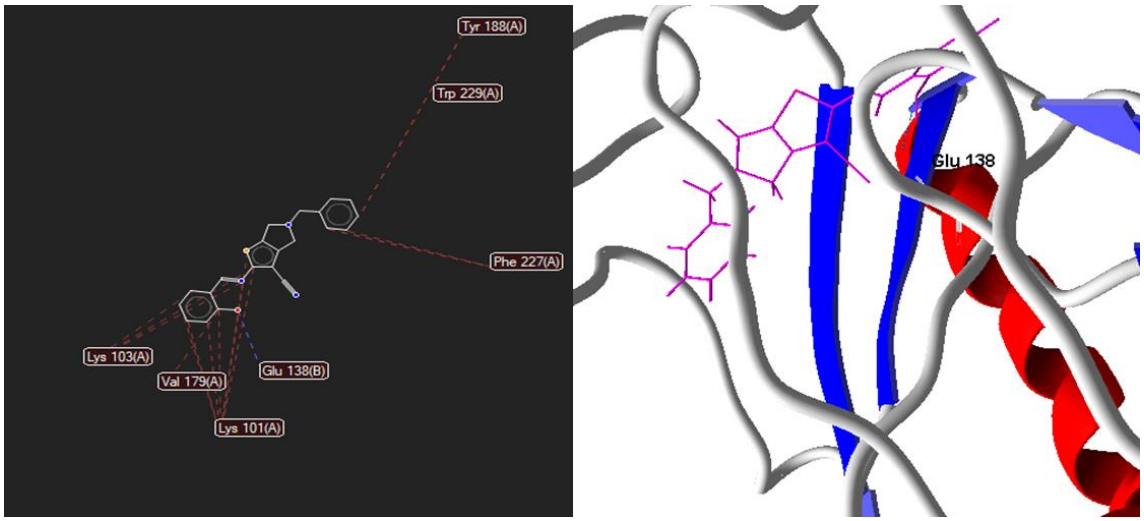

Figura 24. Docking molecular do ALX025 (PDB ID 1DTQ).

Para o composto ALX025 diferentemente das demais estruturas discutidas anteriormente, a interação de hidrogênio foi com o resíduo de aminoácido Glu138 com o oxigênio da hidroxila orto substituída do anel do grupo

benzil ligado a amina alifática da estrutura. Com diversas interações estéticas, pode-se iniciar apontando a com o resíduo Lys101, que também está presente nas demais estruturas acima, interagindo com o enxofre do anel tiofeno e mais uma vez com a amina alifática presente na posição 2 do anel tiofeno, outras interações estéricas podem ser identificadas com o próprio Lys101, 1Val179, 3Lys103, 2Phe227 e 1Tyr188.

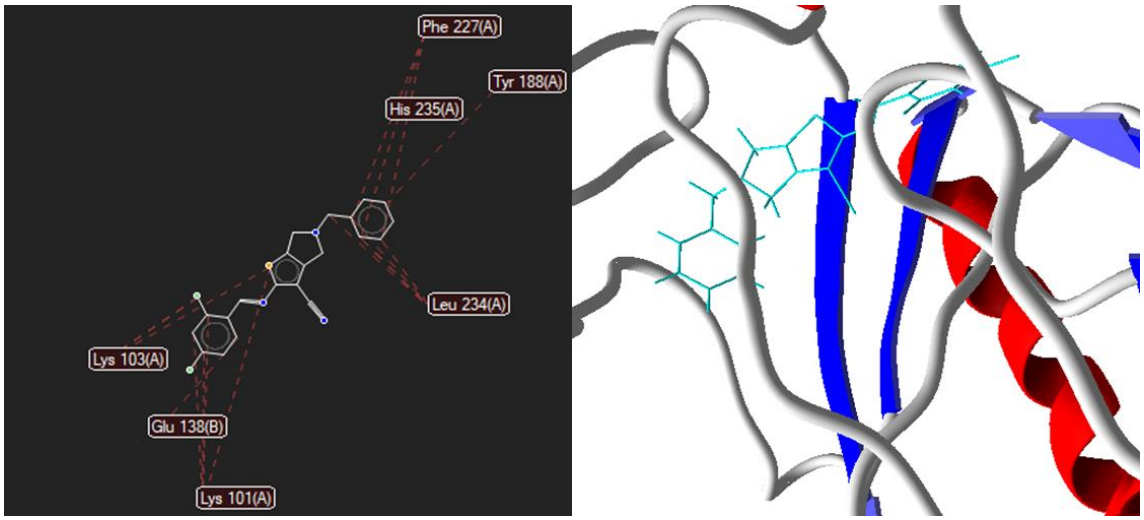

Figura 25. Docking molecular do ALX024 (PDB ID 1DTQ).

Conforme mostrado na figura anterior, o composto ALX024 não estabeleceu nenhuma interação de hidrogênio, contudo, apresentou várias interações estéricas, inclusive com resíduos comuns em outras moléculas, dentre elas pode-se apontar 3Phe227, 1Tyr188, >4Leu234, o cloro na posição orto do anel aromático do substituinte da amina alifática estabeleceu interação com Lys103, assim como com o átomo de enxofre do anel tiofeno, 1Glu138 e 4Lys101.

Avaliando os resultados encontrados para os compostos com melhor perfil inibidor frente a proteína transcriptase PDB ID 1DTQ, foi possível perceber que os compostos com melhores resultados ALX138 e ALX1025 assim como o inibidor e o fármaco efavirez apresentaram interação do tipo de hidrogênio com o resíduo Lys101, assim como interações estéricas comuns com os resíduos Lys101, Lys103 e Tyr188, levando a acreditar que essas interações pontuadas são importantes para o efeito inibitório.

5.3.2 Transcriptase reversa PDB ID 1EP4

Desta vez foi utilizada uma estrutura cristalizada disponível gratuitamente sob o código PDB ID 1EP4, que corresponde a transcriptase reversa cristalizada com a molécula S-1153 (5-(3,5-DICHLOROPHENIL) THIO-4-ISOPROPIL-1-(PIRIDIN-4-YL-METIL) -1H-IMIDAZOL-2-YL-METIL CARBAMATO), abaixo mostra a representação gráfica dos valores de energia de acoplamento mostrados na Figura 26:

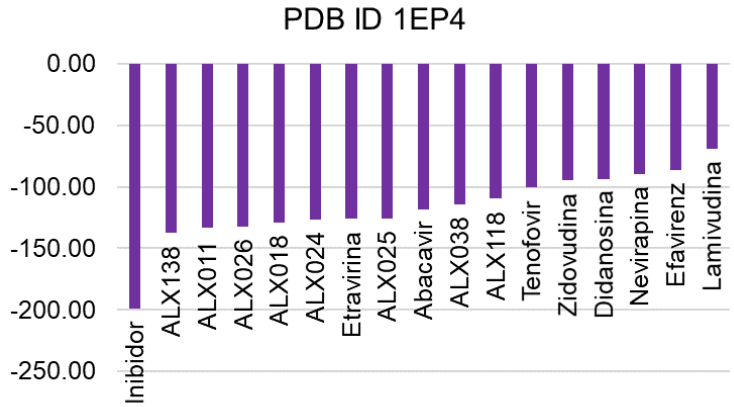

Figura 26. Gráfico representando graficamente os valores de energia no docking molecular para o PDB ID 1EP4.

Conforme a última proteína estudada, o composto ALX138 também apresentou a melhor energia total de acoplamento ligante-receptor, contudo desta vez os compostos ALX011 (-133.47 Kcal/mol), ALX024 (-126.86 Kcal/mol) e ALX026 (-132.05 Kcal/mol) apresentaram também boas condições de docking molecular sobre todos os fármacos utilizados como controle. De acordo com os resultados obtidos para essa proteína, o efavirez apresentou a segunda maior energia, diferentemente da proteína anterior. O inibidor apresentou a mais baixa energia corroborando a literatura que apontou esta estrutura como um dos melhores inibidores para RT (-198.84 Kcal/mol).

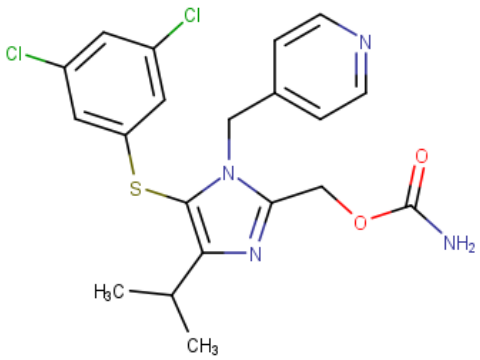

Inibidor

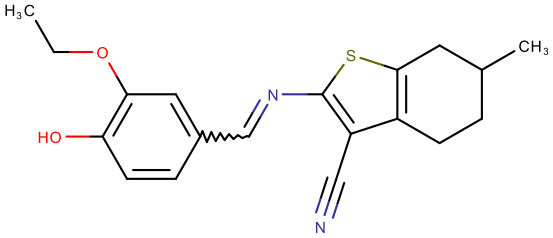

ALX011

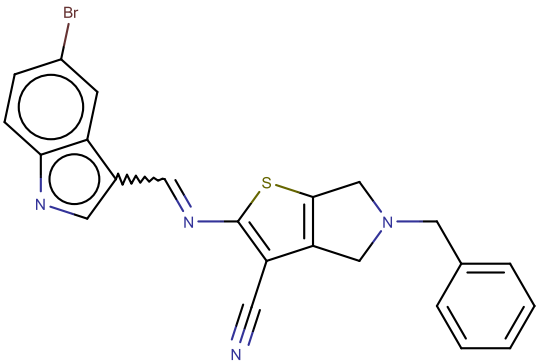

ALX026

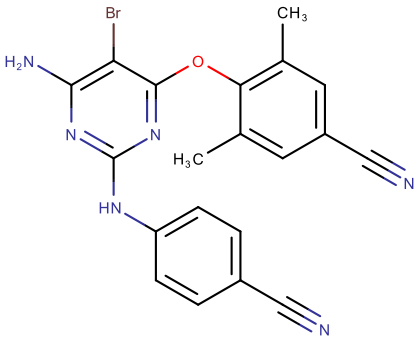

Etravirina

Figura 27. Estruturas 2D do PETT-1, Efavirez, ALX011 e ALX026.

O inibidor é um composto polifuncionado, com três anéis aromáticos, dos quais dois são hexaciclico (um piridinico) e um pentacíclico (imidazólico), apresenta átomo de enxofre alifático, com um carbamato não substituído. De acordo com os resultados obtidos no docking molecular foi possível obter informações sobre a interação com resíduos de aminoácidos importantes, conforme mostradas na figura abaixo:

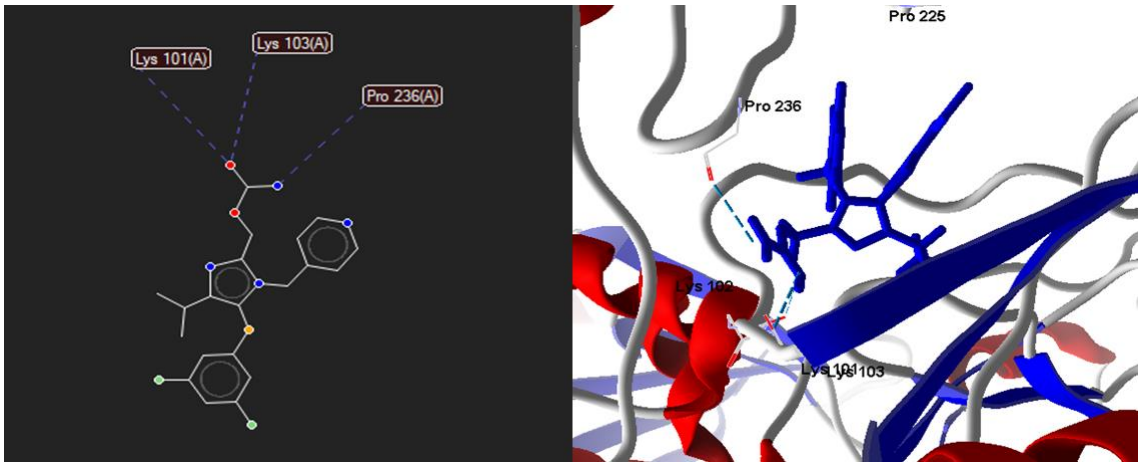

Figura 28. Docking molecular do inibidor (PDB ID 1EP4).

A molécula ALX138 apresentou o melhor resultado conforme visto, contudo não apresentou ligação de hidrogênio, mas sim, 7 interações estéricas importantes, o anel pentacíclico conjugado ao anel tiofeno estabeleceu duas interações uma com o resíduo Pro236 e outra com a Val106, o enxofre e a amina com Phe227, o anel aromático do substituinte da amina com o Tyr181 e Leu234, e por último a hidroxila com Trp229, conforme mostrado na figura abaixo:

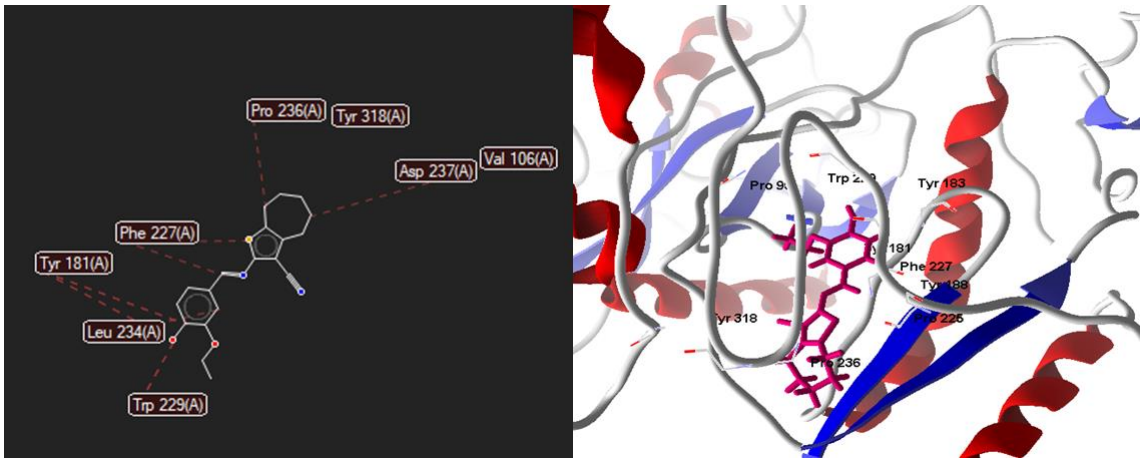

Figura 29. Docking molecular do ALX138 (PDB ID 1EP4).

Segundo os resultados obtidos, o inibidor complexado junto a proteína não apresentou ligações estéricas, contudo apresentou três interações de hidrogênio, na região do carbamato da estrutura, com os resíduos Lys101 que também esteve presente ao longo de toda a análise desses compostos frente a proteína anterior, Lys103 e Pro236.

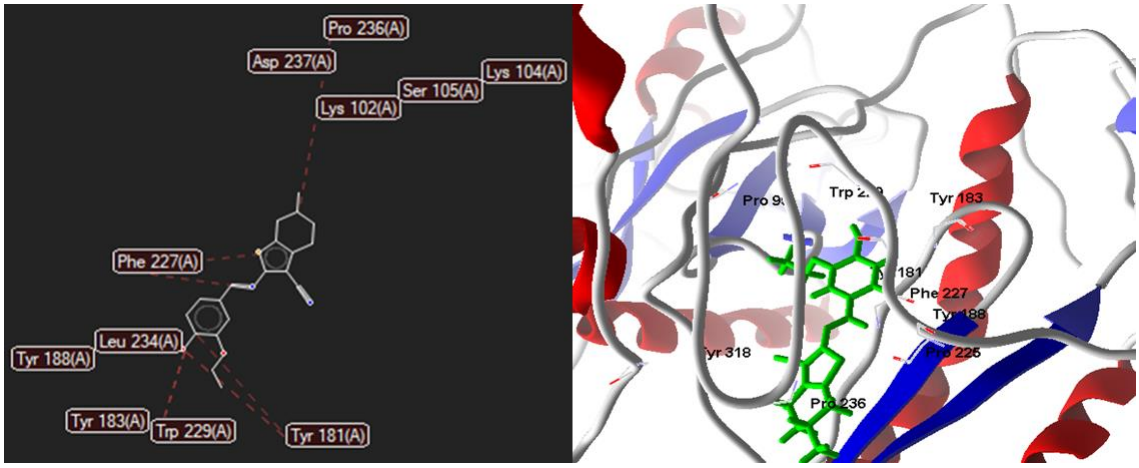

Figura 30. Docking molecular do ALX011 (PDB ID 1EP4).

O composto ALX011 é um composto que apresenta um penta anel tiofeno condensado com um ciclohexano, cuja amina alifática da posição 2 do tiofeno forma dupla ligação com o grupo 3-etoxi-4-hidroxi-benzil, este por sua vez apresentou duas interações estéricas com os resíduos Trp229 e Tyr181, assim como semelhantemente ao ALX0138, neste derivado 2-aminotiofeno o enxofre e a amina interagiu estericamente com o resíduo Phe227, outra interações estérica encontrada foi a que o carbono que contem a hidroxila no substituinte da amina estabeleceu com o resíduo Tyr181, estruturalmente a diferença entre os compostos ALX011 e ALX138 está no anel conjugado ao anel tiofeno, assim, observou-se interações e regiões de interações semelhantes.

Mais uma vez, assim como já mostrado na discussão acima nesta pesquisa, o enxofre também participa da interação ligante-receptor, assim como os substituintes do grupo benzil ligado a amina presente na estrutura.

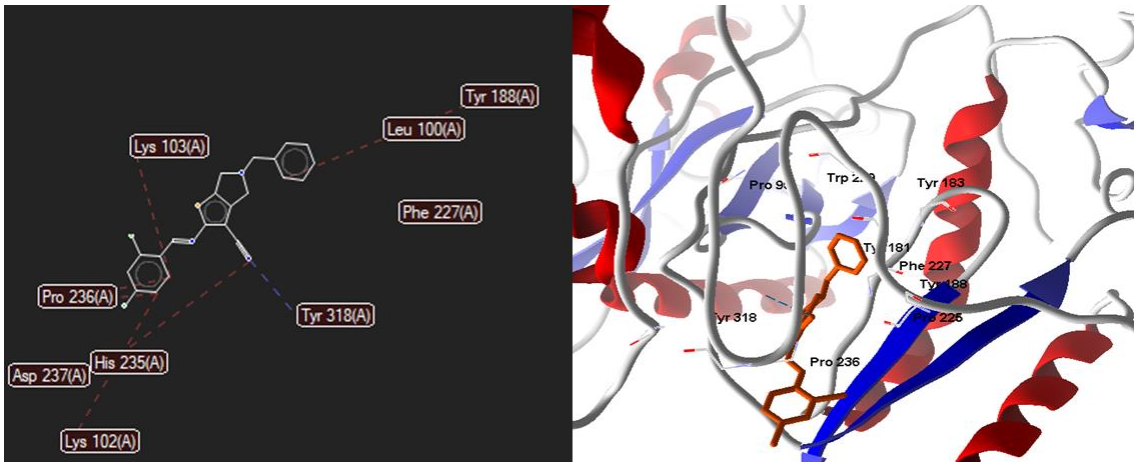

Figura 31. Docking molecular do ALX026 (PDB ID 1EP4).

O composto ALX026 foi o terceiro derivado do 2-aminotiofeno estudado a apresentar melhor energia ligante-receptor frente a proteína estudada, apresente o substituinte 2,4-dicloro-benzil formando ligação dupla com a amina alifática de anel tiofeno pentacíclico conjugado com uma ciclopentamina substituída por um grupo benzil não substituído.

É possível perceber até então, analisando os dados para a proteína PDB ID 1EP4 que os melhores resultados até então discutidos pertencem as moléculas poliaromáticas, com a presença de grupos eletroretiradores que substituem um ou mais posições no grupo benzíla da amina alifática. Como visto na proteína anterior, o efeito de ressonância é importante, várias regiões desses anéis também estabelecem acoplamento ligante-receptor, contudo, nesta proteína vemos moléculas com grupos eletronegativos com as melhores energias de docking molecular.

Finalizando a discussão do docking molecular desta proteína utilizada, conforme mostrado na figura abaixo, o composto ALX024 (Figura 32a) e o fármaco Etravirina (Figura 32b) apresentam interação estérica em comum, assim como os compostos já discutidos acima o Pro236. Com relação ao derivado 2-aminotiofeno, além dessa interação estérica ainda apresenta uma com o resíduo Lys102 e outra com Lys103, já o fármaco usado como controle apresentou interação de hidrogênio com Lys100, estéricas com 1Trp229, 1Tyr188, 1Leu100, 2Pro236 e 1Phe227, sendo mais uma vez observado que os heteroátomos que substituem os anéis aromáticos os responsáveis pela maioria das interações.

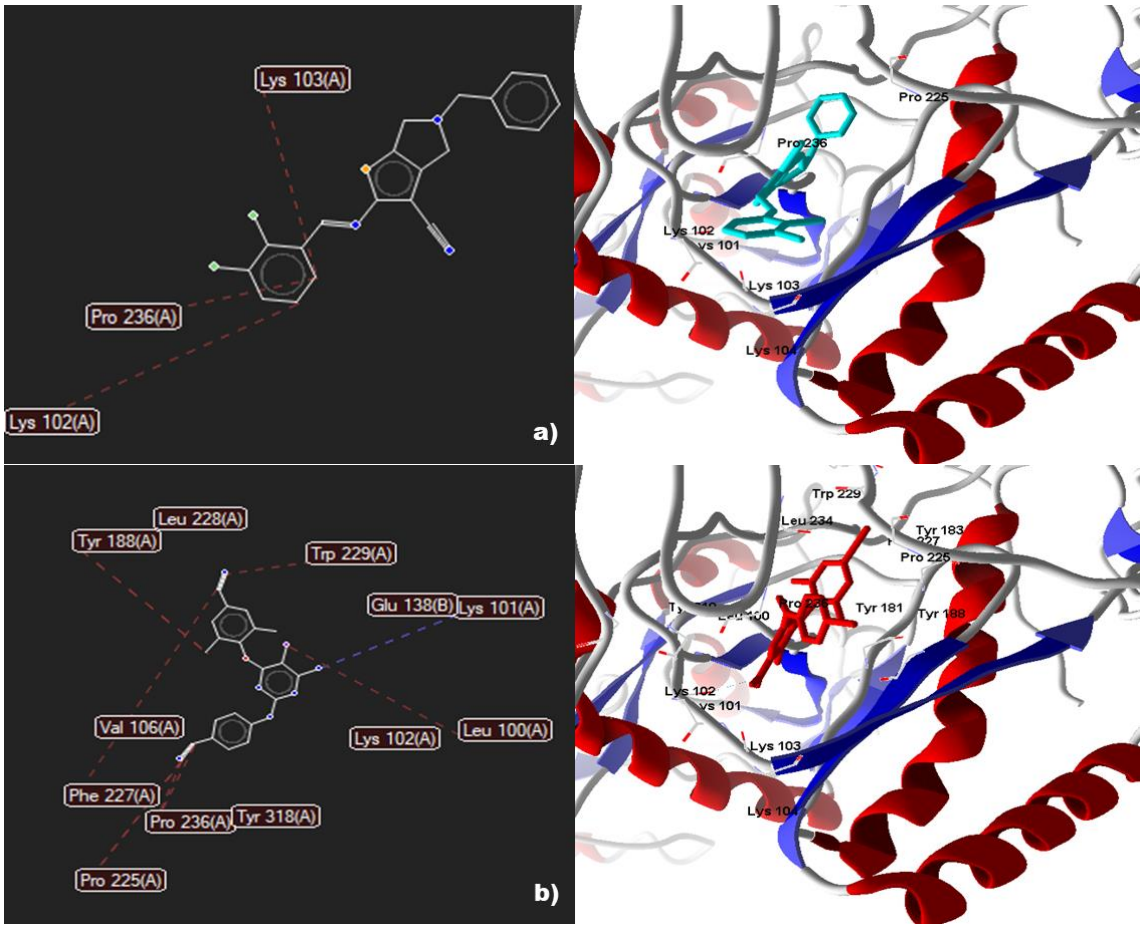

Figura 32. Docking molecular do a) ALX024, b) Etravirina (PDB ID 1EP4).

5.4 Simulação metabólica dos compostos

Os 8 compostos apresentaram afinidades frente as proteínas selecionadas de transcriptase reversa, estas foram submetidas ao METASITE para predição de seus metabólitos hepáticos, os 25 metabólitos secundários com probabilidade de formação a partir de 75% estão dispostos na Tabela 14:

Tabela 14. Dados da predição metabólica hepática dos compostos aprovados.

ID	Molécula	%PROB	TOX	Estrutura
MET011	ALX011	100.00	Não	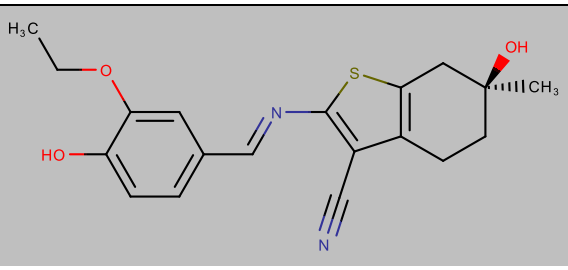

MET022	ALX011	100.00	Não	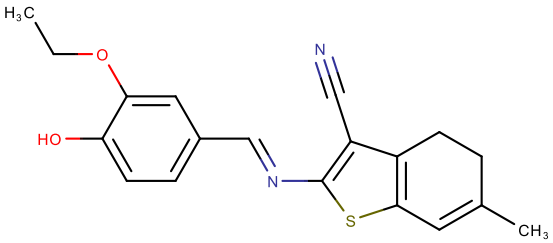
MET018	ALX011	79.22	Não	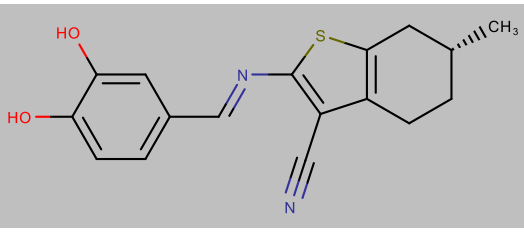
MET019	ALX011	79.22	Não	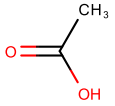
MET023	ALX011	79.22	Sim	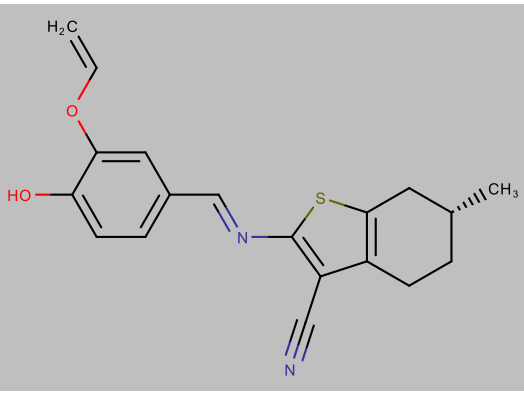
MET039	ALX024	100.00	Não	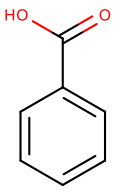
MET059	ALX024	100.00	Não	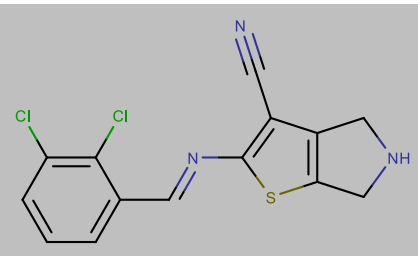
MET067	ALX024	100.00	Não	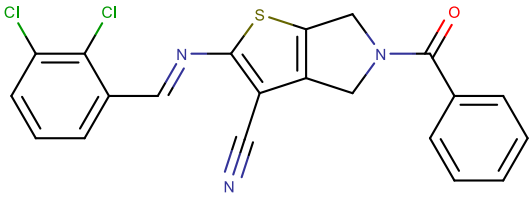

MET039	ALX025	100.00	Não	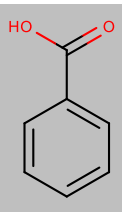
MET081	ALX025	100.00	Não	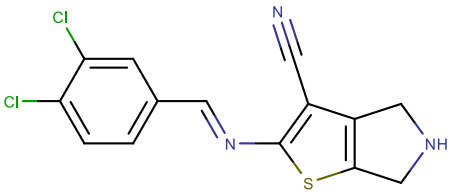
MET089	ALX025	100.00	Não	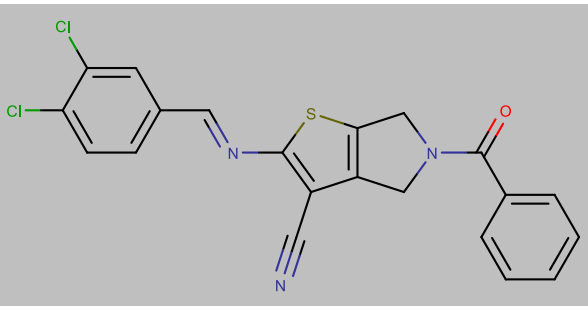
MET039	ALX026	100.00	Não	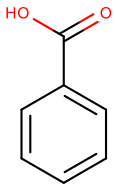
MET102	ALX026	100.00	Não	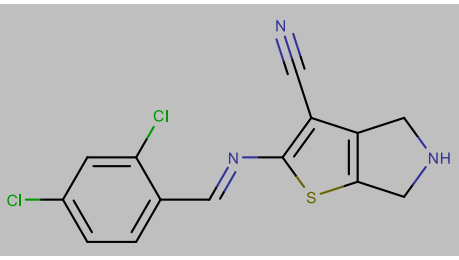
MET110	ALX026	100.00	Não	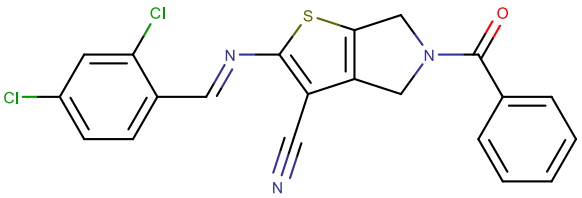
MET034	ALX038	100.00	Não	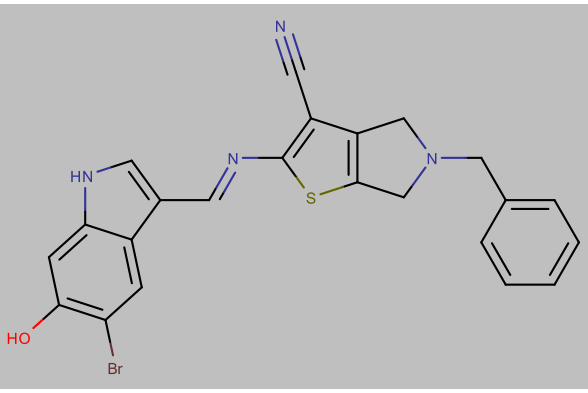

MET019	ALX118	100.00	Não	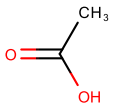
MET122	ALX118	100.00	Não	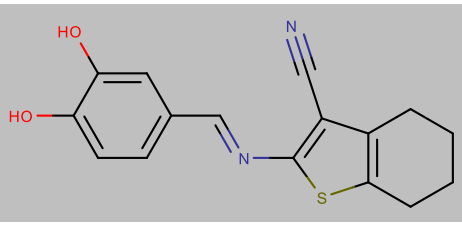
MET126	ALX118	100.00	Não	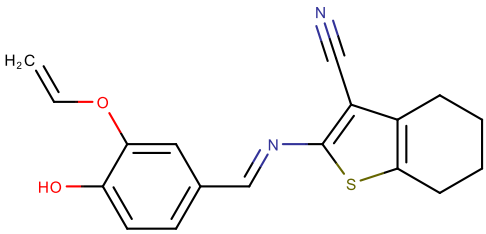
MET117	ALX118	86.58	Não	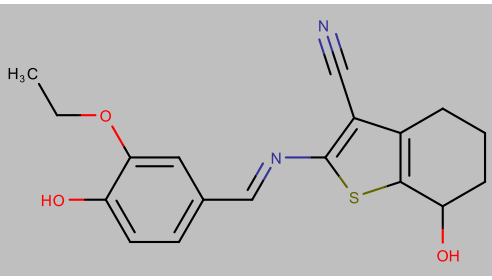
MET123	ALX118	86.58	Não	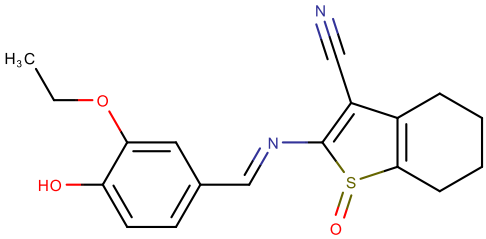
MET125	ALX118	86.58	Não	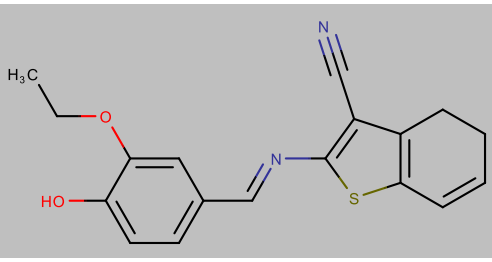
MET128	ALX118	86.58	Não	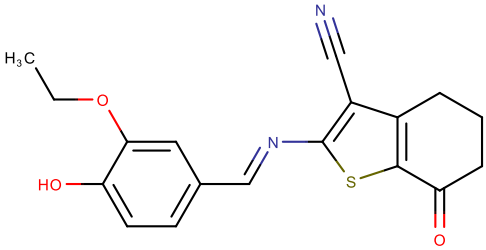
MET019	ALX138	100.00	Não	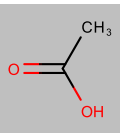

MET141	ALX138	100.00	Não	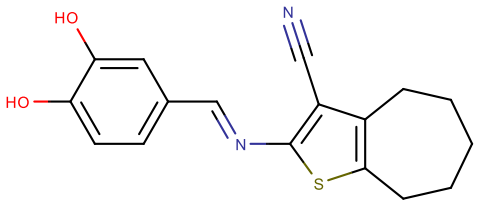
MET145	ALX138	100.00	Não	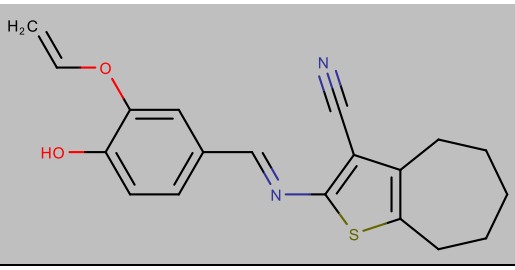

%PROP = Probabilidade de formação

De acordo com os dados obtidos na predição metabólica hepática apresentada na tabela anterior, apenas o metabólito MET023 originário da desidrogenação molécula ALX011 apresentou toxidade segundo o OSIRIS, fazendo com que o derivado 2-aminotiofeno não fosse considerado mais promissor, tendo em vista que seu metabólito apresenta 79,22% de probabilidade de formação, segundo o esquema de reação simplificado mostrado abaixo:

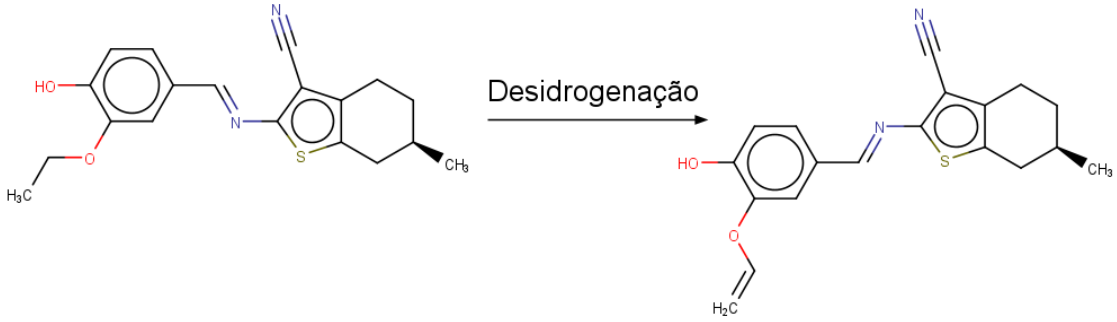

Figura 33. Esquema simplificado de desidrogenação do composto ALX011.

É possível perceber que a metoxila do substituinte da amina perdeu um átomo de hidrogênio, que rapidamente forma uma dupla ligação para estabilizar a estrutura, com essa desidrogenação a molécula apresentou riscos de toxidade segundo as predições, assim, esse tipo de reação não favorece estruturas promissoras para essa unidade farmacofórica, e por isso o composto ALX011 não seguirá para as próximas análises desta pesquisa.

Como os metabólitos com probabilidade de formação a partir de 75% correspondem a um dos parâmetros norteadores para a proposição de bioativos de melhores perfis após a triagem, os 20 metabólitos referentes aos derivados ALX024, ALX025, ALX026, ALX038, ALX118 e ALX138 foram submetidos a um modelo de predição de atividade anti-HIV, HIA e CACO-2 conforme foi realizado com os derivados 2-aminotiofenos já discutidos, com isso, os resultados obtidos estão dispostos na tabela a seguir:

Tabela 15. Predição da atividade anti-HIV por consenso.

ID	CDK			VOLSURF			CONSENSO		
	Dom.	ATV	%ATV	Dom.	ATV	%ATV	Dom.	ATV	%ATV
MET039	C	Inativo	9	C	Inativo	21	C	Inativo	15
MET059	C	Inativo	42.5	C	Ativo	53	C	Inativo	48
MET067	C	Ativo	54.5	C	Ativo	78	C	Ativo	66
MET039	C	Inativo	9	C	Inativo	21	C	Inativo	15
MET081	C	Inativo	42.5	C	Ativo	55.5	C	Inativo	49
MET089	C	Ativo	54	C	Ativo	82	C	Ativo	68
MET039	C	Inativo	9	C	Inativo	21	C	Inativo	15
MET102	C	Inativo	46	C	Ativo	53.5	C	Ativo	50
MET110	C	Ativo	53	C	Ativo	80.5	C	Ativo	67
MET034	C	Ativo	54	C	Ativo	68	C	Ativo	61
MET019	NC	Inativo	15	NC	Inativo	25	NC	Inativo	20
MET122	C	Inativo	37	C	Inativo	47.75	C	Inativo	42
MET126	C	Inativo	31	C	Ativo	63.5	C	Inativo	47
MET117	C	Inativo	36	C	Inativo	35	C	Inativo	36
MET123	C	Inativo	35	C	Inativo	30	C	Inativo	33
MET125	C	Inativo	35.5	C	Ativo	60.5	C	Inativo	48
MET128	C	Inativo	38.5	C	Ativo	60.5	C	Ativo	50
MET019	NC	Inativo	15	NC	Inativo	25	NC	Inativo	20
MET141	C	Inativo	42	C	Ativo	54	C	Inativo	48
MET145	C	Inativo	37.5	C	Ativo	62.25	C	Ativo	50

ATV = Atividade
%ATV = Probabilidade de atividade
C = Confiável
NC = Não confiável
Dom. = Domínio

De acordo com a predição, 7 metabólitos secundários apresentaram possível atividade anti-HIV segundo o consenso entre os modelos de predição utilizando descritores CDK e Volsurf, conforme mostrado na Tabela 15, sendo o MET034 metabólito do composto ALX038, o MET067 do ALX024, o MET089 do ALX025, os MET102 e MET110 do ALX026 o MET128 do ALX118 e MET 145 do

ALX138. Contudo, o composto ALX026 apresentou dois metabólitos com probabilidade de possível atividade segundo a predição realizada, sendo este derivado o composto que apresentou a 3º melhor energia de acoplamento ligante-receptor dentre os derivados estudados frente a proteína PDB ID 1EP4 e a 4º frente a PDB ID 1DTQ, já discutidos anteriormente na seção de docking molecular.

6. CONCLUSÃO

Com base nos dados apresentados pela triagem virtual, os compostos testados apresentaram caráter anti-HIV promissor, que direciona o teste biológico para validar esses dados *in silico*, assim como o teste de citotoxicidade é necessário para confirmar através de testes biológicos antes da proposição desses compostos a novos medicamentos retrovirais.

Esta pesquisa limitou-se apenas às análises computacionais desse grupo de 2-aminotiofênicos, a partir dessas análises os compostos apresentaram interações para os 2 alvos escolhidos de transcriptase reversa contra o HIV-1. Complementando essa conclusão com os dados de risco de citotoxicidade dos metabólitos análogos, com isso, pesquisas futuras podem investir na possível comprovação da atividade anti-HIV através de teste biológicos desses compostos, em especial o composto ALX026 (5-benzil-2-[(E)-[(2,4-diclorofenil)metilideno]amino]-4H,5H,6H-tieno[2,3-c]pirrole-3-carbonitrila).

Os dados apresentados corroboram as pesquisas na área de planejamento de novos fármacos anti-HIV, que apontam os heterocíclicos como moléculas promissores para estudos, cujo objetivo é a proposição de novos agentes retrovirais. Sendo este estudo importante para que futuros pesquisadores possam pesquisar detalhadamente a possibilidade de proposição dos derivados 2-aminotiofenos como drogas no combate ao HIV.

REFERÊNCIAS BIBLIOGRÁFICAS

ADZHUBEI, A. A. *et al.* Direct interaction between ABCA1 and HIV-1 Nef: Molecular modeling and virtual screening for inhibitors. **Computational and structural biotechnology journal**, 2021. v. 19, p. 3876–3884.

AHSAN, M. J. *et al.* Synthesis and antimicrobial activity of N1-(3-chloro-4-fluorophenyl)-N4-substituted semicarbazone derivatives. **Arabian journal of chemistry**, 2016. v. 9, p. S861–S866.

ANDRIANOV, A. M. *et al.* Application of deep learning and molecular modeling to identify small drug-like compounds as potential HIV-1 entry inhibitors. **Journal of Biomolecular Structure and Dynamics**, 2021. p. 1–19.

ASSAF, R. D. *et al.* Are men who have sex with men at higher risk for HIV in Latin America more aware of PrEP? **Plos one**, 2021. v. 16, n. 8, p. e0255557.

BARI, A.; GHANI, U.; SYED, S. A. Thiosemicarbazide binds with the dicopper center in the competitive inhibition of mushroom tyrosinase enzyme: Synthesis and molecular modeling of theophylline analogues. **Bioorganic & Medicinal Chemistry Letters**, 2021. v. 36, p. 127826.

BERMAN, H. M. *et al.* The Protein Data Bank. **Nucleic Acids Research**, jan. 2000. v. 28, n. 1, p. 235–242.

BHOLE, R. P. *et al.* Pharmacophore model and atom-based 3D quantitative structure activity relationship (QSAR) of human immunodeficiency virus-1 (HIV-1) capsid assembly inhibitors. **Journal of Biomolecular Structure and Dynamics**, 2021. v. 39, n. 2, p. 718–727.

BRIAN, W. **Bioinformatics and machine learning in prevention, detection and treatment of HIV/AIDS**. Brac University.

BROEK, N. VAN DEN. Mini commentary on BJOG-20-1962. R1 'Slower response to treatment of iron deficiency anemia in HIV-infected pregnant women: a prospective cohort study'Anaemia in pregnancy remains a global health problem. **Authorea Preprints**, 2021.

CHEN, Y. *et al.* Comparison of dimension reduction methods on fatty acids food source study. **Scientific reports**, 2021. v. 11, n. 1, p. 1–12.

CILENTO, M. E.; KIRBY, K. A.; SARAFIANOS, S. G. Avoiding drug resistance in hiv reverse transcriptase. **Chemical Reviews**, 2021. v. 121, n. 6, p. 3271–3296.

DEVANATHAN, A. S.; KASHUBA, A. D. M. Human Immunodeficiency Virus Persistence in the Spleen: Opportunities for Pharmacologic Intervention. **AIDS Research and Human Retroviruses**, 2021.

DING, X. *et al.* Combination of 2D and 3D-QSAR Studies on DAPY and DANA Derivatives as Potent HIV-1 NNRTIs. **Journal of Molecular Structure**, 2021. p. 131603.

FASHOTO, S. G. *et al.* Multi-Target Regression Prediction on Cervical Cancer for. **Asian Journal of Information Technology**, 2018. v. 17, n. 2, p. 160–166.

FENG, D. *et al.* Design, synthesis, and evaluation of “dual-site”-binding diarylpyrimidines targeting both NNIBP and the NNRTI adjacent site of the HIV-1 reverse transcriptase. **European Journal of Medicinal Chemistry**, 2021. v. 211, p. 113063.

FERRANTE, N. D.; RE, V. Lo. Epidemiology, natural history, and treatment of hepatitis delta virus infection in HIV/hepatitis B virus coinfection. **Current HIV/AIDS Reports**, 2020. p. 1–10.

FORTI, M. **Técnicas de machine learning aplicadas na recuperação de crédito do mercado brasileiro**.

FRANCA RODRIGUES, K. A. DA *et al.* SB-83, a 2-Amino-thiophene derivative orally bioavailable candidate for the leishmaniasis treatment. **Biomedicine & Pharmacotherapy**, 2018. v. 108, p. 1670–1678.

GIROIR, B. P. The time is now to end the HIV epidemic. **American journal of public health**, 2020. v. 110, n. 1, p. 22–24.

GONZALEZ, M. M. *et al.* β-Carboline derivatives as novel antivirals for herpes simplex virus. **International journal of antimicrobial agents**, 2018. v. 52, n. 4, p. 459–468.

GUERRERO-ALONSO, A.; ANTUNEZ-MOJICA, M.; MEDINA-FRANCO, J. L. Chemoinformatic Analysis of Isothiocyanates: Their Impact in Nature and Medicine. **Molecular Informatics**, 2021.

IMAMICHI, H. *et al.* Defective HIV-1 proviruses produce viral proteins. **Proceedings of the National Academy of Sciences**, 2020. v. 117, n. 7, p. 3704–3710.

IMANI, A. *et al.* Design, Synthesis, Docking Study and Biological Evaluation of 4-Hydroxy-2H-benzo [e][1, 2] thiazine-3-carboxamide 1, 1-dioxide Derivatives as Anti-HIV Agents. **Iranian Journal of Pharmaceutical Research**, 2021. v. 20, n. 3, p. 1–12.

IYER, K. *et al.* Diversity in heat shock protein families: functional implications in virus infection with a comprehensive insight of their role in the HIV-1 life cycle. **Cell Stress and Chaperones**, 2021. p. 1–26.

JIANG, H.; ZHOU, Y.; TANG, W. Maintaining HIV care during the COVID-19 pandemic. **The Lancet HIV**, 2020. v. 7, n. 5, p. e308–e309.

JUNIOR, A. B.; CAMOZZATO, N. M. A PrEP, o HIV e as táticas de desobediência. **Fórum Linguístico**, 2021. v. 18, n. 2, p. 6332–6350.

KUMAR, R. *et al.* Impact of chemoinformatics approaches and tools on current chemical research. **Chemoinformatics and Bioinformatics in the Pharmaceutical Sciences**. [S.l.]: Elsevier, 2021, p. 1–26.

LANGARIZADEH, M. A. *et al.* Phlorotannins as HIV Vpu inhibitors, an in silico virtual screening study of marine natural products. **Biotechnology and Applied Biochemistry**, 2021. v. 68, n. 4, p. 918–926.

LI, J. J. Gewald Aminothiophene Synthesis. **Name Reactions**. [S.l.]: Springer, 2021, p. 218–220.

LI, Y. *et al.* Drug resistance mutations in HIV provirus are associated with defective proviral genomes with hypermutation. **AIDS**, 2021. v. 35, n. 7, p. 1015–1020.

LUNA, I. S. Síntese e avaliação do potencial antimicrobiano de novos derivados 2-amino-tiofênicos obtidos a partir de 1, 4-ditiano-2, 5-diol. 2017.

MACHADO-ZALDÍVAR, L. Y. *et al.* Pretreatment HIV Drug-resistance Surveillance as a Tool for Monitoring and Control of the HIV/AIDS Epidemic in Cuba. **MEDICC review**, 2021. v. 23, n. 2.

MALAS, T. B. *et al.* Drug repurposing using a semantic knowledge graph. **DATA-DRIVEN KNOWLEDGE DISCOVERY IN POLYCYSTIC KIDNEY**, 2021. p. 75.

MELO, G. C. De *et al.* Tempo de sobrevida e distância para acesso a tratamento especializado por pessoas vivendo com HIV/Aids no estado de Alagoas, Brasil. **Revista Brasileira de Epidemiologia**, 2021. v. 24.

MONICA, G. La *et al.* Off-Target-Based Design of Selective HIV-1 PROTEASE Inhibitors. **International Journal of Molecular Sciences**, 2021. v. 22, n. 11, p. 6070.

MONTE, F. G. D.; OLIVEIRA ALVIM, H. G. DE. PLANEJAMENTO E SÍNTESE RACIONAL DE DERIVADOS DO NÚCLEO TETRAHIDROQUINOLINODIONA PARA PRODUÇÃO DE FÁRMACOS ANTICANCERÍGENOS. **Revista JRG de Estudos Acadêmicos**, 2021. v. 4, n. 8, p. 173–187.

NARENDER, G. Antimicrobial Activity of 2-Aminothiophene Derivatives. **BR Nahata Smriti Sansthan International Journal of Phramaceutical Sciences & Clinical Research**, 2021. v. 1, n. 1.

NEVES, W. W. *et al.* Incorporation of 2-amino-thiophene derivative in nanoparticles: enhancement of antifungal activity. **Brazilian Journal of Microbiology**, 2020. v. 51, n. 2, p. 647–655.

PRESANIS, A. M. *et al.* Trends in undiagnosed HIV prevalence in England and implications for eliminating HIV transmission by 2030: an evidence synthesis model. **The Lancet Public Health**, 2021. v. 6, n. 10, p. e739–e751.

REES, S. AZT/ABACAVIR. **Journal of Prescribing Practice**, 2021. v. 3, n. 4, p. 132.

ROCHA, J. C. Da. **A química do ranelato: aspectos fundamentais da estrutura eletrônica e reatividade**. Universidade de São Paulo.

SABNIS, R. W. **Novel Histone Deacetylase Inhibitors for Treating HIV Infection**. ACS Publications.

SADRAEIAN, M. *et al.* Selective cytotoxicity of a novel immunotoxin based on pulchellin A chain for cells expressing HIV envelope. **Scientific reports**, 2017. v. 7, n. 1, p. 7579.

SAHIN, K. Investigation of novel indole-based HIV-1 protease inhibitors using virtual screening and text mining. **Journal of Biomolecular Structure and Dynamics**, 2021. v. 39, n. 10, p. 3638–3648.

SAÚDE, M. Da. Protocolo clínico e diretrizes terapêuticas para manejo da

infecção pelo HIV em adultos. **Aids**, 2013.

SCANDELAI, G. A. B. **Avaliação in vitro e in silico das atividades inibidoras de urease e de acetilcolinesterase de chás comercializados em sachês**. Universidade Tecnológica Federal do Paraná.

SRIVASTAVA, V.; SELVARAJ, C.; SINGH, S. K. Chemoinformatics and QSAR. **Advances in Bioinformatics**. [S.l.]: Springer, 2021, p. 183–212.

STEENKAMP, P. Imidazo [1, 2-a] pyridin-3-amines as potential HIV-1 non-nucleoside reverse transcriptase inhibitors. [s.d.].

STOLBOV, L. *et al.* AntiHIV-Pred: web-resource for in silico prediction of anti-HIV/AIDS activity. **Bioinformatics**, 2020. v. 36, n. 3, p. 978–979.

STONE, J. *et al.* Estimating the contribution of key populations towards HIV transmission in South Africa. **Journal of the International AIDS Society**, 2021. v. 24, n. 1, p. e25650.

SUÁREZ, J. A. Q. *et al.* Synthesis of Tetrasubstituted Thiophenes Starting from Amino Mercaptoacrylates and α-brominated Acetamides. **Current Organic Chemistry**, 2021. v. 25, n. 6, p. 748–756.

TANEJA, V. **Methods and materials for assessing and treating arthritis**. Google Patents.

TEIRA, R. *et al.* Real world effectiveness of standard of care triple therapy versus two-drug combinations for treatment of people living with HIV. **PloS one**, 2021. v. 16, n. 4, p. e0249515.

TUNCBILEK, M. *et al.* Synthesis of novel 6-substituted amino-9-(β-d-ribofuranosyl) purine analogs and their bioactivities on human epithelial cancer cells. **Bioorganic & medicinal chemistry letters**, 2018. v. 28, n. 3, p. 235–239.

VAZ, T. A. Modelo de dados para treinamento de inteligência artificial na pesquisa em saúde: um estudo prático sobre infecções hospitalares. 2017.

WATERS, L. *et al.* The evidence for using tenofovir disoproxil fumarate plus lamivudine as a nucleoside analogue backbone for the treatment of HIV. **Journal of Virus Eradication**, 2021. p. 100028.

XIAO, T.; CAI, Y.; CHEN, B. HIV-1 Entry and Membrane Fusion Inhibitors. **Viruses**, 2021. v. 13, n. 5, p. 735.

YEO, J. Y. *et al.* Spontaneous mutations in HIV-1 gag, protease, RT p66 in the first replication cycle and how they appear: insights from an in vitro assay on mutation rates and types. **International Journal of Molecular Sciences**, 2021. v. 22, n. 1, p. 370.

ZHAO, J. *et al.* Human immune deficiency virus-related structural alterations in the brain are dependent on age. **Human brain mapping**, 2021.

ZHU, M. *et al.* Design and evaluation of novel piperidine HIV-1 protease inhibitors with potency against DRV-resistant variants. **European Journal of Medicinal Chemistry**, 2021. v. 220, p. 113450.

ANEXOS

Anexo I – Resumos expandidos

1. MONTEIRO, A.F.M.; SCOTTI, M. T. ; SCOTTI, L. . MOLECULAR DOCKING OF FRUCTOSE-DERIVED NUCLEOSIDE ANALOGS AGAINST REVERSE TRANSCRIPTASE OF HIV-1. In: MOL2NET 2019, International Conference on Multidisciplinary Sciences, 5th edition, 2019, João Pessoa. MOL2NET 2019, International Conference on Multidisciplinary Sciences, 5th edition, 2019.

2. **MONTEIRO, ALEX FRANCE MESSIAS**; MOURA, E. P. ; SOUSA, N. F. ; SANTANA, S. M. ; MURATOV, E. ; SCOTTI, M. T. ; SCOTTI, L. . In silico study of thiophenic heterocycles against Staphylococcus aureus target. In: MOL2NET 2019, International Conference on Multidisciplinary Sciences, 5th edition, 2019, João Pessoa. MOL2NET 2019, International Conference on Multidisciplinary Sciences, 5th edition, 2019. v. 1. p. 1-1.

3. MONTEIRO, ALEX FRANCE M.; SOUSA, N. F. ; MOURA, E. P. ; DAMASCENO, M. A. B. ; MURATOV, E. ; SCOTTI, MARCUS TULLIUS ; SCOTTI, LUCIANA . IN SILICO STUDIES FOR BIOACTIVE PROPOSAL AGAINST HUMAN RETINOBLASTOMA FROM 3,4,5-TRIHYDROXYCINAMIC ACID DERIVATIVES. In: MOL2NET 2019, International Conference on Multidisciplinary Sciences, 5th edition, 2019. MOL2NET 2019, International Conference on Multidisciplinary Sciences, 5th edition.

4. **MONTEIRO, ALEX FRANCE M.**; BEZERRA, A. H. R. ; MOURA, E. P. ; SOUSA, N. F. ; MURATOV, E. ; SCOTTI, M. T. ; SCOTTI, L. . Prediction of antifungal activity, cytotoxicity risks and molecular docking against Malassezia furfur of constituents of citronella essential oil (Cymbopogon winterianus). In: International Conference on Multidisciplinary Sciences, 2019, Joao Pessoa. International Conference on Multidisciplinary Sciences, 2019. v. 5. p. 0-0.

5. MOURA, E. P. ; **MONTEIRO, ALEX FRANCE M.** ; MAIA, M. ; RODRIGUES, G. ; MURATOV, E. ; SCOTTI, M. T. ; SCOTTI, L. . In silico study of various

compounds from essential oil of Cymbopogon winterianus against Pseudomonas aeruginosa targets. In: International Conference on Multidisciplinary Sciences, 2019, Joao Pessoa. International Conference on Multidisciplinary Sciences, 2019. v. 5. p. 0.

6. FRANCE, ALEX M. M.; LUNA, I. S. ; SCOTTI, M. T. ; SCOTTI, L. . In silico analysis of cytotoxicity, rate of absorption and molecular docking of natural products against protease, integrase and HIV-1 reverse transcriptase. In: I Simpósio Paraibano de Estudos Químicos de Produtos Naturais, 2018, João Pessoa. I Simpósio Paraibano de Estudos Químicos de Produtos Naturais, 2018.

7. Monteiro AFM; SCOTTI, M. T. ; SCOTTI, L. . MOLECULAR MODELING OF NUCLEOTIDE DERIVATIVES OF 2.5-DIHYDROFURAN-2,5-DIOL FOR EVALUATION OF POTENTIAL ANTITUBERCULAR ACTIVITY. In: International Conference on Multidisciplinary Sciences, 2018, Miami. MOL2NET 2018, International Conference on Multidisciplinary Sciences, 4th edition, 2018.

8. FRANCE, Alex M. M.; VIANA, J. O. ; BARROS, R. P. C. ; SCOTTI, M. T. ; SCOTTI, L. . PROPOSITION IN SILICO OF BENZOIC ANALOGS AGAINST Staphylococcus aureus. In: SRI-10: Summer Research Institute Symposium, MDC, Miami, FL, USA, 2018, 2018, Miami. MOL2NET 2018, International Conference on Multidisciplinary Sciences, 4th edition, 2018.

9. BEZERRA-FILHO, C.S.M. ; BARBOZA, J.N. ; **MONTEIRO, A.F.M.** ; LIMA, T. C. ; FERREIRA, A.R. ; MORAIS, MAYARA ; R.H. SILVA, N. ; OLIVEIRA, A.J.M.S. ; SILVA, C.R. ; CAMPOS, R.S. ; J.B. NETO, A. ; H.I. MAGALHÃES, F. ; H.V. JÚNIOR, N. ; CAVALCANTI, B. C. ; PERGENTINO DE SOUSA, DAMIÃO . ATIVIDADE ANTIFÚNGICA DE ÉSTERES BENZÓICOS E RELAÇÃO ESTRUTURA-ATIVIDADE (REA). In: ANAIS DO 5º ENCONTRO BRASILEIRO

PARA INOVAçãO TERAPêUTICA, 2017. Anais do 5º Encontro Brasileiro para Inovação Terapêutica, 2017.

10. BARBOZA, J.N. ; OLIVEIRA, A.J.M.S. ; **MONTEIRO, A.F.M.** ; FERREIRA, A.R. ; CAVALCANTI, B. C. ; SILVA, C.R. ; BEZERRA-FILHO, C.S.M. ; J.B. NETO, A. ; H.I. MAGALHÃES, F. ; H.V. JÚNIOR, N. ; MORAIS, MAYARA ; R.H. SILVA, N. ; CAMPOS, R.S. ; LIMA, T. C. ; PERGENTINO DE SOUSA, DAMIÃO . AVALIAÇÃO DA INIBIÇÃO DO CRESCIMENTO DE ESPÉCIES DE CANDIDA APÓS TRATAMENTO COM DERIVADOSCINÂMICOS. In: ANAIS DO 5º ENCONTRO BRASILEIRO PARA INOVAçãO TERAPêUTICA, 2017. Anais do 5º Encontro Brasileiro para Inovação Terapêutica, 2017.

Anexo I – Artigos Publicados

1. CAVALCANTI, ANDREZA B.S. ; DE FIGUEIREDO, PEDRO T.R. ; VELOSO, CARLOS A.G. ; RODRIGUES, GABRIELA C.S. ; DOS S. MAIA, MAYARA ; **MONTEIRO, ALEX FRANCE MESSIAS** ; RODRIGUES, VALNÊS S. ; CASTELO-BRANCO, ANA P.O.T. ; DE F. AGRA, MARIA ; FILHO, RAIMUNDO B. ; DA SILVA, MARCELO S. ; TAVARES, JOSEAN F. ; DE O. COSTA, VICENTE C. ; SCOTTI, LUCIANA ; SCOTTI, MARCUS T. . A new labdane diterpene from the aerial segments of Leptohyptis macrostachys (L'Hérit.) Harley & J.F.B. Pastore. Phytochemistry Letters JCR, v. 43, p. 117-122, 2021.

2. ALVES, D. ; COSTA, T. ; **FRANCE, Alex M. M.** ; LAZARANI, J. ; SCOTTI, M. T. ; ROSALEN, P. ; CASTRO, R. ; SCOTTI, LUCIANA . BIOSYNTHETIC CINNAMALDEHYDE: IN SILICO AND IN VITRO STUDY OF ANTIFUNGAL ACTIVITY AGAINST Candida spp. (OF CLINICAL INTEREST). MOLECULES JCR , v. 1, p. 1, 2020.

3. MONTEIRO AFM; SCOTTI, L. ; SCOTTI, M. T. . In Silico Studies of Potentially Active 2-Amino-Thiophenic Derivatives Against HIV-1. International Journal of Quantitative Structure-Property Relationships, v. 5, p. 100-119, 2020.

4. MAIA, MAYARA DOS SANTOS ; SILVA, JOANDA PAOLLA RAIMUNDO E ; NUNES, THAÍS AMANDA DE LIMA ; SOUSA, JULYANNE MARIA SARAIVA DE ; RODRIGUES, GABRIELA CRISTINA SOARES ; **MONTEIRO, ALEX FRANCE MESSIAS** ; TAVARES, JOSEAN FECHINE ; RODRIGUES, KLINGER ANTONIO DA FRANCA ; MENDONÇA-JUNIOR, FRANCISCO JAIME B. ; SCOTTI, LUCIANA ; SCOTTI, MARCUS TULLIUS . Virtual Screening and the In Vitro Assessment of the Antileishmanial Activity of Lignans. MOLECULES JCR, v. 25, p. 2281, 2020.

5. DOS SANTOS MAIA, MAYARA ; DE SOUSA, NATÁLIA FERREIRA ; RODRIGUES, GABRIELA CRISTINA SOARES ; **MONTEIRO, ALEX FRANCE MESSIAS** ; SCOTTI, MARCUS TULLIUS ; SCOTTI, LUCIANA . Lignans and Neolignans anti-tuberculosis identified by QSAR and Molecular Modeling.

COMBINATORIAL CHEMISTRY & HIGH THROUGHPUT SCREENING JCR, v. 23, p. 1, 2020.

6. RODRIGUES, GABRIELA CRISTINA SOARES ; DOS SANTOS MAIA, MAYARA ; DE MENEZES, RENATA PRISCILA BARROS ; CAVALCANTI, ANDREZA BARBOSA SILVA ; DE SOUSA, NATÁLIA FERREIRA ; DE MOURA, ÉRIKA PAIVA ; **MONTEIRO, ALEX FRANCE MESSIAS** ; SCOTTI, LUCIANA ; SCOTTI, MARCUS TULLIUS . Ligand- and structure-based virtual screening of Lamiaceae diterpenes with potential activity against a novel coronavirus (2019-nCoV). CURRENT TOPICS IN MEDICINAL CHEMISTRY JCR, v. 20, p. 1, 2020.

7. LUNA, EMANUELA COUTINHO ; LUNA, ISADORA SILVA ; SCOTTI, LUCIANA ; **MONTEIRO, ALEX FRANCE M.** ; SCOTTI, MARCUS TULLIUS ; DE MOURA, RICARDO OLÍMPIO ; DE ARAÚJO, RODRIGO SANTOS AQUINO ; MONTEIRO, KADJA LUANA CHAGAS ; DE AQUINO, THIAGO MENDONÇA ; RIBEIRO, FREDERICO FÁVARO ; MENDONÇA, FRANCISCO JAIME BEZERRA . Active Essential Oils and Their Components in Use against Neglected Diseases and Arboviruses. Oxidative Medicine and Cellular Longevity JCR, v. 2019, p. 1-52, 2019.

8. MONTEIRO, ALEX FRANCE MESSIAS; DE OLIVEIRA VIANA, JESSIKA ; MURATOV, ENGENE ; SCOTTI, MARCUS TULLIUS ; SCOTTI, LUCIANA . In Silico and Molecular Docking Studies That Address Viral (Std) Transmission Points. CURRENT PROTEIN & PEPTIDE SCIENCE JCR, v. 20, p. 1-1, 2019.

9. FRANCE, ALEX M. M.; VIANA, J. O. ; SCOTTI, M. T. ; SCOTTI, L. . The Azoles in Pharmacochemistry: Perspectives on the Synthesis of New Compounds and Chemoinformatic Contributions. CURRENT PHARMACEUTICAL DESIGN JCR, v. 25, p. 1-1, 2019.

10. MONTEIRO, ALEX FRANCE MESSIAS; DE OLIVEIRA VIANA, JESSIKA ;

JUNIOR, FRANCISCO JAIME BM ; ISHIKI, HAMIILTON M ; TCHOUBOUN, ERNESTINE NKWENGOUA ; DE ARAÚJO, RODRIGO SANTOS ; SCOTTI, MARCUS TULLIUS ; SCOTTI, LUCIANA . Recent Theoretical Studies Concerning Important Tropical Infections. CURRENT MEDICINAL CHEMISTRY JCR, v. 26, p. 1, 2019.

11. MONTEIRO, ALEX FRANCE MESSIAS; SCOTTI, MARCUS TULLIUS ; SPECK-PLANCHE, ALEJANDRO ; BARROS, RENATA PRISCILA COSTA ; SCOTTI, LUCIANA . In Silico Studies For Bacterystic Evaluation Against Staphylococcus Aureus Of 2-Naftomic Acid Analogues. CURRENT TOPICS IN MEDICINAL CHEMISTRY JCR, v. 19, p. 1-1, 2019.

12. SCOTTI, L. ; SCOTTI, M. T. ; **MONTEIRO AFM** ; VIANA, J. O. ; ISHIKI, H. M. ; YARLA, N. S. . Dengue Virus Inhibition Targets: A Review and Docking Study. CURRENT TOPICS IN MEDICINAL CHEMISTRY JCR, v. 18, p. 1522-1530, 2018.

13. **MONTEIRO, ALEX FRANCE M.**; VIANA, JÉSSIKA DE O. ; NAYARISSERI, ANURAJ ; ZONDEGOUMBA, ERNESTINE N. ; MENDONÇA JUNIOR, FRANCISCO JAIME B. ; SCOTTI, MARCUS TULLIUS ; SCOTTI, LUCIANA . Computational Studies Applied to Flavonoids against Alzheimer?s and Parkinson?s Diseases. Oxidative Medicine and Cellular Longevity JCR, v. 2018, p. 1-21, 2018.

14. SCOTTI, LUCIANA ; **MONTEIRO, ALEX FRANCE MESSIAS** ; DE OLIVEIRA VIANA, JESSIKA ; MENDONCA, FRANCISCO JAIME BEZERRA ; ISHIKI, HAMILTON M. ; TCHOUBOUN, ERNESTINE NKWENGOUA ; SANTOS, RODRIGO ; SCOTTI, MARCUS TULLIUS . Multi-Target Drugs Against Metabolic Disorders. Endocrine Metabolic & Immune Disorders-Drug Targets JCR, v. 19, p. 1-1, 2018.

Anexo III – Artigos relevantes ao tema da tese

Artigo 1: *In silico* studies of potentially active 2-amino-thiophenic derivatives against HIV-1

International Journal of Quantitative Structure-Property Relationships
Volume 5 • Issue 2 • April-June 2020

In Silico Studies of Potentially Active 2-Amino-Thiophenic Derivatives Against HIV-1

Alex France Messias Monteiro, Universidade Federal da Paraíba, Brazil
Marcus Tullius Scotti, Universidade Federal da Paraíba, Brazil
Luciana Scotti, Universidade Federal da Paraíba, Brazil
https://orcid.org/0000-0003-1866-4107

ABSTRACT

HIV is a virus that affects more than 37 million people worldwide, where only 23.3 million were receiving retroviral treatment by 2018, according to the World Health Organization (WHO). Three important enzymatic targets in the life cycle of HIV are: reverse transcriptase, protease and integrase; disease progression causes a decrease in CD4 + T lymphocytes, makes the infected organism vulnerable to opportunistic diseases. Therefore, much research aims to inhibit these enzymes to try to fight AIDS. This research aims to verify the use of silico techniques for an inhibitory activity of a set of 2-aminothiophenic drugs against these three enzymes, based on rational drug planning, virtual screening, and molecular modeling. To this end, many computational tools were used to generate data that improve the expectation of potential activity of these compounds. After all analyses, it was concluded that 12 of the 180 compounds tested may have potential activity against HIV-1 with low toxicological effects.

KEYWORDS

HIV, In Silico, Integrase, Molecular Modeling, Protease, Reverse Transcriptase

1. INTRODUCTION

Before the first clinical reports of HIV in 1981, the only knowledge of the disease was that it had a relationship with the human immune system and the bloodstream. The United States and some African countries performed intensive research on HIV since 1982, and from the results, the disease became known as AIDS (acquired immunodeficiency syndrome). In the mid-1980s in Brazil, the disease became known as the disease of the 5H: homosexuals, hemophiliacs, Haitians, heroin addicts and hookers (Goodkin et al., 2017; Goulart et al., 2018).

According to the World Health Organization (WHO), about 38 million people live with HIV worldwide, of these only 23.3 million infected received treatment by the end of 2018, accounting for 62% of the total infected. These numbers are increasingly attracting research in search of new anti-HIV drug candidates that offer a therapeutic effect with less negative impact on humans due to toxicity.

DOI: 10.4018/IJQSPR.2020040104

Because the life cycle of HIV is well elucidated, most research involving anti-HIV treatment assumes the need for inhibition of the 3 enzymes involved in viral multiplication: protease (PR), integrase (IN) and reverse transcriptase (RT). These are the most widely studied therapeutic targets for HIV-1 in Patel, Homaei, El-Seedi, & Akhtar, (2018).

Cheminformatics has grown over the years, and has made important contributions to pharmaceutical sciences, including the possibility to rationally design bioactive molecules for the treatment of diseases, by either the creation of new drugs or the structural modification existing drugs (Pinheiro-de-oliveira et al., 2018).

In silico methods have helped synthetic chemists, phytochemical specialists, and pharmacologists lower their input costs and time, as screening for a specific biological activity can be done using computational tools, with fewer resources than a classical laboratory experiment (Alves, 2014; Trossini, 2008).

With modern tools, it is possible to screen the candidate molecules based on molecular characteristics suitable for specific biological activity, to analyze the energies and ligand-receptor interactions at a given active site, to verify the stability and dynamic behavior of a ligand at a given receptor, and to perform chemometric analyses such as partial least squares (PLS), principal component analysis (PCA) and consensus PCA (CPCA), and theoretical pharmacophoric studies until proposing more promising biological profile structures (Cruz, 2016; Lopes & Figueiredo, 2018).

The aim of this research is the discussion of in silico studies involving 2-aminothiophenic against HIV-1, through the enzymatic inhibition of targets involved in the retroviral life cycle, and it is expected to contribute studies with retroviral activity, mainly HIV.

2. MATERIALS AND METHODS

In this paper, a virtual hybrid screening with 180 2-aminothiophenic compounds was initially performed (https://doi.org/10.6084/m9.figshare.9722099). The compounds were synthesized in the Synthesis Laboratory and Vectorization of molecules at UEPB (Paraíba State University) whose structures were provided by Professor Dr. Francisco Jaime Mendonça Júnior. This study consists of a ligand-based approach together with a combined form of protein-based approach. Thus, it is possible to obtain molecules with better pharmacological profiles in silico by analyzing bioavailability, absorption, cytotoxicity risks, ligand-receptor interaction, active site stability and prediction of biological activity (Hansmann, Miyaji, & Dressman, 2018).

Virtual screening is the classification of substances based on the characteristics that best explain observed biological activity. These features may serve as activity analogs and can be used to make improvements. This approach is known as rational drug planning and is widely used in drug research, contributing to the reduction of bench time in the synthesis of new bioactive compounds (Cavalcanti, 2018; Paz, 2017; Ellena, 2017; Santos, 2017).

The methodology of this research can be divided into 4 major steps, as shown in Figure 1: a) ADMET prediction: screening through prediction models (biological activity, absorption and intestinal permeability), prediction of cytotoxicity risks, oral absorption rate (% ABS) and Lipinski rule violations (LIP), b) multi-target molecular docking, c) *in silico* analysis of hepatic metabolites, and d) CPCA.

We perform *in silico* analysis of 2-amino-thiophenic compounds against the three HIV-1 proteins. The molecules were initially designed with the aid of ChemAxon MarvinSketch 18.4.0 software to obtain their 2D structures and then imported into HyperChemTM 7.5 software (800 cycles and RMS 0.1 kcal.Å-1.mol-1) for structure optimization using molecular mechanics (MM +) and semi-empirical (AM1) methods. The 3D structures of each molecule were obtained for the conformation calculated to have the lowest energy(Munir & Begum, 2019).

We used eighteen drugs marketed for HIV treatment via different pathways as controls, including protease inhibitors (iPR), integrase inhibitors (iIN), and transcriptase inhibitors (iRT). The analysis

Figure 1. Methodological scheme of this research

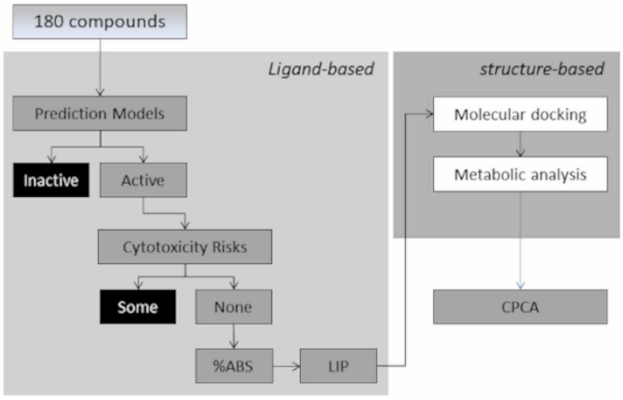

of the controls was performed following the same procedure outlined in the preceding paragraph. The controls used are shown in Table 1.

2.1. Molecular Descriptors

Molecular descriptors correspond to the structural characteristics of each molecule, and can be divided into 5 types: hybrid descriptors, constitutional descriptors, topological descriptors,

Table 1. Marketed anti-HIV drugs that served as controls in this research

ID	Inhibition	Name	Initials	%ABS	MUT	CAR	ESR	IRR	TOX
C01	iPR	Ritonavir	RTV	39.22	No	No	No	No	No
C02	iPR	Fosamprenavir	FPV	41.41	No	No	No	No	No
C03	iPR	Atazanavir	ATV	49.93	No	No	No	No	No
C04	iPR	Saquinavir	SQV	51.47	No	No	No	No	No
C05	iIN	Raltegravir	RAL	57.24	No	No	No	No	No
C06	iPR	Darunavir	DRV	57.66	No	No	No	No	No
C07	iRT	Tenofovir	TDF	58.56	No	No	No	No	No
C08	iPR	Nelfinavir	NFV	65.12	No	No	No	No	No
C09	iRT	Etravirine	ETR	67.38	No	No	No	No	No
C10	iPR	Lopinavir	LPV	67.60	No	No	No	Yes	Yes
C11	iPR	Tipranavir	TPV	69.68	No	No	No	No	No
C12	iRT	Lamivudine	3TC	69.86	No	No	Yes	No	Yes
C13	iRT	Zidovudine	AZT	72.83	Yes	Yes	Yes	No	Yes
C14	iRT	Abacavir	ABC	73.85	No	No	No	No	No
C15	iIN	Dolutegravir	DTG	74.78	No	No	No	No	No
C16	iRT	Didanosine	DDL	78.38	No	No	No	No	No
C17	iRT	Nevirapine	NVP	88.95	No	No	No	No	No
C18	iRT	Efavirenz	EFZ	95.78	No	Yes	No	No	Yes

% ABS = absorption rate; MUT = mutagenicity; CAR = carcinogenicity; IRR = tissue irritability; ESR = toxic effect on the reproductive system and TOX = risk of cytotoxicity.

electronic descriptors and geometric descriptors. The descriptors were calculated from the input file (usually an SDF file) containing all chemical structures to be analyzed. There are many programs for generating molecular descriptors, both simple, such as the free application at Java CDK Descriptor Calculator 4.8 (http://www.rguha.net/code/java/cdkdesc.html) (Pereira, Szwarc, Mondragao, Lima, & Pereira, 2018), and highly complex, such as the commercial Volsurf+ software (Sakagami et al., 2017).

Since the descriptors are essential for the construction of a prediction model and different software programs calculate different descriptors, two predictive models were made, one based on the descriptors calculated by CDK, and the other with the descriptors calculated by Volsurf+. It is possible to obtain a prediction by consensus by combining the two predictions. The reliability of the combined method is higher, and it provides more robustness (Moreira, 2014).

2.2. Ligand-Based Virtual Screening (LBVS)

2.2.1. Prediction Models of Activity, Intestinal Absorption and Intestinal Permeability

Prediction of biological activity is made using the statistical software KNIME Analytics Platforms 3.6 (Kausar & Falcao, 2018) to create a self-organizing map, integrating several data nodes to form the prediction model. The workflow used in this research can be found online (https://doi.org/10.6084/m9.figshare.7588595).

The model uses machine learning to classify each structure whose activity is to be predicted, based on its structural characteristics. This comparison is based on molecules classified as active at the time of model construction. Once the characteristics of active and inactive molecules are known, classification of molecules with unknown biological activity can be predicted by comparison (Barros et al., 2018).

We used a random forest (RF), which consists of a set of decision trees that randomly analyze molecules, for classification. The input compounds were partitioned into training (80%) and testing (20%) sets. Each tree in the forest makes a prediction, and the molecule is classified based on the class predicted by the majority of trees (Veríssimo et al., 2019).

Similarity is analyzed based on the molecular descriptors, where the descriptors of the model molecules are compared with those of the molecules whose activity is unknown. The table of molecules used in the construction of the model was divided into two equal groups based on the following criterion: molecules with the higher pIC50 (-log (IC50)) are assigned the label "A" (active) and others as "I" (inactive). Thus, classification of any structure that is within the model's applicability domain can be performed (Barros et al., 2018).

For the prediction to be statistically acceptable, the molecule must be within the applicability domain. This domain ensures that the characteristics of the molecules tested are known by the model. As the model is based on comparison by similarity, the applicability domain ensures that the predicted molecule has structural characteristics represented in the chemical space of the molecules used in the model construction. When the molecules used for testing and training are within same chemical space, prediction reliability is increased. The higher the percentage of applicability, the more reliable the prediction for the analyzed molecule (Acevedo, Scotti, & Scotti, 2018).

Weka Predictor 3.7 was used to predict activity by classifying molecules whose anti-HIV activity is not known. Adding RF machine learning and WPRED classification, the self-organizing map created with KNIME workflows has gained the attention of many researchers in the field of cheminformatics for its predictive efficiency and ease of configuration (Gultepe & Rashed, 2019).

In addition to the biological activity based on the IC50 of known anti-HIV molecules, prediction of intestinal permeability and absorption was performed using the spreadsheets provided by admetSAR @ LMMD. In this research, the same workflow created for the prediction of biological activity was used for predicting intestinal permeability and absorption, varying only the tables for the construction of the models.

2.2.2. Prediction of Cytotoxicity Risks

The molecules were imported into the free OSIRIS DataWarrior 5.0 software (http://www.openmolecules.org/datawarrior). In this program, the risk of toxicity is predicted by searching for known fragments in the molecules analyzed and comparing with an internal database. When found, the fragments generate a cytotoxicity alert with four parameters: mutagenicity, carcinogenicity, effect on the reproductive system and skin irritability. Total cytotoxicity is assigned a value of "No" when a molecule has no warnings for any of the four parameters analyzed by OSIRIS (Daggupati, Pamanji, & Yeguvapalli, 2018).

When necessary, cytotoxicity risk is used as a parameter to select molecules. When there is no cytotoxicity alert for any of the parameters, the likelihood of the molecule having toxic effect is low.

2.2.3. Oral Absorption Rate and Violations to Lipinski's Rule

To estimate violations to Lipinski's rule, we used the free program DruLiTo (http://www.niper.gov.in/pi_dev_tools/DruLiToWeb/DruLiTo_index.html), in which molecules are imported. The mass, LopP, hydrogen bond acceptors and donors, TPSA, total number of atoms and other structural characteristics can also be calculated simultaneously (Fereidoonnezhad, Mostoufi, Eskandari, Zali, & Aliyan, 2018).

The vast majority of retroviral drugs used in anti-HIV treatment come in the form of tablets or capsules and are easily administered orally to infected patients. Thus, it is possible to calculate the absorption rate of bioactive molecules based on their surface area. The total topological analysis was performed using the equation:

$$\%ABS = 109 - (TPSA \times 0.345)$$ (Zhao et al., 2002)

When using the absorption rate as an exclusion parameter in virtual screening, only molecules with % ABS greater than or equal to the lowest rate of the control drugs (ritonavir with 39.22%) are considered.

2.2.4. Consensus Principal Component Analysis – CPCA

Consensus principal component analysis was performed using the Volsurf + 1.0.7 software, which considered only the descriptor blocks that mostly contribute to data variability, making it possible to understand which electronic and structural properties are the most representative. In the data set studied, the estimated physicochemical characteristics may be hydrophobicity, lipophilicity, amphiphilicity and others (Huang et al., 2018).

Each block of descriptors has different relevance weights, after excluding descriptors that contribute to reducing the explanation of variance, and the most relevant blocks and descriptors for the set of molecules as a whole can be determined. This information is very important data for future work on the rational planning of new drugs (Scotti et al., 2014).

The SDF file containing the molecular structures used in the model construction was imported into the Volsurf+ software, which automatically calculates the 128 descriptors as the basis for CPCA analysis. As a parameter for accepting data from this analysis, many researchers consider values above 70%. Using this value for the remaining descriptors, as well as their blocks, the best represented set of molecules are studied (Scotti et al., 2012).

Interpretation of this analysis is possible by studying the blocks and the descriptors at the end of the model and determining which structural characteristics are most representative of the set of molecules. This data can be combined with data obtained from a study of the relationship between chemical structure and biological activity to plan new bioactive molecules (de Oliveira, 2016).

Interpretation of the descriptors after CPCA analysis is performed with the help of the software manual which is also available online with free registration: http://www.moldiscovery.com/product/

manual/vsplus. The manual describes all descriptors and their value ranges (when appropriate), which is used to decide on the acceptability of the values obtained for the compounds.

2.3. Structure Based Virtual Screening (SBVS)

2.3.1. Molecular Docking

Molecular docking was performed using the Molegro Virtual Docker 6.0 (MVD) program, and coupling was performed with the 3 proteins involved in the HIV-1 protease viral multiplication process (PR - PDB ID: 6DIF; Wong-Sam et al., 2018), integrase (IN - PDB ID: 1QS4; Goldgur et al., 1999) and reverse transcriptase (TR - PDB ID: 3LP0; Su et al., 2010). For interaction analysis, MolDockScores were considered to be interaction energies. The analogues that presented better values (lower values) of the total ligand-receptor interaction energy simultaneously for the 3 proteins were used for classification. The complexed ligands attached to each protein are shown in Figure 2.

As shown in Figure 2, each protein used presented a complexed ligand. For the construction of the coupling system, a template was created using these ligands as a reference, thus delimiting the region of the active site involved in molecular docking. With general standard strength, an energy grid resolution of 0.40Å was used for the MolDock Score [GRID], considering 1500 maximum interactions, a maximum population size of 50, an energy threshold of 100, and a neighbor distance factor equal to one. All water molecules were taken off the grid.

Thus, it is possible to map the interactions of common amino acid residues between the proteins studied and the analogues considered up to this stage of screening and determine the possibility of multi-target bioactivity for HIV-1. For this, we considered the median values for each data set containing the interaction energies of each protein, and the values below the median were classified as the best interaction profiles in the molecular docking as they presented the lowest energies for each data set.

All proteins studied had inhibitors coupled to their crystallographic structure taken from the Protein Data Bank (PDB) website (https://www.rcsb.org) with resolutions of 1.2Å to 6DIF, 2.1Å to 1QS4 and 2.79Å for 3LP0. These inhibitors were important because their presence was used to delimit the active site of each protein.

Figure 2. Binders of each protein used in this study

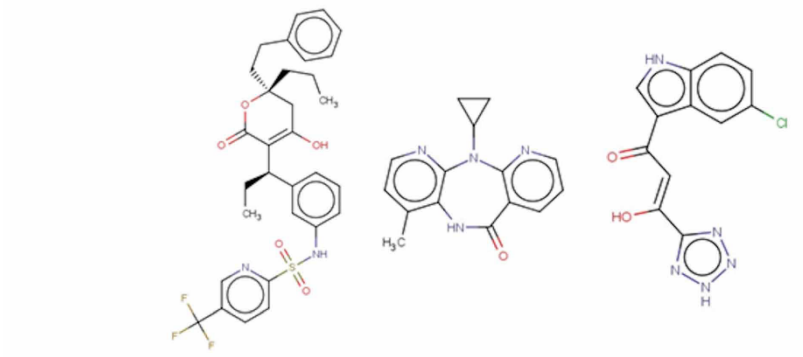

ID	TVP	NVP	100
PDB ID	6DIF	3LP0	1QS4
Formula	$C_{12}H_8ClN_3O_2$	$C_{15}H_{14}N_4O$	$C_{12}H_8ClN_3O_2$
Mol. Weight	289.68 g.mol^{-1}	266.30 g.mol^{-1}	289.68 g.mol^{-1}

For molecular docking validation, redocking was performed by calculating the RMSD (Hanwarinroj et al., 2019) for each protein, using the same parameters considered in the analogous docking. This RMSD was calculated based on the overlapping quality of the best complexed ligand-protein conformation.

2.3.2. Prediction of Hepatic Metabolites and Prediction of Risk of Metabolite Toxicity

To perform a metabolic study using computational methods, Molecular Discovery's METASITE 6.0 non-free software was used in this research. The software predicts the possible transformations suffered by a set of molecules in one or more cytochromes in some specific body regions such as skin, brain, liver and others. Each cytochrome is basically a protein responsible for transforming ingested substances through chemical reactions to promote its elimination by polarizing the structure (Latacz et al., 2019).

The 3D chemical structures of secondary metabolites from metabolism in the liver, brain and/or skin can be estimated by the software. This research considered only the liver transformations. The secondary metabolites generated were submitted to a biological activity prediction model, and cytotoxicity risks were compared to their respective metabolic abundances.

The cytotoxicity risk of each secondary metabolite was predicted using OSIRIS. Bioactive compounds that generated metabolites (having abundance above 75%) with cytotoxic parameters such as high mutagenicity and/or high carcinogenicity were disregarded in the selection of nucleoside analogues with the best profile. It is understood from this research that a drug candidate and its most abundant metabolites should have low or no cytotoxicity.

3. RESULTS AND DISCUSSION

It is possible to verify which of the 180 compounds initially submitted for prediction of biological activity against HIV-1 showed activity against any of the enzymes of interest involved in the retroviral replication cycle. Among these compounds, the model predicted that thirteen structures presented activity with probability ranging from 50.50% to 62.50%.

Based on the statistical data shown in Table 3, test and cross-validation (ROC) curves are shown graphically in Figure 3.

We obtained an accuracy (ACC) value of 0.813 for the test set, which is considered. For the biological activity of the compounds in the training set, a satisfactory accuracy value of 0.841 was obtained. other statistical parameters were also calculated to prove the model performance and reliability. The Matthews coefficient (MCC), which expresses the total correlation between the observed and the predicted data, was determined using the confusion matrix data. We obtained MCC values of 0.627 and 0.683 for the test and training data sets, respectively.

Table 3 shows the precision, sensitivity, specificity, positive predictive values and negative predictive values obtained. All values presented in Table 3 show satisfactory performance of the model, with values above 50%. Thus, the prediction of anti-HIV activity with our model is acceptable, having good data classification capacity (sensitivity and specificity) and high proportions of both true positives and true negatives.

After determining which molecules showed biological activity against HIV, it is necessary to discuss the prediction of internal absorption and intestinal permeability for these 13 active compounds. All compounds showed absorption and permeability in the intestine, suggesting their potential as new drugs candidates, as biological action depends on these pharmacological parameters (shown in Table 4). The compound ALX03 presented high intestinal permeability (CACO2), similar to the other compounds; however, its structure did not go through the domain of similarity, making the prediction less reliable. For intestinal absorption (HIA) all compounds have positive absorption, and all predictions were reliable according to the domain of similarity. Thus, compound ALX03 was

Table 2. Molecules approved by the prediction model of biological activity

ID	Structure	Domain	Activity	% Activity
ALX01	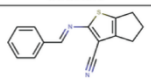	Reliable	A	51.00
ALX02	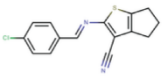	Reliable	A	50.50
ALX03	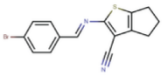	Reliable	A	54.00
ALX04	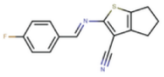	Reliable	A	56.50
ALX05	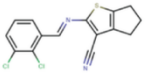	Reliable	A	53.00
ALX06	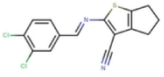	Reliable	A	51.50
ALX07	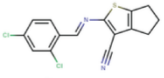	Reliable	A	55.50
ALX08	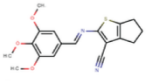	Reliable	A	56.00
ALX09	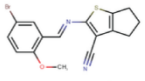	Reliable	A	55.50
ALX10	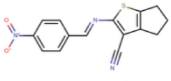	Reliable	A	50.00
ALX11	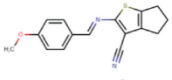	Reliable	A	62.50
ALX12	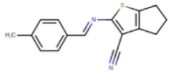	Reliable	A	53.00

Table 3. Sensitivity data, specificity and predictive values

	SENS	ESPEC	VPP	VPN
Test	0.788	0838	0,825	0,801
Validation	0,834	0,848	0,849	0,833

SENS = sensitivity; ESPEC = specificity; PPV = positive predictive value and NPV = negative predictive value.

Figure 3. Graphical representation of the performance of the KNIME activity prediction model

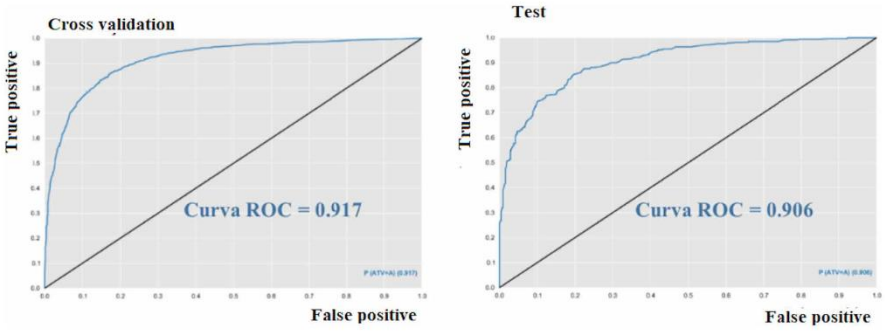

Table 4. Results of predictions of intestinal permeability and absorption

ID	CACO2	%CACO2	Domain CACO2	HIA	%HIA	Domain HIA
ALX01	High	97.5	Reliable	HIA+	97.0	Reliable
ALX02	High	93.0	Reliable	HIA+	97.0	Reliable
ALX03	High	94.0	Unreliable	HIA+	96.0	Reliable
ALX04	High	95.0	Reliable	HIA+	97.0	Reliable
ALX05	High	91.0	Reliable	HIA+	95.0	Reliable
ALX06	High	85.5	Reliable	HIA+	93.5	Reliable
ALX07	High	91.5	Reliable	HIA+	94.5	Reliable
ALX08	High	90.0	Reliable	HIA+	94.0	Reliable
ALX09	High	96.0	Reliable	HIA+	96.0	Reliable
ALX10	High	82.0	Reliable	HIA+	86.5	Reliable
ALX11	High	95.5	Reliable	HIA+	95.0	Reliable
ALX12	High	96.0	Reliable	HIA+	95.0	Reliable
ALX13	High	96.0	Reliable	HIA+	97.0	Reliable

also considered for the other analyses discussed in this paper. The probability that the results will be positive for both permeability and absorption ranges from 82.0% to 97.5%.

As discussed above, the statistical data of the anti-HIV biological activity model is shown in Table 3. In Table 5 we show statistical data for intestinal absorption and permeability predictions. The data show that the models created have good predictive capacity. The ROC curve data for the CACO2 model was 0.857 for the test group and 0.895 for the internal validation, while for the HIA model values of 0.828 and 0.962 were obtained for the test and validation sets, respectively.

Table 5. Statistical data of the intestinal absorption and permeability prediction model

		SENS	ESPEC	MCC	ACC	ROC
CACO2	Test	0.961	0.500	0.542	0.822	0.857
	Validation	0.966	0.501	0.567	0.855	0.895
HIA	Test	0.990	0.550	0.503	0.888	0.828
	Validation	0.993	0.500	0.618	0.922	0.962

In addition, the accuracy for both models ranged from 0.822 to 0.922 (where the accuracy measures how well the model makes correct predictions), as shown in Table 5, and the Matthews coefficient was above 0.5.

The generated model presented high sensitivity ranging from 0.990 to 0.961. That is, the model correctly classifies positive data points. In general, the intestinal absorption and permeability models have good predictive capacity and great true positive rates, making the models applicable for this research.

The next stage of screening is the prediction of cytotoxicity risks, taking into account the parameters MUT, CAR, IRR, And ESR (as mentioned in the methodology) with the aid of the free OSIRIS software. The results are shown in Table 6. Only the ALX09 compound presented high risk of mutagenicity, and therefore will not be considered for the next virtual screening steps proposed by this study. Only the remaining 12 compounds were considered in the next screening step.

In the third screening stage, the oral absorption rate was calculated based on the topological polar surface area of the molecules. According to the computational data obtained, the absorption rate of the 12 compounds was greater than 86%, with up to a single violation of Lipinski's rule, as shown in Table 7. By combining this data with the intestinal absorption and intestinal permeability data discussed earlier, it is possible to expect acceptable bioavailability for the compounds analyzed, since bioavailability also depends on these pharmacokinetic parameters. Obviously, bioavailability also depends on non-structural factors, and the structural factors discussed give hope for the good availability of these bioactive compounds in the body.

For the fourth stage of virtual screening, three molecular docking studies were performed with the 12 studied 2-aminothiophenic compounds. The compounds showed promising ligand-receptor interaction energies (shown in Table 8): between -90.892 and -101.77550 kcal·mol^{-1} for protease (PDB ID-6DIF); between -49.6111 and -62.7756 kcal·mol^{-1} for integrase (PDB ID 1QS4); and between -69.2519 and -104.2340 kcal·mol^{-1} for reverse transcriptase (PDB ID 3LP0). It is worth noting that the RMSD values for protease, integrase and reverse transcriptase are to 0.6460Å, 0.1685Å, and 0.0921Å, respectively, proving that the data discussed for molecular anchoring are reliable.

Table 6. OSIRIS cytotoxicity (TOX) risk prediction data on mutagenicity (MUT), carcinogenicity (CAR), skin irritability (IRR) and reproductive toxicity (ESR)

ID	MUT	CAR	ESR	IRR	TOX
ALX01	None	None	None	None	No
ALX02	None	None	None	None	No
ALX03	None	None	None	None	No
ALX04	None	None	None	None	No
ALX05	None	None	None	None	No
ALX06	None	None	None	None	No
ALX07	None	None	None	None	No
ALX08	None	None	None	None	No
ALX09	High	None	None	None	Yes
ALX10	None	None	None	None	No
ALX11	None	None	None	None	No
ALX12	None	None	None	None	No
ALX13	None	None	None	None	No

Table 7. Oral absorption rate and violations to Lipinski's rule

ID	LIP	TPSA	%ABS
ALX01	0	45.38	93.34
ALX02	0	65.61	86.36
ALX03	0	36.15	96.53
ALX04	0	45.38	93.34
ALX05	1	36.15	96.53
ALX06	1	36.15	96.53
ALX07	1	36.15	96.53
ALX08	0	45.38	93.34
ALX10	0	55.45	89.87
ALX11	0	64.68	86.69
ALX12	0	84.91	79.71
ALX13	0	41.46	94.70

Table 8. Interaction energies [kcal·mol^{-1}] of 2-aminothiophenes and controls for the studied targets of HIV-1

ID	Protease enzyme (PDB ID 6DIF)	Integrase enzyme (PDB ID 1QS4)	Reverse transcriptase enzyme (PDB ID 3LP0)
ALX01	-90.8942	-58.7974	-76.2132
ALX02	-99.6043	-55.5293	-84.1309
ALX03	-94.8946	-49.8185	-83.9773
ALX04	-100.8580	-58.4837	-84.8189
ALX05	-97.3425	-48.4355	-70.7422
ALX06	-104.7070	-54.2600	-90.5419
ALX07	-93.7137	-61.5629	-88.6091
ALX08	-109.1880	-49.6111	-100.1410
ALX10	-96.7010	-55.9553	-92.5705
ALX11	-98.2041	-59.0573	-86.5163
ALX12	-100.7390	-57.0031	-69.2519
ALX13	-101.7550	-62.7756	-87.3791
C01	-84.9299	-77.3905	-82.6159
C02	-72.4624	-75.5680	-177.3560
C03	-76.2692	-96.4926	-157.9830
C04	-115.2570	-71.3740	-183.0290
C05	-63.4924	-86.1126	-113.6810
C06	-127.4050	-84.9255	-219.2790
C07	-103.0210	-148.4980	-116.8440
C08	-69.6643	-41.6490	-150.5600
C09	-26.9554	-67.2550	-95.4293
C10	-48.5037	-65.1455	-129.9620
C11	-47.6569	-68.6211	-125.0450
C12	-38.1601	-68.7104	-96.2246
C13	-34.5039	-49.4436	-84.4204
C14	-77.1986	-77.0027	-125.6800
C15	-27.6528	-63.3550	-104.3090
C16	-54.3136	-54.2284	-112.8810
C17	-28.3280	-40.8529	-114.3160
C18	-34.0594	-59.7443	-119.0220

Based on the data presented in Table 8, it is possible to rank the synthetic compounds derived from 2-aminothiophene, the eighteen controls considered in this research and the respective ligands complexed together with each enzyme used (inhibitor, -186.2840 kcal·mol^{-1}). Regarding protease, as shown in Figure 4, compounds ALX08 and ALX06 showed better ligand-receptor interaction results than all controls studied, followed by compounds ALX02, ALX04, ALX12, ALX13. These compounds showed better results with the C12, C13, C14, C15, C16, and C17 controls (-86.9380, -76.8993, -96.7212, -98.3940, -62.5355 and -74.7124 kcal·mol^{-1}, respectively) that are not protease-specific inhibitors, i.e., none of the 2-aminothiophenics studied in this research showed better results in molecular docking against the protease enzyme.

For integrase (Figure 5), the controls C02, C03, C05 and C07 showed better values than the protein complexed ligand itself (-77.6691, -102.2670, -87.8983, and -77.4944 kcal·mol^{-1}, respectively).

Figure 4. Rank between 2-aminothiophenics, the ligand complexed with the chosen protein and the controls against HIV-1 protease

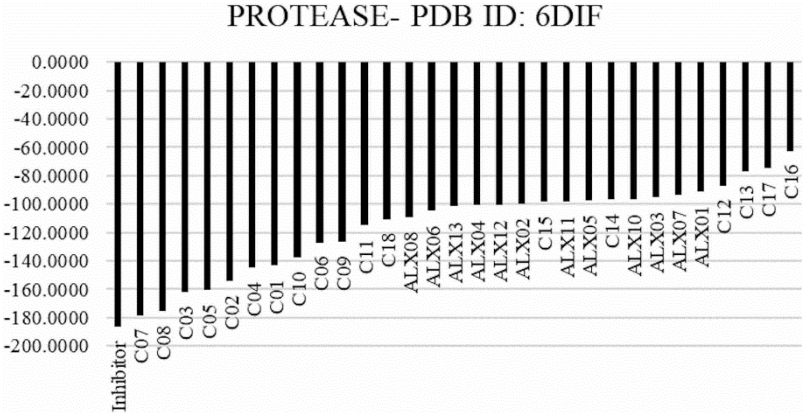

Figure 5. Rank between 2-aminothiophenics, the ligand complexed with the chosen protein and the controls against HIV-1 integrase

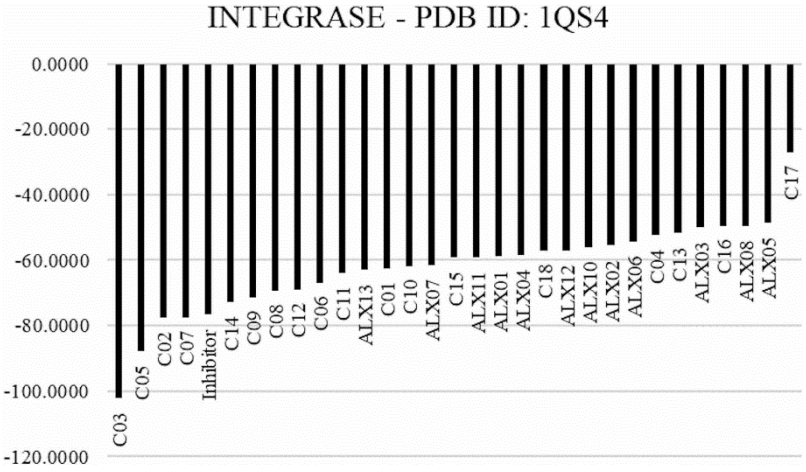

Compound ALX13 had a better total ligand-receptor interaction energy result than the commercial specific inhibitor and control C15 (Dolutegravir, -59.2802 kcal.mol-1); however, C05 (Raltegravir), another integrase inhibitor considered in this research, presented the second best energy result against the integrase used (PDB ID 1QS4), just after the C03 control (Atazanavir) which is a protease inhibitor.

The reverse transcriptase dose of the eighteen controls had better results in molecular docking, including on the ligand complexed with the chosen enzyme PDB ID 3LP0 (-112.1650 kcal·mol^{-1}). According to Figure 6, compound ALX08 showed better ligand-receptor interaction energy than controls C09 (Etravirin, -97,6803 kcal·mol^{-1}) and C13 (Zidovudine, -84.3775 kcal.mol-1); compounds ALX04, ALX06, ALX07, ALX10, ALX11 and ALX13 also showed better results than AZT in molecular docking with the PDB ID 3LP0 enzyme.

We examine the interactions between the amino acid residues of each protein with the best four poses of the ligand-protein complexes. The amino acid residues and interactions of some molecular docking poses are shown in Table 9. The protease inhibitor presented two hydrogen bond type interactions with the Arg25 and Ile50 residues; the latter can also be found in the control C04 (Saquinavir, commercial protease inhibitor), also as hydrogen bond, and as a steric interaction in the ALX10 compound.

For integrase, the C05 control (Raltegravir, commercial integrase inhibitor) showed lower energy and hydrogen bond type interactions with Asn155, Asp64, Gln148 and Asp116 residues, where Asn155 can also undergoes hydrogen bonding with the complex inhibitor. Together with the protein (which had the second lowest energy for this enzyme), residues Thr66, Lys156 and Lys159 are present as steric interaction in all poses selected for this protein.

For reverse transcriptase, the control C18 (Efavirenz, commercial reverse transcriptase inhibitor) showed hydrogen bond type interactions with residues Tyr181, Tyr318, His235 and Pro236, where Tyr181 residue also has steric interactions in all poses. Pro236 and His235 residues showed steric interactions in pose ALX08. The interactions described in Table 9 are shown graphically for all four poses selected for each of the three proteins in Figure 7.

In order to finalize the virtual screening proposed in this research, the possible hepatic metabolites for the compound doses analyzed were predicted. In addition, the cytotoxicity risks (mutagenicity, carcinogenicity, toxic effect on the reproductive system and tissue

Figure 6. Ranking between the 2-aminothiophenics, the ligand complexed with the chosen protein and the controls against HIV-1 reverse transcriptase

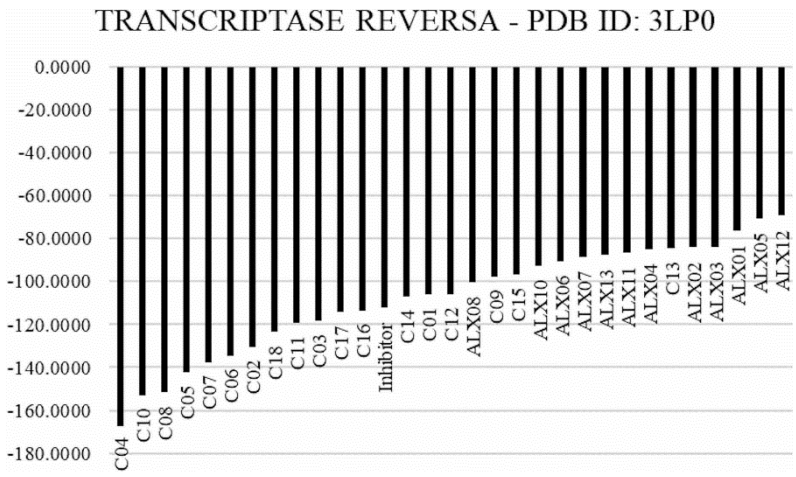

Table 9. Interaction type and amino acids residues in molecular docking study

Protein	Pose	Energy [kcal.mol-1]	Residues of aminoacid	
			Interaction type	Residues
6DIF	Inhibitor	-186.28	H-Bond	Arg25 and Ile50
			Steric	Arg8 and 2(Val82)
6DIF	C04	-144.78	H-Bond	Ile50
			Steric	2(Ile50), Gly27, Ile84 and 3(Pro81)
6DIF	ALX13	-101.75	H-Bond	Asp25
			Steric	Gly48
6DIF	ALX10	-96.70	H-Bond	None
			Steric	Ile50
1QS4	C05	-87.89	H-Bond	Asn155, Asp64, Gln148 and Asp116
			Steric	4(Leu63), Asp116, 2(Thr115), 2(Lys159), 2(Thr66), Lys156, 3(Asp64), 2(Asn155), 2(Ile152) and 3(Glu152)
1QS4	Inhibitor	-70.60	H-Bond	2(Thr66), Asn155, Lys156 and Lys159
			Steric	2(Glu152) and Lys159
1QS4	ALX13	-62.77	H-Bond	Glu152
			Steric	Asn155, Lys156, Lys159, Thr66, Asp64 and Gln148
1QS4	ALX12	-57.00	H-Bond	None
			Steric	Thr66, Lys159, Lys156, Asp64 and Gln148
3LP0	C18	-123.53	H-Bond	Tyr181, Tyr318, His235 and Pro236
			Steric	5(Tyr181), Pro95, 3(Trp229), Leu234, His235, Pro236, Gly190, 4(Val174), Ile100 and Lys101
3LP0	Inhibitor	-112.16	H-Bond	None
			Steric	Tyr188 and Lys101
3LP0	ALX08	-100.14	H-Bond	None
			Steric	2(Leu234), Pro236, His235, Val106, Tyr235, 2(Pro95) and 2(Tyr181)
3LP0	ALX02	-84.13	H-Bond	None
			Steric	3(Tyr181)

irritability) were estimated as detailed in the methodology. Compound ALX01 showed no cytotoxicity risks in any of the four parameters for the ten metabolites generated. Similarly, we find no cytotoxicity risk for the metabolites of ALX02-ALX04 and ALX10. Low and high cytotoxicity risks were found for the remaining compounds with some of the studied toxicological parameters; however, none of the 2-aminothiophenic compounds approved in the prediction model of biological activity presented cytotoxic risks for the highest scoring metabolites (above 60%). Thus, none of the compounds were excluded from this last step of the proposed virtual screening. Liver metabolite analysis data can be found in the spreadsheet available online at https://doi.org/10.6084/m9.figshare.9794288.

The higher-scoring metabolites did not present cytotoxicity (shown graphically in Table 10). The plots in Table 10 correspond to each sample analyzed by METASITE. According to these graphs, the compound ALX01 presented four metabolites with a score of 100%, where the abscissa axes correspond to the predicted metabolite codes. Thus, in the spreadsheet provided, it is possible the smiles of each metabolite for each 2-aminothiophene derivative are shown, in addition to the cytotoxicity risks. As the following figure already shows which metabolites have the highest scores (in red), and the objective of this analysis is to verify the cytotoxicity risks of the highest scoring metabolites, no further discussion of the graphs is necessary.

Some properties must be defined to finalize the hybrid virtual screening proposed in this research. For this, a CPCA analysis was performed for the approved molecular screening dose molecules,

Figure 7. Interactions between poses and their studied proteins: (a) protease inhibitor; (b) C04 protease control; (c) ALX13 with protease; (d) ALX10 with protease; (e) C05 control with integrase; (f) Integrase inhibitor; (g) ALX13 with integrase; (h) ALX12 with integrase; (i) C18 control with RT; (j) RT inhibitor; (k) ALX08 with RT; and l) ALX02 with RT. Blue dotted lines correspond to hydrogen bonds, and red dotted lines to steric interactions.

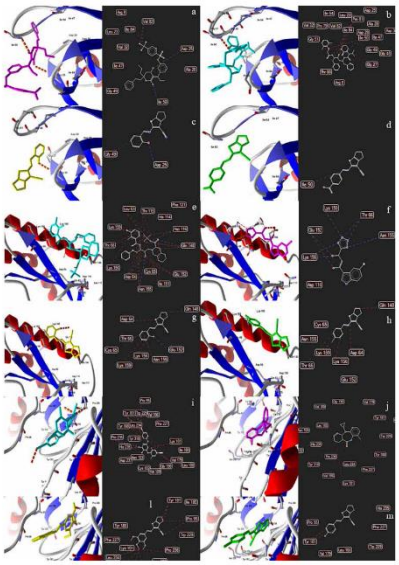

so it was expected to verify the possibility of amphiphilicity through the descriptor blocks. From these 2-aminothiophenic derivatives the molecules were imported into Volsurf +, and the molecular descriptor blocks that best explain the biological activity were determined, as shown in the descriptor blocks that explained the variability of the data in 95.28% STRUCT, MISC, LOGD, TOPP, FLU, DRY, MODEL and LOGS (Figure 8).

From the loading graph generated after performing the Volsurf+ CPCA analysis, there are 8 descriptors that are worth highlighting. These descriptors are shown in Table 11: four of the descriptors correspond to hydrophobic regions of the molecule and the remaining four correspond to hydrophilic regions, leading to the assumption of an amphiphilic character of the molecule.

However, the Volsurf+ software calculates an amphiphilic moment descriptor (A) for this, which is not among the descriptors used for the CPCA model. The descriptor corresponds to the vector from the hydrophobic center to the hydrophilic center, and its length corresponds to the amphiphilic capacity of compounds needed to permeate a membrane. An average of the estimated for the moment of amphiphilicity of the compounds was 4.6017. The thiophene derivatives, ALX02, ALX04, ALX05, ALX08, ALX08 and ALX10, presented above average values of A, while the compounds ALX01, ALX03, ALX11 and ALX12 showed an A value greater than or equal to 4.3024. From the data presented in Table 12, eleven of the analyzed compounds have amphiphilic character, while ALX13 does not, with A = 1.6312.

4. CONCLUSION

Based on the data presented by the virtual screening and CPCA, the tested compounds showed promising anti-HIV character, and should be tested biologically to validate the *in silico* results.

Table 10. Plots of hepatic metabolite ranking for 2-aminothiophenic derived doses

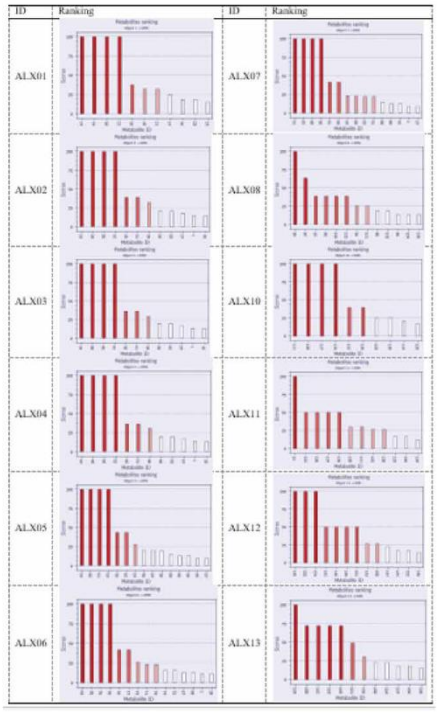

Figure 8. Graphic of block weights for CPCA

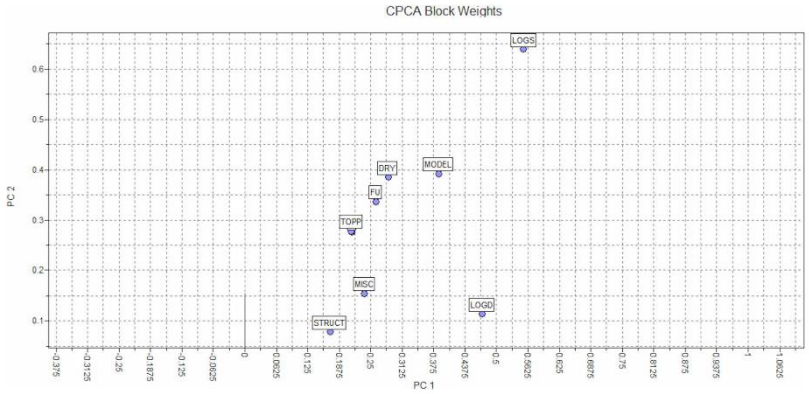

Table 11. Descriptors generated from CPCA

Descriptors	Description	Regions
D1	Hydrophobic Volumes	Hydrophobic
D6		
CD3	Capacity Factors	
CD4		
WO4	H-donor volumes	Hydrophilic
WO5		
HL1	Hydrophilic-lipophilic balance	
HL2		

Table 12. Amphiphilic moment descriptor for the 2-aminothiophenes studied

ID	A
ALX01	4.3396
ALX02	4.6126
ALX03	4.4654
ALX04	4.6349
ALX05	5.2862
ALX06	4.3024
ALX07	5.0413
ALX08	4.6159
ALX10	7.5628
ALX11	4.3210
ALX12	4.4077
ALX13	1.6312

In addition, cytotoxicity tests are necessary to confirm that these compounds can be used new retroviral drugs.

The results presented in this research are encouraging, as it indicates 13 possible candidates for new retroviral drugs, with the possibility of reduced toxic effects when compared to many commercial drugs according to the results of this study. Research such as this is expected to direct studies of new bioactive drugs against HIV, reducing the toxic effects of AIDS therapy.

Based on these analyses, the compounds presented interactions with the three chosen targets against HIV-1: protease, integrase and reverse transcriptase. Complementing this conclusion with the cytotoxicity risk data of the metabolite analogues, a therapeutic response can be expected from the lowest to the highest concentrations.

REFERENCES

Acevedo, C. H., Scotti, L., & Scotti, M. T. (2018). In Silico Studies Designed to Select Sesquiterpene Lactones with Potential Antichagasic Activity from an In-House Asteraceae Database. *ChemMedChem*, *13*(6), 634–645. doi:10.1002/cmdc.201700743 PMID:29323468

Alves, V. de M. (2014). Desenvolvimento de modelos de QSAR e análise quimioinformática da sensibilização e permeabilidade da pele.

Barros, R. P. C., da Cunha, E. V. L., Catão, R. M. R., Scotti, L., Souza, M. S. R., Brás, A. A. Q., & Scotti, M. T. (2018). Virtual screening of secondary metabolites of the genus Solanum with potential antimicrobial activity. *Revista Brasileira de Farmacognosia*, *28*(6), 686–691. doi:10.1016/j.bjp.2018.08.003

Berto Pereira, G., Szwarc, B., Mondragao, M. A., Lima, P. A., & Pereira, F. (2018). A Ligand-Based Approach to the Discovery of Lead-Like Po tassium Channel KV1. 3 Inhibitors.

Cavalcanti, É. B. V. S. (2018). Estudos quimiotaxonômicos e triagem virtual de flavonoides isolados da família asteraceae com potencial atividade leishmanicida.

Cruz, S. M. D. M. da. (2016). Desenvolvimento de uma abordagem computacional para a descoberta de compostos-líderes para fármacos anticancerígenos.

Daggupati, T., Pamanji, R., & Yeguvapalli, S. (2018). In silico screening and identification of potential GSK3β inhibitors. *Journal of Receptors and Signal Transduction*, *38*(4), 279–289. doi:10.1080/10799893.2018.1478854 PMID:29947280

Ellena, J. A. (2017). Caracterização no estado sólido de fármacos anti-HIV: planejamento racional de novas formas cristalinas.

Félix, M. B., de Souza, E. R., de Lima, M. D. C., Frade, D. K. G., Serafim, V. D. L., Rodrigues, K. A. D. F., & de Aquino, T. M. et al. (2016). Antileishmanial activity of new thiophene–indole hybrids: Design, synthesis, biological and cytotoxic evaluation, and chemometric studies. *Bioorganic & Medicinal Chemistry*, *24*(18), 3972–3977.

Fereidoonnezhad, M., Mostoufi, A., Eskandari, M., Zali, S., & Aliyan, F. (2018). Multitarget Drug Design, Molecular Docking and PLIF Studies of Novel Tacrine– Coumarin Hybrids for the Treatment of Alzheimer's Disease (Autumn 2018). *Iranian Journal of Pharmaceutical Research*. PMID:30568682

Goldgur, Y., Craigie, R., Cohen, G. H., Fujiwara, T., Yoshinaga, T., Fujishita, T., & Davies, D. R. et al. (1999). Structure of the HIV-1 integrase catalytic domain complexed with an inhibitor: A platform for antiviral drug design. *Proceedings of the National Academy of Sciences of the United States of America*, *96*(23), 13040–13043. doi:10.1073/pnas.96.23.13040 PMID:10557269

Goodkin, K., Miller, E. N., Cox, C., Reynolds, S., Becker, J. T., Martin, E., & Sacktor, N. C. et al. (2017). Effect of ageing on neurocognitive function by stage of HIV infection: Evidence from the Multicenter AIDS Cohort Study. *The Lancet. HIV*, *4*(9), e411–e422. doi:10.1016/S2352-3018(17)30098-X PMID:28716545

Goulart, A., da Silva, D. V., de Carvalho Carnevali, A., Reis, E. de F. P., Dias, R. A. P., & Carlos-Bender, J. (2018). O conhecimento de estudantes sobre o hiv/aids e a importância de jogos e teatro na reconstrução de conceitos relacionados ao tema. *Ensino, Saude e Ambiente*, *11*(2).

Gultepe, Y., & Rashed, S. (2019). The Use of Data Mining Techniques in Heart Disease Prediction.

Hansmann, S., Miyaji, Y., & Dressman, J. (2018). An in silico approach to determine challenges in the bioavailability of ciprofloxacin, a poorly soluble weak base with borderline solubility and permeability characteristics. *European Journal of Pharmaceutics and Biopharmaceutics*, *122*, 186–196. doi:10.1016/j.ejpb.2017.10.019 PMID:29111469

Hanwarinroj, C., Phusi, N., Batthong, S., Chayajarus, K., Ariyachaokun, K., Kamsri, P., … Suttisintong, K. (2019). Elucidating the binding interaction and binding free energy of DprE1 inhibitors via molecular docking calculations and molecular dynamics simulations.

Huang, S., Zhang, D., Mei, H., Kevin, M., Qu, S., Pan, X., & Lu, L. (2018). SMD-based interaction-energy fingerprints can predict accurately the dissociation rate constants of HIV-1 protease inhibitors. *Journal of Chemical Information and Modeling*, *59*(1), 159–169. doi:10.1021/acs.jcim.8b00567 PMID:30422654

Kausar, S., & Falcao, A. O. (2018). An automated framework for QSAR model building. *Journal of Cheminformatics*, *10*(1), 1. doi:10.1186/s13321-017-0256-5 PMID:29340790

Latacz, G., Lubelska, A., Jastrzębska-Więsek, M., Partyka, A., Marć, M. A., Satała, G., & Kamińska, K. et al. (2019). The 1, 3, 5-Triazine Derivatives as Innovative Chemical Family of 5-HT6 Serotonin Receptor Agents with Therapeutic Perspectives for Cognitive Impairment. *International Journal of Molecular Sciences*, *20*(14), 3420. doi:10.3390/ijms20143420 PMID:31336820

Lopes, D. A., & Figueiredo, Â. (2018). Fios que tecem a história: o cabelo crespo entre antigas e novas formas de ativismo. *Opará: Etnicidades, Movimentos Sociais e Educação*, *6*(8).

Moreira, R. F. (2014). Determinação do perfil farmacocinético de medicamentos contendo fármacos de ação central.

Munir, S., & Begum, M. (2019). Computational investigations of a novel photoactive material for potential application in dye sensitized solar cells. *Asian Journal of Green Chemistry, 3*, 91–102. doi:10.22034/ajgc.2018.136899.1077

Patel, S., Homaei, A., El-Seedi, H. R., & Akhtar, N. (2018). Cathepsins: Proteases that are vital for survival but can also be fatal. *Biomedicine and Pharmacotherapy*, *105*(April), 526–532. doi:10.1016/j.biopha.2018.05.148 PMID:29885636

Paz, O. S. (2017). Triagem in silico e avaliação in vitro de compostos antifalcizantes.

Pinheiro-de-Oliveira, T. F., Fonseca Jr, A. A., Camargos, M. F., Laguardia-Nascimento, M., de Oliveira, A. M., Cottorello, A. C., ... Barbosa-Stancioli, E. F. (2018). Development of a droplet digital RT-PCR for the quantification of foot-and-mouth virus RNA. Journal of virological methods, 259, 129-134. doi:10.1016/j.jviromet.2018.06.015

Sakagami, H., Uesawa, Y., Masuda, Y., Tomomura, M., Yokose, S., Miyashiro, T., & Terakubo, S. et al. (2017). Quantitative structure–cytotoxicity relationship of newly synthesized piperic acid esters. *Anticancer Research*, *37*(11), 6161–6168. PMID:29061797

Santos, M. L. A. dos. (2017). Estudos químicos-computacionais, farmacocinéticos e toxicológicos in silico de derivados azaindóis do ácido hidroxâmico, inibidores da enzima integrase do HIV-1.

Scotti, L., Tullius Scotti, M., Barros Silva, V., Regina Lima Santos, S., & Cavalcanti, C. H. (2014). Chemometric studies on potential larvicidal compounds against Aedes aegypti. *Medicinal Chemistry (Shariqah, United Arab Emirates)*, *10*(2), 201–210. doi:10.2174/15734064113099990005 PMID:23676010

Scotti, L., Tullius Scotti, M., de Oliveira Lima, E., Sobral da Silva, M., do Carmo Alves de Lima, M., da Rocha Pitta, I., & Bezerra Mendonça, F. J. et al. (2012). Experimental methodologies and evaluations of computer-aided drug design methodologies applied to a series of 2-aminothiophene derivatives with antifungal activities. *Molecules (Basel, Switzerland)*, *17*(3), 2298–2315. doi:10.3390/molecules17032298 PMID:22367025

Su, H. P., Yan, Y., Prasad, G. S., Smith, R. F., Daniels, C. L., Abeywickrema, P. D., & Munshi, S. et al. (2010). Structural basis for the inhibition of RNase H activity of HIV-1 reverse transcriptase by RNase H active site-directed inhibitors. *Journal of Virology*, *84*(15), 7625–7633. doi:10.1128/JVI.00353-10 PMID:20484498

Trossini, G. H. G. (2008). Antichagásicos potenciais: busca racional de compostos com ação seletiva pela cruzaína. <ALIGNMENT.qj></ALIGNMENT>10.11606/T.9.2008.tde-17102014-152528

Veríssimo, G. C., Dutra, E. F. M., Dias, A. L. T., de Oliveira Fernandes, P., Kronenberger, T., Gomes, M. A., & Maltarollo, V. G. (2019). HQSAR and random forest-based QSAR models for anti-T. vaginalis activities of nitroimidazoles derivatives. *Journal of Molecular Graphics & Modelling*, *90*, 180–191. doi:10.1016/j.jmgm.2019.04.007 PMID:31100677

Wong-Sam, A., Wang, Y. F., Zhang, Y., Ghosh, A. K., Harrison, R. W., & Weber, I. T. (2018). Drug Resistance Mutation L76V Alters Nonpolar Interactions at the Flap-Core Interface of HIV-1 Protease. *ACS Omega*, *3*(9), 12132–12140. doi:10.1021/acsomega.8b01683 PMID:30288468

Zhao, Y. H., Abraham, M. H., Le, J., Hersey, A., Luscombe, C. N., Beck, G., & Cooper, I. et al. (2002). Rate-limited steps of human oral absorption and QSAR studies. *Pharmaceutical Research*, *19*(10), 1446–1457. doi:10.1023/A:1020444330011 PMID:12425461

Currently, there has been a frequent use of molecular docking in the planning and discovery of drug candidates by their coupling in the protein targets, being able to predict the orientation of the ligand when it is bound to a protein receptor or enzyme using shape, H-bond and electrostatic interactions to quantify it [8]. In this type of orientation the binding affinity between the two molecules can be observed by calculating scoring functions [9, 10], which represents potentiality of binding.

In the last decades, the number of docking tools and programs have been developed for academic and commercial, like FlexX [11], GOLD [12], AutoDock [13, 14], DOCK, Cdocker and LigandFit [15], Surflex [16], MCDock, FRED [17], Glide [18], AutoDock Vina [19], MOE-Dock [20], LeDock [21] Dock [22], among others. The strategies of positioning of the binder differ for each software used, varying with the use of predictive algorithms such as genetic algorithms (GOLD), systematic technique (Glide) and Monte Carlo simulation (LigandFit).

In the study by Wang *et al.* (2016) [23] the accuracy of the AutoDock Vina, GOLD and MOE-Dock programs was observed, possessing the abilities in producing the correct binding mode of a ligand. However, interactions between small molecules and receptors still depend on experimental methods, since current anchoring methods do not simulate solvent effects, entropic effects, and protonation stages of residues in the active site. The accelerated rhythm of research in this field has been very usual in several fields of research and can be approached more accurately in the near future.

3. EBOLA VIRUS DISEASE

The agent that causes Ebola Virus Disease (EVD) is an RNA virus belonging to the Filoviridae family and Ebolavirus genus. There are currently about five different Ebolavirus strains, the species *Zaire ebolavirus* (EBOV), *Sudan ebolavirus* (SUDV), *Tai Forest ebolavirus* (TAFV), *Bundibugyo ebolavirus* (BDBV) and *Reston ebolavirus* (RESTV). EBOV occurs in a higher proportion [24] for being the most lethal of the five strains [25]; and RESTV is not pathogenic for humans.

The World Health Organization (WHO) reported the incidence of Ebola as epidemic and as a public health emergency in 2014, registering a total of 6,553 new cases, with 3,083 deaths. These increasing levels have been aggravated by economic, and sociocultural factors, as well as by delays in identification of the disease, which involve lack of supplies to control the infection, a shortage of healthcare professionals in the affected localities and the absence of epidemiological surveillance to identify new cases [26].

In the Congo, Ebola birth rates have reached an incidence of up to 90%. The incubation period ranges from 2 to 21 days, with symptoms ranging from fever, weakness, vomiting, diarrhea, headache, and throat pain, to internal and external hemorrhages with multiple dysfunctions [27]. Infections can occur as caused by infected hosts, such as nonhuman primates; by direct contact between humans through body fluids or contaminated surfaces [28]; by manipulation of the bodies of deceased [29] with high viral loads presenting transmission through direct contact in cases of unsafe burials; and among health workers who are not fully protected. A fourth point of transmission can occur through sexual intercourse, skin-to-skin contact, and body secretions. Studies have reported the presence of the virus in vaginal, rectal, and seminal fluids [30], and in some cases the presence of the virus in semen samples has been reported after 157 days.

The persistence of EBOV, particularly in the semen of male survivors, raises the risks of sexual transmission [31]. Previously, EVD survivors had been advised to practice sexual abstinence or to use a condom during sexual activity until 3 months after recovery. These recommendations were based on EBOV detection results from semen samples obtained from eight survivors of EVD and/or Marburg virus disease in prior epidemics. The longest period that the infectious virus was detected in the semen after the onset of symptoms was 82 days [32].

Subsequent investigations revealed EBOV RNA in a survivor's semen at 199 days after the onset of symptoms; the genetic sequence coincided with the sample obtained from the patient of the case [33]. Although no infectious virus has been detected in such semen specimens; the possibility remains that infectious EBOV could persist in the semen of the survivor for up to 6 months after the onset of symptoms. This led the WHO and the Center for Disease Control (CDC) to revise their guidelines as to the time that survivors should practice safe sex through sexual abstinence or in particular, with the use of condoms [28, 34].

Mate *et al.* (2015) [35] demonstrated sexual transmission from a male EVD survivor to his partner after 179 days of the disease. The assembled blood and semen genomes confirmed direct sexual transmission, and presented three substitutions that were not present in other EVD sequences of West Africa.

Despite occasional reports of Ebola virus RNA in patients without evidence of sexual transmission, the suggestion that there are theoretical reasons to consider sexual transmission of the contagion has maintained relevance. Because of the potential risk, EVD survivors need to abstain from sex, or use condoms for up to 3 months after the disease's onset [36]. There is also a need to provide guidance to patients and health agents on the subject. Genomic surveillance, as used to elucidate viral origin and transmission [37], may well help to determine the relevance of sexual transmission and its role. All the while, no drugs or vaccines are yet available to cure EBOV.

3.1. Targets

Genetic studies are being used to identify better measures against the disease. The EBOV RNA genome encodes seven polypeptides, including glycoprotein (GP), nucleoprotein (NP), RNA-dependent RNA polymerase (L), and viral proteins VP35, VP30, VP40 and VP24 [38, 39]. Study of these targets serves to understand their functions and promotes the development of potential drug inhibitors [40]. Studies that address structure-based drug design include the 3D structure of the proteins in docking studies with individual small molecules. Such studies calculate docking scores and binding energies, and identify lead compounds which present the

properties and appropriate profiles needed for clinical development [41]. In this review, molecular docking studies in EVD proteins to develop potential inhibitors for the disease will be reported.

3.1.1. Glycoprotein

Infection with EBOV initiates through fusion between the host cell membrane and the viral glycoprotein (GP) membrane [42]. The GP is formed by a trimer of three disulfide-linked GP1-GP2 heterodimers which are produced during virus assembly through proteolytic cleavage of the GP0 precursor polypeptide [43]. The process occurs via the GP1 subunit, which mediates adhesion to host cells, while the GP2 subunit carries out membrane fusion [44]. Similar fusion processes are observed in other viruses, such as the protein envelope (Env) of the human immunodeficiency virus (HIV), and hemagglutinin (HA) of the influenza virus [45].

EBOV GP is a principal target for designing vaccines and inhibitors [46]. The virus enters the cell through receptor-mediated endocytosis through clathrin-coated pits and caveolae, followed by actin and microtubule-dependent transport to the endosome, where GP is further processed by endosomal cathepsins [47].

In molecular docking studies developed by Ahmad *et al.* (2017) [48] to simulate their constructed models; 5 strong interactions between the glycoprotein and inhibitors derived from dronedarone, amiodarone, and benzofurano were observed. A good score and interaction affinity with residues Arg164 and Ala109 were respectively observed in portions of the arene-arene interaction with benzene ring, and with the hydrogen atom of the hydroxyl group (Fig. **1a**).

In studies of ADMET properties and molecular docking with the Ebola virus glycoprotein another *in silico* study [49] demonstrated potential antiviral drug activities for Fostemsavir and 20 Vicriviroc analogues. The drug screen selected molecules which presented considerable binding energies. One of the analogues, AC1LA8DY, formed bonds with the target protein and interacted with the Thr217, Thr223, Asn257, Thr216, Glu258, and Ala114 residues (Fig. **1b**).

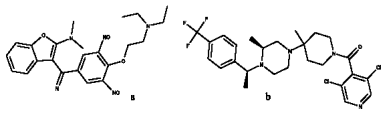

Fig. (1). Compounds presenting activity against Ebola virus glycoprotein **a**) Amiodarone; **b**) AC1LA8DY.

3.1.2. VP35

The Ebola VP35 protein has become a strong target candidate; it acts as a component of the viral RNA polymerase complex. Its activity hinders host interferon (IFN) production, and is vital to the virulence of the Ebola virus. Studies have reported that dsRNA-binding when focused on Arg312 has a high conservation rate and can be considered as a crucial factor for the virulence of EBOV [50]. Reynard and coworkers (2011) [51] reported that disruption of the VP35 protein leads to reduced viral amplification and mortality rates in rats, it is considered a target in the development of drugs against the Ebola virus.

Molecular docking studies for VP35 have been developed by several research groups. In studies carried out by Ekins *et al.* (2014) [52] molecular docking studies were performed using the inhibitors amodiaquine, chloroquine, clomiphene and toremifene. From the pharmacophoric characteristics of compounds with VP35 structures, it was observed that amodiaquine and chloroquine presented the best scores for the protein, with residues Lys248, Ile295, and Gln244 being essential for the activity (Figs. **2a-b**).

Glanzer (2016) [53] employed molecular docking with the VP35 structure to enrich a population of compounds for further *in vitro* testing to approximately 80,000 compounds. Virtual screening triggered the selection of four compounds with IC_{50} of 20 μM, and one compound at 4 μM; demonstrating that Arg305 and Lys339 permit large degrees of freedom, Lys319 and Arg322 present lower degrees of freedom, and Lys309 and Arg312 present bimodal activity. These studies demonstrate the value of *in silico* docking when enriching compounds for *in vitro* testing (Fig. **2c**).

In another study, Ren and coworkers (2016) [54] collected 144 inhibitors of VP35 (EBV) containing the same core scaffolds. Applying virtual screening methodologies and employing docking studies to predict pharmacophore, and a 3D QSAR models triggered identification of seven potential inhibitors with novel scaffolds identified as new VP35 inhibitors. Interactions with Gln241, Lys248, Ile195, Ile303, Pro304 and Phe328 were essential for the activity (Fig. **2d**).

Sulaiman (2018) [55] virtually screened docking and ADME predictions for almost 36 million compounds based on the VP35 structure. In total, 5 compounds with high receptor affinities were selected, of which compound A appeared to be a potential lead compound, with interactions that include interaction with Ala221 and Ile295; alkyl interactions with Lys248, Val245 and Pro 293; hydrogen bonding with Gln241 and Gln244; cation interaction with Lys248; interaction with Ile295; amide stacked interaction with Cys247; and alkyl interactions with Pro304, which could further directing study (Fig. **2e**).

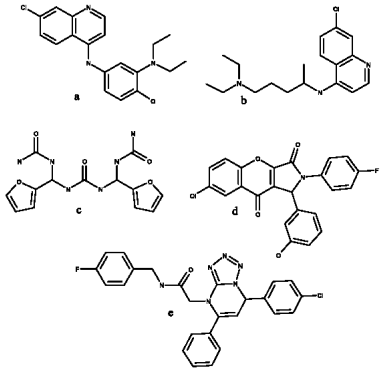

Fig. (2). Compounds presenting activity against Ebola virus VP35 **a**) amodiaquine; **b**) Chloroquine; **c**) ZINC5328460; **d**) CPD5; and **e**) compound A.

3.1.3. VP30

VP30 also acts in the formation of viral mRNAs. Due to its homo-oligomerization function, VP30 is a potential target for antiviral treatment [56]. The protein is about 30 kD in size and presents phospho-proteins that shield the RNA in the presence of zinc [57] and is associated with the viral RNA synthesis machinery [58]. Studies have also implicated VP30 in regulation of co-transcriptional editing of viral glycoprotein mRNAs, and in re-initiation of viral transcription [59].

Raj *et al.* (2016) [40] carried out predictive ADME property studies and molecular docking with four Ebola virus proteins VP40, VP35, VP30 and VP4 using flavonoid derivatives to identify potential lead compounds. The screening used 4500 compounds. Gossypetin and Taxifolin presented the best docking scores and binding energies for the four study proteins; superior to the study's control drug (BCX4430) (Fig. **3a-b**).

Shah and coworkers (2015) [60] evaluated 56 compounds anchored to the VP40, VP35 and VP24 proteins. As a result, they found that the compounds Deslanoside and Digoxin had the best interaction energy values with Asn130 (acting as a common residue in all compounds). Residues that could be considered essential for activity were Asn130 and Gln329 for VP35, and Ser151, Arg154, Ser155 and Lys39 for VP24 (Fig. **3c-d**).

Setlur and coworkers (2016) [61] screened 150 herbal compounds to identify their potential activity in the VP24, VP30, VP35 and VP40 proteins using computational ADMET property studies and molecular docking. Limonin, Samarcandin and Gummosin derivatives demonstrated high affinity with the VP24 and VP35 enzymes, curcumin presented strong inhibition for VP30 (Fig. **3e-g**).

3.1.4. VP40

One of the most abundant proteins in the viral bilayer; VP40 is responsible for structural integrity, is formed in the plasma membrane, and requires lipid raft micro-domains [62]. It performs important viral roles involving the viral RNA and the host cell [63]. Its structure is based on the connection of N-terminal and C-terminal domains by residues of up to 200 amino acids. The C-terminal domain of VP40 acts as a potential target drug because of its role in membrane association [64]. The N-terminal domain is responsible for oligomerization of the protein. The C-terminal domain comprises a proline rich region conserved in the VP40 EBOV receptor and ranges from 205-219 amino acids.

Mirza *et al.* (2016) [65] performed virtual screening of 145,329 natural products, evaluating the pharmacokinetic properties of predicted metabolic sites and molecular docking against the VP35 and VP40 proteins. For molecular docking, the best virtual hits were selected; with Lys251 being a critical residue for VP35, and Thr123, Phe125 and Arg134 being critical for VP40 (Fig. **4a**).

El-Din (2016) [66] performed molecular docking to the VP40 protein using the Lamarckian Genetic Algorithm with 1800 molecules drawn from the PubChem database based on the structure of pyrimidine-2,4-dione. In total, 7 molecules presented promising results against EBOV, with interactions present at Arg134 and Asn136, and according to Lipinsk's rules they were nontoxic (Fig. **4b**).

Abazari (2015) [67] analyzed a library containing 120,000 molecules for ADME properties and simulated potential activity against the EBOV VP40 protein. In this virtual screening, 10 compounds were selected that presented the best profiles, and which resulted in 4 chemicals that could bind VP40 subunits in a manner which (by steric interference) condenses and prevents protein matrix oligomerization. They are being considered as structural hits for anti-Ebola treatment (Fig. **4c**).

Karthick (2016) [68] performed virtual screening of the PLANTS package, an algorithm designed to efficiently rank potential candidates and find a lead compound (against the VP40 protein) based on docking scores, Lipinski rules, and molecular dynamics simulations. The study showed that emodin-8-beta-D-glucoside from the Traditional Chinese Medicine Database (TCMD) qualifies as a lead candidate with critical interaction residues at Phe125 and Arg134, and interactions as an inhibitor of amino acids vital to viral replication (Fig. **4d**).

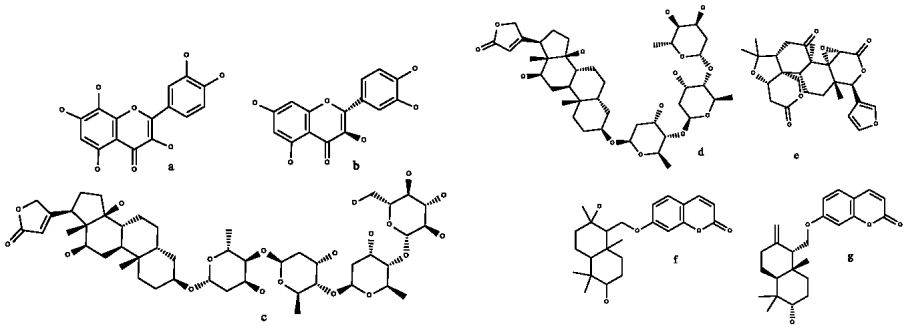

Fig. (3). Compounds presenting activity against Ebola virus VP30. **a**) Gossypentin; **b**) Taxifolin; **c**) Deslanoside; **d**) Digoxin; **e**) Limonin; **f**) Samarcandin; **g**) Gummosin.

Further studies, based on the construction of VP40 protein inhibitors and to find possible alignments between them were carried out by Patel (2013) [69]. The construction of these models and docking studies performed with 1500 drug compounds from the COPICAT server led to the selection of 4 ligands with potential anti-Ebola activity (Fig. **4e**).

Skarivachan (2016) [70] studied the therapeutic potential of metabolites extracted from bacteria associated with the marine sponge (*Cliona sp.*) and tested against the Ebola virus VP40 target. *In vitro* studies, computational virtual screening, and molecular docking were used. In this study, the natural products Gymnastatin, Sorbicillactone, Marizomib and Daryamide were found through molecular docking to possess high protein energy affinity, with strong hydrogen interactions at the residues Leu32, Gly126, Lys127, Ala128 and Phe135, suggesting their potential as lead molecules for novel drugs (Fig. **4f**).

Tamilvanan and Hopper (2013) [71] applied High Throughput Virtual Screening and molecular docking studies to the Traditional Chinese Medicine and Asinex compound databases to find inhibitors against VP40. The Thr123, Phe125, Arg134 residues were found to be essential for binding to the protein, 10 compounds were identified as potent inhibitors of the VP40 matrix protein (Fig. **4g**).

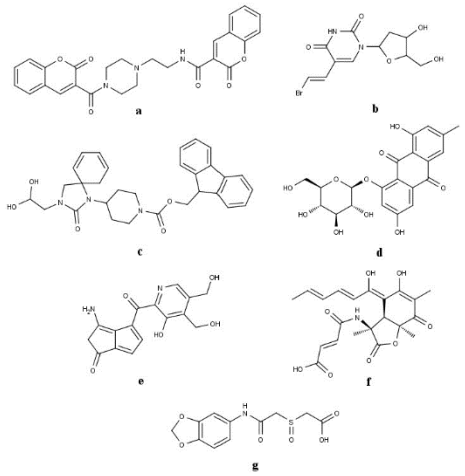

Fig. (4). Compounds presenting activity against Ebola virus VP40. **a**) 2-Oxo-N-(2-{4-((2-oxo-2H-chromen-3-yl)carbonyl)-1-piperazinyl}ethyl)-2H-chromene-3-carboxamide; **b**) Pubchem416724; **c**) compound A; **d**) Emodin-8-β-Glucoside; **e**) compound 1 (Patel, 2013); **f**) Sorbicillactone A; **g**) ASN03576800.

3.1.5. VP24

The EBV VP24 structural protein has been shown to inhibit host interferon (IFN) signaling [72], and also influence transcription and replication in a region of the EBOV genome [73]. The role of the VP24 protein is not yet fully understood; however, it is known to act as a structural protein and may play a role in the virion assembly process. The VP24 protein is expressed in a set with nucleoprotein (NP), and VP35 [74].

Tambunan (2016) [75] virtually screened 2,020 natural Indonesian products from various sources and carried out analyses of their molecular and pharmacological characteristics, Molecular docking simulations were also performed. Cycloartocarpine presented the best potential for anti-Ebola activity (Fig. **5a**).

Tambunan *et al.* in 2018, [76] through *in silico* experiments also identified other VP24 protein inhibitors. In their study, 242,520 compounds were submitted to virtual screening based on pharmacological properties and molecular docking analysis. The compounds, L833, L217 and L595 presented the best results; and compound L595 was considered the most promising lead candidate for inhibiting Ebola virus VP24 (Fig. **5b**).

Sharmila and coworkers (2016) [77] evaluated the activity of andrographolide using molecular docking against three Ebola virus proteins: VP40, VP35, and VP24. The high affinity of the compound for the three proteins of the study, hydrogen bonds and hydrophobic interactions between the compound and the active site of the receptor were found to be responsible for mediating the biological activity (Fig. **5c**).

Sharma (2017) [78] using amino acid sequence homology generated a VP24 protein model and then anchored structural derivatives of Oseltamivir, (which is the first-line drug used to treat Ebola hemorrhagic fevers). From the study, 20 new compounds were found that presented good scores and are potential VP40 inhibitors (Fig. **5d**).

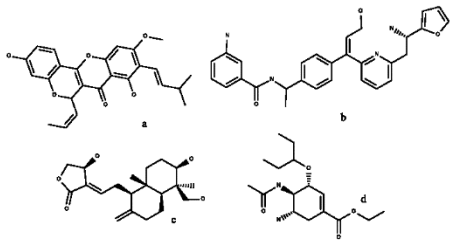

Fig. (5). Compounds presenting activity against Ebola virus VP24. **a**) Cycloartocalpin; **b**) L595; **c**) Andrographolide; **d**) Oseltamivir.

3.1.6. Nucleoprotein

The RNA genome of the Ebola virus exists in its encapsulated form because nucleoprotein (NP) forms a ribonucleoprotein (RNP) complex together with RdRp [79]. RNA serves as a co-packaged (and RNA-dependent) RNA polymerase complex (RdRp) transcribing mRNA of the viral genome. After the virus enters the host cell via glycoproteins, RNP is released from the virion. The function of the nucleocapsid is to protect ssRNAs from degradation [80].

Baikerikar (2017) [81], in molecular docking studies demonstrated the potential activity of curcumin derivatives against the VP40, VP30, VP35, GP and NP proteins of Ebola. The derivative bisdemethoxycurcumin presented excel-

lent binding affinity; with interactions at residues Pro131, Ala128 and Pro165 for VP40; Thr335, Val294 and Leu249 for VP35; Ala246 and Phe181 for VP30; Arg154, Leu158 for VP24; Leu593 and Trp597 for Glycoprotein (GP). If taken as a separated group; (VP35, GP, and VP30); tetrahydrocurcumin presented better binding affinity than curcumin. The molecular docking performed for nucleoprotein presented interactions at residues Arg559, Leu561, Phe630, Ala562 and Leu558. Curcumin binds to NP at residues required for the formation of nucleocapsid structures and replication of the viral genome, thus interrupting its activity (Fig. **6**).

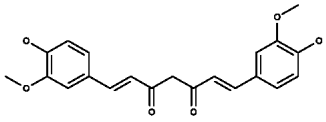

Fig. (6). Curcumin compounds present activity against Ebola virus nucleoprotein.

4. HERPES DISEASE

Herpes simplex virus (HSV), affecting the lives of human hosts through cold sores and genital herpes takes two forms: that of herpes simplex virus type 1 (HSV-1), and herpes simplex virus type 2 (HSV-2) [82]. After entering latency, HSV remains present at nerve ganglia and may emerge later to cause a recurrent and active infection. Herpes viruses are divided into three groups: α herpes viruses which include herpes simplex virus types 1 and 2 and varicella-zoster virus; β herpes viruses which include cytomegalovirus and human herpes viruses 6 and 7; and γ herpes viruses which include Epstein-Barr virus and human herpes virus 8 [83].

HSV-1 causes an oropharyngeal infection, and is transmitted primarily by non-genital contact. HSV-2 is almost exclusively sexually transmitted, causing genital herpes, which can cause ulcerative and vesicular lesions in adults [84]. Ulceration of the genital area may evolve into transmission of the human immunodeficiency virus (HIV) [85].

In the United States HSV-2 is one of the most common sexually transmitted diseases. Many more cases are recorded in Africa (31.5%), followed by the Americas (14.4%), and these exists a high prevalence in women [86]. HSV-2 is transmitted via exposure to the surface of the genital mucosa, leading to latency in the sacral ganglia. Several studies have explored treatments during pharmacological interventions, and vaccines have been developed for Herpes Simplex Virus Type 2 [87].

In many cases HSV is asymptomatic. However, when symptoms do occur, small genital or anal blisters are often characterized, and may include ulcers at the site of infection with fevers, body aches, and swollen lymph glands [85]. Even if the disease is not lethal, the resurgence of the disease can dramatically affect one's life. To treat HSV, several studies have reported the use of synthetic analogues, such as the nucleosides acyclovir, valacyclovir, famcyclovir and penciclovir [88]. Upon activation by viral thymidine kinase these drugs inhibit the activity of viral DNA polymerase [89]. However, if treatment is delayed until late in the infectious process or until after reactivation of the disease, it hinders the effectiveness of the treatment, making cases of viral resistance increasingly reported in compromised individuals [90].

Kolb *et al.* (2017) [91] performed sequential analyses and phylogenetic comparison of 6 HSV-2 isolates, determining the existence of genomic mosaicism and 4 polymorphisms, as well as low inter-strain diversity for HSV-2. Thus, significantly improved anti-HSV agents with broad therapeutic efficacy are being targeted by those in the field of drug research.

4.1. Targets

HSV codes seven proteins that act in the replication and propagation of the virus [92], they include helicase activity, binding proteins, heterodimeric DNA polymerase, single-stranded (ss) DNA-binding protein, and heterotrimeric helicase-primase. However, for the development of inhibitors, few receptors present sufficient capacity as targets [93].

4.1.1. Herpes Simplex Virus Type II Protease

Herpes Simplex Virus Type II Protease is a homodimeric structure comprised of a seven-stranded β -barrel structure with seven α -helices. The active site of the protease is in a shallow groove along the β -barrel surface [94]. For serine proteases, the catalytic mechanism involves a serine nucleic attack on the carbonyl carbon of the scissile bond of the substrate, resulting in an enzyme-serine acyl intermediate awaiting further hydrolysis [95].

Searching the literature, only one article on molecular docking as applied to HSV type II; Arunkumar and Rajarajan (2018) [96] evaluated the efficacy of compounds obtained through *Punica granatum* by means of *in vitro* and *in silico* studies of ADMET properties and HSV-2 protein targets with molecular docking. The compound punicalagin presented moderate absorption, low permeability, and low blood brain barrier penetration. For viral protease, punicalagin presented hydrogen bond interactions with amino acids Arg157, Ser131, Ser129, and Thr132, at the active site of the protease.

4.1.2. Regulator Complex gH/gL

Among the accessory proteins that act as HSV machinery glycoproteins gB, gD, gH and gL, mediate membrane fusion events for entry and virus-induced cell fusion. Deletion of any of these four glycoproteins results in mutant virions that cannot penetrate host cells [97]. Normally, activated forms of gD interact with gH/gL to carryout virus-cell or cell-cell fusion. However, the details of this path still remain unknown [98]. The gH/gL heterodimeric complex acts as a fusion component of all herpes viruses, being considered a target of HSV neutralizing antibodies. In HSV-2 the gH protein contains 3 domains: An N-terminal domain that binds gL, a central helical domain and a C-terminal β -sandwich domain; the second and third domains are conserved in EBV and HSV [99].

In the same article by Arunkumar and Rajarajan (2018) [96] molecular docking with the same set of molecules as potential inhibitors of the gH/gL complex was performed. For the gH/gL herpes virus regulator complex, they found

that punicalagin presented amino acid interactions at Arg527, Trp634, Tyr486, Leu421 and Gly420. This study, using *in vitro* and *in silico* studies revealed good binding results for punicalagin, potential evidence to be used in the development of anti-HSV-2 compounds (Fig. **7**).

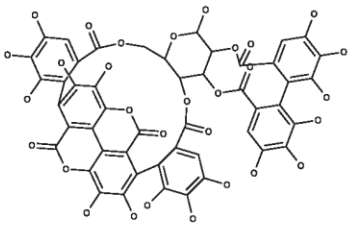

Fig. (7). The compound Punicalagin; presents activity against the Herpes virus Protease and Regulator Complex gH/gL.

5. HUMAN IMMUNODEFICIENCY VIRUS - HIV

Acquired immunodeficiency syndrome (AIDS) is caused by chronic HIV infection and is responsible for a gradual decrease in defense cells of the infected organism. According to WHO, 36.9 million people worldwide are living with HIV; of which in 2017, 59% were receiving treatment.

According to UNAIDS/WHO estimates, in 2017 children under the age of 15 living with HIV numbered 1.8 million, with an estimated 180,000 new cases of children last year. More than 51% of adult HIV cases occurred in women in 2017.

Currently the infection is treatable. With treatment, the infected individual can have a higher quality of life and control over the disease. However, to reduce the risk of transmission and to inhibit contagion, certain actions are essential; such as condom use, not sharing needles, prenatal care, and others.

5.1 Targets

Current HIV treatment is viewed mainly as inhibition of three important proteins; protease (PR), integrase (IN) and reverse transcriptase (RT). Due to HIV mutations and resistance, as well as to the cytotoxicity of the drugs used for treatment, many research groups are actively working to develop and test new anti-HIV bioactive molecules [100, 101].

5.1.1. Enzyme Protease

Protease (PR) is an enzyme responsible for cleavage of peptide bonds between proteins, thus activating or deactivating enzymes. Viral proteins are encoded in peptide chains, and are cleaved by proteases. When viral proteins take on an active conformation they contribute to viral multiplication and proliferation triggering the infectious process.

Using PDB ID 1HXB [102], the authors sought to predict its molecular affinity with HIV protease type 1; the study's prediction model obtained 98% accuracy. HIV protease type 1 is responsible for the cleavage of certain polyproteins present in HIV, this forms mature proteins that will spread throughout the infected organism and lead to the development of the chronic AIDS infection. The protease has now caught the attention of the world's researchers. The same target was used by Mohammdi *et al.* [103] who studied 9 tetrahydropyridine derivatives (obtained using diastereoselective synthesis) which presented promising values against HIV-1 protease. The results as compared to the inhibitor saquinavir were good; where hydrogen bonds in common with the standard drug were perceived for all of the derivatives at the active site of the protease, highlighting residues such as Gly27, Ile50, Val82, Gly48, Asp25 and Asp29.

Tong *et al.* [104] analyzed the interactions, relational structures, and biological activities of 34 urea cycle derivatives using a similarity index, the target was PDB 1AJV. Carboxylic grouping of the molecules interacting with the Asp25 amino acid residue was found to contribute significantly to biological activity, as well as the hydrogen bond involved.

Zondagh *et al.* [105] performed molecular dynamics simulations with HIV-1 (South African wild - Subtype C) targeting PDB 3U71 protease (chosen for close homology with N37T), to study the dynamics (20ns) of 3 anti-HIV bioactives: lopinavir, atazanavir, and darunavir. It was found that HIV mutation had reduced susceptibility to these drugs.

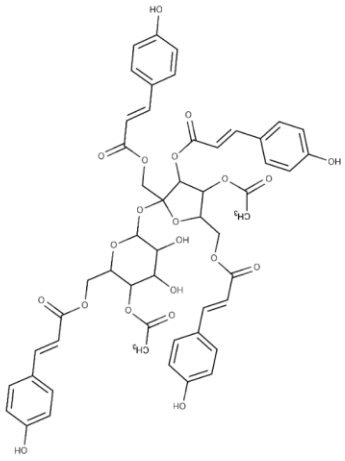

Fig. (8). 2D Structure of Polygonumins A.

A natural product which presents a combination of four phenylpropanoid esters and a unit of sucrose was extracted from the Malaysian Medicinal Plant; *Polygonum minus* (*Persicaria minor*)[106]. Polygonumins A (Fig. **8**) exhibits antiproliferative activity against human leukemia, human breast adenocarcinoma, and colorectal cancer. In addition, study results presented anti-HIV activity; moderately inhibiting the protease PDB 3OXC target by 56%, with an interaction energy in the range of -10.5 to -11.3 kcal/mol. This is the first bioactive from this plant to be considered as protease inhibitor for HIV-1.

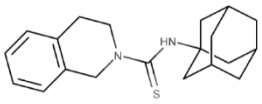

Fig. (9). 2D Structure of N-(Adamantan-1-yl)-1,2,3,4-tetra-hydro-iso-quinoline-2-carbo-thio-amide.

Studies [107] show that N-(Adamantan-1-yl)-1,2,3,4-tetrahydroisoquinoline-2-carbothioamide (Fig. **9**) may present inhibitory activity against HIV-1 protease. Molecular docking using the PDB 1EBY protein revealed the best energy of the calculated poses as -8.1 kcal/mol with significant interactions at amino acid residues Ala128, Arg8, Val82, Pro81, Gly148, Gly149 and Ile147, and a hydrogen bond with residue Gly12. Many studies have focused on the adamantane aggregation at the pharmacophore group of protease inhibitors for HIV-1. For this study, Ghosh *et al.* [108] (whose research discusses molecular docking) evaluated the interaction between a number of synthetic compounds using the adamantanyl group with PDB 5JFP, 5JFU and 5JG1 proteins as targets.

5.1.2. Enzyme Integrase

Integrase (IN) is responsible for integrating the viral DNA into the host cell DNA. This process represents an irreversible step in the cycle of viral reproduction, and once integrated, the infected cell continues expression of the viral gene.

Debnath *et al.* [109] studied the potential pharmacological effect of N-hydroxy-substituted 2-arylacetamide bioactives against the HIV-1 integrase protein. The study highlighted 6 compounds with *in vitro* inhibition of greater than 50%. Molecular docking performed with the PDB 1QS4 protein, revealed important integrations for anti-HIV activity, and hydrophobic and hydrogen bonding interactions with amino acid residues Asn155, Lys156 and Lys159 were observed. Other studies with the same protein can be found in the literature. Vyas *et al.* [110] studied a data set of 71 compounds derived from azoindol-hydroxamic, and azaindol-N-methylhydroxamic acids, together with N-hydroxydihydronaphthyridines collected from the literature. In the molecular docking results, the residues important for pharmacological action were Lys156, Lys159 and Gln148.

Using virtual screening, Chander *et al.* [111] concluded that seven compounds from a database of 200,000 molecules present inhibitory activity for both integrase and reverse transcriptase. For the molecular docking studies, the PDB 3OYA IN protein was used. The drug raltegravir was used as a control. Important interactions for activity with residues Tyr212, Pro214, Pro211, Pro161, Ala188, Try535, Pro537, Ala538, Lys540 were discovered. This same integrase protein was studied by Faridoon *et al.* [112] with a series of 4-arylimino-3-hydroxybutanoic acid derivatives (Fig. **10**); five of which presented HIV-1 inhibitory activity. The control drugs used were tegravir, elvitegravir and dolutegravir and interactions with important residues for activity at: Glu221, Asp128 and Asp185 were detected.

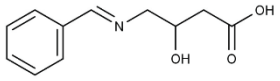

Fig. (10). 2D Structure of 4-arylimino-3-hydroxybutanoic acid.

Zhang *et al.* [113] studied integrase inhibitory activity in a series of 3-hydroxypicolinamides (Fig. **11**) with the PDB 3LPU protein. In this study, residues Ile365, Leu102, Ala128, Ala129, Trp132, Thr174, Met178, Asp36, His171, Ile365 , Gln168, Lys173, Met178, Leu102, Ala128, Ala129, Trp131 and Trp132 presented significance for anti-HIV activity. The same protein was also used in a study by Panwar & Singh [114] where 3 compounds studied showed promising integrase inhibitory activity.

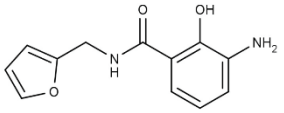

Fig. (11). 2D Structure of 3-hydroxypicolinamide.

Natural products with anti-HIV pharmacological action are also reported in the literature, Srivastav & Tiwari [115] studied 26 coumarin derivative dockings (Fig. **12**) (using raltegravir as the control) with the PDB 3NF7 protein. The molecules were subjected to a QSAR regression model with Q2 = 0.8307. The interactions at Arg199, Leu158, Met154, Lys188, Val150, Arg199, Lys186 and Ala196 were shown to be important for activity. Ericksen *et al.* [116] has even used molecular docking with the PDB 3NF7 protein in a Machine Learning Consensus Scoring study to evaluate software performance.

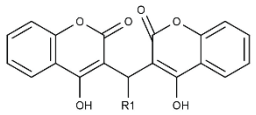

Fig. (12). 2D Structure of coumarin derivatives.

5.1.3. Reverse Transcriptase

RT also known as RNA-dependent DNA polymerase synthesizes viral DNA molecules from the viral RNA present in the virus; genetic material that becomes available for incorporation into host cells.

Jin *et al.* [117] studied a new series of biphenyl-substituted diarylpyrimidines (Fig. **13a**) against wild type and mutant HIV reverse transcriptase, aiming to inhibit its activity. Of twenty-two (22) ligand-receptor interactions calculated through molecular docking with the PDB 2ZD1 protein, five presented high potency with EC_{50s} of less than 2 nM. Maruti & Dhawale [118] also performed a study with 24 derivative malonamide compounds (Fig. **13b**) analyzing *in silico* molecular docking of ligand-receptor interactions against reverse transcriptase with the PDB 2ZD1 protein.

The study revealed the contribution of interactions at amino acid residues Asp64, Asp116, Leu100, Tyr18, Trp229, Val106, Val179 and Phe227.

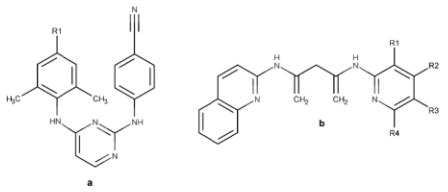

Fig. (13). 2D Structures of **a**) biphenyl-substituted diarylpyrimidines, and **b**) malonamide derivatives.

Liu *et al.* [119] analyzed the interactions of 52 diarylpyrimidine analogues (DAPYs) using molecular docking for the PDB 3MEC protein; indicating a contribution of the phenyl ring at the C4 position of the pyrimidine ring that presented better results than cycloalkanes. The authors pointed out certain amino acid residues which are important for HIV-1 reverse transcriptase inhibitory action: Lys 101, Tyr318, Tyr232, Phe 227, Trp239, Trp229, Pro225, Pro226, Met230, Ile94, and Val189, Leu100, Lys103, Val179, Gly190, Leu234, His235, Tyr188, Tyr181, and Trp229. The same protein is found in many chemoinformatic studies [120-122].

Samanta & Das [123] studied reverse transcriptase inhibition in certain di-ether catechols, performing molecular docking for the PDB: 4H4M, 4RW4, 4RW6, 4RW7, 4RW8 and 4RW9 proteins in differing *in silico* modeling software showing significant interactions with residues Lys103, Val106, Asn103, Pro236, Val179, Tyr181, Leu100, Leu234, Pro95, Lys102, Tyr188 and Trp229. These PDB proteins are found in other works [124], including Monforte *et al* [125] who performed molecular docking of N1-aryl-2-arylthioacetamido-benzimidazole derivatives with the PDB 3DLG protein using the drugs nevirapine and efavirenz. Two compounds with promising anti-HIV profiles were highlighted.

Cabrera *et al.* [126] developed a double inhibition study with molecular modeling of 320 quinoline derivatives (Fig. **14**) for reverse transcriptase and integrase using the PDB: 2BAN, 2B5J and 3L2U proteins. In conclusion, 4 structures presented the possibility of having binary pharmacological activities, with interactions similar to the drug elvitegravir and important interactions with amino acid residues: Pro236 or Lys103.

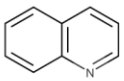

Fig. (14). 2D Structure of quinoline.

Tang *et al.* [127] synthesized and modeled 2-hydroxyisoquinoline-1,3-dione derivatives. Two of which (Fig. **15**) presented potent and selective inhibition of HIV-1 reverse transcriptase-associated RNase H in molecular docking studies, with affinities for the Arg448, Lys65, Arg72, Gln151, Asn103, Tyr188, Tyr181, and Trp229 residues in PDB: 3LP1 and 1RTD proteins.

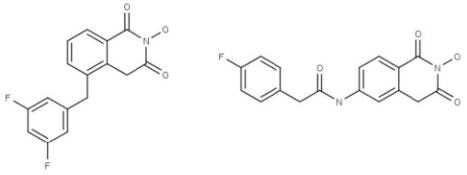

Fig. (15). 2D structures of the most potent and selective bioactives against the PDB: 3LP1 and 1RTD proteins.

6. HEPATITIS C VIRUS

In Babylon, more than 2,500 years ago, reports of jaundice (yellowing of the skin) have been found. Around 400 a.C the greek physician named Hipocrates characterized jaundice as being an infectious disease whose origin was in liver-related problems [128-131].

Bianch JB was the first to use the term "hepatitis", publishing in 1725 with his work titled as *Historia hepatica without theoria et praxis omnius morborum hepatitis et bilis*. Hepatitis is an infectious disease caused by viruses, which when reaching a chronic state causing cirrhosis, it is advisable to transplant the liver, when starting the treatment the patient is advised not to ingest alcoholic beverages and not to consume toxic foods to the liver [132-136].

The hepatitis virus attacks hepatocyte cells (which produce proteins) in the liver, once infected, the virus binds to the hepatocytes (cells found in the liver) through the proteins of its viral envelope crossing the cellular cytoplasm and losing its capsid upon entering the nucleus, in which the polymerase present in the cellular medium biosynthesizes the viral genetic material [137-140].

In 1970 Harvey J. Alter through an investigation realized that most cases of hepatitis did not correspond to the types A and B, but only in 2000 through the scientists Alter and Houghton that gained the premo Lasker that the virus of Hepatitis C happened to be known. According to the WHO, an estimated 71 million people are infected with hepatitis C worldwide, of which almost 400,000 die each year. Treatments with current medications can achieve 95% cure, yet according to estimates about 30% of those infected develop liver cirrhosis within 20 years after infection.

6.1. Targets

6.1.1. Inhibition of ns5b

NS5B is an RNA polymerase protein present in hepatitis C virus, with which the virus can multiply itself by replicating its RNA, using viral RNA as a template during its replication. Inhibition can occur basically by three chemical agents: nucleoside inhibitors, non-nucleoside allosteric inhibitors and pyrophosphate analogues. As drugs widely used as inhibitors of BS5B we have sofosbuvir and ledipasvir (Fig. **16**).

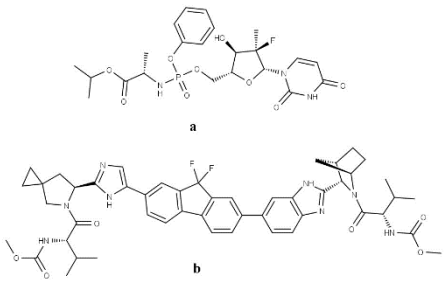

Fig. (16). 2D structures of NS5B inhibitory drugs. **a**) sofosbuvir and **b**) ledipasvir.

Patel *et al.* [141] studied the inhibitory action of NS5B by 67 benzoimidazole heterocyclic compounds through QSAR 3D studies and molecular anchoring using PDB ID 2DXS for action against Hepatitis C virus (HCV), as a conclusion compound 22 (Fig. **17**) presented a better antiviral profile in the light against hepatitis, with pIC_{50} equal to 2.10. This same protein is present in some computational chemistry studies such as Vani *et al.* [142] using 65 compounds selected through the ADMET properties of 89 compounds selected from the platform online PubChem NCBI (https://pubchem. ncbi.nlm.nih.gov), estes compostos foram submetidos a docking molecular usando o software iGEM dock (http:// gemdock.life.nctu.edu.tw/dock/igemdock.php) presenting good anchorage results with the protein, of which 4 presented better results: daidzin, ononin, colecoxib, rofecoxib.

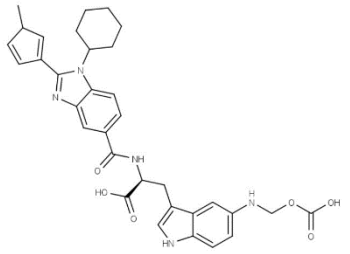

Fig. (17). 2D structures of the compound with the best result in the study of Patel *et al.* [141].

Other heterocyclic compounds can be readily found in studies proposing candidates for anti-HCV drugs, for example benzothiadiazine derivatives, which is a compound with two rings containing two nitrogen atoms and one sulfur atom (Fig. **18a**). Wang *et al.* [143] developed mock-chemistry studies using 3D QSAR, molecular docking and molecular dynamics with 239 benzothiadiazinic compounds, in this study molecular anchoring was performed using the PDB ID 3H98 protein using SYBYL 6.9 exhibiting important interactions with amino acid residues Glu446, Gly449, Asn291 and Asp318. Anithaa *et al.* [144] carried out a QSAR and molecular docking study of 52 1,1-Dioxo-2H-benzothiadiazine compounds acting against HCV, this study pointed out that the increase of hydrogen donors and acceptors and hydrophobic groups in some regions of these benzothiadiazines proved to be potentiators of antiviral activity.

Natural products are also studied for antiviral action against hepatitis C, as an example it is possible to point out the study of Liu *et al.* [145] which addresses the possibility of using flavonoids in hepatitis treatment through a pharmacophoric research combined with molecular docking using the PDB ID 1C2P protein and 39 flavonoids through GOLD software of which 20 of these compounds showed EC 50 μM results, two which have a natural occurrence: apigenin and luteolin (Fig. **18b-c**).

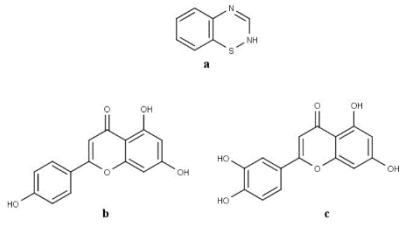

Fig. (18). General structure of **a**) benzothiadiazine, **b**) apigenin and **c**) luteolin.

6.1.2. Inhibition of Other Targets

Protease is also a therapeutic target widely studied by researchers seeking new drugs for Hepatitis C, because it is a peptide cleavage enzyme and plays a key role in cell life and HCV proteases such as NS2, NS3, NS4A, NS4B, NS5A and NS5B [146-148].

Bailey *et al.* [149] developed a study with 27 2,4-disubstituted thiazole substituted for evaluation, in this study a molecular docking study was developed to understand the interactions between amino acid residues that contribute significantly to activity against Hepatitis C, thus, this study concludes that the Asp81, His57 and Tyr56 residues are present in the ligand-receptor interaction region. The biological results through the IC 50 validated the *in silico* results, obtaining as a result the possibility of using these triazoles as a good therapeutic alternative in the fight against HCV, the example of which is in compound 11 of that study that presented $IC_{50} = 0.74$nm (Fig. **19a**).

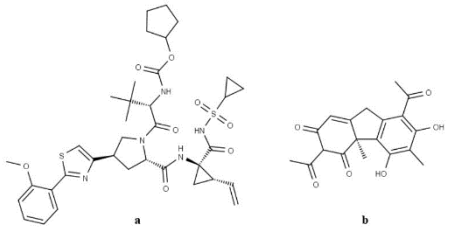

Fig. (19). Structure 2D **a**) of the compound with the lowest inhibitory concentration [149] and **b**) (+)-usnic acid.

Wei *et al.* [150] studied the antiviral action of 8 compounds present in the organic extract with ethyl acetate from the plant *Daphne papyracea*, According to their study, these compounds showed an inhibitory effect of NS3 / NS4A protease, among the results (+)-usnic acid (Fig. **19b**) presented better results. Plants, as well as their natural products, are widely studied as a source of HCV bioactives, as in the *in silico* Ashfaq *et al.* [151] which consists of the molecular docking of phytochemical components of Azadirachta indica leaves with the objective of identifying potential inhibitors of hepatitis C NS3, in this study, the 3-Deacetyl-3-cinnamoyl-azadirachtin compound presented a better antiviral profile interacting with the residue Gln526.

A survey of Shaw *et al.* [152] consisted of the virtual screening of 12 compounds available from ChemBridge Corporation, KeyOrganics, Sigma Aldrich and MedChem Express, which were subjected to molecular docking using the PDB ID 2HD0 protein, in order to track new NS2 inhibitors, as validation of the *in silico* method through *In vitro* test, as conclusion of this study it is shown that compound 160 (Fig. **20a**) presented good results against the inhibitory action of the NS3 protease, as well as its derivatives 160-1 (Fig. **20b**) and 160-2 (Fig. **20c**).

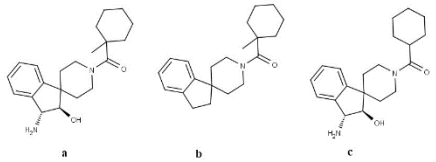

Fig. (20). 2D Structure of Shaw *et al.* [152]. **a**) compound 160, **b**) compound 160-1 and **c**) compound 160-2.

The PDB ID 2HD0 target was also used in other studies, an example was the search for Lulu *et al.* [153] which consisted in verifying by molecular docking the possibility of inhibitory action of Hepatitis C NS2 using AutoDock4.2 proving the potential anti-hepatic action of naringenin and quercetin.

In addition to the proteases, inhibition of protein targets present in viral envelopes are also studied as possibilities in the rational planning of new drugs in the fight against hepatitis C, some studies regard proteins E1 and E2 as promising examples. Uddin *et al.* [154] performed the molecular modeling using benzoimidazole B5 with the objective of inhibiting the E1 viral envelope protein, in this study included molecular docking between these compounds and the protein PDB ID 1MBN, through the computational data obtained in their research, the authors realized the possibility of using this azolic as a bioactive against hepatitis C Another example of a study involving envelope proteins is the Hung *et al.* [155] in which the use of berberine as a molecule with anti-HCV action, in its study the results of molecular docking using 4UOI and 4MWF proteins were validated with the tests *in vitro*.

CONCLUSION

This review addressed sexually transmitted diseases; chronic infections that afflict people from all over the world regardless of sex, class, or financial means which are caused by viruses and maintain certain protein targets. These diseases constitute a public health concern, and new bioactives have been emerging that may reduce cases of resistance and avoid the cytotoxicity of existing drugs.

Computational chemistry, when included in pharmaceutical and medicinal chemistry provides a tool for rational drug screening and planning. Molecular docking; the study of ligand-receptor interactions contributed to all of the studies presented. The objective is to understand structural contributions and interactions involved in inhibiting the activity of target proteins which are necessary to serious pathologies such as Ebola, HIV and herpes.

In this study, our purpose was to inform as to the nature and/or class of the compounds reviewed together with their targets in *in silico* studies, so that new research may emerge through appropriating this knowledge towards the development of new drugs.

CONSENT FOR PUBLICATION

Not applicable.

FUNDING

We would like to thank the Conselho Nacional de Desenvolvimento Científico e Tecnológico (CNPq) and the Coordenação de Aperfeiçoamento de Pessoal de Nível Superior (Capes) for financial support.

CONFLICT OF INTEREST

The authors declare no conflict of interest, financial or otherwise.

ACKNOWLEDGEMENTS

Declared none.

REFERENCES

[1] Singh, S.K. *Diagnostics to Pathogenomics of Sexually Trans-mitted Infections*, 1st ed; Wiley Blackwell, **2018**.

[2] Satterwhite, C.L.; Torrone, E.; Meites, E.; Dunne, E.F.; Mahajan, R.; Ocfemia, M.C.B.; Su, J.; Xu, F.; Weinstock, H. Sexually transmitted infections among US women and men: prevalence and incidence estimates, 2008. *Sex. Transm. Dis.*, **2013**, *40*(3), 187-193.

[3] World Health Organization: Sexually transmitted infections, 2016. http://www.who.int/news-room/fact-sheets/detail/sexually-transmitted-infections-(stis) (Accessed Set 15, 2018)

[4] Friedman, A.L.; Kachur, R.E.; Noar, S.M.; McFarlane, M. Health communication and social marketing campaigns for sexually transmitted disease prevention and control: What is the evidence of their effectiveness? *Sex. Transm. Dis.*, **2016**, *43*(2)(Suppl. 1), S83-S101.

[5] Center of Disease Control: Sexually transmitted diseases treatment guidelines, 2010. https://www.cdc.gov/std/treatment/2010/std-treatment-2010-rr5912.pdf (Accessed Set 15, 2018)

[6] Ferreira, L.G.; Dos Santos, R.N.; Oliva, G.; Andricopulo, A.D. Molecular docking and structure-based drug design strategies. *Molecules*, **2015**, *20*(7), 13384-13421.

[7] Chen, Y.; Shoichet, B.K. Molecular docking and ligand specificity in fragment-based inhibitor discovery. *Nat. Chem. Biol.*, **2009**, *5*(5), 358-364.

[8] Kitchen, D.B.; Decornez, H.; Furr, J.R.; Bajorath, J. Docking and scoring in virtual screening for drug discovery: methods and applications. *Nat. Rev. Drug Discov.*, **2004**, *3*(11), 935-949.

[9] Wang, R.; Lu, Y.; Wang, S. Comparative evaluation of 11 scoring functions for molecular docking. *J. Med. Chem.,* **2003**, *46*(12), 2287-2303.

[10] Warren, G.L.; Andrews, C.W.; Capelli, A.M.; Clarke, B.; LaLonde, J.; Lambert, M.H.; Lindvall, M.; Nevins, N.; Semus, S.F.; Senger, S.; Tedesco, G.; Wall, I.D.; Woolven, J.M.; Peishoff, C.E.; Head, M.S. A critical assessment of docking programs and scoring functions. *J. Med. Chem.,* **2006**, *49*(20), 5912-5931.

[11] Rarey, M.; Kramer, B.; Lengauer, T.; Klebe, G. A fast flexible docking method using an incremental construction algorithm. *J. Mol. Biol.,* **1996**, *261*(3), 470-489.

[12] Jones, G.; Willett, P.; Glen, R.C.; Leach, A.R.; Taylor, R. Development and validation of a genetic algorithm for flexible docking. *J. Mol. Biol.,* **1997**, *267*(3), 727-748.

[13] Österberg, F.; Morris, G.M.; Sanner, M.F.; Olson, A.J.; Goodsell, D.S. Automated docking to multiple target structures: incorporation of protein mobility and structural water heterogeneity in AutoDock. *Proteins,* **2002**, *46*(1), 34-40.

[14] Morris, G.M.; Huey, R.; Lindstrom, W.; Sanner, M.F.; Belew, R.K.; Goodsell, D.S.; Olson, A.J. AutoDock4 and AutoDockTools4: Automated docking with selective receptor flexibility. *J. Comput. Chem.,* **2009**, *30*(16), 2785-2791.

[15] Venkatachalam, C.M.; Jiang, X.; Oldfield, T.; Waldman, M. LigandFit: a novel method for the shape-directed rapid docking of ligands to protein active sites. *J. Mol. Graph. Model.,* **2003**, *21*(4), 289-307.

[16] Jain, A.N. Surflex: Fully automatic flexible molecular docking using a molecular similarity-based search engine. *J. Med. Chem.,* **2003**, *46*(4), 499-511.

[17] McGann, M.R.; Almond, H.R.; Nicholls, A.; Grant, J.A.; Brown, F.K. Gaussian docking functions. *Biopolymers,* **2003**, *68*(1), 76-90.

[18] Friesner, R.A.; Banks, J.L.; Murphy, R.B.; Halgren, T.A.; Klicic, J.J.; Mainz, D.T.; Repasky, M.P.; Knoll, E.H.; Shelley, M.; Perry, J.K.; Shaw, D.E.; Francis, P.; Shenkin, P.S. Glide: a new approach for rapid, accurate docking and scoring. 1. Method and assessment of docking accuracy. *J. Med. Chem.,* **2004**, *47*(7), 1739-1749.

[19] Trott, O.; Olson, A.J. AutoDock Vina: improving the speed and accuracy of docking with a new scoring function, efficient optimization, and multithreading. *J. Comput. Chem.,* **2010**, *31*(2), 455-461.

[20] Corbeil, C.R.; Williams, C.I.; Labute, P. Variability in docking success rates due to dataset preparation. *J. Comput. Aided Mol. Des.,* **2012**, *26*(6), 775-786.

[21] Zhao, H.; Caflisch, A. Discovery of ZAP70 inhibitors by high-throughput docking into a conformation of its kinase domain generated by molecular dynamics. *Bioorg. Med. Chem. Lett.,* **2013**, *23*(20), 5721-5726.

[22] Allen, W.J.; Balius, T.E.; Mukherjee, S.; Brozell, S.R.; Moustakas, D.T.; Lang, P.T.; Case, D.A.; Kuntz, I.D.; Rizzo, R.C. DOCK 6: Impact of new features and current docking performance. *J. Comput. Chem.,* **2015**, *36*(15), 1132-1156.

[23] Wang, Z.; Sun, H.; Yao, X.; Li, D.; Xu, L.; Li, Y.; Tian, S.; Hou, T. Comprehensive evaluation of ten docking programs on a diverse set of protein-ligand complexes: the prediction accuracy of sampling power and scoring power. *Phys. Chem. Chem. Phys.,* **2016**, *18*(18), 12964-12975.

[24] Leroy, E.M.; Kumulungui, B.; Pourrut, X.; Rouquet, P.; Hassanin, A.; Yaba, P.; Délicat, A.; Paweska, J.T.; Gonzalez, J.P.; Swanepoel, R. Fruit bats as reservoirs of Ebola virus. *Nature,* **2005**, *438*(7068), 575-576.

[25] Briand, S.; Bertherat, E.; Cox, P.; Formenty, P.; Kieny, M.P.; Myhre, J.K.; Roth, C.; Shindo, N.; Dye, C. The International Ebola Emergency. *N. Engl. J. Med.,* **2014**, *371*, 1180-1183.sis.nlm.nih.gov/Tox/ToxMain.html (Accessed May 23, 2004)

[26] World Health Organization: Ebola situation report, 2016. http://apps.who.int/ebola/current-situation/ebola-situation-report-30-march-2016 (Accessed Oct 9, 2018).

[27] Bwaka, M.A.; Bonnet, M.J.; Calain, P.; Colebunders, R.; De Roo, A.; Guimard, Y.; Katwiki, K.R.; Kibadi, K.; Kipasa, M.A.; Kuvula, K.J.; Mapanda, B.B.; Massamba, M.; Mupapa, K.D.; Muyembe-Tamfum, J.J.; Ndaberey, E.; Peters, C.J.; Rollin, P.E.; Van den Enden, E.; Van den Enden, E. Ebola hemorrhagic fever in Kikwit, Democratic Republic of the Congo: clinical observations in 103 patients. *J. Infect. Dis.,* **1999**, *179*(Suppl. 1), S1-S7.

[28] Centers for Disease Control and Prevention: Transmission Of Ebola (Ebola Virus Disease), 2014. https://www.cdc.gov/vhf/ebola/transmission/index.html (Accessed Sep 18, 2018)

[29] Hewlett, B.S.; Amola, R.P. Cultural contexts of Ebola in northern Uganda. *Emerg. Infect. Dis.,* **2003**, *9*(10), 1242-1248. [http://dx.doi.org/10.3201/eid0910.020493]

[30] Rodriguez, L.L.; De Roo, A.; Guimard, Y.; Trappier, S.G.; Sanchez, A. Bressler, Williams, D.A.J.; Rowe, A.K.; Bertolli, J.; Khan, A.S.; Ksiazek, T.G.; Peters, C.J.; Nichol, S.T. Persis-tence and genetic stability of Ebola virus during the outbreak in Kikwit, Democratic Republic of the Congo, 1995. *J. Infect. Dis.,* **1999**, *179*, 170-176.

[31] Rogstad, K.E.; Tunbridge, A. Ebola virus as a sexually transmitted infection. *Curr. Opin. Infect. Dis.,* **2015**, *28*(1), 83-85.

[32] Deen, G.F.; Broutet, N.; Xu, W.; Knust, B.; Sesay, F.R.; McDonald, S.L.; Ervin, E.; Marrinan, J.E.; Gaillard, P.; Habib, N.; Liu, H.; Liu, W.; Thorson, A.E.; Yamba, F.; Mas-saquoi, T.A.; James, F.; Ariyarajah, A.; Ross, C.; Bernstein, K.; Coursier, A.; Klena, J.; Carino, M.; Wurie, A.H.; Zhang, Y.; Dumbuya, M.S.; Abad, N.; Idriss, B.; Wi, T.; Bennett, S.D.; Davies, T.; Ebrahim, F.K.; Meites, E.; Naidoo, D.; Smith, S.J.; Ongpin, P.; Malik, T.; Banerjee, A.; Erickson, B.R.; Liu, Y.; Liu, Y. Xu, K.; Brault, A.; Durski, K.N.; Winter, J.; Sealy, T.; Nichol S.T.; Lamunu, M.; Bangura, J.; Landoulsi, S.; Jambai, A.; Morgan, A.; Wu, G.; Liang, M.; Su, Q.; Lan, Y.; Hao, Y.; Formenty, P.; Ströher, U.; Sahr, F. Ebola RNA persistence in semen of Ebola virus disease survivors. *N. Engl. J. Med.,* **2017**, *377*(15), 1428-1437.

[33] Christie, A.; Davies-Wayne, G.J.; Cordier-Lassalle, T.; Blackley, D.J.; Laney, A.S.; Williams, D.E.; Shinde, S.A.; Badio, M.; Lo, T.; Mate, S.E.; Ladner, J.T.; Wiley, M.R.; Kugelman, J.R.; Palacios, G.; Holbrook, M.R.; Janosko, K.B.; de Wit, E.; van Doremalen, N.; Munster, V.J.; Pettitt, J.; Schoepp, R.J.; Verhenne, L.; Evlampidou, I.; Kollie, K.K.; Sieh, S.B.; Gasasira, A.; Bolay, F.; Kateh, F.N.; Nyenswah, T.G.; De Cock, K.M. Possible sexual transmission of Ebola virus - Liberia, 2015. *MMWR Morb. Mortal. Wkly. Rep.,* **2015**, *64*(17), 479-481.

[34] World Health Organization. Interim advice on the sexual transmission of the Ebola virus disease, 2016. . http://www.who.int/reproductivehealth/topics/rtis/ebola-virus-semen/en/ (Accessed Set 21, 2018).

[35] Mate, S.E.; Kugelman, J.R.; Nyenswah, T.G.; Ladner, J.T.; Wiley, M.R.; Cordier-Lassalle, T.; Christie, A.; Schroth, G.P.; Gross, S.M.; Davies-Wayne, G.J.; Shinde, S.A.; Murugan, R.; Sieh, S.B.; Badio, M.; Fakoli, L.; Taweh, F.; de Wit, E.; van Doremalen, N.; Munster, V.J.; Pettitt, J.; Prieto, K.; Humrighouse, B.W.; Ströher, U.; DiClaro, J.W.; Hensley, L.E.; Schoepp, R.J.; Safronetz, D.; Fair, J.; Kuhn, J.H.; Blackley, D.J.; Laney, A.S.; Williams, D.E.; Lo, T.; Gasasira, A.; Nichol, S.T.; Formenty, P.; Kateh, F.N.; De Cock, K.M.; Bolay, F.; Sanchez-Lockhart, M.; Palacios, G. Molecular evidence of sexual transmission of Ebola virus. *N. Engl. J. Med.,* **2015**, *373*(25), 2448-2454.

[36] Judson, S.; Prescott, J.; Munster, V. Understanding ebola virus transmission. *Viruses,* **2015**, *7*(2), 511-521.

[37] Gire, S.K.; Goba, A.; Andersen, K.G.; Sealfon, R.S.G.; Park, D.J.; Kanneh, L. Jalloh, s.; Momoh, M.; Fullah, M.; Dudas, G.; Wohl, S.; Moses, L.M.; Yozwiak, N.L.; Winnicki, S.; Matranga, C.B.; Malboeyf, C.M.; Qu, J.; Glandden, A.D.; Schaffner, S.F.; Yang, X.; Jiang, P.P.; Nekoui, M.; Colubri, A.; Coomber, M.R.; Fonnie, M.; Moigboi, A.; Gbakie, M.; Kama-ra, F.K.; Tucker, V.; Konuwa, E.; Saffa, S.; Sellu, J.; Jalloh, A.A.; Jovoma, A.; Koninga, J.; Mustapha, I.; Kargbo, K.; Fo-day, M.; Yillah, M.; Kanneh, F.; Robert, W.; Massally, J.L.B.; Chapman, S.B.; Bochicchio, J.; Murphy, C.; Nusbaum, C.; Young, S.; Birren, B.W.; Grant, D.S.; Scheiffelin, J.S.; Lander, E.S.; Happi, C.; Gevao, S.M.; Gnirke, A.; Rambaut, A.; Garry, R.F.; Khan, S.H.; Sabeti, P.C. Genomic surveillance elucidates Ebola virus origin and transmission during the 2014 outbreak. *Science,* **2014**, *345*, 1369-1372.

[38] Hulo, C.; de Castro, E.; Masson, P.; Bougueleret, L.; Bairoch, A.; Xenarios, I.; Le Mercier, P. ViralZone: A knowledge resource to understand virus diversity. *Nucleic Acids Res.,* **2011**, *39*(Database issue), D576-D582.

[39] Nanbo, A.; Watanabe, S.; Halfmann, P.; Kawaoka, Y. The spatio-temporal distribution dynamics of Ebola virus proteins and RNA in infected cells. *Sci. Rep.,* **2013**, *3*, 1206.

[40] Raj, U.; Varadwaj, P.K. Flavonoids as multi-target inhibitors for proteins associated with Ebola virus: In silico discovery using vir-

tual screening and molecular docking studies. *Interdiscip. Sci.,* **2016**, *8*(2), 132-141.
[41] Chou, K.C. Impacts of bioinformatics to medicinal chemistry. *Med. Chem.,* **2015**, *11*(3), 218-234.
[42] Diehl, W.E.; Lin, A.E.; Grubaugh, N.D.; Carvalho, L.M.; Kim, K.; Kyawe, P.P.; McCauley, S.M.; Donnard, E.; Kucukural, A.; McDonel, P.; Schaffner, S.F.; Garber, M.; Rambaut, A.; Andersen, K.G.; Sabeti, P.C.; Luban, J. Ebola virus glycopro-tein with increased infectivity dominated the 2013-2016 epi-demic. *Cell,* **2016**, *167*(4), 1088-1098.e6.
[43] Weissenhorn, W.; Carfí, A.; Lee, K.H.; Skehel, J.J.; Wiley, D.C. Crystal structure of the Ebola virus membrane fusion subunit, GP2, from the envelope glycoprotein ectodomain. *Mol. Cell,* **1998**, *2*(5), 605-616.
[44] Takada, A.; Robison, C.; Goto, H.; Sanchez, A.; Murti, K.G.; Whitt, M.A.; Kawaoka, Y. A system for functional analysis of Ebola virus glycoprotein. *Proc. Natl. Acad. Sci. USA,* **1997**, *94*(26), 14764-14769.
[45] Earp, L.J.; Delos, S.E.; Park, H.E.; White, J.M. The many mechanisms of viral membrane fusion proteins. *Mem-brane trafficking in viral replication*; Marsh, M., Ed.; Springer: Berlin, Heidelberg, **2004**, Vol. *285*, pp. 25-66.
[46] Sakurai, Y.; Kolokoltsov, A.A.; Chen, C.C.; Tidwell, M.W.; Bauta, W.E.; Klugbauer, N.; Grimm, C.; Wahl-Schott, C.; Biel, M.; Davey, R.A. Ebola virus. Two-pore channels control Ebola virus host cell entry and are drug targets for disease treatment. *Science,* **2015**, *347*(6225), 995-998.
[47] Lee, J.E.; Fusco, M.L.; Hessell, A.J.; Oswald, W.B.; Burton, D.R.; Saphire, E.O. Structure of the Ebola virus glycoprotein bound to an antibody from a human survivor. *Nature,* **2008**, *454*(7201), 177-182.
[48] Ahmad, N.; Farman, A.; Badshah, S.L.; Ur Rahman, A.; Ur Rashid, H.; Khan, K. Molecular modeling, simulation and docking study of ebola virus glycoprotein. *J. Mol. Graph. Model.,* **2017**, *72*, 266-271.
[49] Shinyguruce, A.; Sathya, D.; Keerthiga, K.; Pavithra, P.; Vin-itha, M.; Vaidheeswari, R.; Eswara, P.B. *In Silico* Antiviral Drug Screening and Molecular Docking Studies Against Ebola Virus Glycoprotein. *J. Appl. Sci. Comput.,* **2018**, *5*(9), 211-216.
[50] Basler, C.F.; Mikulasova, A.; Martinez-Sobrido, L.; Paragas, J.; Mühlberger, E.; Bray, M.; Klenk, H.D.; Palese, P.; García-Sastre, A. The Ebola virus VP35 protein inhibits activation of interferon regulatory factor 3. *J. Virol.,* **2003**, *77*(14), 7945-7956.
[51] Reynard, O.; Nemirov, K.; Page, A.; Mateo, M.; Raoul, H.; Weissenhorn, W.; Volchkov, V.E. Conserved proline-rich re-gion of Ebola virus matrix protein VP40 is essential for plas-ma membrane targeting and virus-like particle release. *J. Infect. Dis.,* **2011**, *204*, 884-891.
[52] Ekins, S.; Freundlich, J.S.; Coffee, M. A common feature pharmacophore for FDA-approved drugs inhibiting the Ebola virus. *F1000 Res.,* **2014**, *3*, 277.
[53] Glanzer, J.G.; Byrne, B.M.; McCoy, A.M.; James, B.J.; Frank, J.D.; Oakley, G.G. *In silico* and *in vitro* methods to identify ebola virus VP35-dsRNA inhibitors. *Bioorg. Med. Chem.,* **2016**, *24*(21), 5388-5392.
[54] Ren, J.X.; Zhang, R.T.; Zhang, H.; Cao, X.S.; Liu, L.K.; Xie, Y. Identification of novel VP35 inhibitors: Virtual screening driven new scaffolds. *Biomed. Pharmacother.,* **2016**, *84*, 199-207.
[55] Sulaiman, K.O.; Kolapo, T.U.; Onawole, A.T.; Islam, A.; Adegoke, R.O.; Badmus, S.O. Molecular dynamics and com-bined docking studies for the identification of *Zaire Ebola* Vi-rus inhibitors. *J. Biomol. Struct. Dyn.,* **2018**, *2018*, 1-31.
[56] Hartlieb, B.; Muziol, T.; Weissenhorn, W.; Becker, S. Crystal structure of the C-terminal domain of Ebola virus VP30 reveals a role in transcription and nucleocapsid association. *Proc. Natl. Acad. Sci. USA,* **2007**, *104*(2), 624-629.
[57] John, S.P.; Wang, T.; Steffen, S.; Longhi, S.; Schmaljohn, C.S.; Jonsson, C.B. Ebola virus VP30 is an RNA binding protein. *J. Virol.,* **2007**, *81*(17), 8967-8976.
[58] Biedenkopf, N.; Hartlieb, B.; Hoenen, T.; Becker, S. Phosphorylation of Ebola virus VP30 influences the composition of the viral nucleocapsid complex: impact on viral transcription and replication. *J. Biol. Chem.,* **2013**, *288*(16), 11165-11174.
[59] Martínez, M.J.; Biedenkopf, N.; Volchkova, V.; Hartlieb, B.; Alazard-Dany, N.; Reynard, O.; Becker, S.; Volchkov, V. Role of Ebola virus VP30 in transcription reinitiation. *J. Virol.,* **2008**, *82*(24), 12569-12573.
[60] Shah, R.; Panda, P.K.; Patel, P.; Panchal, H. Pharmacophore based virtual screening and molecular docking studies of inherited compounds against ebola virus receptor proteins. *World J. Pharm. Pharm. Sci.,* **2015**, *4*(5), 1268-1282.
[61] Setlur, A.S.; Naik, S.Y.; Skariyachan, S. Herbal lead as ideal bioactive compounds against probable drug targets of ebola virus in comparison with known chemical analogue: A computational drug discovery perspective. *Interdiscip. Sci.,* **2017**, *9*(2), 254-277.
[62] Vecchio, K.D.; Shwarz, A.; Saphire, E.O.; Stahelin, R. The ebola virus matrix protein vp40 interacts selectively with plasma membrane lipids to promote viral egress. *FASEB J.,* **2017**, *31*, 945-951.
[63] Gomis-Rüth, F.X.; Dessen, A.; Timmins, J.; Bracher, A.; Kolesnikowa, L.; Becker, S.; Klenk, H.D.; Weissenhorn, W. The matrix protein VP40 from Ebola virus octamerizes into pore-like structures with specific RNA binding properties. *Structure,* **2003**, *11*(4), 423-433.
[64] Scianimanico, S.; Schoehn, G.; Timmins, J.; Ruigrok, R.H.; Klenk, H.D.; Weissenhorn, W. Membrane association induces a conformational change in the Ebola virus matrix protein. *EMBO J.,* **2000**, *19*(24), 6732-6741.
[65] Mirza, M.U.; Ikram, N. Integrated computational approach for virtual hit identification against ebola viral proteins VP35 and VP40. *Int. J. Mol. Sci.,* **2016**, *17*(11), 1748.
[66] M Alam El-Din, H.; A Loutfy, S.; Fathy, N.; H Elberry, M.; M Mayla, A.; Kassem, S.; Naqvi, A. Molecular docking based screening of compounds against VP40 from Ebola virus. *Bioinformation,* **2016**, *12*(3), 192-196.
[67] Abazari, D.; Moghtadaei, M.; Behvarmanesh, A.; Ghannadi, B.; Aghaei, M.; Behruznia, M.; Rigi, G. Molecular docking based screening of predicted potential inhibitors for VP40 from Ebola virus. *Bioinformation,* **2015**, *11*(5), 243-247.
[68] Karthick, V.; Nagasundaram, N.; Doss, C.G.P.; Chakraborty, C.; Siva, R.; Lu, A.; Zhang, G.; Zhu, H. Virtual screening of the inhibitors targeting at the viral protein 40 of Ebola virus. *Infect. Dis. Poverty,* **2016**, *5*, 12.
[69] Patel, J.; Chipkar, Y.; Momin, A. Comparitive study of vari-ous ebola virus Vp40 strains with modelling and docking studies to treat ebola virus infection. *Intl. J. Pharm. Drug Res.,* **2013**, *2*(1), 1-10.
[70] Skariyachan, S.; Acharya, A.B.; Subramaniyan, S.; Babu, S.; Kulkarni, S.; Narayanappa, R. Secondary metabolites extracted from marine sponge associated Comamonas testosteroni and *Citrobacter freundii* as potential antimicrobials against MDR pathogens and hypothetical leads for VP40 matrix protein of Ebola virus: an *in vitro* and *in silico* investigation. *J. Biomol. Struct. Dyn.,* **2016**, *34*(9), 1865-1883.
[71] Tamilvanan, T.; Hopper, W. High-throughput virtual screening and docking studies of matrix protein vp40 of ebola virus. *Bioinformation,* **2013**, *9*(6), 286-292.
[72] Reid, S.P.; Leung, L.W.; Hartman, A.L.; Martinez, O.; Shaw, M.L.; Carbonnelle, C.; Volchkov, V.E.; Nichol, S.T.; Basler, C.F. Ebola virus VP24 binds karyopherin alpha1 and blocks STAT1 nuclear accumulation. *J. Virol.,* **2006**, *80*(11), 5156-5167.
[73] Watanabe, S.; Noda, T.; Halfmann, P.; Jasenosky, L.; Kawaoka, Y. Ebola virus (EBOV) VP24 inhibits transcription and replication of the EBOV genome. *J. Infect. Dis.,* **2007**, *196*(Suppl. 2), S284-S290.
[74] Hoenen, T.; Jung, S.; Herwig, A.; Groseth, A.; Becker, S. Both matrix proteins of Ebola virus contribute to the regulation of viral genome replication and transcription. *Virology,* **2010**, *403*(1), 56-66.
[75] Tambunan, U.S.F.; Nasution, M.A.F. Identification of novel Ebola virus (EBOV) VP24 inhibitor from Indonesian natural products through in silico drug design approach. *AIP Conf. Proc.,* **2017**, *1862*(1)030091
[76] Tambunan, U.S.F.; Siregar, S.; Toepak, E.P. Ebola viral protein 24 (Vp24) inhibitor discovery by *in silico* fragment-based design. *Intl. J. Geom.,* **2018**, *15*(49), 59-64.
[77] Sharmila, R.; Jaikumar, B. Molecular docking study of bioac-tive compound of andrographolide against ebola virus. *Intl.. J. Pharm. Sci. Res.,* **2016**, *7*(5), 250-253.
[78] Sharma, D.; Pathak, M.; Sharma, R.; Tyagi, P.; Chawla, R.; Basu, M.; Ojha, H. Homology modeling and docking studies of VP24 protein of Ebola virus with an antiviral drug and its derivatives. *Chem. Biol. Lett.,* **2017**, *4*(1), 27-32.

[79] Sun, Y.; Guo, Y.; Lou, Z. A versatile building block: the structures and functions of negative-sense single-stranded RNA virus nucleocapsid proteins. *Protein Cell,* **2012**, *3*(12), 893-902.

[80] Zhou, H.; Sun, Y.; Guo, Y.; Lou, Z. Structural perspective on the formation of ribonucleoprotein complex in negative-sense single-stranded RNA viruses. *Trends Microbiol.,* **2013**, *21*(9), 475-484.

[81] Baikerikar, S. Curcumin and natural derivatives inhibit ebola viral proteins: An *in silico* approach. *Pharmacog. Res.,* **2017**, *9*(Suppl. 1), S15-S22.

[82] Slots, J. Periodontal herpesviruses: prevalence, pathogenicity, systemic risk. *Periodontol. 2000,* **2015**, *69*(1), 28-45.

[83] Whitley, R.J. Herpesviruses.*University of Texas Medical Branch at Gal-veston*; Microbiology, M.; Sam-uel, B., Eds.; Galveston, Texas, **1996**.

[84] Robbins, G.; Lammert, S.; Rompalo, A.; Riley, L.; Daskalakis, D.; Morrow, R.; Lee, H.; Shui, A.; Gaydos, C.; Detrick, B.; Rosenber, E.; Crochiere, D.; Cunningham, K.; Bradley, H.; Markowitz, L.; Xu, F.; Felsenstein, D. Serologic assays for the diagnosis of herpes virus 1 (HSV-1) herpes virus 2 (HSV-2): test characteristics of FDA approved type-specific assays in an ethnically, racially, and economi-cally diverse patient population In: *Open Forum Infectious Diseases,*; Oxford University Press., **2015**; 2.

[85] Rohner, E.; Wyss, N.; Heg, Z.; Faralli, Z.; Mbulaiteye, S.M.; Novak, U.; Zwahlen, M.; Egger, M.; Bohlius, J. HIV and human herpesvirus 8 co-infection across the globe: Systematic review and meta-analysis. *Int. J. Cancer,* **2016**, *138*(1), 45-54.

[86] World Health Organization: Herpes simplex virus, 2017. . http://www.who.int/news-room/fact-sheets/detail/herpes-simplex-virus (Accessed Oct 2, 2018)

[87] Burn, C.; Ramsey, N.; Garforth, S.J.; Almo, S.; Jacobs, W.R., Jr; Herold, B.C. A herpes simplex virus (HSV)-2 single-cycle candidate vaccine deleted in glycoprotein D protects male mice from lethal skin challenge with clinical isolates of HSV-1 and HSV-2. *J. Infect. Dis.,* **2018**, *217*(5), 754-758.

[88] Sripiboon, S.; Angkawanish, T.; Boonprasert, K.; Sombutputorn, P.; Langkaphin, W.; Ditcham, W.; Warren, K. Successful treatment of a clinical elephant endotheliotropic herpesvirus infection: The dynamics of viral load, genotype analysis, and treatment with acyclovir. *J. Zoo Wildl. Med.,* **2017**, *48*(4), 1254-1259.

[89] Troszok, A.; Kolek, L.; Szczygiel, J.; Wawrzeczko, J.; Borzym, E.; Reichert, M.; Kamińska, T.; Ostrowski, T.; Jurecka, P.; Adamek, M.; Rakus, K.; Irnazarow, I. Acyclovir inhibits Cyprinid herpesvirus 3 multiplication *in vitro*. *J. Fish Dis.,* **2018**, *41*(11), 1709-1718.

[90] Piret, J.; Boivin, G. *Herpesvirus Resistance to Antiviral Drugs*; Antimicrobial Drug Resistance, **2017**, pp. 1185-1211.

[91] Kolb, A.W.; Larsen, I.V.; Cuellar, J.A.; Brandt, C.R. Genomic, phylogenetic, and recombinational characterization of herpes simplex virus 2 strains. *J. Virol.,* **2015**, *89*(12), 6427-6434.

[92] Lehman, I.R.; Boehmer, P.E. Replication of herpes simplex virus DNA. *J. Biol. Chem.,* **1999**, *274*(40), 28059-28062.

[93] Matthews, J.T.; Terry, B.J.; Field, A.K. The structure and function of the HSV DNA replication proteins: Defining novel antiviral targets. *Antiviral Res.,* **1993**, *20*(2), 89-114.

[94] Hoog, S.S.; Smith, W.W.; Qiu, X.; Janson, C.A.; Hellmig, B.; McQueney, M.S.; O'Donnell, K.; O'Shannessy, D.; DiLella, A.G.; Debouck, C.; Abdel-Meguid, S.S. Active site cavity of herpesvirus proteases revealed by the crystal structure of herpes simplex virus protease/inhibitor complex. *Biochemistry,* **1997**, *36*(46), 14023-14029.

[95] Kashyap, K.; Kakkar, R. *Herpesvirus Proteases: Structure, Function, and Inhibition*; Viral Proteases and Their Inhibitors, **2017**, pp. 411-439.

[96] Arunkumar, J.; Rajarajan, S. Study on antiviral activities, drug-likeness and molecular docking of bioactive compounds of Punica granatum L. to Herpes simplex virus - 2 (HSV-2). *Microb. Pathog.,* **2018**, *118*, 301-309.

[97] Chowdary, T.K.; Cairns, T.M.; Atanasiu, D.; Cohen, G.H.; Eisenberg, R.J.; Heldwein, E.E. Crystal structure of the conserved herpesvirus fusion regulator complex gH-gL. *Nat. Struct. Mol. Biol.,* **2010**, *17*(7), 882-888.

[98] Atanasiu, D.; Cairns, T.M.; Whitbeck, J.C.; Saw, W.T.; Rao, S.; Eisenberg, R.J.; Cohen, G.H. Regulation of herpes simplex virus gB-induced cell-cell fusion by mutant forms of gH/gL in the absence of gD and cellular receptors. *MBio,* **2013**, *4*(2), e00046-e13.

[99] Connolly, C. S.A.; Jackson, J.O.; Jardetzky, T.S.; Longnecker, R. Fusing structure and function: a structural view of the her-pesvirus entry machinery. *Nat. Rev. Microbiol.,* **2011**, *9*(5), 369.

[100] Boyer, C.B.; Greenberg, L.; Chutuape, K.; Walker, B.; Monte, D.; Kirk, J.; Ellen, J.M.; Belzer, M.; Martinez, M.; Dudek, J. Adolescent medicine trials network. exchange of sex for drugs or money in adolescents and young adults: An examination of sociodemographic factors, HIV-related risk, and community context. *J. Commun. Health,* **2017**, *42*(1), 90-100.

[101] Strategies, P.; Therapy, F.O.R.A.; Tecnol, D.; Cruz, O. Estratégias farmacológicas para a terapia anti-aids Emerson Poley Peçanha* e Octavio A. C. *Antunes.,* **2002**, *25*(6), 1108-1116.

[102] Morris, P.; DaSilva, Y.; Clark, E.; Hahn, W.E.; Barenholtz, E. Convolutional Neural Networks for Predicting Molecular Binding Affinity to HIV-1 Proteins. In: 2018 ACM International Conference on Bioinformatics, Computational Biology, and Health Informatics (BCB '18). ACM, New York, NY, USA, 220-225. DOI: https://doi.org/10.1145/3233547.3233596

[103] Mohammadi, A.A.; Taheri, S.; Amouzegar, A.; Ahdenov, R.; Halvagar, M.R.; Sadr, A.S. Diastereoselective synthesis and molecular docking studies of novel fused tetrahydro-pyridine derivatives as new inhibitors of HIV protease. *J. Mol. Struct.,* **2017**, *1139*, 166-174.

[104] Tong, J.; Wu, Y.; Bai, M.; Zhan, P. 3D-QSAR and molecular docking studies on HIV protease inhibitors. *J. Mol. Struct.,* **2017**, *1129*, 17-22.

[105] Zondagh, J.; Balakrishnan, V.; Achilonu, I.; Dirr, H.W.; Sayed, Y. Molecular dynamics and ligand docking of a hinge region variant of South African HIV-1 subtype C protease. *J. Mol. Graph. Model.,* **2018**, *82*, 1-11.

[106] Ahmad, R.; Sahidin, I.; Taher, M.; Low, C.; Noor, N.M.; Sillapachaiyaporn, C.; Chuchawankul, S.; Sarachana, T.; Tencomnao, T.; Iskandar, F.; Rajab, N.F.; Baharum, S.N. Polygonumins A, a newly isolated compound from the stem of Polygonum minus Huds with potential medicinal activities. *Sci. Rep.,* **2018**, *8*(1), 4202.

[107] Al-Shehri, M.M.; Al-Majed, A.R.A.; Aljohar, H.I.; El-Emam, A.A.; Pathak, S.K.; Sachan, A.K.; Prasad, O.; Sinha, L. First principle study of a potential bioactive molecule with tetrahydroisoquinoline, carbothiomide and adamantane scaffolds. *J. Mol. Struct.,* **2017**, *1143*, 204-216.

[108] Ghosh, A.K.; Osswald, H.L.; Glauninger, K.; Agniswamy, J.; Wang, Y-F.; Hayashi, H.; Aoki, M.; Weber, I.T.; Mitsuya, H. Probing lipophilic adamantyl group as the P1-ligand for HIV-1 protease inhibitors: Design, synthesis, protein X-ray structural studies, and biological evaluation. *J. Med. Chem.,* **2016**, *59*(14), 6826-6837.

[109] Debnath, U.; Kumar, P.; Agarwal, A.; Kesharwani, A.; Gupta, S.K.; Katti, S.B. N-hydroxy-substituted 2-aryl acetamide analogs: A novel class of HIV-1 integrase inhibitors. *Chem. Biol. Drug Des.,* **2017**, *90*(4), 527-534.

[110] Vyas, V.K.; Shah, S.; Ghate, M. Generation of new leads as HIV-1 integrase inhibitors: 3D QSAR, docking and molecular dynamics simulation. *Med. Chem. Res.,* **2017**, *26*(3), 532-550.

[111] Chander, S.; Pandey, R.K.; Penta, A.; Choudhary, B.S.; Sharma, M.; Malik, R.; Prajapati, V.K.; Murugesan, S. Molecular docking and molecular dynamics simulation based approach to explore the dual inhibitor against HIV-1 reverse transcriptase and integrase. *Comb. Chem. High Throughput Screen.,* **2017**, *20*(8), 734-746.

[112] Faridoon; Mnkandhla, D.; Isaacs, M.; Hoppe, H. C.; Kaye, P. T. Synthesis and evaluation of substituted 4-arylimino-3-hydroxybutanoic acids as potential HIV-1 integrase inhibitors. *Bioorg. Med. Chem. Lett.,* **2018**, *28*(6), 1067-1070.

[113] Zhang, F.H.; Debnath, B.; Xu, Z.L.; Yang, L.M.; Song, L.R.; Zheng, Y.T.; Neamati, N.; Long, Y.Q. Discovery of novel 3-hydroxypicolinamides as selective inhibitors of HIV-1 integrase-LEDGF/p75 interaction. *Eur. J. Med. Chem.,* **2017**, *125*, 1051-1063.

[114] Panwar, U.; Singh, S.K. Structure-based virtual screening toward the discovery of novel inhibitors for impeding the protein-protein interaction between HIV-1 integrase and hu-man lens epithelium-derived growth factor (LEDGF/P75). *J. Biomol. Struct. Dyn.,* **2018**, *36*(12), 3199-3217.

[115] Srivastav, V.K.; Tiwari, M. QSAR and Docking studies of coumarin derivatives as potent HIV-1 integrase inhibitors. *Arab. J. Chem.,* **2017**, *10*, S1081-S1094.

[116] Ericksen, S.S.; Wu, H.; Zhang, H.; Michael, L.A.; Newton, M.A.; Hoffmann, F.M.; Wildman, S.A. Machine learning consensus scor-

ing improves performance across targets in structure-based virtual screening. *J. Chem. Inf. Model.,* **2017**, *57*(7), 1579-1590.

[117] Jin, K.; Yin, H.; De Clercq, E.; Pannecouque, C.; Meng, G.; Chen, F. Discovery of biphenyl-substituted diarylpyrimidines as non-nucleoside reverse transcriptase inhibitors with high potency against wild-type and mutant HIV-1. *Eur. J. Med. Chem.,* **2018**, *145*, 726-734.

[118] Kashid, A.M.; Dhawale, S. Design, Synthesis and Biological Screening of N 1 - (Substituted Pyridine-2-Yl) -N 3 - (Quinoline-2-Yl). *Malonamide as Novel Anti-HIV-I Agents., Ind. J. Chem. Sec. B Org. Med. Chem.,* **2018**, *57*, 870-879.

[119] Liu, G.; Wang, W.; Wan, Y.; Ju, X.; Gu, S. Application of 3D-QSAR, Pharmacophore, and Molecular Docking in the Molec-ular Design of Diarylpyrimidine Derivatives as HIV-1 Nonnucleoside Reverse Transcriptase Inhibitors. *Int. J. Mol. Sci.,* **2018**, *19*(5), 1436.

[120] Singh, A.; Singh, V.K.; Verma, R.; Singh, R.K. In Silico Studies on N - (Pyridin- 2-Yl) Thiobenzamides as NNRTIs against Wild and Mutant HIV-1 Strains. *Philipp. J. Sci.,* **2018**, *147*(March), 37-46.

[121] Peddi, S.R.; Mohammed, N.A.; Hussein, A.A.; Sivan, S.K.; Manga, V. Multiple-Receptor Conformation Docking, Dock Pose Clustering, and 3D QSAR-Driven Approaches Exploring New HIV-1 RT Inhibitors. *Struct. Chem.,* **2018**, *29*(4), 999-1012.

[122] Zhang, H.; Tian, Y.; Kang, D.; Huo, Z.; Zhou, Z.; Liu, H.; De Clercq, E.; Pannecouque, C.; Zhan, P.; Liu, X. Discovery of uracil-bearing DAPYs derivatives as novel HIV-1 NNRTIs *via* crystallographic overlay-based molecular hybridization. *Eur. J. Med. Chem.,* **2017**, *130*, 209-222.

[123] Samanta, P.N.; Das, K.K. Inhibition activities of catechol diether based non-nucleoside inhibitors against the HIV reverse transcriptase variants: Insights from molecular docking and ONIOM calculations. *J. Mol. Graph. Model.,* **2017**, *75*, 294-305.

[124] Poongavanam, V.; Namasivayam, V.; Vanangamudi, M.; Al Shamaileh, H.; Veedu, R.N.; Kihlberg, J.; Murugan, N.A. Integrative Approaches in HIV-1 Non-Nucleoside Reverse Transcriptase Inhibitor Design. *Wiley Interdiscip. Rev. Comput. Mol. Sci.,* **2018**, *8*(1), 1-26.

[125] Monforte, A.M.; De Luca, L.; Buemi, M.R.; Agharbaoui, F.E.; Pannecouque, C.; Ferro, S. Structural optimization of N_1-aryl-benzimidazoles for the discovery of new non-nucleoside reverse transcriptase inhibitors active against wild-type and mutant HIV-1 strains. *Bioorg. Med. Chem.,* **2018**, *26*(3), 661-674.

[126] Cabrera, A.; Huerta, H.L.; Chávez, D.; Medina-Franco, J.L. Molecular Modeling of Potential Dual Inhibitors of HIV Reverse Transcriptase and Integrase. *Comput. Mol. Biosci.,* **2018**, *8*, 1-41.

[127] Tang, J.; Vernekar, S.K.V.; Chen, Y.L.; Miller, L.; Huber, A.D.; Myshakina, N.; Sarafianos, S.G.; Parniak, M.A.; Wang, Z. Synthesis, biological evaluation and molecular modeling of 2-Hydroxyisoquinoline-1,3-dione analogues as inhibitors of HIV reverse transcriptase associated ribonuclease H and polymerase. *Eur. J. Med. Chem.,* **2017**, *133*, 85-96.

[128] Barberato, C.; Neto, Z. G. A AÇÃO coletiva como instrumento de tutela e concretização do direito à saúde. *Jus Popul.,* **2018**, *1*(3), 129-146.

[129] Sousa, S.J.F.E.; Sousa, S.B.F.E. Eye bank procedures: donor selection criteria. *Arq. Bras. Oftalmol.,* **2018**, *81*(1), 73-79.

[130] Lemon, S.M.; Walker, C.M.; Hepatitis, A. Virus and Hepatitis E Virus: Emerging and Re-Emerging Enterically Transmitted Hepatitis Viruses. *Cold Spring Harb. Perspect. Med.,* **2019**, *9*(6), pii. A031823.

[131] Majumdar, A.; Gilliam, B.L.; Arnold, R.; Rock, C.; Croft, L.; Morgan, D.J.; Donnenberg, M.S.; Majid, A.; McAninch, J.; Morgan, D.J. Grazoprevir Potassium. HCV NS3 NS4A Prote-ase Inhibitor, Anti-Hepatitis C Virus Drug. *Drugs Future,* **2016**, *41*(2), 85-109.

[132] Pontarolo, R.; Borba, H. H. L.; Ferreira, V. L.; Pedroso, M. L. A.; Souza, A. W.; Siqueira, F. M. Direct-Acting Antivirals For Chronic Hepatitis C Treatment, ed. Berlin, Germany: Arid Science, **2017**, v., p.t.

[133] Stanaway, J.D.; Flaxman, A.D.; Naghavi, M.; Fitzmaurice, C.; Vos, T.; Abubakar, I.; Abu-Raddad, L.J.; Assadi, R.; Bhala, N.; Cowie, B.; Forouzanfour, M.H.; Groeger, J.; Hanafiah, K.M.; Jacobsen, K.H.; James, S.L.; MacLachlan, J.; Malekzadeh, R.; Martin, N.K.; Mokdad, A.A.; Mokdad, A.H.; Murray, C.J.L.; Plass, D.; Rana, S.; Rein, D.B.; Richardus, J.H.; Sanabria, J.; Saylan, M.; Shahraz, S.; So, S.; Vlassov, V.V.; Weiderpass, E.; Wiersma, S.T.; Younis, M.; Yu, C.; El Sayed Zaki, M.; Cooke, G.S. The global burden of viral hepatitis from 1990 to 2013: findings from the Global Burden of Disease Study 2013. *Lancet,* **2016**, *388*(10049), 1081-1088.

[134] Liver, E.A.F.T.S.O.T. EASL 2017 Clinical Practice Guidelines on the management of hepatitis B virus infection. *J. Hepatol.,* **2017**, *67*(2), 370-398.

[135] Kimberlin, D. W.; Brady, M. T.; Jackson, M. A.; Long, S. S. *Red Book: 2015 Report of the Committee on Infec-tious Diseases,* 30th ed.; American Academy of Pediatrics; Elk Grove Village, IL, **2015**.

[136] Giesecke, J. *Modern Infectious Disease Epidemiology*; CRC Press, **2017**.

[137] Pilot-Matias, T.; Tripathi, R.; Cohen, D.; Gaultier, I.; Dekhtyar, T.; Lu, L.; Reisch, T.; Irvin, M.; Hopkins, T.; Pithawalla, R.; Middleton, T.; Ng, T.; McDaniel, K.; Or, Y.S.; Menon, R.; Kempf, D.; Molla, A.; Collins, C. *In vitro* and *in vivo* antiviral activity and resistance profile of the hepatitis C virus NS3/4A protease inhibitor ABT-450. *Antimicrob. Agents Chemother.,* **2015**, *59*(2), 988-997.

[138] Foureau, D.M.; Walling, T.L.; Maddukuri, V.; Anderson, W.; Culbreath, K.; Kleiner, D.E.; Ahrens, W.A.; Jacobs, C.; Watkins, P.B.; Fontana, R.J.; Chalasani, N.; Talwalkar, J.; Lee, W.M.; Stolz, A.; Serrano, J.; Bonkovsky, H.L. Comparative analysis of portal hepatic infiltrating leucocytes in acute drug-induced liver injury, idiopathic autoimmune and viral hepatitis. *Clin. Exp. Immunol.,* **2015**, *180*(1), 40-51.

[139] Sarrazin, C.; Lathouwers, E.; Peeters, M.; Daems, B.; Buelens, A.; Witek, J.; Wyckmans, Y.; Fevery, B.; Verbinnen, T.; Ghys, A.; Schlag, M.; Baldini, A.; De Meyer, S.; Lenz, O. Prevalence of the hepatitis C virus NS3 polymorphism Q80K in genotype 1 patients in the European region. *Antiviral Res.,* **2015**, *116*, 10-16.

[140] Appleby, T. C.; Perry, J. K.; Murakami, E.; Barauskas, O.; Feng, J.; Cho, A.; Fox, D.; Wetmore, D. R.; McGrath, M. E.; Ray, A. S. Structural Basis for RNA Replication by the Hepatitis C Virus Polymerase. *Science,* **2015**, *347*(6223), 771-775.

[141] Patel, P.D.; Patel, M.R.; Kaushik-Basu, N.; Talele, T.T. 3D QSAR and molecular docking studies of benzimidazole derivatives as hepatitis C virus NS5B polymerase inhibitors. *J. Chem. Inf. Model.,* **2008**, *48*(1), 42-55.

[142] Vani, G.S.; Rajarajan, S. A Study on *In-Silico* Analysis of Phytochemicals Targeting the Proteins of Hepatitis B and C Virus. *Int. J. Curr. Microbiol. Appl. Sci.,* **2015**, *4*(12), 683-691.

[143] Wang, X.; Yang, W.; Xu, X.; Zhang, H.; Li, Y.; Wang, Y. Studies of benzothiadiazine derivatives as hepatitis C virus NS5B polymerase inhibitors using 3D-QSAR, molecular docking and molecular dynamics. *Curr. Med. Chem.,* **2010**, *17*(25), 2788-2803.

[144] Anithaa, K.; Singhb, N.; Shaikc, B.; Ahmadc, I.; Agrawald, V.K.; Guptac, S.P. QSAR and Docking Studies on 1, 1-Dioxo-2H-Benzothiadiazines Acting as HCV NS5B Polymerase In-hibitors. *J. Mod. Med. Chem.,* **2015**, *3*, 49-68.

[145] Liu, M-M.; Zhou, L.; He, P-L.; Zhang, Y-N.; Zhou, J-Y.; Shen, Q.; Chen, X-W.; Zuo, J-P.; Li, W.; Ye, D-Y. Discovery of flavonoid derivatives as anti-HCV agents via pharmacophore search combining molecular docking strategy. *Eur. J. Med. Chem.,* **2012**, *52*, 33-43.

[146] Scull, M.A.; Schneider, W.M.; Flatley, B.R.; Hayden, R.; Fung, C.; Jones, C.T.; van de Belt, M.; Penin, F.; Rice, C.M. The N-terminal Helical Region of the Hepatitis C Virus p7 Ion Channel Protein Is Critical for Infectious Virus Production. *PLoS Pathog.,* **2015**, *11*(11), e1005297.

[147] Boukadida, C.; Fritz, M.; Blumen, B.; Fogeron, M-L.; Penin, F.; Martin, A. NS2 proteases from hepatitis C virus and related hepaciviruses share composite active sites and previously unrecognized intrinsic proteolytic activities. *PLoS Pathog.,* **2018**, *14*(2), e1006863.

[148] Lisboa Neto, G.; Noble, C.; Pinho, J.R.R.; Malta, F.M.; Gomes-Gouvea, M.S.; Alvarado-Mora, M.V.; Silva, M.H.; Leite, A.G.; Piccoli, L.Z.; Carrilho, F.J. Characterization of clinical predictors of naturally oc-curring ns3/ns4a protease polymorphism in genotype 1 hepatitis c virus infected patients. *J. Hepatol.,* Elsevier Science BV, **2015**, Vol. *62*, pp. S686-S686.

[149] Bailey, M.D.; Halmos, T.; Lemke, C.T. Discovery of novel P2 substituted 4-biaryl proline inhibitors of hepatitis C virus NS3 serine protease. *Bioorg. Med. Chem. Lett.,* **2013**, *23*(15), 4436-4440.

[150] Wei, Y.; Yang, J.; Kishore Sakharkar, M.; Wang, X.; Liu, Q.; Du, J.; Zhang, J-J. Evaluating the Inhibitory Effect of Eight Compounds from Daphne Papyracea against the NS3/4A Pro-tease of Hepatitis C Virus. *Nat. Prod. Res.,* **2018**, *17,* 1-4.

[151] Ashfaq, U.A.; Jalil, A.; Ul Qamar, M.T. Antiviral phytochemicals identification from Azadirachta indica leaves against HCV NS3 protease: an *in silico* approach. *Nat. Prod. Res.,* **2016**, *30*(16), 1866-1869.

[152] Shaw, J.; Harris, M.; Fishwick, C.W.G. Identification of a lead like inhibitor of the hepatitis C virus non-structural NS2 autoprotease. *Antiviral Res.,* **2015**, *124*, 54-60.

[153] Lulu, S.S.; Thabitha, A.; Vino, S.; Priya, A.M.; Rout, M. Naringenin and quercetin--potential anti-HCV agents for NS2 protease targets. *Nat. Prod. Res.,* **2016**, *30*(4), 464-468.

[154] Uddin, R.; Downard, K.M. Molecular basis of benzimidazole inhibitors to hepatitis C virus envelope glycoprotein. *Chem. Biol. Drug Des.,* **2018**, *92*(3), 1638-1646.

[155] Hung, T-C.; Jassey, A.; Liu, C-H.; Lin, C-J.; Lin, C-C.; Wong, S.H.; Wang, J.Y.; Yen, M-H.; Lin, L-T. Berberine inhibits hepatitis C virus entry by targeting the viral E2 glycoprotein. *Phytomedicine,* **2019**, *53*, 62-69.

Artigo 2: *In Silico* Studies against Viral Sexually Transmitted Diseases

Current Protein and Peptide Science, 2019, *20*, 1135-1150

REVIEW ARTICLE

In Silico Studies against Viral Sexually Transmitted Diseases

Alex F.M. Monteiro[1], Jessika de Oliveira Viana[1], Engene Muratov[3], Marcus T. Scotti[1] and Luciana Scotti[1,2,*]

[1]*Program of Natural and Synthetic Bioactive Products (PgPNSB), Health Sciences Center, Federal University of Paraíba, João Pessoa-PB, Brazil;* [2]*Teaching and Research Management - University Hospital, Federal University of Paraíba, Campus I, 58051-900, João Pessoa-PB, Brazil;* [3]*Laboratory for Molecular Modeling, Division of Medicinal Chemistry and Natural Products, Eshelman School of Pharmacy, University of North Carolina, Beard Hall 301, CB#7568, Chapel Hill, NC, 27599, USA*

ARTICLE HISTORY

Received: December 10, 2018
Revised: January 17, 2019
Accepted: January 18, 2019

DOI:
10.2174/1389203720666190311142747

Abstract: Sexually Transmitted Diseases (STDs) refer to a variety of clinical syndromes and infections caused by pathogens that can be acquired and transmitted through sexual activity. Among STDs widely reported in the literature, viral sexual diseases have been increasing in a number of cases globally. This emphasizes the need for prevention and treatment. Among the methods widely used in drug planning are Computer-Aided Drug Design (CADD) studies and molecular docking which have the objective of investigating molecular interactions between two molecules to better understand the three -dimensional structural characteristics of the compounds. This review will discuss molecular docking studies applied to viral STDs, such as Ebola virus, Herpes virus and HIV, and reveal promising new drug candidates with high levels of specificity to their respective targets.

Keywords: Sexually transmitted diseases, antiviral drugs, *in silico*, molecular docking, HIV, infection.

1. INTRODUCTION

Sexually Transmitted Diseases (STDs) are syndromes and infections caused by pathogens that have been acquired or transmitted through sexual activity. STDs are part of the global disease burden. STDs, as connected to afflicted individuals generally present high emotional costs and social stigma, as well as economic burdens on the affected individuals and the healthcare system [1]. STDs affect men and women of all backgrounds, irrespective of their economic status [2]. They can be acquired and transmitted through unsafe sexual practices and from various pathogens, including bacteria, fungi, viruses and parasites.

WHO estimates that about 1 million sexually transmitted diseases (STDs) are acquired every day worldwide through sexual contact alone, and involve more than 30 different types of bacteria, viruses, and parasites; among these infections, we will highlight 3 incurable viral infections: herpes simplex virus (HSV or herpes), HIV, and Ebola virus (EVD) [3].

Transmission of these diseases can be reduced through prevention, as in comprehensive sexuality education and safe sex/risk-reduction counseling [4]. Symptoms can generally be reduced or modified through treatment. Yet though antivirals can modulate the course of the disease, they do not cure definitively [3].

*Address correspondence to this author at the Health Sciences Center, Federal University of Paraíba, Campus I, 58051-970, João Pessoa-PB, Brazil; Fax 55-83-3291-1528; E-mail: luciana.scotti@gmail.com

Many guidelines have been formulated to help fight STDs, emphasizing treatment, prevention strategies, and other recommendations. Such documents include the CDC's Sexually Transmitted Diseases Treatment Guidelines, 2010 [5], which is often applied in areas that treat patients at risk for STDs.

The need for efforts to control, eliminate, and eradicate STDs has increased in the recent years, both in more efficient health systems and particularly in the design of more potent drugs that attenuate or cure the disease. Often mentioned, molecular docking is a well-accepted tool in the field of drug discovery and is based on the analysis of small molecule-protein interactions, similar to drug-receptor models found in medicinal chemistry [6].

This article provides an overview of sexually transmitted diseases, including the most common viral infections that compromise sexual health, and of molecular docking as applied to protein targets, through comparison of prototypes as reported in the literature to their respective drug standards.

2. DOCKING APPROACHES

In the area of molecular modeling, docking fits as a method of predicting the possible orientation of a molecule relative to a second molecule, forming a stable complex [7]. Therefore, docking has been useful in predicting the intensity of the type of signal transduction produced by various biologically relevant proteins.

1875-5550/19 $58.00+.00

Currently, there has been a frequent use of molecular docking in the planning and discovery of drug candidates by their coupling in the protein targets, being able to predict the orientation of the ligand when it is bound to a protein receptor or enzyme using shape, H-bond and electrostatic interactions to quantify it [8]. In this type of orientation the binding affinity between the two molecules can be observed by calculating scoring functions [9, 10], which represents potentiality of binding.

In the last decades, the number of docking tools and programs have been developed for academic and commercial, like FlexX [11], GOLD [12], AutoDock [13, 14], DOCK, Cdocker and LigandFit [15], Surflex [16], MCDock, FRED [17], Glide [18], AutoDock Vina [19], MOE-Dock [20], LeDock [21] Dock [22], among others. The strategies of positioning of the binder differ for each software used, varying with the use of predictive algorithms such as genetic algorithms (GOLD), systematic technique (Glide) and Monte Carlo simulation (LigandFit).

In the study by Wang *et al.* (2016) [23] the accuracy of the AutoDock Vina, GOLD and MOE-Dock programs was observed, possessing the abilities in producing the correct binding mode of a ligand. However, interactions between small molecules and receptors still depend on experimental methods, since current anchoring methods do not simulate solvent effects, entropic effects, and protonation stages of residues in the active site. The accelerated rhythm of research in this field has been very usual in several fields of research and can be approached more accurately in the near future.

3. EBOLA VIRUS DISEASE

The agent that causes Ebola Virus Disease (EVD) is an RNA virus belonging to the Filoviridae family and Ebolavirus genus. There are currently about five different Ebolavirus strains, the species *Zaire ebolavirus* (EBOV), *Sudan ebolavirus* (SUDV), *Tai Forest ebolavirus* (TAFV), *Bundibugyo ebolavirus* (BDBV) and *Reston ebolavirus* (RESTV). EBOV occurs in a higher proportion [24] for being the most lethal of the five strains [25]; and RESTV is not pathogenic for humans.

The World Health Organization (WHO) reported the incidence of Ebola as epidemic and as a public health emergency in 2014, registering a total of 6,553 new cases, with 3,083 deaths. These increasing levels have been aggravated by economic, and sociocultural factors, as well as by delays in identification of the disease, which involve lack of supplies to control the infection, a shortage of healthcare professionals in the affected localities and the absence of epidemiological surveillance to identify new cases [26].

In the Congo, Ebola birth rates have reached an incidence of up to 90%. The incubation period ranges from 2 to 21 days, with symptoms ranging from fever, weakness, vomiting, diarrhea, headache, and throat pain, to internal and external hemorrhages with multiple dysfunctions [27]. Infections can occur as caused by infected hosts, such as nonhuman primates; by direct contact between humans through body fluids or contaminated surfaces [28]; by manipulation of the bodies of deceased [29] with high viral loads presenting transmission through direct contact in cases of unsafe burials; and among health workers who are not fully protected. A fourth point of transmission can occur through sexual intercourse, skin-to-skin contact, and body secretions. Studies have reported the presence of the virus in vaginal, rectal, and seminal fluids [30], and in some cases the presence of the virus in semen samples has been reported after 157 days.

The persistence of EBOV, particularly in the semen of male survivors, raises the risks of sexual transmission [31]. Previously, EVD survivors had been advised to practice sexual abstinence or to use a condom during sexual activity until 3 months after recovery. These recommendations were based on EBOV detection results from semen samples obtained from eight survivors of EVD and/or Marburg virus disease in prior epidemics. The longest period that the infectious virus was detected in the semen after the onset of symptoms was 82 days [32].

Subsequent investigations revealed EBOV RNA in a survivor's semen at 199 days after the onset of symptoms; the genetic sequence coincided with the sample obtained from the patient of the case [33]. Although no infectious virus has been detected in such semen specimens; the possibility remains that infectious EBOV could persist in the semen of the survivor for up to 6 months after the onset of symptoms. This led the WHO and the Center for Disease Control (CDC) to revise their guidelines as to the time that survivors should practice safe sex through sexual abstinence or in particular, with the use of condoms [28, 34].

Mate *et al.* (2015) [35] demonstrated sexual transmission from a male EVD survivor to his partner after 179 days of the disease. The assembled blood and semen genomes confirmed direct sexual transmission, and presented three substitutions that were not present in other EVD sequences of West Africa.

Despite occasional reports of Ebola virus RNA in patients without evidence of sexual transmission, the suggestion that there are theoretical reasons to consider sexual transmission of the contagion has maintained relevance. Because of the potential risk, EVD survivors need to abstain from sex, or use condoms for up to 3 months after the disease's onset [36]. There is also a need to provide guidance to patients and health agents on the subject. Genomic surveillance, as used to elucidate viral origin and transmission [37], may well help to determine the relevance of sexual transmission and its role. All the while, no drugs or vaccines are yet available to cure EBOV.

3.1. Targets

Genetic studies are being used to identify better measures against the disease. The EBOV RNA genome encodes seven polypeptides, including glycoprotein (GP), nucleoprotein (NP), RNA-dependent RNA polymerase (L), and viral proteins VP35, VP30, VP40 and VP24 [38, 39]. Study of these targets serves to understand their functions and promotes the development of potential drug inhibitors [40]. Studies that address structure-based drug design include the 3D structure of the proteins in docking studies with individual small molecules. Such studies calculate docking scores and binding energies, and identify lead compounds which present the

properties and appropriate profiles needed for clinical development [41]. In this review, molecular docking studies in EVD proteins to develop potential inhibitors for the disease will be reported.

3.1.1. Glycoprotein

Infection with EBOV initiates through fusion between the host cell membrane and the viral glycoprotein (GP) membrane [42]. The GP is formed by a trimer of three disulfide-linked GP1-GP2 heterodimers which are produced during virus assembly through proteolytic cleavage of the GP0 precursor polypeptide [43]. The process occurs via the GP1 subunit, which mediates adhesion to host cells, while the GP2 subunit carries out membrane fusion [44]. Similar fusion processes are observed in other viruses, such as the protein envelope (Env) of the human immunodeficiency virus (HIV), and hemagglutinin (HA) of the influenza virus [45].

EBOV GP is a principal target for designing vaccines and inhibitors [46]. The virus enters the cell through receptor-mediated endocytosis through clathrin-coated pits and caveolae, followed by actin and microtubule-dependent transport to the endosome, where GP is further processed by endosomal cathepsins [47].

In molecular docking studies developed by Ahmad *et al.* (2017) [48] to simulate their constructed models; 5 strong interactions between the glycoprotein and inhibitors derived from dronedarone, amiodarone, and benzofurano were observed. A good score and interaction affinity with residues Arg164 and Ala109 were respectively observed in portions of the arene-arene interaction with benzene ring, and with the hydrogen atom of the hydroxyl group (Fig. **1a**).

In studies of ADMET properties and molecular docking with the Ebola virus glycoprotein another *in silico* study [49] demonstrated potential antiviral drug activities for Fostemsavir and 20 Vicriviroc analogues. The drug screen selected molecules which presented considerable binding energies. One of the analogues, AC1LA8DY, formed bonds with the target protein and interacted with the Thr217, Thr223, Asn257, Thr216, Glu258, and Ala114 residues (Fig. **1b**).

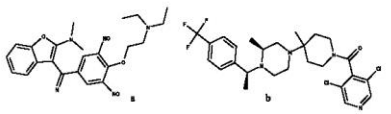

Fig. (1). Compounds presenting activity against Ebola virus glycoprotein **a**) Amiodarone; **b**) AC1LA8DY.

3.1.2. VP35

The Ebola VP35 protein has become a strong target candidate; it acts as a component of the viral RNA polymerase complex. Its activity hinders host interferon (IFN) production, and is vital to the virulence of the Ebola virus. Studies have reported that dsRNA-binding when focused on Arg312 has a high conservation rate and can be considered as a crucial factor for the virulence of EBOV [50]. Reynard and coworkers (2011) [51] reported that disruption of the VP35 protein leads to reduced viral amplification and mortality rates in rats, it is considered a target in the development of drugs against the Ebola virus.

Molecular docking studies for VP35 have been developed by several research groups. In studies carried out by Ekins *et al.* (2014) [52] molecular docking studies were performed using the inhibitors amodiaquine, chloroquine, clomiphene and toremifene. From the pharmacophoric characteristics of compounds with VP35 structures, it was observed that amodiaquine and chloroquine presented the best scores for the protein, with residues Lys248, Ile295, and Gln244 being essential for the activity (Figs. **2a-b**).

Glanzer (2016) [53] employed molecular docking with the VP35 structure to enrich a population of compounds for further *in vitro* testing to approximately 80,000 compounds. Virtual screening triggered the selection of four compounds with IC_{50} of 20 μM, and one compound at 4 μM; demonstrating that Arg305 and Lys339 permit large degrees of freedom, Lys319 and Arg322 present lower degrees of freedom, and Lys309 and Arg312 present bimodal activity. These studies demonstrate the value of *in silico* docking when enriching compounds for *in vitro* testing (Fig. **2c**).

In another study, Ren and coworkers (2016) [54] collected 144 inhibitors of VP35 (EBV) containing the same core scaffolds. Applying virtual screening methodologies and employing docking studies to predict pharmacophore, and a 3D QSAR models triggered identification of seven potential inhibitors with novel scaffolds identified as new VP35 inhibitors. Interactions with Gln241, Lys248, Ile195, Ile303, Pro304 and Phe328 were essential for the activity (Fig. **2d**).

Sulaiman (2018) [55] virtually screened docking and ADME predictions for almost 36 million compounds based on the VP35 structure. In total, 5 compounds with high receptor affinities were selected, of which compound A appeared to be a potential lead compound, with interactions that include interaction with Ala221 and Ile295; alkyl interactions with Lys248, Val245 and Pro 293; hydrogen bonding with Gln241 and Gln244; cation interaction with Lys248; interaction with Ile295; amide stacked interaction with Cys247; and alkyl interactions with Pro304, which could further directing study (Fig. **2e**).

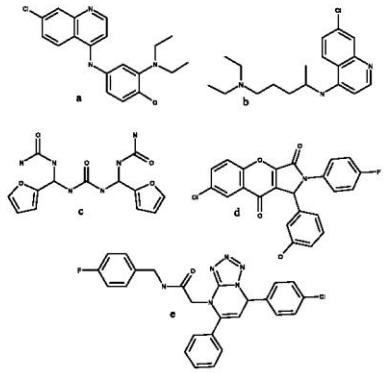

Fig. (2). Compounds presenting activity against Ebola virus VP35 **a**) amodiaquine; **b**) Chloroquine; **c**) ZINC5328460; **d**) CPD5; and **e**) compound A.

3.1.3. VP30

VP30 also acts in the formation of viral mRNAs. Due to its homo-oligomerization function, VP30 is a potential target for antiviral treatment [56]. The protein is about 30 kD in size and presents phospho-proteins that shield the RNA in the presence of zinc [57] and is associated with the viral RNA synthesis machinery [58]. Studies have also implicated VP30 in regulation of co-transcriptional editing of viral glycoprotein mRNAs, and in re-initiation of viral transcription [59].

Raj *et al.* (2016) [40] carried out predictive ADME property studies and molecular docking with four Ebola virus proteins VP40, VP35, VP30 and VP4 using flavonoid derivatives to identify potential lead compounds. The screening used 4500 compounds. Gossypetin and Taxifolin presented the best docking scores and binding energies for the four study proteins; superior to the study's control drug (BCX4430) (Fig. **3a-b**).

Shah and coworkers (2015) [60] evaluated 56 compounds anchored to the VP40, VP35 and VP24 proteins. As a result, they found that the compounds Deslanoside and Digoxin had the best interaction energy values with Asn130 (acting as a common residue in all compounds). Residues that could be considered essential for activity were Asn130 and Gln329 for VP35, and Ser151, Arg154, Ser155 and Lys39 for VP24 (Fig. **3c-d**).

Setlur and coworkers (2016) [61] screened 150 herbal compounds to identify their potential activity in the VP24, VP30, VP35 and VP40 proteins using computational ADMET property studies and molecular docking. Limonin, Samarcandin and Gummosin derivatives demonstrated high affinity with the VP24 and VP35 enzymes, curcumin presented strong inhibition for VP30 (Fig. **3e-g**).

3.1.4. VP40

One of the most abundant proteins in the viral bilayer; VP40 is responsible for structural integrity, is formed in the plasma membrane, and requires lipid raft micro-domains [62]. It performs important viral roles involving the viral RNA and the host cell [63]. Its structure is based on the connection of N-terminal and C-terminal domains by residues of up to 200 amino acids. The C-terminal domain of VP40 acts as a potential target drug because of its role in membrane association [64]. The N-terminal domain is responsible for oligomerization of the protein. The C-terminal domain comprises a proline rich region conserved in the VP40 EBOV receptor and ranges from 205-219 amino acids.

Mirza *et al.* (2016) [65] performed virtual screening of 145,329 natural products, evaluating the pharmacokinetic properties of predicted metabolic sites and molecular docking against the VP35 and VP40 proteins. For molecular docking, the best virtual hits were selected; with Lys251 being a critical residue for VP35, and Thr123, Phe125 and Arg134 being critical for VP40 (Fig. **4a**).

El-Din (2016) [66] performed molecular docking to the VP40 protein using the Lamarckian Genetic Algorithm with 1800 molecules drawn from the PubChem database based on the structure of pyrimidine-2,4-dione. In total, 7 molecules presented promising results against EBOV, with interactions present at Arg134 and Asn136, and according to Lipinsk's rules they were nontoxic (Fig. **4b**).

Abazari (2015) [67] analyzed a library containing 120,000 molecules for ADME properties and simulated potential activity against the EBOV VP40 protein. In this virtual screening, 10 compounds were selected that presented the best profiles, and which resulted in 4 chemicals that could bind VP40 subunits in a manner which (by steric interference) condenses and prevents protein matrix oligomerization. They are being considered as structural hits for anti-Ebola treatment (Fig. **4c**).

Karthick (2016) [68] performed virtual screening of the PLANTS package, an algorithm designed to efficiently rank potential candidates and find a lead compound (against the VP40 protein) based on docking scores, Lipinski rules, and molecular dynamics simulations. The study showed that emodin-8-beta-D-glucoside from the Traditional Chinese Medicine Database (TCMD) qualifies as a lead candidate with critical interaction residues at Phe125 and Arg134, and interactions as an inhibitor of amino acids vital to viral replication (Fig. **4d**).

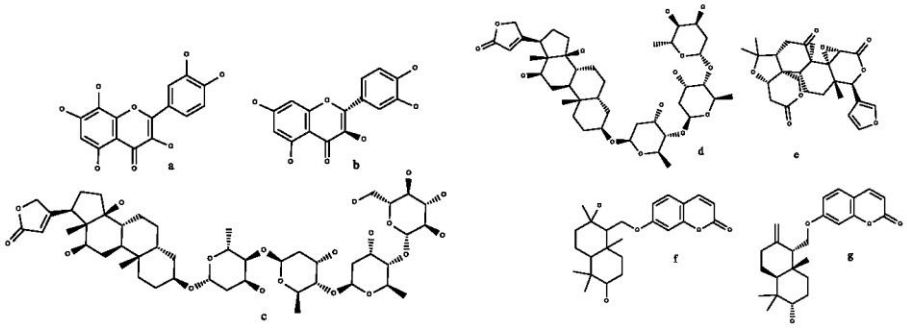

Fig. (3). Compounds presenting activity against Ebola virus VP30. **a**) Gossypentin; **b**) Taxifolin; **c**) Deslanoside; **d**) Digoxin; **e**) Limonin; **f**) Samarcandin; **g**) Gummosin.

Further studies, based on the construction of VP40 protein inhibitors and to find possible alignments between them were carried out by Patel (2013) [69]. The construction of these models and docking studies performed with 1500 drug compounds from the COPICAT server led to the selection of 4 ligands with potential anti-Ebola activity (Fig. **4e**).

Skarivachan (2016) [70] studied the therapeutic potential of metabolites extracted from bacteria associated with the marine sponge (*Cliona sp.*) and tested against the Ebola virus VP40 target. *In vitro* studies, computational virtual screening, and molecular docking were used. In this study, the natural products Gymnastatin, Sorbicillactone, Marizomib and Daryamide were found through molecular docking to possess high protein energy affinity, with strong hydrogen interactions at the residues Leu32, Gly126, Lys127, Ala128 and Phe135, suggesting their potential as lead molecules for novel drugs (Fig. **4f**).

Tamilvanan and Hopper (2013) [71] applied High Throughput Virtual Screening and molecular docking studies to the Traditional Chinese Medicine and Asinex compound databases to find inhibitors against VP40. The Thr123, Phe125, Arg134 residues were found to be essential for binding to the protein, 10 compounds were identified as potent inhibitors of the VP40 matrix protein (Fig. **4g**).

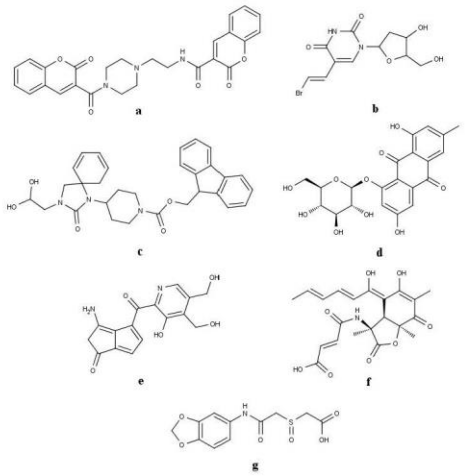

Fig. (4). Compounds presenting activity against Ebola virus VP40. **a**) 2-Oxo-N-(2-{4-((2-oxo-2H-chromen-3-yl)carbonyl)-1-piperazinyl}ethyl)-2H-chromene-3-carboxamide; **b**) Pubchem416724; **c**) compound A; **d**) Emodin-8-β-Glucoside; **e**) compound 1 (Patel, 2013); **f**) Sorbicillactone A; **g**) ASN03576800.

3.1.5. VP24

The EBV VP24 structural protein has been shown to inhibit host interferon (IFN) signaling [72], and also influence transcription and replication in a region of the EBOV genome [73]. The role of the VP24 protein is not yet fully understood; however, it is known to act as a structural protein and may play a role in the virion assembly process. The VP24 protein is expressed in a set with nucleoprotein (NP), and VP35 [74].

Tambunan (2016) [75] virtually screened 2,020 natural Indonesian products from various sources and carried out analyses of their molecular and pharmacological characteristics, Molecular docking simulations were also performed. Cycloartocarpine presented the best potential for anti-Ebola activity (Fig. **5a**).

Tambunan *et al.* in 2018, [76] through *in silico* experiments also identified other VP24 protein inhibitors. In their study, 242,520 compounds were submitted to virtual screening based on pharmacological properties and molecular docking analysis. The compounds, L833, L217 and L595 presented the best results; and compound L595 was considered the most promising lead candidate for inhibiting Ebola virus VP24 (Fig. **5b**).

Sharmila and coworkers (2016) [77] evaluated the activity of andrographolide using molecular docking against three Ebola virus proteins: VP40, VP35, and VP24. The high affinity of the compound for the three proteins of the study, hydrogen bonds and hydrophobic interactions between the compound and the active site of the receptor were found to be responsible for mediating the biological activity (Fig. **5c**).

Sharma (2017) [78] using amino acid sequence homology generated a VP24 protein model and then anchored structural derivatives of Oseltamivir, (which is the first-line drug used to treat Ebola hemorrhagic fevers). From the study, 20 new compounds were found that presented good scores and are potential VP40 inhibitors (Fig. **5d**).

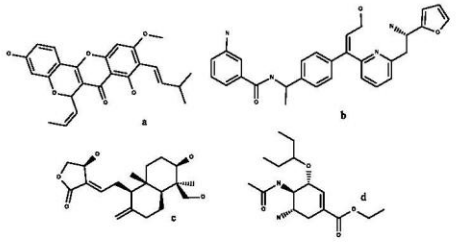

Fig. (5). Compounds presenting activity against Ebola virus VP24. **a**) Cycloartocalpin; **b**) L595; **c**) Andrographolide; **d**) Oseltamivir.

3.1.6. Nucleoprotein

The RNA genome of the Ebola virus exists in its encapsulated form because nucleoprotein (NP) forms a ribonucleoprotein (RNP) complex together with RdRp [79]. RNA serves as a co-packaged (and RNA-dependent) RNA polymerase complex (RdRp) transcribing mRNA of the viral genome. After the virus enters the host cell via glycoproteins, RNP is released from the virion. The function of the nucleocapsid is to protect ssRNAs from degradation [80].

Baikerikar (2017) [81], in molecular docking studies demonstrated the potential activity of curcumin derivatives against the VP40, VP30, VP35, GP and NP proteins of Ebola. The derivative bisdemethoxycurcumin presented excel-

lent binding affinity; with interactions at residues Pro131, Ala128 and Pro165 for VP40; Thr335, Val294 and Leu249 for VP35; Ala246 and Phe181 for VP30; Arg154, Leu158 for VP24; Leu593 and Trp597 for Glycoprotein (GP). If taken as a separated group; (VP35, GP, and VP30); tetrahydrocurcumin presented better binding affinity than curcumin. The molecular docking performed for nucleoprotein presented interactions at residues Arg559, Leu561, Phe630, Ala562 and Leu558. Curcumin binds to NP at residues required for the formation of nucleocapsid structures and replication of the viral genome, thus interrupting its activity (Fig. **6**).

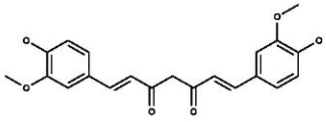

Fig. (6). Curcumin compounds present activity against Ebola virus nucleoprotein.

4. HERPES DISEASE

Herpes simplex virus (HSV), affecting the lives of human hosts through cold sores and genital herpes takes two forms: that of herpes simplex virus type 1 (HSV-1), and herpes simplex virus type 2 (HSV-2) [82]. After entering latency, HSV remains present at nerve ganglia and may emerge later to cause a recurrent and active infection. Herpes viruses are divided into three groups: α herpes viruses which include herpes simplex virus types 1 and 2 and varicella-zoster virus; β herpes viruses which include cytomegalovirus and human herpes viruses 6 and 7; and γ herpes viruses which include Epstein-Barr virus and human herpes virus 8 [83].

HSV-1 causes an oropharyngeal infection, and is transmitted primarily by non-genital contact. HSV-2 is almost exclusively sexually transmitted, causing genital herpes, which can cause ulcerative and vesicular lesions in adults [84]. Ulceration of the genital area may evolve into transmission of the human immunodeficiency virus (HIV) [85].

In the United States HSV-2 is one of the most common sexually transmitted diseases. Many more cases are recorded in Africa (31.5%), followed by the Americas (14.4%), and these exists a high prevalence in women [86]. HSV-2 is transmitted via exposure to the surface of the genital mucosa, leading to latency in the sacral ganglia. Several studies have explored treatments during pharmacological interventions, and vaccines have been developed for Herpes Simplex Virus Type 2 [87].

In many cases HSV is asymptomatic. However, when symptoms do occur, small genital or anal blisters are often characterized, and may include ulcers at the site of infection with fevers, body aches, and swollen lymph glands [85]. Even if the disease is not lethal, the resurgence of the disease can dramatically affect one's life. To treat HSV, several studies have reported the use of synthetic analogues, such as the nucleosides acyclovir, valacyclovir, famcyclovir and penciclovir [88]. Upon activation by viral thymidine kinase these drugs inhibit the activity of viral DNA polymerase [89]. However, if treatment is delayed until late in the infectious process or until after reactivation of the disease, it hinders the effectiveness of the treatment, making cases of viral resistance increasingly reported in compromised individuals [90].

Kolb *et al.* (2017) [91] performed sequential analyses and phylogenetic comparison of 6 HSV-2 isolates, determining the existence of genomic mosaicism and 4 polymorphisms, as well as low inter-strain diversity for HSV-2. Thus, significantly improved anti-HSV agents with broad therapeutic efficacy are being targeted by those in the field of drug research.

4.1. Targets

HSV codes seven proteins that act in the replication and propagation of the virus [92], they include helicase activity, binding proteins, heterodimeric DNA polymerase, single-stranded (ss) DNA-binding protein, and heterotrimeric helicase-primase. However, for the development of inhibitors, few receptors present sufficient capacity as targets [93].

4.1.1. Herpes Simplex Virus Type II Protease

Herpes Simplex Virus Type II Protease is a homodimeric structure comprised of a seven-stranded β-barrel structure with seven α-helices. The active site of the protease is in a shallow groove along the β-barrel surface [94]. For serine proteases, the catalytic mechanism involves a serine nucleic attack on the carbonyl carbon of the scissile bond of the substrate, resulting in an enzyme-serine acyl intermediate awaiting further hydrolysis [95].

Searching the literature, only one article on molecular docking as applied to HSV type II; Arunkumar and Rajarajan (2018) [96] evaluated the efficacy of compounds obtained through *Punica granatum* by means of *in vitro* and *in silico* studies of ADMET properties and HSV-2 protein targets with molecular docking. The compound punicalagin presented moderate absorption, low permeability, and low blood brain barrier penetration. For viral protease, punicalagin presented hydrogen bond interactions with amino acids Arg157, Ser131, Ser129, and Thr132, at the active site of the protease.

4.1.2. Regulator Complex gH/gL

Among the accessory proteins that act as HSV machinery glycoproteins gB, gD, gH and gL, mediate membrane fusion events for entry and virus-induced cell fusion. Deletion of any of these four glycoproteins results in mutant virions that cannot penetrate host cells [97]. Normally, activated forms of gD interact with gH/gL to carryout virus-cell or cell-cell fusion. However, the details of this path still remain unknown [98]. The gH/gL heterodimeric complex acts as a fusion component of all herpes viruses, being considered a target of HSV neutralizing antibodies. In HSV-2 the gH protein contains 3 domains: An N-terminal domain that binds gL, a central helical domain and a C-terminal β-sandwich domain; the second and third domains are conserved in EBV and HSV [99].

In the same article by Arunkumar and Rajarajan (2018) [96] molecular docking with the same set of molecules as potential inhibitors of the gH/gL complex was performed. For the gH/gL herpes virus regulator complex, they found

that punicalagin presented amino acid interactions at Arg527, Trp634, Tyr486, Leu421 and Gly420. This study, using *in vitro* and *in silico* studies revealed good binding results for punicalagin, potential evidence to be used in the development of anti-HSV-2 compounds (Fig. **7**).

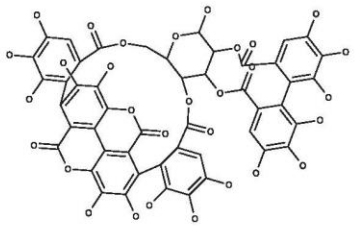

Fig. (7). The compound Punicalagin; presents activity against the Herpes virus Protease and Regulator Complex gH/gL.

5. HUMAN IMMUNODEFICIENCY VIRUS - HIV

Acquired immunodeficiency syndrome (AIDS) is caused by chronic HIV infection and is responsible for a gradual decrease in defense cells of the infected organism. According to WHO, 36.9 million people worldwide are living with HIV; of which in 2017, 59% were receiving treatment.

According to UNAIDS/WHO estimates, in 2017 children under the age of 15 living with HIV numbered 1.8 million, with an estimated 180,000 new cases of children last year. More than 51% of adult HIV cases occurred in women in 2017.

Currently the infection is treatable. With treatment, the infected individual can have a higher quality of life and control over the disease. However, to reduce the risk of transmission and to inhibit contagion, certain actions are essential; such as condom use, not sharing needles, prenatal care, and others.

5.1 Targets

Current HIV treatment is viewed mainly as inhibition of three important proteins; protease (PR), integrase (IN) and reverse transcriptase (RT). Due to HIV mutations and resistance, as well as to the cytotoxicity of the drugs used for treatment, many research groups are actively working to develop and test new anti-HIV bioactive molecules [100, 101].

5.1.1. Enzyme Protease

Protease (PR) is an enzyme responsible for cleavage of peptide bonds between proteins, thus activating or deactivating enzymes. Viral proteins are encoded in peptide chains, and are cleaved by proteases. When viral proteins take on an active conformation they contribute to viral multiplication and proliferation triggering the infectious process.

Using PDB ID 1HXB [102], the authors sought to predict its molecular affinity with HIV protease type 1; the study's prediction model obtained 98% accuracy. HIV protease type 1 is responsible for the cleavage of certain polyproteins present in HIV, this forms mature proteins that will spread throughout the infected organism and lead to the development of the chronic AIDS infection. The protease has now caught the attention of the world's researchers. The same target was used by Mohammdi *et al.* [103] who studied 9 tetrahydropyridine derivatives (obtained using diastereoselective synthesis) which presented promising values against HIV-1 protease. The results as compared to the inhibitor saquinavir were good; where hydrogen bonds in common with the standard drug were perceived for all of the derivatives at the active site of the protease, highlighting residues such as Gly27, Ile50, Val82, Gly48, Asp25 and Asp29.

Tong *et al.* [104] analyzed the interactions, relational structures, and biological activities of 34 urea cycle derivatives using a similarity index, the target was PDB 1AJV. Carboxylic grouping of the molecules interacting with the Asp25 amino acid residue was found to contribute significantly to biological activity, as well as the hydrogen bond involved.

Zondagh *et al.* [105] performed molecular dynamics simulations with HIV-1 (South African wild - Subtype C) targeting PDB 3U71 protease (chosen for close homology with N37T), to study the dynamics (20ns) of 3 anti-HIV bioactives: lopinavir, atazanavir, and darunavir. It was found that HIV mutation had reduced susceptibility to these drugs.

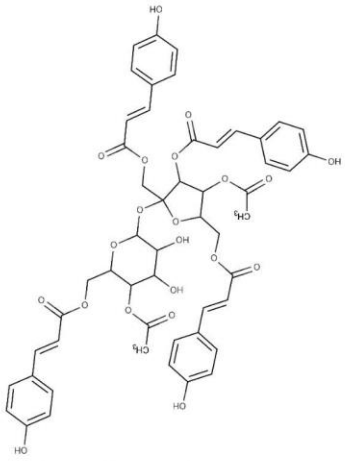

Fig. (8). 2D Structure of Polygonumins A.

A natural product which presents a combination of four phenylpropanoid esters and a unit of sucrose was extracted from the Malaysian Medicinal Plant; *Polygonum minus* (*Persicaria minor*)[106]. Polygonumins A (Fig. **8**) exhibits antiproliferative activity against human leukemia, human breast adenocarcinoma, and colorectal cancer. In addition, study results presented anti-HIV activity; moderately inhibiting the protease PDB 3OXC target by 56%, with an interaction energy in the range of -10.5 to -11.3 kcal/mol. This is the first bioactive from this plant to be considered as protease inhibitor for HIV-1.

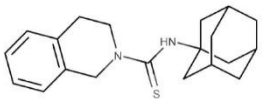

Fig. (9). 2D Structure of N-(Adamantan-1-yl)-1,2,3,4-tetra-hydro-iso-quinoline-2-carbo-thio-amide.

Studies [107] show that N-(Adamantan-1-yl)-1,2,3,4-tetrahydroisoquinoline-2-carbothioamide (Fig. **9**) may present inhibitory activity against HIV-1 protease. Molecular docking using the PDB 1EBY protein revealed the best energy of the calculated poses as -8.1 kcal/mol with significant interactions at amino acid residues Ala128, Arg8, Val82, Pro81, Gly148, Gly149 and Ile147, and a hydrogen bond with residue Gly12. Many studies have focused on the adamantane aggregation at the pharmacophore group of protease inhibitors for HIV-1. For this study, Ghosh *et al.* [108] (whose research discusses molecular docking) evaluated the interaction between a number of synthetic compounds using the adamantanyl group with PDB 5JFP, 5JFU and 5JG1 proteins as targets.

5.1.2. Enzyme Integrase

Integrase (IN) is responsible for integrating the viral DNA into the host cell DNA. This process represents an irreversible step in the cycle of viral reproduction, and once integrated, the infected cell continues expression of the viral gene.

Debnath *et al.* [109] studied the potential pharmacological effect of N-hydroxy-substituted 2-arylacetamide bioactives against the HIV-1 integrase protein. The study highlighted 6 compounds with *in vitro* inhibition of greater than 50%. Molecular docking performed with the PDB 1QS4 protein, revealed important integrations for anti-HIV activity, and hydrophobic and hydrogen bonding interactions with amino acid residues Asn155, Lys156 and Lys159 were observed. Other studies with the same protein can be found in the literature. Vyas *et al.* [110] studied a data set of 71 compounds derived from azoindol-hydroxamic, and azaindol-N-methylhydroxamic acids, together with N-hydroxydihydronaphthyridines collected from the literature. In the molecular docking results, the residues important for pharmacological action were Lys156, Lys159 and Gln148.

Using virtual screening, Chander *et al.* [111] concluded that seven compounds from a database of 200,000 molecules present inhibitory activity for both integrase and reverse transcriptase. For the molecular docking studies, the PDB 3OYA IN protein was used. The drug raltegravir was used as a control. Important interactions for activity with residues Tyr212, Pro214, Pro211, Pro161, Ala188, Try535, Pro537, Ala538, Lys540 were discovered. This same integrase protein was studied by Faridoon *et al.* [112] with a series of 4-arylimino-3-hydroxybutanoic acid derivatives (Fig. **10**); five of which presented HIV-1 inhibitory activity. The control drugs used were tegravir, elvitegravir and dolutegravir and interactions with important residues for activity at: Glu221, Asp128 and Asp185 were detected.

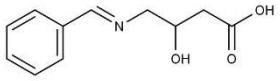

Fig. (10). 2D Structure of 4-arylimino-3-hydroxybutanoic acid.

Zhang *et al.* [113] studied integrase inhibitory activity in a series of 3-hydroxypicolinamides (Fig. **11**) with the PDB 3LPU protein. In this study, residues Ile365, Leu102, Ala128, Ala129, Trp132, Thr174, Met178, Asp36, His171, Ile365 , Gln168, Lys173, Met178, Leu102, Ala128, Ala129, Trp131 and Trp132 presented significance for anti-HIV activity. The same protein was also used in a study by Panwar & Singh [114] where 3 compounds studied showed promising integrase inhibitory activity.

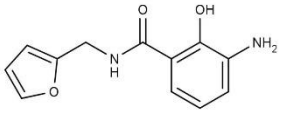

Fig. (11). 2D Structure of 3-hydroxypicolinamide.

Natural products with anti-HIV pharmacological action are also reported in the literature, Srivastav & Tiwari [115] studied 26 coumarin derivative dockings (Fig. **12**) (using raltegravir as the control) with the PDB 3NF7 protein. The molecules were subjected to a QSAR regression model with Q2 = 0.8307. The interactions at Arg199, Leu158, Met154, Lys188, Val150, Arg199, Lys186 and Ala196 were shown to be important for activity. Ericksen *et al.* [116] has even used molecular docking with the PDB 3NF7 protein in a Machine Learning Consensus Scoring study to evaluate software performance.

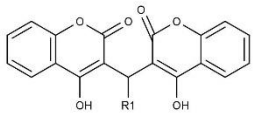

Fig. (12). 2D Structure of coumarin derivatives.

5.1.3. Reverse Transcriptase

RT also known as RNA-dependent DNA polymerase synthesizes viral DNA molecules from the viral RNA present in the virus; genetic material that becomes available for incorporation into host cells.

Jin *et al.* [117] studied a new series of biphenyl-substituted diarylpyrimidines (Fig. **13a**) against wild type and mutant HIV reverse transcriptase, aiming to inhibit its activity. Of twenty-two (22) ligand-receptor interactions calculated through molecular docking with the PDB 2ZD1 protein, five presented high potency with EC_{50s} of less than 2 nM. Maruti & Dhawale [118] also performed a study with 24 derivative malonamide compounds (Fig. **13b**) analyzing *in silico* molecular docking of ligand-receptor interactions against reverse transcriptase with the PDB 2ZD1 protein.

The study revealed the contribution of interactions at amino acid residues Asp64, Asp116, Leu100, Tyr18, Trp229, Val106, Val179 and Phe227.

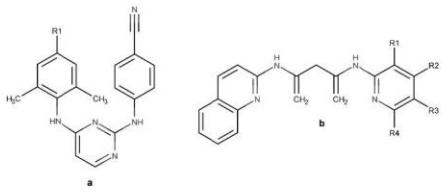

Fig. (13). 2D Structures of **a**) biphenyl-substituted diarylpyrimidines, and **b**) malonamide derivatives.

Liu *et al.* [119] analyzed the interactions of 52 diarylpyrimidine analogues (DAPYs) using molecular docking for the PDB 3MEC protein; indicating a contribution of the phenyl ring at the C4 position of the pyrimidine ring that presented better results than cycloalkanes. The authors pointed out certain amino acid residues which are important for HIV-1 reverse transcriptase inhibitory action: Lys 101, Tyr318, Tyr232, Phe 227, Trp239, Trp229, Pro225, Pro226, Met230, Ile94, and Val189, Leu100, Lys103, Val179, Gly190, Leu234, His235, Tyr188, Tyr181, and Trp229. The same protein is found in many chemoinformatic studies [120-122].

Samanta & Das [123] studied reverse transcriptase inhibition in certain di-ether catechols, performing molecular docking for the PDB: 4H4M, 4RW4, 4RW6, 4RW7, 4RW8 and 4RW9 proteins in differing *in silico* modeling software showing significant interactions with residues Lys103, Val106, Asn103, Pro236, Val179, Tyr181, Leu100, Leu234, Pro95, Lys102, Tyr188 and Trp229. These PDB proteins are found in other works [124], including Monforte *et al* [125] who performed molecular docking of N1-aryl-2-arylthioacetamido-benzimidazole derivatives with the PDB 3DLG protein using the drugs nevirapine and efavirenz. Two compounds with promising anti-HIV profiles were highlighted.

Cabrera *et al.* [126] developed a double inhibition study with molecular modeling of 320 quinoline derivatives (Fig. **14**) for reverse transcriptase and integrase using the PDB: 2BAN, 2B5J and 3L2U proteins. In conclusion, 4 structures presented the possibility of having binary pharmacological activities, with interactions similar to the drug elvitegravir and important interactions with amino acid residues: Pro236 or Lys103.

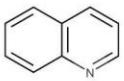

Fig. (14). 2D Structure of quinoline.

Tang *et al.* [127] synthesized and modeled 2-hydroxyisoquinoline-1,3-dione derivatives. Two of which (Fig. **15**) presented potent and selective inhibition of HIV-1 reverse transcriptase-associated RNase H in molecular docking studies, with affinities for the Arg448, Lys65, Arg72, Gln151, Asn103, Tyr188, Tyr181, and Trp229 residues in PDB: 3LP1 and 1RTD proteins.

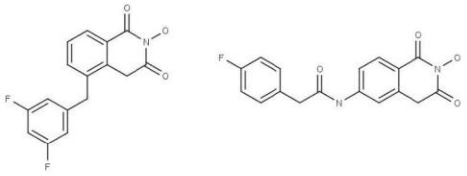

Fig. (15). 2D structures of the most potent and selective bioactives against the PDB: 3LP1 and 1RTD proteins.

6. HEPATITIS C VIRUS

In Babylon, more than 2,500 years ago, reports of jaundice (yellowing of the skin) have been found. Around 400 a.C the greek physician named Hipocrates characterized jaundice as being an infectious disease whose origin was in liver-related problems [128-131].

Bianch JB was the first to use the term "hepatitis", publishing in 1725 with his work titled as *Historia hepatica without theoria et praxis omnius morborum hepatitis et bilis*. Hepatitis is an infectious disease caused by viruses, which when reaching a chronic state causing cirrhosis, it is advisable to transplant the liver, when starting the treatment the patient is advised not to ingest alcoholic beverages and not to consume toxic foods to the liver [132-136].

The hepatitis virus attacks hepatocyte cells (which produce proteins) in the liver, once infected, the virus binds to the hepatocytes (cells found in the liver) through the proteins of its viral envelope crossing the cellular cytoplasm and losing its capsid upon entering the nucleus, in which the polymerase present in the cellular medium biosynthesizes the viral genetic material [137-140].

In 1970 Harvey J. Alter through an investigation realized that most cases of hepatitis did not correspond to the types A and B, but only in 2000 through the scientists Alter and Houghton that gained the premo Lasker that the virus of Hepatitis C happened to be known. According to the WHO, an estimated 71 million people are infected with hepatitis C worldwide, of which almost 400,000 die each year. Treatments with current medications can achieve 95% cure, yet according to estimates about 30% of those infected develop liver cirrhosis within 20 years after infection.

6.1. Targets

6.1.1. Inhibition of ns5b

NS5B is an RNA polymerase protein present in hepatitis C virus, with which the virus can multiply itself by replicating its RNA, using viral RNA as a template during its replication. Inhibition can occur basically by three chemical agents: nucleoside inhibitors, non-nucleoside allosteric inhibitors and pyrophosphate analogues. As drugs widely used as inhibitors of BS5B we have sofosbuvir and ledipasvir (Fig. **16**).

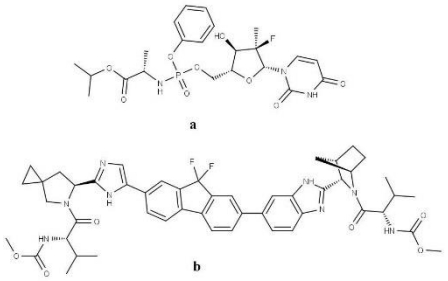

Fig. (16). 2D structures of NS5B inhibitory drugs. **a**) sofosbuvir and **b**) ledipasvir.

Patel *et al.* [141] studied the inhibitory action of NS5B by 67 benzoimidazole heterocyclic compounds through QSAR 3D studies and molecular anchoring using PDB ID 2DXS for action against Hepatitis C virus (HCV), as a conclusion compound 22 (Fig. **17**) presented a better antiviral profile in the fight against hepatitis, with pIC_{50} equal to 2.10. This same protein is present in some computational chemistry studies such as Vani *et al.* [142] using 65 compounds selected through the ADMET properties of 89 compounds selected from the platform online PubChem NCBI (https://pubchem. ncbi.nlm.nih.gov), estes compostos foram submetidos a docking molecular usando o software iGEM dock (http:// gemdock.life.nctu.edu.tw/dock/igemdock.php) presenting good anchorage results with the protein, of which 4 presented better results: daidzin, ononin, colecoxib, rofecoxib.

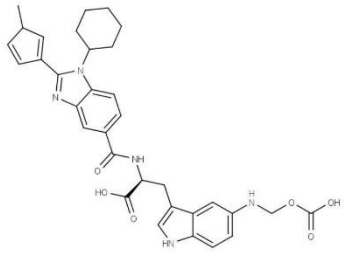

Fig. (17). 2D structures of the compound with the best result in the study of Patel *et al.* [141].

Other heterocyclic compounds can be readily found in studies proposing candidates for anti-HCV drugs, for example benzothiadiazine derivatives, which is a compound with two rings containing two nitrogen atoms and one sulfur atom (Fig. **18a**). Wang *et al.* [143] developed mock-chemistry studies using 3D QSAR, molecular docking and molecular dynamics with 239 benzothiadiazinic compounds, in this study molecular anchoring was performed using the PDB ID 3H98 protein using SYBYL 6.9 exhibiting important interactions with amino acid residues Glu446, Gly449, Asn291 and Asp318. Anithaa *et al.* [144] carried out a QSAR and molecular docking study of 52 1,1-Dioxo-2H-benzothiadiazine compounds acting against HCV, this study pointed out that the increase of hydrogen donors and acceptors and hydrophobic groups in some regions of these benzothiadiazines proved to be potentiators of antiviral activity.

Natural products are also studied for antiviral action against hepatitis C, as an example it is possible to point out the study of Liu *et al.* [145] which addresses the possibility of using flavonoids in hepatitis treatment through a pharmacophoric research combined with molecular docking using the PDB ID 1C2P protein and 39 flavonoids through GOLD software of which 20 of these compounds showed EC 50 μM results, two which have a natural occurrence: apigenin and luteolin (Fig. **18b-c**).

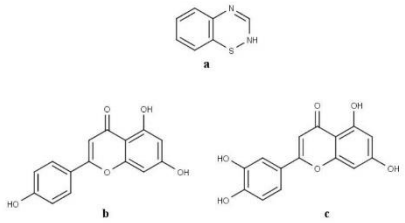

Fig. (18). General structure of **a**) benzothiadiazine, **b**) apigenin and **c**) luteolin.

6.1.2. Inhibition of Other Targets

Protease is also a therapeutic target widely studied by researchers seeking new drugs for Hepatitis C, because it is a peptide cleavage enzyme and plays a key role in cell life and HCV proteases such as NS2, NS3, NS4A, NS4B, NS5A and NS5B [146-148].

Bailey *et al.* [149] developed a study with 27 2,4-disubstituted thiazole substituted for evaluation, in this study a molecular docking study was developed to understand the interactions between amino acid residues that contribute significantly to activity against Hepatitis C, thus, this study concludes that the Asp81, His57 and Tyr56 residues are present in the ligand-receptor interaction region. The biological results through the IC 50 validated the *in silico* results, obtaining as a result the possibility of using these triazoles as a good therapeutic alternative in the fight against HCV, the example of which is in compound 11 of that study that presented $IC_{50} = 0.74$nm (Fig. **19a**).

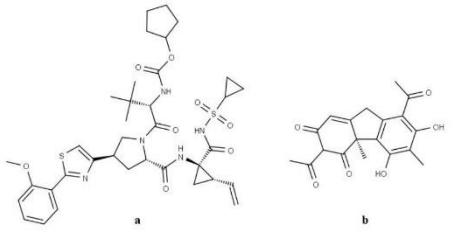

Fig. (19). Structure 2D **a**) of the compound with the lowest inhibitory concentration [149] and **b**) (+)-usnic acid.

Wei *et al.* [150] studied the antiviral action of 8 compounds present in the organic extract with ethyl acetate from the plant *Daphne papyracea*, According to their study, these compounds showed an inhibitory effect of NS3 / NS4A protease, among the results (+)-usnic acid (Fig. **19b**) presented better results. Plants, as well as their natural products, are widely studied as a source of HCV bioactives, as in the *in silico* Ashfaq *et al.* [151] which consists of the molecular docking of phytochemical components of Azadirachta indica leaves with the objective of identifying potential inhibitors of hepatitis C NS3, in this study, the 3-Deacetyl-3-cinnamoyl-azadirachtin compound presented a better antiviral profile interacting with the residue Gln526.

A survey of Shaw *et al.* [152] consisted of the virtual screening of 12 compounds available from ChemBridge Corporation, KeyOrganics, Sigma Aldrich and MedChem Express, which were subjected to molecular docking using the PDB ID 2HD0 protein, in order to track new NS2 inhibitors, as validation of the *in silico* method through *In vitro* test, as conclusion of this study it is shown that compound 160 (Fig. **20a**) presented good results against the inhibitory action of the NS3 protease, as well as its derivatives 160-1 (Fig. **20b**) and 160-2 (Fig. **20c**).

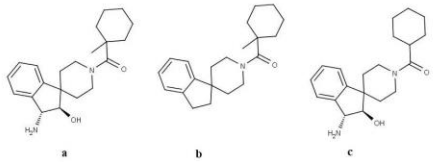

Fig. (20). 2D Structure of Shaw *et al.* [152]. **a**) compound 160, **b**) compound 160-1 and **c**) compound 160-2.

The PDB ID 2HD0 target was also used in other studies, an example was the search for Lulu *et al.* [153] which consisted in verifying by molecular docking the possibility of inhibitory action of Hepatitis C NS2 using AutoDock4.2 proving the potential anti-hepatic action of naringenin and quercetin.

In addition to the proteases, inhibition of protein targets present in viral envelopes are also studied as possibilities in the rational planning of new drugs in the fight against hepatitis C, some studies regard proteins E1 and E2 as promising examples. Uddin *et al.* [154] performed the molecular modeling using benzoimidazole B5 with the objective of inhibiting the E1 viral envelope protein, in this study included molecular docking between these compounds and the protein PDB ID 1MBN, through the computational data obtained in their research, the authors realized the possibility of using this azolic as a bioactive against hepatitis C Another example of a study involving envelope proteins is the Hung *et al.* [155] in which the use of berberine as a molecule with anti-HCV action, in its study the results of molecular docking using 4UOI and 4MWF proteins were validated with the tests *in vitro*.

CONCLUSION

This review addressed sexually transmitted diseases; chronic infections that afflict people from all over the world regardless of sex, class, or financial means which are caused by viruses and maintain certain protein targets. These diseases constitute a public health concern, and new bioactives have been emerging that may reduce cases of resistance and avoid the cytotoxicity of existing drugs.

Computational chemistry, when included in pharmaceutical and medicinal chemistry provides a tool for rational drug screening and planning. Molecular docking; the study of ligand-receptor interactions contributed to all of the studies presented. The objective is to understand structural contributions and interactions involved in inhibiting the activity of target proteins which are necessary to serious pathologies such as Ebola, HIV and herpes.

In this study, our purpose was to inform as to the nature and/or class of the compounds reviewed together with their targets in *in silico* studies, so that new research may emerge through appropriating this knowledge towards the development of new drugs.

CONSENT FOR PUBLICATION

Not applicable.

FUNDING

We would like to thank the Conselho Nacional de Desenvolvimento Científico e Tecnológico (CNPq) and the Coordenação de Aperfeiçoamento de Pessoal de Nível Superior (Capes) for financial support.

CONFLICT OF INTEREST

The authors declare no conflict of interest, financial or otherwise.

ACKNOWLEDGEMENTS

Declared none.

REFERENCES

[1] Singh, S.K. *Diagnostics to Pathogenomics of Sexually Trans-mitted Infections,* 1st ed; Wiley Blackwell, **2018**.

[2] Satterwhite, C.L.; Torrone, E.; Meites, E.; Dunne, E.F.; Mahajan, R.; Ocfemia, M.C.B.; Su, J.; Xu, F.; Weinstock, H. Sexually transmitted infections among US women and men: prevalence and incidence estimates, 2008. *Sex. Transm. Dis.*, **2013**, *40*(3), 187-193.

[3] World Health Organization: Sexually transmitted infections, 2016. http://www.who.int/news-room/fact-sheets/detail/sexually-transmitted-infections-(stis) (Accessed Set 15, 2018)

[4] Friedman, A.L.; Kachur, R.E.; Noar, S.M.; McFarlane, M. Health communication and social marketing campaigns for sexually transmitted disease prevention and control: What is the evidence of their effectiveness? *Sex. Transm. Dis.*, **2016**, *43*(2)(Suppl. 1), S83-S101.

[5] Center of Disease Control: Sexually transmitted diseases treatment guidelines, 2010. https://www.cdc.gov/std/treatment/2010/std-treatment-2010-rr5912.pdf (Accessed Set 15, 2018)

[6] Ferreira, L.G.; Dos Santos, R.N.; Oliva, G.; Andricopulo, A.D. Molecular docking and structure-based drug design strategies. *Molecules*, **2015**, *20*(7), 13384-13421.

[7] Chen, Y.; Shoichet, B.K. Molecular docking and ligand specificity in fragment-based inhibitor discovery. *Nat. Chem. Biol.*, **2009**, *5*(5), 358-364.

[8] Kitchen, D.B.; Decornez, H.; Furr, J.R.; Bajorath, J. Docking and scoring in virtual screening for drug discovery: methods and applications. *Nat. Rev. Drug Discov.*, **2004**, *3*(11), 935-949.

[9] Wang, R.; Lu, Y.; Wang, S. Comparative evaluation of 11 scoring functions for molecular docking. *J. Med. Chem.,* **2003**, *46*(12), 2287-2303.

[10] Warren, G.L.; Andrews, C.W.; Capelli, A.M.; Clarke, B.; LaLonde, J.; Lambert, M.H.; Lindvall, M.; Nevins, N.; Semus, S.F.; Senger, S.; Tedesco, G.; Wall, I.D.; Woolven, J.M.; Peishoff, C.E.; Head, M.S. A critical assessment of docking programs and scoring functions. *J. Med. Chem.,* **2006**, *49*(20), 5912-5931.

[11] Rarey, M.; Kramer, B.; Lengauer, T.; Klebe, G. A fast flexible docking method using an incremental construction algorithm. *J. Mol. Biol.,* **1996**, *261*(3), 470-489.

[12] Jones, G.; Willett, P.; Glen, R.C.; Leach, A.R.; Taylor, R. Development and validation of a genetic algorithm for flexible docking. *J. Mol. Biol.,* **1997**, *267*(3), 727-748.

[13] Österberg, F.; Morris, G.M.; Sanner, M.F.; Olson, A.J.; Goodsell, D.S. Automated docking to multiple target structures: incorporation of protein mobility and structural water heterogeneity in AutoDock. *Proteins,* **2002**, *46*(1), 34-40.

[14] Morris, G.M.; Huey, R.; Lindstrom, W.; Sanner, M.F.; Belew, R.K.; Goodsell, D.S.; Olson, A.J. AutoDock4 and AutoDockTools4: Automated docking with selective receptor flexibility. *J. Comput. Chem.,* **2009**, *30*(16), 2785-2791.

[15] Venkatachalam, C.M.; Jiang, X.; Oldfield, T.; Waldman, M. LigandFit: a novel method for the shape-directed rapid docking of ligands to protein active sites. *J. Mol. Graph. Model.,* **2003**, *21*(4), 289-307.

[16] Jain, A.N. Surflex: Fully automatic flexible molecular docking using a molecular similarity-based search engine. *J. Med. Chem.,* **2003**, *46*(4), 499-511.

[17] McGann, M.R.; Almond, H.R.; Nicholls, A.; Grant, J.A.; Brown, F.K. Gaussian docking functions. *Biopolymers,* **2003**, *68*(1), 76-90.

[18] Friesner, R.A.; Banks, J.L.; Murphy, R.B.; Halgren, T.A.; Klicic, J.J.; Mainz, D.T.; Repasky, M.P.; Knoll, E.H.; Shelley, M.; Perry, J.K.; Shaw, D.E.; Francis, P.; Shenkin, P.S. Glide: a new approach for rapid, accurate docking and scoring. 1. Method and assessment of docking accuracy. *J. Med. Chem.,* **2004**, *47*(7), 1739-1749.

[19] Trott, O.; Olson, A.J. AutoDock Vina: improving the speed and accuracy of docking with a new scoring function, efficient optimization, and multithreading. *J. Comput. Chem.,* **2010**, *31*(2), 455-461.

[20] Corbeil, C.R.; Williams, C.I.; Labute, P. Variability in docking success rates due to dataset preparation. *J. Comput. Aided Mol. Des.,* **2012**, *26*(6), 775-786.

[21] Zhao, H.; Caflisch, A. Discovery of ZAP70 inhibitors by high-throughput docking into a conformation of its kinase domain generated by molecular dynamics. *Bioorg. Med. Chem. Lett.,* **2013**, *23*(20), 5721-5726.

[22] Allen, W.J.; Balius, T.E.; Mukherjee, S.; Brozell, S.R.; Moustakas, D.T.; Lang, P.T.; Case, D.A.; Kuntz, I.D.; Rizzo, R.C. DOCK 6: Impact of new features and current docking performance. *J. Comput. Chem.,* **2015**, *36*(15), 1132-1156.

[23] Wang, Z.; Sun, H.; Yao, X.; Li, D.; Xu, L.; Li, Y.; Tian, S.; Hou, T. Comprehensive evaluation of ten docking programs on a diverse set of protein-ligand complexes: the prediction accuracy of sampling power and scoring power. *Phys. Chem. Chem. Phys.,* **2016**, *18*(18), 12964-12975.

[24] Leroy, E.M.; Kumulungui, B.; Pourrut, X.; Rouquet, P.; Hassanin, A.; Yaba, P.; Délicat, A.; Paweska, J.T.; Gonzalez, J.P.; Swanepoel, R. Fruit bats as reservoirs of Ebola virus. *Nature,* **2005**, *438*(7068), 575-576.

[25] Briand, S.; Bertherat, E.; Cox, P.; Formenty, P.; Kieny, M.P.; Myhre, J.K.; Roth, C.; Shindo, N.; Dye, C. The International Ebola Emergency. *N. Engl. J. Med.,* **2014**, *371*, 1180-1183.sis.nlm.nih.gov/Tox/ToxMain.html (Accessed May 23, 2004)

[26] World Health Organization: Ebola situation report, 2016. http://apps.who.int/ebola/current-situation/ebola-situation-report-30-march-2016 (Accessed Oct 9, 2018).

[27] Bwaka, M.A.; Bonnet, M.J.; Calain, P.; Colebunders, R.; De Roo, A.; Guimard, Y.; Katwiki, K.R.; Kibadi, K.; Kipasa, M.A.; Kuvula, K.J.; Mapanda, B.B.; Massamba, M.; Mupapa, K.D.; Muyembe-Tamfum, J.J.; Ndaberey, E.; Peters, C.J.; Rollin, P.E.; Van den Enden, E.; Van den Enden, E. Ebola hemorrhagic fever in Kikwit, Democratic Republic of the Congo: clinical observations in 103 patients. *J. Infect. Dis.,* **1999**, *179*(Suppl. 1), S1-S7.

[28] Centers for Disease Control and Prevention: Transmission Of Ebola (Ebola Virus Disease), 2014. https://www.cdc.gov/vhf/ebola/transmission/index.html (Accessed Sep 18, 2018)

[29] Hewlett, B.S.; Amola, R.P. Cultural contexts of Ebola in northern Uganda. *Emerg. Infect. Dis.,* **2003**, *9*(10), 1242-1248. [http://dx.doi.org/10.3201/eid0910.020493]

[30] Rodriguez, L.L.; De Roo, A.; Guimard, Y.; Trappier, S.G.; Sanchez, A. Bressler, Williams, D.A.J.; Rowe, A.K.; Bertolli, J.; Khan, A.S.; Ksiazek, T.G.; Peters, C.J.; Nichol, S.T. Persis-tence and genetic stability of Ebola virus during the outbreak in Kikwit, Democratic Republic of the Congo, 1995. *J. Infect. Dis.,* **1999**, *179*, 170-176.

[31] Rogstad, K.E.; Tunbridge, A. Ebola virus as a sexually transmitted infection. *Curr. Opin. Infect. Dis.,* **2015**, *28*(1), 83-85.

[32] Deen, G.F.; Broutet, N.; Xu, W.; Knust, B.; Sesay, F.R.; McDonald, S.L.; Ervin, E.; Marrinan, J.E.; Gaillard, P.; Habib, N.; Liu, H.; Liu, W.; Thorson, A.E.; Yamba, F.; Mas-saquoi, T.A.; James, F.; Ariyarajah, A.; Ross, C.; Bernstein, K.; Coursier, A.; Klena, J.; Carino, M.; Wurie, A.H.; Zhang, Y.; Dumbuya, M.S.; Abad, N.; Idriss, B.; Wi, T.; Bennett, S.D.; Davies, T.; Ebrahim, F.K.; Meites, E.; Naidoo, D.; Smith, S.J.; Ongpin, P.; Malik, T.; Banerjee, A.; Erickson, B.R.; Liu, Y.; Liu, Y. Xu, K.; Brault, A.; Durski, K.N.; Winter, J.; Sealy, T.; Nichol S.T.; Lamunu, M.; Bangura, J.; Landoulsi, S.; Jambai, A.; Morgan, A.; Wu, G.; Liang, M.; Su, Q.; Lan, Y.; Hao, Y.; Formenty, P.; Ströher, U.; Sahr, F. Ebola RNA persistence in semen of Ebola virus disease survivors. *N. Engl. J. Med.,* **2017**, *377*(15), 1428-1437.

[33] Christie, A.; Davies-Wayne, G.J.; Cordier-Lassalle, T.; Blackley, D.J.; Laney, A.S.; Williams, D.E.; Shinde, S.A.; Badio, M.; Lo, T.; Mate, S.E.; Ladner, J.T.; Wiley, M.R.; Kugelman, J.R.; Palacios, G.; Holbrook, M.R.; Janosko, K.B.; de Wit, E.; van Doremalen, N.; Munster, V.J.; Pettitt, J.; Schoepp, R.J.; Verhenne, L.; Evlampidou, I.; Kollie, K.K.; Sieh, S.B.; Gasasira, A.; Bolay, F.; Kateh, F.N.; Nyenswah, T.G.; De Cock, K.M. Possible sexual transmission of Ebola virus - Liberia, 2015. *MMWR Morb. Mortal. Wkly. Rep.,* **2015**, *64*(17), 479-481.

[34] World Health Organization. Interim advice on the sexual transmission of the Ebola virus disease, 2016. . http://www.who.int/reproductivehealth/topics/rtis/ebola-virus-semen/en/ (Accessed Set 21, 2018).

[35] Mate, S.E.; Kugelman, J.R.; Nyenswah, T.G.; Ladner, J.T.; Wiley, M.R.; Cordier-Lassalle, T.; Christie, A.; Schroth, G.P.; Gross, S.M.; Davies-Wayne, G.J.; Shinde, S.A.; Murugan, R.; Sieh, S.B.; Badio, M.; Fakoli, L.; Taweh, F.; de Wit, E.; van Doremalen, N.; Munster, V.J.; Pettitt, J.; Prieto, K.; Humrighouse, B.W.; Ströher, U.; DiClaro, J.W.; Hensley, L.E.; Schoepp, R.J.; Safronetz, D.; Fair, J.; Kuhn, J.H.; Blackley, D.J.; Laney, A.S.; Williams, D.E.; Lo, T.; Gasasira, A.; Nichol, S.T.; Formenty, P.; Kateh, F.N.; De Cock, K.M.; Bolay, F.; Sanchez-Lockhart, M.; Palacios, G. Molecular evidence of sexual transmission of Ebola virus. *N. Engl. J. Med.,* **2015**, *373*(25), 2448-2454.

[36] Judson, S.; Prescott, J.; Munster, V. Understanding ebola virus transmission. *Viruses,* **2015**, *7*(2), 511-521.

[37] Gire, S.K.; Goba, A.; Andersen, K.G.; Sealfon, R.S.G.; Park, D.J.; Kanneh, L. Jalloh, s.; Momoh, M.; Fullah, M.; Dudas, G.; Wohl, S.; Moses, L.M.; Yozwiak, N.L.; Winnicki, S.; Matranga, C.B.; Malboeyf, C.M.; Qu, J.; Glandden, A.D.; Schaffner, S.F.; Yang, X.; Jiang, P.P.; Nekoui, M.; Colubri, A.; Coomber, M.R.; Fonnie, M.; Moigboi, A.; Gbakie, M.; Kama-ra, F.K.; Tucker, V.; Konuwa, E.; Saffa, S.; Sellu, J.; Jalloh, A.A.; Jovoma, A.; Koninga, J.; Mustapha, I.; Kargbo, K.; Fo-day, M.; Yillah, M.; Kanneh, F.; Robert, W.; Massally, J.L.B.; Chapman, S.B.; Bochicchio, J.; Murphy, C.; Nusbaum, C.; Young, S.; Birren, B.W.; Grant, D.S.; Scheiffelin, J.S.; Lander, E.S.; Happi, C.; Gevao, S.M.; Gnirke, A.; Rambaut, A.; Garry, R.F.; Khan, S.H.; Sabeti, P.C. Genomic surveillance elucidates Ebola virus origin and transmission during the 2014 outbreak. *Science,* **2014**, *345*, 1369-1372.

[38] Hulo, C.; de Castro, E.; Masson, P.; Bougueleret, L.; Bairoch, A.; Xenarios, I.; Le Mercier, P. ViralZone: A knowledge resource to understand virus diversity. *Nucleic Acids Res.,* **2011**, *39*(Database issue), D576-D582.

[39] Nanbo, A.; Watanabe, S.; Halfmann, P.; Kawaoka, Y. The spatio-temporal distribution dynamics of Ebola virus proteins and RNA in infected cells. *Sci. Rep.,* **2013**, *3*, 1206.

[40] Raj, U.; Varadwaj, P.K. Flavonoids as multi-target inhibitors for proteins associated with Ebola virus: In silico discovery using vir-

tual screening and molecular docking studies. *Interdiscip. Sci.,* **2016**, *8*(2), 132-141.
[41] Chou, K.C. Impacts of bioinformatics to medicinal chemistry. *Med. Chem.,* **2015**, *11*(3), 218-234.
[42] Diehl, W.E.; Lin, A.E.; Grubaugh, N.D.; Carvalho, L.M.; Kim, K.; Kyawe, P.P.; McCauley, S.M.; Donnard, E.; Kucukural, A.; McDonel, P.; Schaffner, S.F.; Garber, M.; Rambaut, A.; Andersen, K.G.; Sabeti, P.C.; Luban, J. Ebola virus glycopro-tein with increased infectivity dominated the 2013-2016 epi-demic. *Cell,* **2016**, *167*(4), 1088-1098.e6.
[43] Weissenhorn, W.; Carfí, A.; Lee, K.H.; Skehel, J.J.; Wiley, D.C. Crystal structure of the Ebola virus membrane fusion subunit, GP2, from the envelope glycoprotein ectodomain. *Mol. Cell,* **1998**, *2*(5), 605-616.
[44] Takada, A.; Robison, C.; Goto, H.; Sanchez, A.; Murti, K.G.; Whitt, M.A.; Kawaoka, Y. A system for functional analysis of Ebola virus glycoprotein. *Proc. Natl. Acad. Sci. USA,* **1997**, *94*(26), 14764-14769.
[45] Earp, L.J.; Delos, S.E.; Park, H.E.; White, J.M. The many mechanisms of viral membrane fusion proteins. *Mem-brane trafficking in viral replication*; Marsh, M., Ed.; Springer: Berlin, Heidelberg, **2004**, Vol. *285*, pp. 25-66.
[46] Sakurai, Y.; Kolokoltsov, A.A.; Chen, C.C.; Tidwell, M.W.; Bauta, W.E.; Klugbauer, N.; Grimm, C.; Wahl-Schott, C.; Biel, M.; Davey, R.A. Ebola virus. Two-pore channels control Ebola virus host cell entry and are drug targets for disease treatment. *Science,* **2015**, *347*(6225), 995-998.
[47] Lee, J.E.; Fusco, M.L.; Hessell, A.J.; Oswald, W.B.; Burton, D.R.; Saphire, E.O. Structure of the Ebola virus glycoprotein bound to an antibody from a human survivor. *Nature,* **2008**, *454*(7201), 177-182.
[48] Ahmad, N.; Farman, A.; Badshah, S.L.; Ur Rahman, A.; Ur Rashid, H.; Khan, K. Molecular modeling, simulation and docking study of ebola virus glycoprotein. *J. Mol. Graph. Model.,* **2017**, *72*, 266-271.
[49] Shinyguruce, A.; Sathya, D.; Keerthiga, K.; Pavithra, P.; Vin-itha, M.; Vaidheeswari, R.; Eswara, P.B. *In Silico* Antiviral Drug Screening and Molecular Docking Studies Against Ebola Virus Glycoprotein. *J. Appl. Sci. Comput.,* **2018**, *5*(9), 211-216.
[50] Basler, C.F.; Mikulasova, A.; Martinez-Sobrido, L.; Paragas, J.; Mühlberger, E.; Bray, M.; Klenk, H.D.; Palese, P.; García-Sastre, A. The Ebola virus VP35 protein inhibits activation of interferon regulatory factor 3. *J. Virol.,* **2003**, *77*(14), 7945-7956.
[51] Reynard, O.; Nemirov, K.; Page, A.; Mateo, M.; Raoul, H.; Weissenhorn, W.; Volchkov, V.E. Conserved proline-rich re-gion of Ebola virus matrix protein VP40 is essential for plas-ma membrane targeting and virus-like particle release. *J. Infect. Dis.,* **2011**, *204*, 884-891.
[52] Ekins, S.; Freundlich, J.S.; Coffee, M. A common feature pharmacophore for FDA-approved drugs inhibiting the Ebola virus. *F1000 Res.,* **2014**, *3*, 277.
[53] Glanzer, J.G.; Byrne, B.M.; McCoy, A.M.; James, B.J.; Frank, J.D.; Oakley, G.G. *In silico* and *in vitro* methods to identify ebola virus VP35-dsRNA inhibitors. *Bioorg. Med. Chem.,* **2016**, *24*(21), 5388-5392.
[54] Ren, J.X.; Zhang, R.T.; Zhang, H.; Cao, X.S.; Liu, L.K.; Xie, Y. Identification of novel VP35 inhibitors: Virtual screening driven new scaffolds. *Biomed. Pharmacother.,* **2016**, *84*, 199-207.
[55] Sulaiman, K.O.; Kolapo, T.U.; Onawole, A.T.; Islam, A.; Adegoke, R.O.; Badmus, S.O. Molecular dynamics and com-bined docking studies for the identification of *Zaire Ebola* Vi-rus inhibitors. *J. Biomol. Struct. Dyn.,* **2018**, *2018*, 1-31.
[56] Hartlieb, B.; Muziol, T.; Weissenhorn, W.; Becker, S. Crystal structure of the C-terminal domain of Ebola virus VP30 reveals a role in transcription and nucleocapsid association. *Proc. Natl. Acad. Sci. USA,* **2007**, *104*(2), 624-629.
[57] John, S.P.; Wang, T.; Steffen, S.; Longhi, S.; Schmaljohn, C.S.; Jonsson, C.B. Ebola virus VP30 is an RNA binding protein. *J. Virol.,* **2007**, *81*(17), 8967-8976.
[58] Biedenkopf, N.; Hartlieb, B.; Hoenen, T.; Becker, S. Phosphorylation of Ebola virus VP30 influences the composition of the viral nucleocapsid complex: impact on viral transcription and replication. *J. Biol. Chem.,* **2013**, *288*(16), 11165-11174.
[59] Martínez, M.J.; Biedenkopf, N.; Volchkova, V.; Hartlieb, B.; Alazard-Dany, N.; Reynard, O.; Becker, S.; Volchkov, V. Role of Ebola virus VP30 in transcription reinitiation. *J. Virol.,* **2008**, *82*(24), 12569-12573.
[60] Shah, R.; Panda, P.K.; Patel, P.; Panchal, H. Pharmacophore based virtual screening and molecular docking studies of inherited compounds against ebola virus receptor proteins. *World J. Pharm. Pharm. Sci.,* **2015**, *4*(5), 1268-1282.
[61] Setlur, A.S.; Naik, S.Y.; Skariyachan, S. Herbal lead as ideal bioactive compounds against probable drug targets of ebola virus in comparison with known chemical analogue: A computational drug discovery perspective. *Interdiscip. Sci.,* **2017**, *9*(2), 254-277.
[62] Vecchio, K.D.; Shwarz, A.; Saphire, E.O.; Stahelin, R. The ebola virus matrix protein vp40 interacts selectively with plasma membrane lipids to promote viral egress. *FASEB J.,* **2017**, *31*, 945-951.
[63] Gomis-Rüth, F.X.; Dessen, A.; Timmins, J.; Bracher, A.; Kolesnikowa, L.; Becker, S.; Klenk, H.D.; Weissenhorn, W. The matrix protein VP40 from Ebola virus octamerizes into pore-like structures with specific RNA binding properties. *Structure,* **2003**, *11*(4), 423-433.
[64] Scianimanico, S.; Schoehn, G.; Timmins, J.; Ruigrok, R.H.; Klenk, H.D.; Weissenhorn, W. Membrane association induces a conformational change in the Ebola virus matrix protein. *EMBO J.,* **2000**, *19*(24), 6732-6741.
[65] Mirza, M.U.; Ikram, N. Integrated computational approach for virtual hit identification against ebola viral proteins VP35 and VP40. *Int. J. Mol. Sci.,* **2016**, *17*(11), 1748.
[66] M Alam El-Din, H.; A Loutfy, S.; Fathy, N.; H Elberry, M.; M Mayla, A.; Kassem, S.; Naqvi, A. Molecular docking based screening of compounds against VP40 from Ebola virus. *Bioinformation,* **2016**, *12*(3), 192-196.
[67] Abazari, D.; Moghtadaei, M.; Behvarmanesh, A.; Ghannadi, B.; Aghaei, M.; Behruznia, M.; Rigi, G. Molecular docking based screening of predicted potential inhibitors for VP40 from Ebola virus. *Bioinformation,* **2015**, *11*(5), 243-247.
[68] Karthick, V.; Nagasundaram, N.; Doss, C.G.P.; Chakraborty, C.; Siva, R.; Lu, A.; Zhang, G.; Zhu, H. Virtual screening of the inhibitors targeting at the viral protein 40 of Ebola virus. *Infect. Dis. Poverty,* **2016**, *5*, 12.
[69] Patel, J.; Chipkar, Y.; Momin, A. Comparitive study of vari-ous ebola virus Vp40 strains with modelling and docking studies to treat ebola virus infection. *Intl. J. Pharm. Drug Res.,* **2013**, *2*(1), 1-10.
[70] Skariyachan, S.; Acharya, A.B.; Subramaniyan, S.; Babu, S.; Kulkarni, S.; Narayanappa, R. Secondary metabolites extracted from marine sponge associated Comamonas testosteroni and *Citrobacter freundii* as potential antimicrobials against MDR pathogens and hypothetical leads for VP40 matrix protein of Ebola virus: an *in vitro* and *in silico* investigation. *J. Biomol. Struct. Dyn.,* **2016**, *34*(9), 1865-1883.
[71] Tamilvanan, T.; Hopper, W. High-throughput virtual screening and docking studies of matrix protein vp40 of ebola virus. *Bioinformation,* **2013**, *9*(6), 286-292.
[72] Reid, S.P.; Leung, L.W.; Hartman, A.L.; Martinez, O.; Shaw, M.L.; Carbonnelle, C.; Volchkov, V.E.; Nichol, S.T.; Basler, C.F. Ebola virus VP24 binds karyopherin alpha1 and blocks STAT1 nuclear accumulation. *J. Virol.,* **2006**, *80*(11), 5156-5167.
[73] Watanabe, S.; Noda, T.; Halfmann, P.; Jasenosky, L.; Kawaoka, Y. Ebola virus (EBOV) VP24 inhibits transcription and replication of the EBOV genome. *J. Infect. Dis.,* **2007**, *196*(Suppl. 2), S284-S290.
[74] Hoenen, T.; Jung, S.; Herwig, A.; Groseth, A.; Becker, S. Both matrix proteins of Ebola virus contribute to the regulation of viral genome replication and transcription. *Virology,* **2010**, *403*(1), 56-66.
[75] Tambunan, U.S.F.; Nasution, M.A.F. Identification of novel Ebola virus (EBOV) VP24 inhibitor from Indonesian natural products through in silico drug design approach. *AIP Conf. Proc.,* **2017**, *1862*(1)030091
[76] Tambunan, U.S.F.; Siregar, S.; Toepak, E.P. Ebola viral protein 24 (Vp24) inhibitor discovery by *in silico* fragment-based design. *Intl. J. Geom.,* **2018**, *15*(49), 59-64.
[77] Sharmila, R.; Jaikumar, B. Molecular docking study of bioac-tive compound of andrographolide against ebola virus. *Intl.. J. Pharm. Sci. Res.,* **2016**, *7*(5), 250-253.
[78] Sharma, D.; Pathak, M.; Sharma, R.; Tyagi, P.; Chawla, R.; Basu, M.; Ojha, H. Homology modeling and docking studies of VP24 protein of Ebola virus with an antiviral drug and its derivatives. *Chem. Biol. Lett.,* **2017**, *4*(1), 27-32.

[79] Sun, Y.; Guo, Y.; Lou, Z. A versatile building block: the structures and functions of negative-sense single-stranded RNA virus nucleocapsid proteins. *Protein Cell,* **2012**, *3*(12), 893-902.

[80] Zhou, H.; Sun, Y.; Guo, Y.; Lou, Z. Structural perspective on the formation of ribonucleoprotein complex in negative-sense single-stranded RNA viruses. *Trends Microbiol.,* **2013**, *21*(9), 475-484.

[81] Baikerikar, S. Curcumin and natural derivatives inhibit ebola viral proteins: An *in silico* approach. *Pharmacog. Res.,* **2017**, *9*(Suppl. 1), S15-S22.

[82] Slots, J. Periodontal herpesviruses: prevalence, pathogenicity, systemic risk. *Periodontol. 2000,* **2015**, *69*(1), 28-45.

[83] Whitley, R.J. Herpesviruses.*University of Texas Medical Branch at Gal-veston*; Microbiology, M.; Sam-uel, B., Eds.; Galveston, Texas, **1996**.

[84] Robbins, G.; Lammert, S.; Rompalo, A.; Riley, L.; Daskalakis, D.; Morrow, R.; Lee, H.; Shui, A.; Gaydos, C.; Detrick, B.; Rosenber, E.; Crochiere, D.; Cunningham, K.; Bradley, H.; Markowitz, L.; Xu, F.; Felsenstein, D. Serologic assays for the diagnosis of herpes virus 1 (HSV-1) herpes virus 2 (HSV-2): test characteristics of FDA approved type-specific assays in an ethnically, racially, and economi-cally diverse patient population In: *Open Forum Infectious Diseases,*; Oxford University Press., **2015**; 2.

[85] Rohner, E.; Wyss, N.; Heg, Z.; Faralli, Z.; Mbulaiteye, S.M.; Novak, U.; Zwahlen, M.; Egger, M.; Bohlius, J. HIV and human herpesvirus 8 co-infection across the globe: Systematic review and meta-analysis. *Int. J. Cancer,* **2016**, *138*(1), 45-54.

[86] World Health Organization: Herpes simplex virus, 2017. . http://www.who.int/news-room/fact-sheets/detail/herpes-simplex-virus (Accessed Oct 2, 2018)

[87] Burn, C.; Ramsey, N.; Garforth, S.J.; Almo, S.; Jacobs, W.R., Jr; Herold, B.C. A herpes simplex virus (HSV)-2 single-cycle candidate vaccine deleted in glycoprotein D protects male mice from lethal skin challenge with clinical isolates of HSV-1 and HSV-2. *J. Infect. Dis.,* **2018**, *217*(5), 754-758.

[88] Sripiboon, S.; Angkawanish, T.; Boonprasert, K.; Sombutputorn, P.; Langkaphin, W.; Ditcham, W.; Warren, K. Successful treatment of a clinical elephant endotheliotropic herpesvirus infection: The dynamics of viral load, genotype analysis, and treatment with acyclovir. *J. Zoo Wildl. Med.,* **2017**, *48*(4), 1254-1259.

[89] Troszok, A.; Kolek, L.; Szczygiel, J.; Wawrzeczko, J.; Borzym, E.; Reichert, M.; Kamińska, T.; Ostrowski, T.; Jurecka, P.; Adamek, M.; Rakus, K.; Irnazarow, I. Acyclovir inhibits Cyprinid herpesvirus 3 multiplication *in vitro*. *J. Fish Dis.,* **2018**, *41*(11), 1709-1718.

[90] Piret, J.; Boivin, G. *Herpesvirus Resistance to Antiviral Drugs*; Antimicrobial Drug Resistance, **2017**, pp. 1185-1211.

[91] Kolb, A.W.; Larsen, I.V.; Cuellar, J.A.; Brandt, C.R. Genomic, phylogenetic, and recombinational characterization of herpes simplex virus 2 strains. *J. Virol.,* **2015**, *89*(12), 6427-6434.

[92] Lehman, I.R.; Boehmer, P.E. Replication of herpes simplex virus DNA. *J. Biol. Chem.,* **1999**, *274*(40), 28059-28062.

[93] Matthews, J.T.; Terry, B.J.; Field, A.K. The structure and function of the HSV DNA replication proteins: Defining novel antiviral targets. *Antiviral Res.,* **1993**, *20*(2), 89-114.

[94] Hoog, S.S.; Smith, W.W.; Qiu, X.; Janson, C.A.; Hellmig, B.; McQueney, M.S.; O'Donnell, K.; O'Shannessy, D.; DiLella, A.G.; Debouck, C.; Abdel-Meguid, S.S. Active site cavity of herpesvirus proteases revealed by the crystal structure of herpes simplex virus protease/inhibitor complex. *Biochemistry,* **1997**, *36*(46), 14023-14029.

[95] Kashyap, K.; Kakkar, R. *Herpesvirus Proteases: Structure, Function, and Inhibition*; Viral Proteases and Their Inhibitors, **2017**, pp. 411-439.

[96] Arunkumar, J.; Rajarajan, S. Study on antiviral activities, drug-likeness and molecular docking of bioactive compounds of Punica granatum L. to Herpes simplex virus - 2 (HSV-2). *Microb. Pathog.,* **2018**, *118*, 301-309.

[97] Chowdary, T.K.; Cairns, T.M.; Atanasiu, D.; Cohen, G.H.; Eisenberg, R.J.; Heldwein, E.E. Crystal structure of the conserved herpesvirus fusion regulator complex gH-gL. *Nat. Struct. Mol. Biol.,* **2010**, *17*(7), 882-888.

[98] Atanasiu, D.; Cairns, T.M.; Whitbeck, J.C.; Saw, W.T.; Rao, S.; Eisenberg, R.J.; Cohen, G.H. Regulation of herpes simplex virus gB-induced cell-cell fusion by mutant forms of gH/gL in the absence of gD and cellular receptors. *MBio,* **2013**, *4*(2), e00046-e13.

[99] Connolly, C. S.A.; Jackson, J.O.; Jardetzky, T.S.; Longnecker, R. Fusing structure and function: a structural view of the her-pesvirus entry machinery. *Nat. Rev. Microbiol.,* **2011**, *9*(5), 369.

[100] Boyer, C.B.; Greenberg, L.; Chutuape, K.; Walker, B.; Monte, D.; Kirk, J.; Ellen, J.M.; Belzer, M.; Martinez, M.; Dudek, J. Adolescent medicine trials network. exchange of sex for drugs or money in adolescents and young adults: An examination of sociodemographic factors, HIV-related risk, and community context. *J. Commun. Health,* **2017**, *42*(1), 90-100.

[101] Strategies, P.; Therapy, F.O.R.A.; Tecnol, D.; Cruz, O. Estratégias farmacológicas para a terapia anti-aids Emerson Poley Peçanha* e Octavio A. C. *Antunes.,* **2002**, *25*(6), 1108-1116.

[102] Morris, P.; DaSilva, Y.; Clark, E.; Hahn, W.E.; Barenholtz, E. Convolutional Neural Networks for Predicting Molecular Binding Affinity to HIV-1 Proteins. In: 2018 ACM International Conference on Bioinformatics, Computational Biology, and Health Informatics (BCB '18). ACM, New York, NY, USA, 220-225. DOI: https://doi.org/10.1145/3233547.3233596

[103] Mohammadi, A.A.; Taheri, S.; Amouzegar, A.; Ahdenov, R.; Halvagar, M.R.; Sadr, A.S. Diastereoselective synthesis and molecular docking studies of novel fused tetrahydro-pyridine derivatives as new inhibitors of HIV protease. *J. Mol. Struct.,* **2017**, *1139*, 166-174.

[104] Tong, J.; Wu, Y.; Bai, M.; Zhan, P. 3D-QSAR and molecular docking studies on HIV protease inhibitors. *J. Mol. Struct.,* **2017**, *1129*, 17-22.

[105] Zondagh, J.; Balakrishnan, V.; Achilonu, I.; Dirr, H.W.; Sayed, Y. Molecular dynamics and ligand docking of a hinge region variant of South African HIV-1 subtype C protease. *J. Mol. Graph. Model.,* **2018**, *82*, 1-11.

[106] Ahmad, R.; Sahidin, I.; Taher, M.; Low, C.; Noor, N.M.; Sillapachaiyaporn, C.; Chuchawankul, S.; Sarachana, T.; Tencomnao, T.; Iskandar, F.; Rajab, N.F.; Baharum, S.N. Polygonumins A, a newly isolated compound from the stem of Polygonum minus Huds with potential medicinal activities. *Sci. Rep.,* **2018**, *8*(1), 4202.

[107] Al-Shehri, M.M.; Al-Majed, A.R.A.; Aljohar, H.I.; El-Emam, A.A.; Pathak, S.K.; Sachan, A.K.; Prasad, O.; Sinha, L. First principle study of a potential bioactive molecule with tetrahydroisoquinoline, carbothiomide and adamantane scaffolds. *J. Mol. Struct.,* **2017**, *1143*, 204-216.

[108] Ghosh, A.K.; Osswald, H.L.; Glauninger, K.; Agniswamy, J.; Wang, Y-F.; Hayashi, H.; Aoki, M.; Weber, I.T.; Mitsuya, H. Probing lipophilic adamantyl group as the P1-ligand for HIV-1 protease inhibitors: Design, synthesis, protein X-ray structural studies, and biological evaluation. *J. Med. Chem.,* **2016**, *59*(14), 6826-6837.

[109] Debnath, U.; Kumar, P.; Agarwal, A.; Kesharwani, A.; Gupta, S.K.; Katti, S.B. N-hydroxy-substituted 2-aryl acetamide analogs: A novel class of HIV-1 integrase inhibitors. *Chem. Biol. Drug Des.,* **2017**, *90*(4), 527-534.

[110] Vyas, V.K.; Shah, S.; Ghate, M. Generation of new leads as HIV-1 integrase inhibitors: 3D QSAR, docking and molecular dynamics simulation. *Med. Chem. Res.,* **2017**, *26*(3), 532-550.

[111] Chander, S.; Pandey, R.K.; Penta, A.; Choudhary, B.S.; Sharma, M.; Malik, R.; Prajapati, V.K.; Murugesan, S. Molecular docking and molecular dynamics simulation based approach to explore the dual inhibitor against HIV-1 reverse transcriptase and integrase. *Comb. Chem. High Throughput Screen.,* **2017**, *20*(8), 734-746.

[112] Faridoon; Mnkandhla, D.; Isaacs, M.; Hoppe, H. C.; Kaye, P. T. Synthesis and evaluation of substituted 4-arylimino-3-hydroxybutanoic acids as potential HIV-1 integrase inhibitors. *Bioorg. Med. Chem. Lett.,* **2018**, *28*(6), 1067-1070.

[113] Zhang, F.H.; Debnath, B.; Xu, Z.L.; Yang, L.M.; Song, L.R.; Zheng, Y.T.; Neamati, N.; Long, Y.Q. Discovery of novel 3-hydroxypicolinamides as selective inhibitors of HIV-1 integrase-LEDGF/p75 interaction. *Eur. J. Med. Chem.,* **2017**, *125*, 1051-1063.

[114] Panwar, U.; Singh, S.K. Structure-based virtual screening toward the discovery of novel inhibitors for impeding the protein-protein interaction between HIV-1 integrase and hu-man lens epithelium-derived growth factor (LEDGF/P75). *J. Biomol. Struct. Dyn.,* **2018**, *36*(12), 3199-3217.

[115] Srivastav, V.K.; Tiwari, M. QSAR and Docking studies of coumarin derivatives as potent HIV-1 integrase inhibitors. *Arab. J. Chem.,* **2017**, *10*, S1081-S1094.

[116] Ericksen, S.S.; Wu, H.; Zhang, H.; Michael, L.A.; Newton, M.A.; Hoffmann, F.M.; Wildman, S.A. Machine learning consensus scor-

ing improves performance across targets in structure-based virtual screening. *J. Chem. Inf. Model.,* **2017**, *57*(7), 1579-1590.

[117] Jin, K.; Yin, H.; De Clercq, E.; Pannecouque, C.; Meng, G.; Chen, F. Discovery of biphenyl-substituted diarylpyrimidines as non-nucleoside reverse transcriptase inhibitors with high potency against wild-type and mutant HIV-1. *Eur. J. Med. Chem.,* **2018**, *145*, 726-734.

[118] Kashid, A.M.; Dhawale, S. Design, Synthesis and Biological Screening of N 1 - (Substituted Pyridine-2-Yl) -N 3 - (Quinoline-2-Yl). *Malonamide as Novel Anti-HIV-I Agents., Ind. J. Chem. Sec. B Org. Med. Chem.,* **2018**, *57*, 870-879.

[119] Liu, G.; Wang, W.; Wan, Y.; Ju, X.; Gu, S. Application of 3D-QSAR, Pharmacophore, and Molecular Docking in the Molec-ular Design of Diarylpyrimidine Derivatives as HIV-1 Nonnucleoside Reverse Transcriptase Inhibitors. *Int. J. Mol. Sci.,* **2018**, *19*(5), 1436.

[120] Singh, A.; Singh, V.K.; Verma, R.; Singh, R.K. In Silico Studies on N - (Pyridin- 2-Yl) Thiobenzamides as NNRTIs against Wild and Mutant HIV-1 Strains. *Philipp. J. Sci.,* **2018**, *147*(March), 37-46.

[121] Peddi, S.R.; Mohammed, N.A.; Hussein, A.A.; Sivan, S.K.; Manga, V. Multiple-Receptor Conformation Docking, Dock Pose Clustering, and 3D QSAR-Driven Approaches Exploring New HIV-1 RT Inhibitors. *Struct. Chem.,* **2018**, *29*(4), 999-1012.

[122] Zhang, H.; Tian, Y.; Kang, D.; Huo, Z.; Zhou, Z.; Liu, H.; De Clercq, E.; Pannecouque, C.; Zhan, P.; Liu, X. Discovery of uracil-bearing DAPYs derivatives as novel HIV-1 NNRTIs *via* crystallographic overlay-based molecular hybridization. *Eur. J. Med. Chem.,* **2017**, *130*, 209-222.

[123] Samanta, P.N.; Das, K.K. Inhibition activities of catechol diether based non-nucleoside inhibitors against the HIV reverse transcriptase variants: Insights from molecular docking and ONIOM calculations. *J. Mol. Graph. Model.,* **2017**, *75*, 294-305.

[124] Poongavanam, V.; Namasivayam, V.; Vanangamudi, M.; Al Shamaileh, H.; Veedu, R.N.; Kihlberg, J.; Murugan, N.A. Integrative Approaches in HIV-1 Non-Nucleoside Reverse Transcriptase Inhibitor Design. *Wiley Interdiscip. Rev. Comput. Mol. Sci.,* **2018**, *8*(1), 1-26.

[125] Monforte, A.M.; De Luca, L.; Buemi, M.R.; Agharbaoui, F.E.; Pannecouque, C.; Ferro, S. Structural optimization of N_1-arylbenzimidazoles for the discovery of new non-nucleoside reverse transcriptase inhibitors active against wild-type and mutant HIV-1 strains. *Bioorg. Med. Chem.,* **2018**, *26*(3), 661-674.

[126] Cabrera, A.; Huerta, H.L.; Chávez, D.; Medina-Franco, J.L. Molecular Modeling of Potential Dual Inhibitors of HIV Reverse Transcriptase and Integrase. *Comput. Mol. Biosci.,* **2018**, *8*, 1-41.

[127] Tang, J.; Vernekar, S.K.V.; Chen, Y.L.; Miller, L.; Huber, A.D.; Myshakina, N.; Sarafianos, S.G.; Parniak, M.A.; Wang, Z. Synthesis, biological evaluation and molecular modeling of 2-Hydroxyisoquinoline-1,3-dione analogues as inhibitors of HIV reverse transcriptase associated ribonuclease H and polymerase. *Eur. J. Med. Chem.,* **2017**, *133*, 85-96.

[128] Barberato, C.; Neto, Z. G. A AÇÃO coletiva como instrumento de tutela e concretização do direito à saúde. *Jus Popul.,* **2018**, *1*(3), 129-146.

[129] Sousa, S.J.F.E.; Sousa, S.B.F.E. Eye bank procedures: donor selection criteria. *Arq. Bras. Oftalmol.,* **2018**, *81*(1), 73-79.

[130] Lemon, S.M.; Walker, C.M.; Hepatitis, A. Virus and Hepatitis E Virus: Emerging and Re-Emerging Enterically Transmitted Hepatitis Viruses. *Cold Spring Harb. Perspect. Med.,* **2019**, *9*(6), pii. A031823.

[131] Majumdar, A.; Gilliam, B.L.; Arnold, R.; Rock, C.; Croft, L.; Morgan, D.J.; Donnenberg, M.S.; Majid, A.; McAninch, J.; Morgan, D.J. Grazoprevir Potassium. HCV NS3 NS4A Prote-ase Inhibitor, Anti-Hepatitis C Virus Drug. *Drugs Future,* **2016**, *41*(2), 85-109.

[132] Pontarolo, R.; Borba, H. H. L.; Ferreira, V. L.; Pedroso, M. L. A.; Souza, A. W.; Siqueira, F. M. Direct-Acting Antivirals For Chronic Hepatitis C Treatment, ed. Berlin, Germany: Arid Science, **2017**, v., p.t.

[133] Stanaway, J.D.; Flaxman, A.D.; Naghavi, M.; Fitzmaurice, C.; Vos, T.; Abubakar, I.; Abu-Raddad, L.J.; Assadi, R.; Bhala, N.; Cowie, B.; Forouzanfour, M.H.; Groeger, J.; Hanafiah, K.M.; Jacobsen, K.H.; James, S.L.; MacLachlan, J.; Malekzadeh, R.; Martin, N.K.; Mokdad, A.A.; Mokdad, A.H.; Murray, C.J.L.; Plass, D.; Rana, S.; Rein, D.B.; Richardus, J.H.; Sanabria, J.; Saylan, M.; Shahraz, S.; So, S.; Vlassov, V.V.; Weiderpass, E.; Wiersma, S.T.; Younis, M.; Yu, C.; El Sayed Zaki, M.; Cooke, G.S. The global burden of viral hepatitis from 1990 to 2013: findings from the Global Burden of Disease Study 2013. *Lancet,* **2016**, *388*(10049), 1081-1088.

[134] Liver, E.A.F.T.S.O.T. EASL 2017 Clinical Practice Guidelines on the management of hepatitis B virus infection. *J. Hepatol.,* **2017**, *67*(2), 370-398.

[135] Kimberlin, D. W.; Brady, M. T.; Jackson, M. A.; Long, S. S. *Red Book: 2015 Report of the Committee on Infec-tious Diseases,* 30th ed.; American Academy of Pediatrics; Elk Grove Village, IL, **2015**.

[136] Giesecke, J. *Modern Infectious Disease Epidemiology*; CRC Press, **2017**.

[137] Pilot-Matias, T.; Tripathi, R.; Cohen, D.; Gaultier, I.; Dekhtyar, T.; Lu, L.; Reisch, T.; Irvin, M.; Hopkins, T.; Pithawalla, R.; Middleton, T.; Ng, T.; McDaniel, K.; Or, Y.S.; Menon, R.; Kempf, D.; Molla, A.; Collins, C. *In vitro* and *in vivo* antiviral activity and resistance profile of the hepatitis C virus NS3/4A protease inhibitor ABT-450. *Antimicrob. Agents Chemother.,* **2015**, *59*(2), 988-997.

[138] Foureau, D.M.; Walling, T.L.; Maddukuri, V.; Anderson, W.; Culbreath, K.; Kleiner, D.E.; Ahrens, W.A.; Jacobs, C.; Watkins, P.B.; Fontana, R.J.; Chalasani, N.; Talwalkar, J.; Lee, W.M.; Stolz, A.; Serrano, J.; Bonkovsky, H.L. Comparative analysis of portal hepatic infiltrating leucocytes in acute drug-induced liver injury, idiopathic autoimmune and viral hepatitis. *Clin. Exp. Immunol.,* **2015**, *180*(1), 40-51.

[139] Sarrazin, C.; Lathouwers, E.; Peeters, M.; Daems, B.; Buelens, A.; Witek, J.; Wyckmans, Y.; Fevery, B.; Verbinnen, T.; Ghys, A.; Schlag, M.; Baldini, A.; De Meyer, S.; Lenz, O. Prevalence of the hepatitis C virus NS3 polymorphism Q80K in genotype 1 patients in the European region. *Antiviral Res.,* **2015**, *116*, 10-16.

[140] Appleby, T. C.; Perry, J. K.; Murakami, E.; Barauskas, O.; Feng, J.; Cho, A.; Fox, D.; Wetmore, D. R.; McGrath, M. E.; Ray, A. S. Structural Basis for RNA Replication by the Hepatitis C Virus Polymerase. *Science,* **2015**, *347*(6223), 771-775.

[141] Patel, P.D.; Patel, M.R.; Kaushik-Basu, N.; Talele, T.T. 3D QSAR and molecular docking studies of benzimidazole derivatives as hepatitis C virus NS5B polymerase inhibitors. *J. Chem. Inf. Model.,* **2008**, *48*(1), 42-55.

[142] Vani, G.S.; Rajarajan, S. A Study on *In-Silico* Analysis of Phytochemicals Targeting the Proteins of Hepatitis B and C Virus. *Int. J. Curr. Microbiol. Appl. Sci.,* **2015**, *4*(12), 683-691.

[143] Wang, X.; Yang, W.; Xu, X.; Zhang, H.; Li, Y.; Wang, Y. Studies of benzothiadiazine derivatives as hepatitis C virus NS5B polymerase inhibitors using 3D-QSAR, molecular docking and molecular dynamics. *Curr. Med. Chem.,* **2010**, *17*(25), 2788-2803.

[144] Anithaa, K.; Singhb, N.; Shaikc, B.; Ahmadc, I.; Agrawald, V.K.; Guptac, S.P. QSAR and Docking Studies on 1, 1-Dioxo-2H-Benzothiadiazines Acting as HCV NS5B Polymerase In-hibitors. *J. Mod. Med. Chem.,* **2015**, *3*, 49-68.

[145] Liu, M-M.; Zhou, L.; He, P-L.; Zhang, Y-N.; Zhou, J-Y.; Shen, Q.; Chen, X-W.; Zuo, J-P.; Li, W.; Ye, D-Y. Discovery of flavonoid derivatives as anti-HCV agents via pharmacophore search combining molecular docking strategy. *Eur. J. Med. Chem.,* **2012**, *52*, 33-43.

[146] Scull, M.A.; Schneider, W.M.; Flatley, B.R.; Hayden, R.; Fung, C.; Jones, C.T.; van de Belt, M.; Penin, F.; Rice, C.M. The N-terminal Helical Region of the Hepatitis C Virus p7 Ion Channel Protein Is Critical for Infectious Virus Production. *PLoS Pathog.,* **2015**, *11*(11), e1005297.

[147] Boukadida, C.; Fritz, M.; Blumen, B.; Fogeron, M-L.; Penin, F.; Martin, A. NS2 proteases from hepatitis C virus and related hepaciviruses share composite active sites and previously unrecognized intrinsic proteolytic activities. *PLoS Pathog.,* **2018**, *14*(2), e1006863.

[148] Lisboa Neto, G.; Noble, C.; Pinho, J.R.R.; Malta, F.M.; Gomes-Gouvea, M.S.; Alvarado-Mora, M.V.; Silva, M.H.; Leite, A.G.; Piccoli, L.Z.; Carrilho, F.J. Characterization of clinical predictors of naturally oc-curring ns3/ns4a protease polymorphism in genotype 1 hepatitis c virus infected patients. *J. Hepatol.,* Elsevier Science BV, **2015**, Vol. *62*, pp. S686-S686.

[149] Bailey, M.D.; Halmos, T.; Lemke, C.T. Discovery of novel P2 substituted 4-biaryl proline inhibitors of hepatitis C virus NS3 serine protease. *Bioorg. Med. Chem. Lett.,* **2013**, *23*(15), 4436-4440.

[150] Wei, Y.; Yang, J.; Kishore Sakharkar, M.; Wang, X.; Liu, Q.; Du, J.; Zhang, J-J. Evaluating the Inhibitory Effect of Eight Compounds from Daphne Papyracea against the NS3/4A Pro-tease of Hepatitis C Virus. *Nat. Prod. Res.,* **2018**, *17*, 1-4.

[151] Ashfaq, U.A.; Jalil, A.; Ul Qamar, M.T. Antiviral phytochemicals identification from Azadirachta indica leaves against HCV NS3 protease: an *in silico* approach. *Nat. Prod. Res.,* **2016**, *30*(16), 1866-1869.

[152] Shaw, J.; Harris, M.; Fishwick, C.W.G. Identification of a lead like inhibitor of the hepatitis C virus non-structural NS2 autoprotease. *Antiviral Res.,* **2015**, *124*, 54-60.

[153] Lulu, S.S.; Thabitha, A.; Vino, S.; Priya, A.M.; Rout, M. Naringenin and quercetin--potential anti-HCV agents for NS2 protease targets. *Nat. Prod. Res.,* **2016**, *30*(4), 464-468.

[154] Uddin, R.; Downard, K.M. Molecular basis of benzimidazole inhibitors to hepatitis C virus envelope glycoprotein. *Chem. Biol. Drug Des.,* **2018**, *92*(3), 1638-1646.

[155] Hung, T-C.; Jassey, A.; Liu, C-H.; Lin, C-J.; Lin, C-C.; Wong, S.H.; Wang, J.Y.; Yen, M-H.; Lin, L-T. Berberine inhibits hepatitis C virus entry by targeting the viral E2 glycoprotein. *Phytomedicine,* **2019**, *53*, 62-69.